MONASH University

Studies of Insulin Dicarba-Peptidomimetics

Synthesis and biological evaluation of novel insulin analogues

Andrew M. Wright

School of Chemistry
Monash University
2018

Supervisor: Prof. Andrea J. Robinson

This page is intentionally left blank

Copyright notice

"*The rich kid becomes a junkie,*

The poor kid, an advertiser.

What a tragic waste of potential.

Being a junkie's not so good either."

- This Is Serious, Mum

Declaration

This thesis contains no material which has been accepted for the award of any other degree or diploma at any university or equivalent institution and that, to the best of my knowledge and belief, this thesis contains no material previously published or written by another person, except where due reference is made in the text of the thesis.

Signature: 

Print Name: Andrew M. Wright

Date: 18/12/18

Table of Contents

Abstract

Insulin presents an intriguing prospect to the chemist and the structural biologist alike; it remains a target of intense scientific investigation and pharmaceutical enterprise. However, despite nearly a century of multidisciplinary endeavour, a complete picture of the functions, interactions and contortions of the peptide remains elusive.

This work seeks to unite catalytic methodologies with novel peptide synthesis to gain insights into the conformational repertoire of insulin. Three distinct synthetic investigations are presented in Chapters 2, 3 and 4 focussing on dicarba-replacement of two of human insulin's three highly conserved disulfide bridges. An examination of these bridges and other aspects of insulin's structure-activity relationship is presented in Chapter 1.

Chapter 2 presents a synthesis of four dicarba-insulin analogues whereby the C_α stereochemistry of the allylglycine residues constituting the A6-A11 intrachain dicarba bridge is systematically inverted. Whilst the *cis*/*trans* geometry of this bridge is known to give rise to disparate activities, its effect in conjunction with chiral mutations at the C_α position was previously unknown. The deleterious effect of these chiral mutations on dicarba-insulin's binding affinity was elucidated, highlighting insulin's remarkable sensitivity to modification in this region.

Chapter 3 details the synthesis and biological assay of dicarba-insulin analogues whereby the intrachain disulfide is alternately replaced by alkyne- and allylcysteine-derived dicarba-linkages. Given the high activity of previously synthesised *cis*-olefinic dicarba-bridged insulins, it was of interest to observe the effects of highly constrained (alkynyl) and conformationally flexible (allylcysteine-derived) linkages. The synthesis of the former was an opportunity to deploy practically challenging chemistry in the form of

highly air-sensitive on-resin ring-closing alkyne metathesis (RCAM). By the diminished binding affinity of each of these analogues, it was inferred that any linkage employed to replace the A6-A11 disulfide must be a four-atom moiety capable of adopting a conformation analogous to a *cis*oid disulfide bridge if receptor binding affinity and activation is to be retained.

Chapter 4 details the development of strategies to enable a biomimetic synthesis of an *interchain* dicarba-bridged insulin analogue. A truncated C-peptide tether was designed and successfully enzymatically cleaved from a single-chain insulin precursor with a view to form the interchain dicarba bridge through ring-closing metathesis (RCM). Additionally, a novel strategy for enabling RCM in reticent peptide sequences by the use of dehydroamino acid residues is described, as well as an optimised synthesis for such species.

Acknowledgements

I'd like to thank the following, without whom this work would not be possible:

- My Supervisor, Prof. Andrea Robinson.
- Academic staff at Monash University who have assisted or mentored me in various ways throughout this project, including: Em. Prof. Roy Jackson, Dr. Kellie Tuck, Dr. Eva Campi, Dr. Patrick Perlmutter, Dr. Katya Pas, Prof. David Lupton, Assoc. Prof. Mike Grace, Em. Prof. Don McNaughton, Dr. Chris Thompson and Dr. David Collins.
- The technical staff who have provided me with invaluable training and assistance in the operation and maintenance of instrumentation, including: Dr. Peter Nichols, Dr. Boujemaa Moubaraki, Dr. Sally Duck, Dr. Georg Beilharz, Dr. Peter Newman and Mr. Phil Holt. Additional thanks to Dr. Barb Kemp-Harper of the Pharmacology Department.
- Past and present members of the Robinson Group, with particular thanks to those who have trained me in the practice of organic chemistry: Dr. Alessia Belgi, Dr. James Burnley, Dr. Nic Spiccia, Dr. Bianca van Lierop and Dr. James Wang.
- My family (esp. Mum, Dad, Kate and David), Alexis and family, my bandmates (esp. Michael, Nina and Miel), the Cave Clan (esp. Critt, Dezi, Chewy, Dougo, Prowler, Dodgy, Gilligan, SiR, Diode and the Drongos) and the 160 m crossband missions (Dave Stuart VK3ASE, Chris Long VK3AML, Steve Langley VK3SL, Ralph Klimek VK3ZZC, John Eggington VK3EGG, David Wilks VK3HDW, the other Peter Godfrey VK3YPG *et al*.).
- Official Australian suppliers to VK3BEK: Cisco's World of Coffee, Cedel Toothpaste, Red Eye Energy Drinks, Kooka's Country Cookies, Big W, Donut King, Pellegrini's Espresso Bar, Mario's and La Bohemia of Noble Park and Toscana's of Murrumbeena.

- Those who have ceaselessly inspired me but have sadly departed too soon: Dr. Peter Godfrey and Prof. Leone Spiccia; Michael ‘Predator’ Carlton and Tony ‘the Branch’ Sanderson. This thesis is dedicated to their memory.

List of Abbreviations

(Δ^4A*y*,*z*) – a C4-unsaturated diaminosuberic acid residue formed by residues y and z within the peptide sequence

^{1}H - proton

^{13}C – carbon 13

Ac – acetyl

Ac_2O – acetic anhydride

Acm – acetamidomethyl

Agl - allylglycine

Alloc – allyloxycarbonyl

ALP - *Acromobacter lyticus* protease

ASTM – American Standard Sieve Series

Boc_2O – di-*tert*-butyl dicarbonate

Bug - butynylglycine

cat. – catalyst

Cbz - carboxybenzyl

CD – circular dichroism

CM – cross metathesis

COD - cyclooctadiene

CR – cysteine-rich

DAS – 2,7-diaminosuberic acid

DCM - dichloromethane

des_{Ax-y} – residues *x* to *y* of native insulin A chain not present

Dhv – 2,3-dehydrovaline

DIPEA – *N*,*N*-diisopropylamine

DM – *diabetes mellitus*

DMAP – 4-dimethylaminopyridine

DMF – *N*,*N*-dimethylformamide

DOI – *des*-octapeptide insulin

DSE – dihedral strain energy

DPDS – 2,2-dipyridyl disulfide

DTI – *des*-tetrapeptide insulin

EGTA – ethylene glycol-bis(β-aminoethyl ether)-*N*,*N*,*N*′,*N*′-tetraacetic acid

EM – electron microscopy

equiv. – molar equivalents

ESI – electrospray ionisation

Et - ethyl

Fmoc – fluorenylmethoxycarbonyl

FTIR – Fourier transform infrared

GII – Grubbs' 2nd Generation Catalyst

h – hours

HATU - (1-[bis(dimethylamino)methylene]-1*H*-1,2,3-triazolo[4,5-b]pyridinium 3-oxide hexafluorophosphate)

HEPES - 4-(2-hydroxyethyl)-1-piperazine-ethanesulfonic acid

HPLC – high performance liquid chromatography

HRMS – high-resolution mass spectrometry

INSL – insulin-like peptide

IGF – insulin-like growth factor

IR – insulin receptor

^{i}Pr – *iso*-propyl

LDA – lithium diisopropylamide

LRMS – low-resolution mass spectrometry

Me – methyl

MS – mass spectrometry

MVW – multivariable wavelength

NCL – native chemical ligation

NMM – *N*-methyl morpholine

NMP – *N*-methyl pyrrolidine

NMR – nuclear magnetic resonance

PDA – photodiode array

PDB – Protein Data Bank

PG – protecting group

PPTS - pyridinium *p*-toluenesulfonate

Pren - prenyl

Prenoc – prenyloxycarbonyl

PTFE – polytetrafluoroethylene (Teflon)

Pyr – pyridyl

RCAM – ring-closing alkyne metathesis

RCM – ring closing metathesis

R_f - retardation factor

RP-HPLC – reverse-phase high performance liquid chromatography

rt – room temperature

Sac – *S*-allylcysteine

SPPS – solid phase peptide synthesis

Su - succinimide

^{t}Bu – *tert*-butyl

TFA – trifluoroacetic acid

THF – tetrahydrofuran

TIPS - triisopropylsilane

TK – tyrosine kinase

TLC – thin-layer chromatography

TNBS – 2,4,6-trinitrobenzenesulfonic acid

TOF – time-of-flight

t_R – retention time

Ts - tosyl

1 The current scope of insulin, its analogues and the relevance of catalysis to its synthesis

1.1 Insulin

Insulin is a 51 amino acid peptide hormone comprised of a 21-residue A-chain and a 30-residue B-chain. A pair of interchain disulfide bridges, Cys^{A7}-Cys^{B7} and Cys^{A20}-Cys^{B19}, links these whilst an additional intrachain disulfide bridge, Cys^{A6}-Cys^{A11}, is present within the A-chain. This arrangement of disulfide bridges is conserved amidst diverse peptides within the insulin superfamily.[1] The elucidation of the structure of hagfish insulin[2-3] suggests that the conserved residues of insulin (Table 1) have remained static from an evolutionary perspective for approximately 500 million years.[3]

Table 1 - Conservation of crucial binding residues throughout vertebrate species. Positions that are universally conserved highlighted in red. Adapted from Conlon.[4]

	A1	A2	A3	A4	A5	A19	A21	B12	B16	B23	B24	B25	B26
Human	Gly	Ile	Val	Glu	Gln	Tyr	Asn	Val	Tyr	Gly	Phe	Phe	Tyr
Guinea pig	-	-	-	Asp	-	-	-	-	-	-	-	-	-
Chinchilla	-	-	-	Asp	-	-	-	-	-	-	-	-	-
Casiragua	-	-	-	Asp	-	-	-	-	-	-	-	Tyr	Arg
Coypu	-	-	-	Asp	-	-	-	-	-	-	-	Tyr	Arg
Porcupine	-	-	-	Asp	-	-	-	-	-	-	-	-	-
Cuis	-	-	-	Asp	-	-	-	-	-	-	-	-	Ser
Degu	-	-	-	Asp	-	-	-	-	-	-	-	Tyr	Arg
Iguana	-	-	-	Gln	-	-	-	-	-	-	-	Tyr	-
Rattlesnake	-	-	-	-	-	-	-	-	Phe	-	-	Tyr	-
Colubrid Snake	-	-	-	-	-	-	-	-	Phe	-	-	Tyr	-
Python	-	-	-	-	-	-	-	-	-	-	-	Tyr	-
Caecilian	-	-	-	-	Lys	-	-	-	-	-	-	-	-
Wood frog	-	-	-	-	-	-	Ser	-	-	-	-	-	-
Surinam toad	-	-	-	-	-	-	-	-	His	-	-	-	-
Australian lungfish	-	-	-	-	-	-	-	-	His	-	-	-	-
African lungfish	-	-	-	-	-	-	-	-	His	-	-	-	-
Cod	-	-	-	Asp	-	-	-	-	-	-	-	-	-
Eel	-	-	-	-	-	-	-	-	-	-	-	-	Phe
Elephantnose	-	-	-	-	-	-	-	-	Phe	-	-	-	Phe
Tilapia	-	-	-	-	Glu	-	-	-	-	-	-	-	-
Bowfin	-	-	-	-	-	-	-	-	Phe	-	-	-	-
Electric ray	-	-	-	-	His	-	-	-	-	-	-	Tyr	-
Spiny dogfish	-	-	-	-	His	-	-	-	-	-	-	Tyr	-
Spotted dogfish	-	-	-	Asp	His	-	-	-	-	-	-	Tyr	-
Hammerhead shark	-	-	-	Asp	His	-	-	-	-	-	-	Tyr	-
Pouched lamprey	-	-	-	-	Lys	-	-	-	-	-	-	Tyr	-
Hagfish	-	-	-	-	-	-	-	-	-	-	-	-	-

Insulin was discovered and isolated from pancreatic secretions by Banting and Best in 1922.[5-6] Its efficacy in the treatment of *diabetes mellitus* (DM) was quickly and dramatically established,[6] beginning almost a century of research dedicated to the compound's biochemistry.[7] Insulin's principal biological function is to regulate blood glucose *via* activation of the insulin receptor, which increases muscular and adipose tissue glucose uptake and inhibits glucose production from glycogen in the liver.[8] As such, it represents a core functional component of vertebrate metabolism.

The biosynthesis of insulin was first elucidated by Steiner *et al*. in the late 1960s.[9-10] Preproinsulin, a 104-residue peptide, is synthesised within pancreatic β cells constrained in clusters called the *islets of Langerhans*.[11] In addition to the 51-residue insulin sequence, preproinsulin also includes a 24-residue signal peptide appended to the B-chain's *N*-terminus and a 29-residue 'C-peptide', bookended by a pair of two-residue cleavage sites, linking the B-chain *C*-terminus to the A-chain *N*-terminus.[12] This initial precursor is converted to proinsulin (Figure 1), which lacks the signal peptide, mostly *via* cotranslational cleavage in the endoplasmic reticulum.[11] Proinsulin is then stored with proteases in storage granules that liberate insulin and C-peptide upon appropriate stimulus (e.g. increase in endogenous glucose).[13]

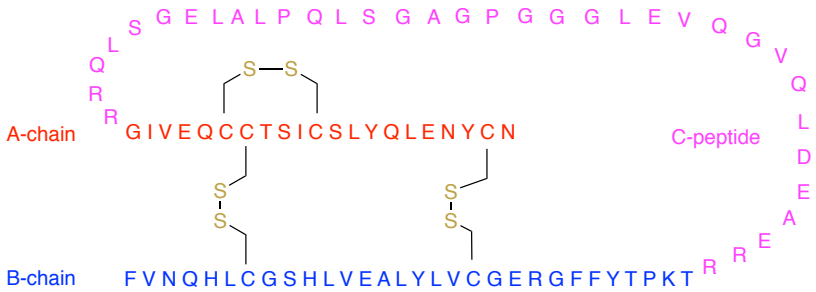

Figure 1 - Proinsulin primary sequence. Insulin residues shown in red and blue, C-peptide shown in pink, disulfide constituents in yellow.

Hodgkin's determination of the crystal structure of porcine insulin was an important milestone in the fields of insulin research and X-ray crystallography - insulin was shown to exist as a Zn^{2+}-coordinated hexamer.[14] This is the storage form of insulin, which dissociates into monomers for transport within the body.[15] Insulin also forms dimers prior to organisation into the hexamer structure (Figure 2).[15]

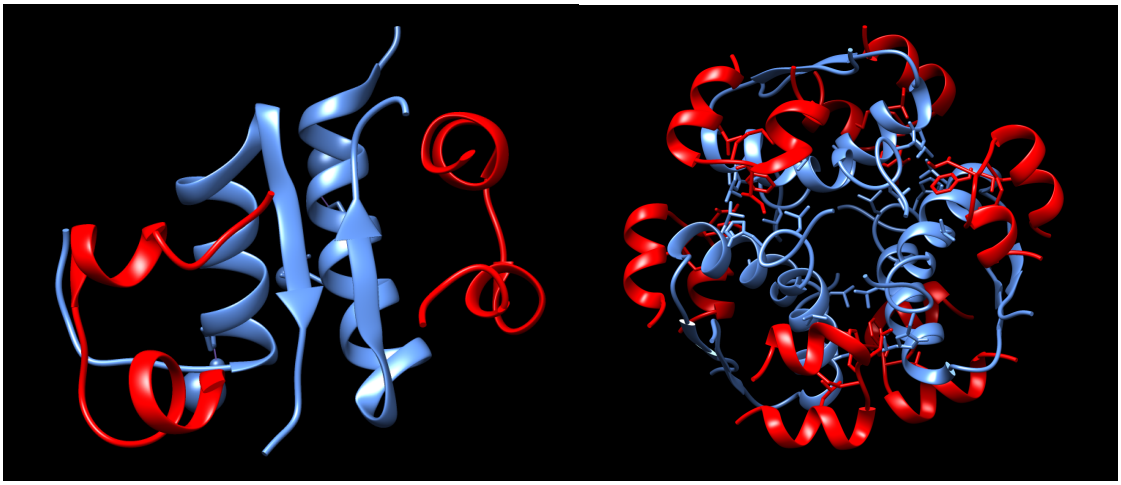

Figure 2 - Insulin dimer (left)[16] and hexamer (right)[17] structures. Rendered by the author from the corresponding PDB data using UCSF Chimera.[18]

Mutations of the insulin sequence at crucial oligomerising residues, preventing formation of the storage hexamer, have formed the basis of 'fast acting' insulin analogues[19] used in the treatment of DM such as insulin lispro[20] (Humalog ®) and insulin aspart[21] (Novolog ®) (Table 2).

Table 2 – Comparison of several commercially available insulin therapeutics. Adapted from Walsh.[22]

	Description	Structure	Company	Approved
Humulin	Recombinant human insulin produced in *E. Coli*	Identical to human insulin	Eli Lilly	1982 (USA)
Humalog (insulin Lispro)	Recombinant short-acting human insulin analogue produced in *E. Coli*	Engineered; inversion of native B28-B29 proline-lysine sequence	Eli Lilly	1996 (USA and EU)
NovoRapid (insulin Aspart)	Recombinant short-acting human insulin analogue produced in *S. cerevisiae*	Engineered; B28 proline replaced by aspartic acid	Novo Nordisk	1999 (EU)
Levemir (insulin Detemir)	Recombinant long-acting human insulin analogue produced in *S. cerevisiae*	Engineered; devoid of B30 threonine and a C14 fatty acid is covalently attached to B29 lysine	Novo Nordisk	2004 (EU)
Apidra (insulin Glulisine)	Recombinant rapid-acting insulin analogue produced in *E. Coli*	Engineered; B28 proline replaced by lysine and B29 lysine replaced by glutamic acid	Aventis Pharmaceuticals	2004 (USA)
Lantus (insulin Glargine)	Recombinant long-acting human insulin analogue produced in *E. Coli*	Engineered; A21 asparagine replaced by glycine and B chain elongated by two arginines	Aventis Pharmaceuticals	2000 (USA and EU)
Tresiba (insulin Degludec)	Recombinant ultralong-acting human insulin analogue produced in *S. cerevisiae*	Engineered; devoid of B30 threonine and hexadecanoic diacid is attached to B29 lysine *via* a glutamyl linker	Novo Nordisk	2015 (USA)

Insulin has since been contextualised as the template of a number of hormone peptides that all share the same conserved disulfide pattern, including human relaxins (H2 and H3 relaxin), insulin-like growth factors (IGF I & II) and the various insulin-like peptides (INSL3-6).[23] It has been demonstrated that insulin and its analogues can activate the heterologous IGF receptor (a tyrosine kinase receptor like the insulin receptor) with the undesirable effect of enacting uncontrolled cell growth (carcinogenicity).[24-25] Maximising receptor specificity with regards to avoiding carcinogenic IGF-I cross-activation is thus of critical concern for the design of therapeutic insulins.

1.1.1 Insulin receptor binding and conformational change

Despite decades of research,[26] a complete understanding of how insulin binds and activates its receptor has not yet been realised. Though NMR and X-Ray crystallographic studies have revealed the structures of insulin, its derivatives and its receptor, a high-resolution structure of the bound insulin-receptor complex (holoreceptor) has not been obtained, ostensibly due to the receptor ectodomain's large size, flexible

morphology, many disulfide bonds and variable glycosylation.[27] Promisingly, recent Cryo-EM studies of the holoreceptor complex have for the first time furnished a complete picture of its exterior conformation.[28] However, the limited resolution achievable using these techniques prevents unequivocal identification of buried binding motifs. Crystallisation of human insulin bound to various combinations of insulin receptor domains furnished several observations pertinent to insulin binding. It has been previously established that two surfaces of insulin directly interact with the insulin receptor during binding,[29] regions that are also associated with dimer and hexamer formation.[30]

The insulin receptor (IR) is a disulfide-linked ($\alpha\beta_2$) tyrosine kinase. The α-subunits comprise the extracellular portion of the receptor (Figure 3). These units bind a single insulin molecule with high affinity. The α-subunits demonstrate negative cooperativity in that upon insulin binding to one α-subunit the binding affinity of the unoccupied site on the other α-subunit is significantly reduced. Isolated αβ receptor heterodimers demonstrate linear Scatchard plots and binding affinity somewhere between the high and low affinity states of full receptor $(\alpha\beta)_2$ heterotetramers.[31]

The primary insulin binding site (site 1*) is distributed across a pair of α-subunits, which may account for the aforementioned negative cooperativity. It is comprised of the central β-sheet (L1-β_2) of the first leucine-rich repeat domain (L1) of one α-subunit and the partially helical *C*-terminal segment (αCT) of the other α-subunit. Binding of the hormone confers a conformational shift, leading to downstream transphosphorylation of the β-subunits' intracellular tyrosine kinase (TK) domains and inducing insulin's biological effects.[32]

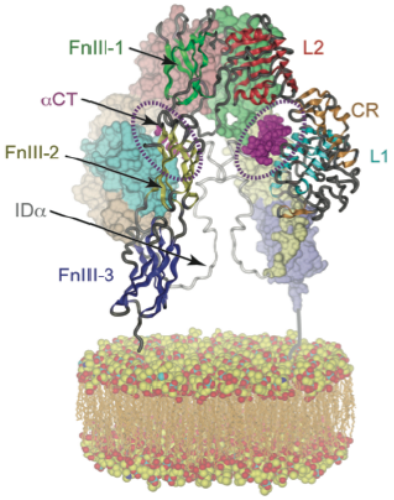

Figure 3 - Insulin receptor ectodomain $(\alpha\beta)_2$ homodimer with important binding subdomains labelled. Reproduced from Ward et al.[33] *with permission. Copyright 2013, John Wiley and Sons.*

The phenylalanine residue pair at B24-B25 has been identified as crucial for both receptor binding and dimerisation. The benzyl side chains of the pair alternately project inward towards the hydrophobic core of insulin (B24) and outward towards the solvation shell to participate in surface interactions (B25) (Figure 4). Phe B24, an invariant residue over insulin's evolution,[4] has been thought to stabilise the β-turn at residues B20-B23 in the *C*-terminus.[34] The β-strand comprised of Phe B24, Phe B25 and Tyr B26 forms an antiparallel β-sheet with that of another insulin molecule, stabilising the dimer form.[35]

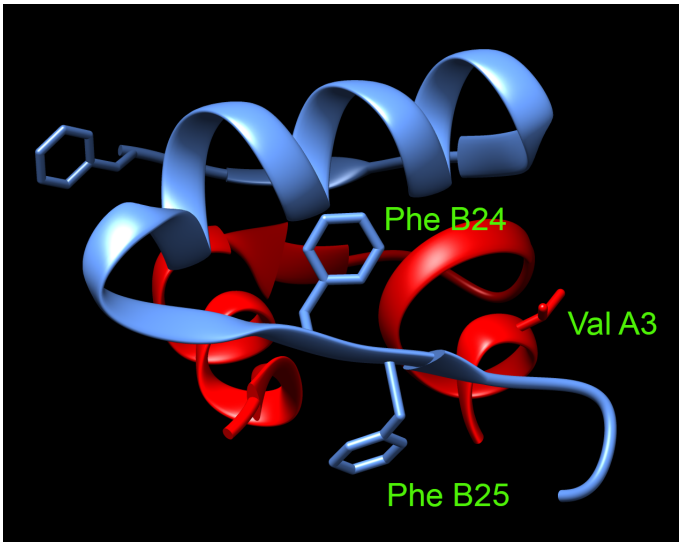

Figure 4 - Human insulin with invariant residues Phe B24, Phe B25 and Val A3 illustrated. Rendered by the author from the corresponding PDB data[36] using UCSF Chimera.[18]

Substitutions at B24 reveal disparate effects on receptor binding. Ser B24 (insulin Los Angeles) and Leu B24 both exhibit significantly diminished binding affinity (~10% affinity).[37-38] However, Gly B24 exhibits only modest-to-substantial loss of binding (22-78% affinity, two different studies)[35, 39] and chiral mutation to D-Phe at B24 improves binding (140-180% affinity, two different studies).[35, 39] Additionally, the D-Ala B24 mutant exhibits increased binding (150% affinity)[39], highlighting the importance of a hydrophobic residue side chain at this position. Based on these observations, Mirmira and Tager suggest that insulin undergoes a conformational change upon receptor binding.[39]

The most popular proposal for insulin's conformational change upon binding involves displacement of the *C*-terminal β-strand of the B-chain (Phe B24-Thr B30) from the hydrophobic helical core, exposing otherwise protected binding residues. The B-chain β-strand attracted further interest when clinical mutations within the region were associated with DM.[40] Photo-cross-linking studies have demonstrated that the β-strand and the core helix residues likely both engage with the receptor upon binding.[41]

2D-NMR studies conducted by Hua *et al*. suggested that the conformational change imbued by the aforementioned Gly B24 substitution was that of a largely disordered B-chain *C*-terminus segment, with residues B20-B30 losing well-defined tertiary structure yet retaining the conformation of the hydrophobic core.[42] The somewhat retained binding affinity of this analogue implies that the core is exposed to the receptor upon binding and that the B-chain *C*-terminus may not directly contact the primary active site of the insulin receptor.[35] This gives weight to the concept of the B-chain *C*-terminal strand playing an initial role in the conformational change undergone by insulin upon binding.

Phe B25 is far less tolerant of substitutions than its adjacent partner. The Leu B25 analogue (insulin Chicago) exhibits only ~2% binding affinity despite minimal disruption to insulin's global structure.[35, 43] The Ala B25 analogue exhibits 8-14% binding affinity with similar retention of global structure.[35] The Ser B25 analogue exhibits an even lower binding affinity (<1%) which may be the result of enhanced structural stabilisation arising from H-bonding between the serine hydroxyl group and the backbone carbonyl of Tyr A19, consequently limiting the conformational freedom required by this region of the peptide for binding.[35]

The full bioactivity of the Tyr B25 analogue[44] (present in a variety of non-mammalian species and IGF-I)[4] demonstrates the necessity of an aromatic residue at the B25 position. However, the inactivity of analogues with elongated and truncated aromatic residues at the B25 position demonstrate that the length of the side chain is absolutely crucial.[43, 45] This implies that Phe B25 either participates in binding directly at the insulin receptor active site or plays a role in directing the conformational change undergone by the B-chain *C*-terminal strand upon receptor approach.

Evidence for the exposure of insulin's hydrophobic core by the B-chain *C*-terminus may be gleaned from the earliest experiments directed towards semisynthesis of human insulin. Young and Carpenter observed that *des*-B23-B30 insulin (*des*-octapeptide-insulin, DOI), a product of trypsin digestion of insulin, possessed virtually no (<1%) bioactivity.[46] However, Katsoyannis *et al*. observed that full biological activity (in mouse convulsion assay) was exhibited by *des*-B28-B30 insulin, *des*-B27-30 insulin (*des*-tetrapeptide insulin, DTI) and *des*-B26-30 (*des*-pentapeptide insulin, DPI).[47-49] This highlights the redundancy of the B26-30 region in receptor binding, a region that normally shields the hydrophobic core of insulin. It may be inferred that these *C*-terminal residues are displaced upon binding.

A recent investigation by Menting *et al*. demonstrates a significant advance towards understanding the receptor binding-induced conformational change underpinning insulin's biological activity.[27] The work describes a 'microreceptor' (μIR) consisting of the L1-CR domain of the α-subunit (IR310.T) and exogenous αCT peptide 704-719.[27] Insulin's interaction with this abridged receptor complex defined a hinge mechanism whereby the B-chain *C*-terminus opens upon remodelling of the αCT between the nonpolar surfaces of L1 and the insulin A-chain. Insulin analogues have been synthesised to study this hinge moiety, including [B20 D-Ala, B23 D-Ala]-insulin and two incorporating (α,β)-dehydrophenylalanine (ΔPhe), [B24 ΔPhe]- and [B25 ΔPhe]-insulin. The study describes the first use of the latter amino acid substitution as a 'β-breaker', disrupting the *C*-terminal β-strand to probe possible induced fit during receptor binding.[32]

Structures of native insulin and analogues bound to the μIR and associated fragments were recently derived,[27] indicating that hormone binding is principally mediated by αCT (receptor residues 711-714). Contrary to expectations, binding of insulin residues to L1 was limited to certain B-chain residues only. Upon insulin binding, αCT was shown to

remodel itself on the L1- β_2 surface, its helix extending at the *C*-terminus to residues 711-714. The positions of residues beyond B21 were not defined in the determined structures, yet the *C*-terminus detachment model was nonetheless supported by the αCT translocating to a region that would otherwise be occupied by insulin B-chain residues B25-B30 had the strand remained static (Figure 5).[27]

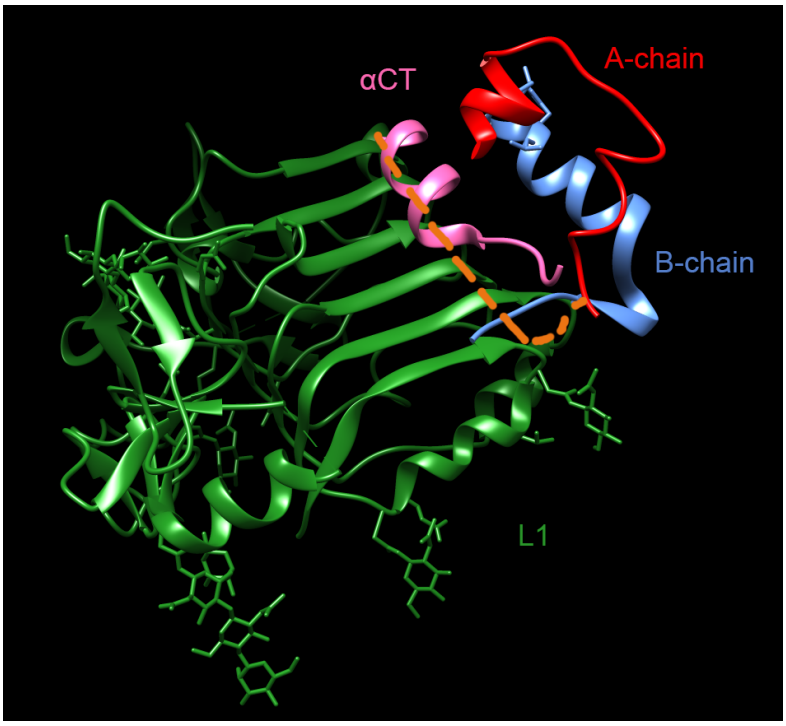

Figure 5 - Human insulin bound to μIR. B-chain residues in blue originally resolved in crystal structure, residues in orange illustrate the typical region occupied by B-chain C-terminus in unbound insulin. Note clash of αCT with B-chain. Rendered by the author from the corresponding PDB data[32] using UCSF Chimera.[18]

In crystal structures of the μIR, the B-chain *C*-terminal region comprised of residues B22-B30 was marked by apparent disorder. To determine whether this was an artefact of receptor truncation or technical or mechanical handling, alanine substitutions were made at Phe B24, Phe B25 and Tyr B26 and the result assessed for similarities to complete holoreceptor binding. Stabilities of the μIR complex correlated well with the affinity of the analogues for the full receptor. The data imply that residues B24-B26 make similar contributions to the binding of insulin to the μIR and full receptor.[32]

The benzyl side chain of Phe B24 was shown to be nestled within a hydrophobic pocket comprised of Val B12, Leu B15, Tyr B16 and Cys B19 as well as receptor residues Asn15, Leu37, Phe39 and Phe714 (Figure 6A). Cys B19 was linked to Phe B24 by continuous density *via* a type 1 β-turn with positive Φ-angles at Gly B20 and Gly B23, similar to native insulin. The B20-B23 β-turn does not directly interact with the μIR. Phe B25 is less resolved in this structure than Phe B24. It resides between αCT residues Val715 and Pro718, projecting away from L1-β_2 region (Figure 6B).[32]

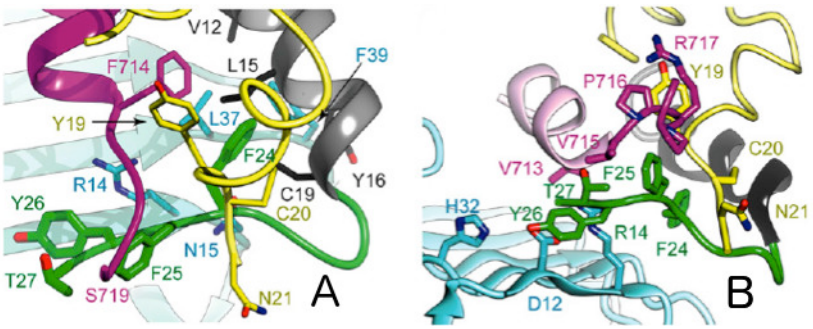

Figure 6 - Environment of Phe B24 (F24) (A) and residues B25-B27 (B) in the insulin-bound μIR complex, Black –B-chain residues 7-19, Green – B-chain residues 20-27, Yellow - A-chain, Magenta/Pink - αCT segment, Cyan - L1 domain. Reproduced from Menting et al.[32] *with permission.*

The work of Menting and coworkers is a substantial leap forward in our understanding of insulin receptor binding and activation. The long suspected conformational change undergone by the B-chain *C*-terminal region of insulin is confirmed and structurally elucidated in receptor fragments. However, the effects of this displacement on distal structural elements of insulin, such as the invariant A-chain *N*-terminal region and the conserved disulfide bridges are yet to be examined in detail. These questions formed the basis of the work undertaken in this thesis.

1.1.2 The role of insulin's disulfide bridges in binding and receptor activation

Owing to the conserved nature of insulin's disulfide bridges,[2, 11, 50] the role that they play in insulin's binding and receptor activation is of considerable interest to structural

biologists and peptide chemists.[51] Though the studies of Menting *et al*. have elucidated an important aspect of insulin binding and activation in terms of a backbone conformational switch, the influence of insulin's disulfides on binding are not given explicit treatment in their investigation.

It has been shown in substitution studies that all three disulfides are crucial for insulin's structural integrity and consequent biological activity.[51-52] Chiral mutations of each constituting cysteine residue have also shown that correctly oriented bridges are integral components of the active insulin species.[53] It has been proposed that at least one of insulin's disulfides undergoes a thiol/disulfide interaction with its receptor upon binding.[54] However, studies involving an insulin dicarba analogue whereby the most likely disulfide for this interaction (A7-B7) is replaced with a saturated carbon linkage suggested that this is not the case as this analogue was a functional insulin, albeit with reduced binding affinity and biological activity.[55]

Insulin's disulfide bridges have additionally been shown to remain covalently bonded during insulin's conversion to amyloid fibrils.[56] Substitution studies whereby each bridging cysteine pair is replaced with glycine residues demonstrate that the presence of the disulfides has a significant impact on insulin's tendency to form amyloid fibrils.[57] For example, substitution of A6-A11 resulted in the greatest degree of oligomerisation and consequent cytotoxicity, though substitution of the A7-B7 interchain disulfide demonstrated the greatest increase in overall amyloidogenicity.[57] The design and synthesis of analogues intended to mitigate the insulin scaffold's tendency towards amyloid formation must thus take into account the importance of the disulfide motif.

The displaced β-strand of the B-chain, principally comprised of residues B24-B30, are not far removed (ca. 5 residues) from insulin's A20-B19 interchain disulfide and could conceivably influence the A-chain conformation *via* displacement-induced strain

conveyed through the disulfide network. In addition, 'hot spot' residues Gly A1, Ile A2, Val A3 adjacent to the A6-A11 intrachain disulfide, Tyr A19 adjacent to Cys A20 and Gly B8 adjacent to Cys B7 make contact with key αCT residues upon binding, which may suggest that the conformation of the nearby disulfides are influenced. This would indicate a potential allosteric capacity for insulin's disulfides, traditionally considered to confer little more than structural stability, and thus an underexplored site for modification and probing.

1.2 Disulfide bridges – their role in peptide function and their modification

1.2.1 Allosteric disulfide bridges

The stabilising effect of the disulfide bridge has long been attributed to the physical impediment to unfolding provided by the bridge. However, calculations performed by Schulz and Schirmer in the late 1970s[58] suggest that the stabilising effect is more likely attributable to the formation of crosslinks in the *unfolded* state, reducing the magnitude of entropy gained by unfolding and thus making the native folded state relatively more favourable than in the absence of disulfides.[59] However, the strained nature of many disulfide linkages appears to counter their apparent contribution to stability.[60] This implies that disulfides have evolved to fulfil roles more complex than simple provision of structural stability.

Peptidic disulfide linkages have traditionally been classified as either structural or functional motifs. These classes are strictly defined as covalently stabilising the peptide's secondary and tertiary structures or participating in redox transformations, respectively. In the past decade, roles for disulfide bridges falling outside these definitions have been postulated. Schmidt *et al*. describe a new taxonomy for the classification of disulfide bridges that includes a third class, the 'allosteric disulfide'.[61] Rather than passively reinforcing structure or participating in chemical transduction, the allosteric disulfide

motif enacts biological function by relaying a conformational change within the peptide's tertiary structure upon redox transformation, often effected by a catalytic disulfide (Figure 7).

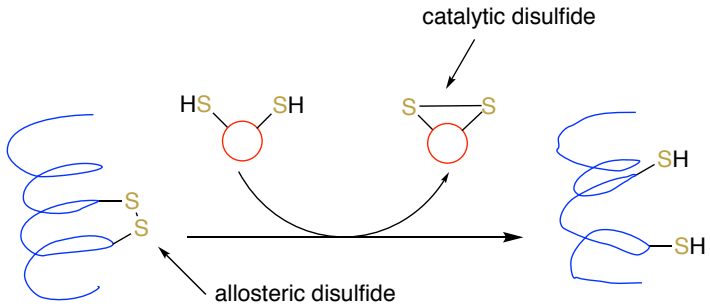

Figure 7 - Allosteric disulfide facilitating conformational change by undergoing reduction by a catalytic disulfide. Adapted from Wong and Hogg.[62]

The work of Schmidt *et al.*[61] approaches the classification of peptidic disulfides in terms of experimentally determined dihedral angles and subsequently calculated potential energy. A computer survey of the Protein Data Bank (PDB) elucidated structural commonalities between disulfide-containing proteins correlating with their suspected biological mechanism.

Structurally reinforcing disulfides were largely found to possess the -LHspiral topology (Figure 8) and the lowest average dihedral strain energy (DSE) of the disulfides surveyed (10.1 kJ mol^{-1}) compared to peptidic disulfides as a species in general (14.8 kJ mol^{-1}). This may be expected as greater DSE directly correlates with greater likelihood of catalytic functionality. Consequently, most peptidic disulfides with a known catalytic redox functionality were found to possess the +/-RHhook topology (Figure 8) with a higher average DSE of 20.8 kJ mol^{-1}.[61]

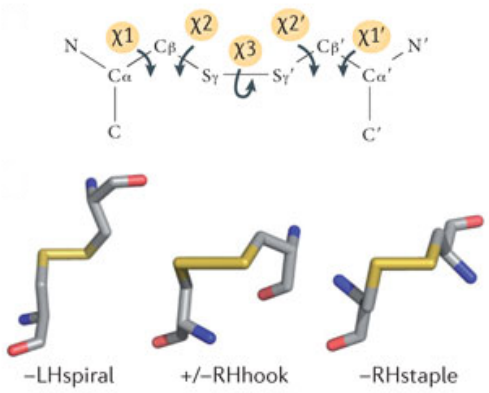

Figure 8 - Classes of allosteric disulfide bonds. Reproduced from Hogg[63] with permission. Copyright 2013, Nature Publishing Group.

The –RHstaple group (Figure 8) was found to contain all known or suspected allosteric disulfides. Their above-average DSE (18.1 kJ mol^{-1}) is consistent with their functional behaviour, though this is lower than that of the +/-RHhook topology associated with traditional redox/catalytic functionality.[61]

Classification of insulin's three disulfide bonds within this taxonomy may be useful for elucidating their respective roles in receptor activation. Given that evidence for the catalytic capacity of insulin's disulfides is limited[54-55] and that the peptide is sensitive to small changes in disulfide orientation,[53] it is tempting to classify at least one of its disulfide bridges as possessing allosteric functionality.

If insulin's disulfides are likely to undergo allosteric rearrangement *via* a redox interaction, the catalytic 'trigger' is likely to arise from interaction with the cysteine-rich (CR) domain of the insulin receptor. The abundance of cysteine residues in this region provide ample opportunities for disulfide exchange. However, Menting *et al.*'s model of binding shows that insulin primarily interacts with the αCT and L1 domain whilst remaining distal to the CR domain.[27] This observation precludes a CR domain redox-modulated allosteric switch and suggests that the allostery of insulin's disulfide

bridges may involve conformational alteration *via* perturbation of insulin's backbone structure and not a redox transformation.

Evaluation of conformational changes undergone by insulin may be accomplished *via* systematic replacement of the native cystine with isosteres of altered geometry. If insulin's disulfide bridges are expected to play a structural role and relay conformational change without undergoing a redox interaction, the use of dicarba bridges in this capacity is attractive due to the latter's tuneable geometry (i.e. *via* hybridisation) and non-reducibility *in vivo/in vitro*.

1.2.2 Disulfide replacement

The relative lability of the disulfide bond in physiological media has lead to the investigation of non-reducible analogues whereby the disulfide moiety is replaced with a more robust, biologically-equivalent linkage (a 'bioisostere'). Moieties used in place of the disulfide include amides,[64-65] esters,[66] diselenides,[67] thioethers[68] and triazoles (Figure 9).[69] Carbon-carbon bonds ('dicarba bridges') have received increasing attention in disulfide replacement due to their chemical robustness, highly isosteric nature, variable hybridisation and geometry (sp, sp^2, sp^3) and diverse and often challenging routes of synthesis.[70]

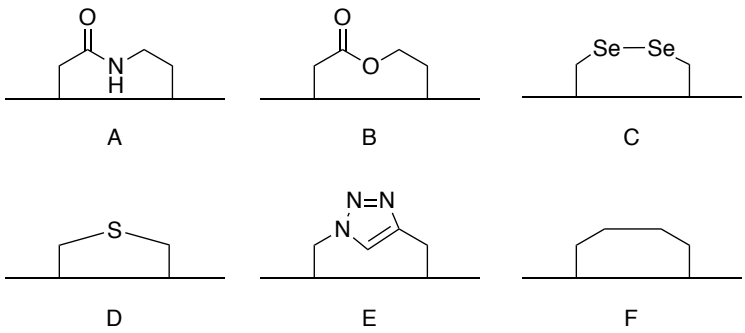

Figure 9 - Disulfide bridge replacements: A – amide bridge; B – ester bridge; C - diselenide bridge; D – thioether bridge; E – triazole bridge; F – dicarba bridge.

Among the first dicarba analogues were the saturated dicarba-oxytocins synthesised by Jost *et al.* in 1973,[71] followed by Keller and Rudinger in 1974.[72] These were followed by Veber's somatostatin analogue in 1976.[73] These analogues were synthesised *via* incorporation of a 2,7-diaminosuberic acid (DAS) residue in place of their native cysteine bridge. Synthetic incorporation of DAS and its homologues remained *de rigeur* for the generation of dicarba peptides for the following twenty years and remains a viable strategy in the synthesis of complex dicarba peptidomimetics.[74]

The advent of olefin metathesis in the early 1990s[75] heralded new approaches to the synthesis of dicarba analogues. The exceptional functional group tolerance of Grubbs' ruthenium alkylidene metathesis catalyst (Figure 10, 2nd Generation species shown) made it a promising candidate for use on peptidic substrates.[76] Early efforts towards metathesis-enabled dicarba bridge formation focused on the synthesis of 2,7-diaminosuberic acid derivatives. Preliminary investigations by Miller and Grubbs demonstrated that ring-closing olefin metathesis (RCM) could be successfully employed in the synthesis of protected amino acid derivatives and small analogues of disulfide-containing peptides.[77] This methodology was extended the following year to include larger ring sizes and solid-supported ('on-resin') synthesis.[78] Further to this, Grubbs and Blackwell later demonstrated that dicarba 'staples' could be used to stabilise α-helixes,[79] a paradigm soon elaborated upon by Verdine *et al*.[80]

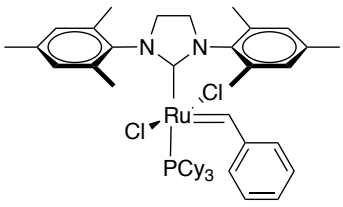

Figure 10 - Grubbs' 2nd Generation Catalyst ('GII'), a ruthenium-alkylidene metathesis catalyst commonly employed in on-resin RCM.

The first synthesis of a biologically active dicarba analogue *via* RCM was that of dicarba-oxytocin reported by Vederas *et al*. in 2003.[81] On-resin RCM was accomplished between two L-allylglycine residues substituted for the native cysteines, affording the *cis*- and *trans*-alkenyl macrocycles. These species were subsequently deprotected, cleaved from the support and reduced to the saturated species by H_2 and Pd/C (Scheme 1).

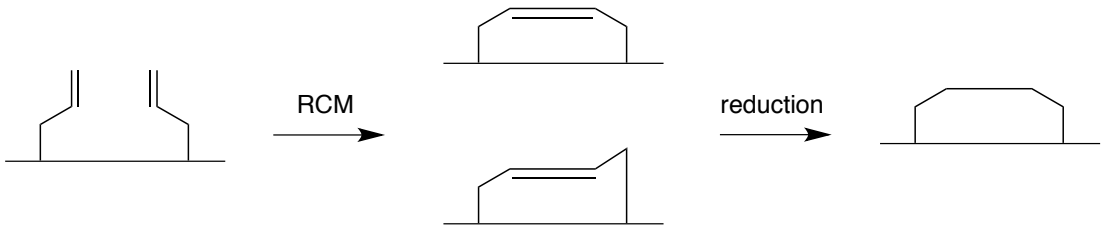

Scheme 1 - General schematic for dicarba bridge formation via RCM and reduction to give the saturated DAS moiety.

Intriguingly, it was observed that the *cis* intermediate demonstrated significantly greater biological activity (EC_{50} = 38 ng/mL) than either the equivalent *trans* species (EC_{50} = 242 ng/mL) or the fully saturated analogue (EC_{50} = 338 ng/mL). Though the *cis* analogue displayed a 14-fold reduction in potency with respect to the native peptide (EC_{50} = 2.7 ng/mL), these results demonstrated that unsaturated dicarba-analogues are potentially useful tools for the elucidation of native disulfide bond conformation and its relation to biological activity.

1.3 Project Background

The Robinson Group has a strong background in the development of catalytic methodologies applicable to peptide synthesis.[82-96] In the course of exploring the applicability of metathesis for the synthesis of various dicarba peptidomimetics, van Lierop and Robinson synthesised insulin analogues whereby the A6-A11 disulfide is replaced by an unsaturated diaminosuberic acid moiety.[91, 95, 97] Due to the non-selective

nature of the olefin metathesis catalyst employed, *E*- and *Z*-isomers were obtained. These isomers were separately combined with the native B-chain to give a complete, two chain analogue (Figure 11, *Z*-isomer shown).

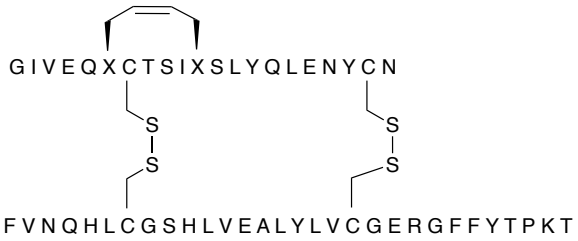

Figure 11 - (L,L)-[Z-Δ⁴A6-A11-dicarba]-insulin, synthesised by van Lierop and Robinson.

Competition binding studies (Eu-labelled insulin displacement within immunocaptured IR-B) of the [A6-A11]-dicarba insulin isomers, conducted by Prof. Briony Forbes (Flinders Medical Centre, Flinders University, Adelaide), revealed that the earlier eluting isomer ('Isomer I') possessed a binding affinity almost identical to that of native human insulin. Conversely and intriguingly, the later eluting isomer ('Isomer II') exhibited affinity diminished by more than two orders of magnitude (Figure 12). Similar results were obtained for [A6-A11]-dicarba DKP-insulin. Encouragingly, these disparate activities were mirrored in insulin receptor activation assays measuring IR-B phosphorylation.[95, 97] An extended synthetic-analytical investigation later revealed that the bioactive species (Isomer I, Figure 11) possessed the *Z*-geometry and the inactive species (Isomer II) possessed the *E*-geometry.[95]

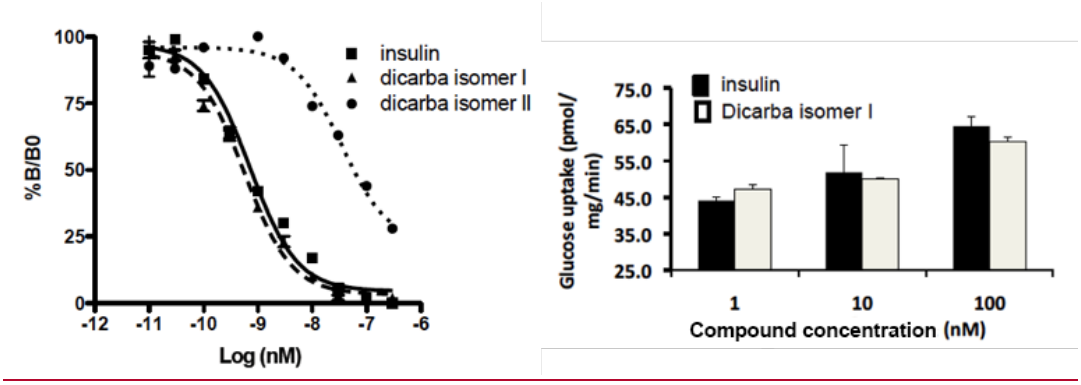

Figure 12 - Binding affinity (left) and regulation of glucose uptake (right) of dicarba insulin analogue(s) compared to native human insulin. Courtesy of Forbes.

In light of these results, it was suggested by van Lierop and Robinson that the A6-A11 disulfide may play a role in structural activation of the otherwise dormant, circulating native insulin. Later circular dichroism (CD) studies conducted by Forbes demonstrated that, whilst the inactive *E*-isomer exhibited some loss of helical content compared to native insulin, the active *Z*-isomer displayed notably more loss. This was the basis for the hypothesis that the A6-A11 enacts its allosteric function by modulating the ordering of the A-chain *N*-terminal helix (residues A1-A5). Indeed, substitution of the A6-A11 bridge with a pair of serine residues has been shown to result in segmental unfolding of the *N*-terminus.[98]

Residues A1-A8 are thought to contact the binding surface of the IR and residues A1-A3 are highly conserved.[1] Mutations in this region are very poorly tolerated, with even minor stereochemical inversions at branched sidechains resulting in severe loss of activity. For example, inversion of the Cβ stereocentre of Ile A2 (to L-alloisoleucine) in DKP insulin resulted in a loss of activity by a factor of 50.[99] Gly A1 appears to tolerate mutation better than the subsequent two residues, although still associated with activity loss in almost all known instances. Omission of Gly A1 in sheep insulin gave an insulin with activity equal to 35% of that of the native species,[100] whilst replacement with β-alanine halved potency.[101] An interesting exception to this trend is the substitution of Gly A1 to D-

alanine (but not L-alanine), furnishing an analogue with almost full activity with respect to native human insulin.[102] This observation was reinforced by evaluation of additional D-amino acid-substitutions at Gly A1, with similar results.[103]

Ile A2 and Val A3 are the least tolerant of mutation amongst the A-chain *N*-terminal residues. As well as the aforementioned C_β chiral inversion,[99] mutation of Ile A2 to glycine, alanine, norleucine and several other amino acids gave analogues with receptor binding affinities of less than 5% of that of the native.[104] Insulin Wakayama, an analogue whereby Val A3 is mutated to leucine, demonstrates a 100-fold loss in binding affinity and a similarly drastic impaired glucose uptake stimulation.[105] The highly conserved nature of these residues plus the generally deleterious impact of their mutation suggests that the A-chain *N*-terminus is a crucial binding motif in all insulins. By extension, modulation of these residues' sidechains by shifts in insulin's secondary and tertiary structure may thus control insulin receptor binding, activation and receptor-mediated clearance.

An X-ray crystal structure of the unbound, active *cis*-dicarba insulin reveals that residues A1-A10 are disordered, with no structural definition of the A-chain *N*-terminal secondary structure evident (Figure 13, right).[95]

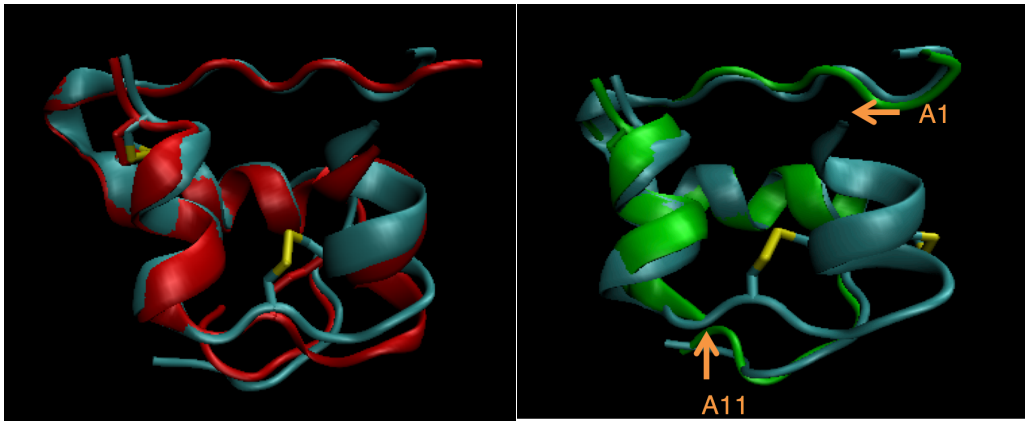

*Figure 13 - X-ray crystal structures of (Δ⁴A6-A11)-dicarba insulin. **Blue** – Native human insulin; Red – Inactive isomer of (Δ⁴A6-A11)-dicarba insulin 6; Green – Active isomer of (Δ⁴A6-A11)-dicarba insulin 6 sans residues A1-A11 (as indicated by arrows).*

This partial 'unwinding' of helix, giving rise to said disorder, results in rotation of the *N*-terminal residues side chains and prevents steric clash with residues within the receptor binding site.[95] These results and subsequent hypotheses provide insight into the role of insulin's disulfide bridges, previously thought to be exclusively structural, in receptor binding and activation.

1.4 Scope of Work

The [A6-A11]-dicarba insulins developed by van Lierop *et al*. provide an intriguing starting point for modification of the A6-A11 linkage. The disorder of the *cis*-[A6-A11]-dicarba insulin A-chain's *N*-terminus in conjunction with the peptide's near-native bioactivity suggests a link between the conformational restraint incurred at the A6-A11 bridge and the modulation of the crucial *N*-terminal binding motif. It is thus of interest to see what indirect modification of the *N*-terminal region through variation of A6-A11 bridge conformation, as opposed to direct mutation of its highly conserved residues, may reveal about insulin's structure-activity relationship. In this way, the A6-A11 may be viewed as a possible 'control handle' or even 'on-off switch' for insulin's binding and bioactivity.

To further probe the A6-A11 disulfide linkage's role as a control handle for insulin, it was envisioned that a number of dicarba derivatives could be synthesised and evaluated for their biological function. These targets varied in synthetic complexity, ranging from a synthesis on par with that of van Lierop's A6-A11 dicarba analogues, to an interchain target requiring significant challenges in chain assembly and metathesis to be overcome with novel strategies. These variations on the dicarba insulin theme are described in subsequent chapters.

2 Variation of C_α stereochemistry (chiral mutation) of the A6-A11 dicarba bridge and its effects on insulin receptor binding

2.1 Overview

Chiral mutagenesis of insulin has not been extensively investigated in the literature, with the notable exception of an *allo*-Ile A2 analogue of DKP insulin synthesised by Xu *et al.* whereby the C_β stereocentre of the native Ile A2 is inverted, giving the *allo*-form.[99] Intriguingly, though native folding and stability were retained by the analogue, it demonstrated a 50-fold loss in binding affinity. It was thus inferred that the A-chain *N*-terminal helix binds within a chirally-sensitive pocket within the IR, exceptionally intolerant of even minor steric variation. This is reinforced by the ubiquitous conservation of these residues across all vertebrate species.[4]

Chiral mutations at the A6 and A11 positions of human insulin have been previously investigated by Sieber *et al.*.[53, 106-107] Substituting the native L-configured cysteine residues with the D-enantiomer during synthesis markedly decreases binding affinity. When A6 was D-Cys substituted, the analogue exhibited a 1.5-fold loss in binding affinity (anti-insulin serum binding) compared with the native species. The same substitutions at A11 and both A6 and A11 (A6+A11) lead to diminished binding by factors of 10 and 14, respectively. Furthermore, an assay of *in vitro* biological activity, glucose oxidation in rat fat cells, revealed 433-, 137- and 3760-fold decreases in potency for the antipodal A6, A11 and A6+A11 analogues, respectively. It was noted by the authors that the very small degree of activity displayed by these analogues may have arisen from trace quantities of insulin present in the samples due to incomplete purification.

These early investigations not only highlight the importance of the A6-A11 disulfide bridge for insulin binding and activity but also demonstrate that modifications to these

moieties result in disparate actions on both. Activity is substantially diminished where binding is relatively less affected. This may be seen as an indication of the crucial role that the A6-A11 bridge plays in the mechanics of insulin conformational change upon binding.

Inspired by these observations, synthesis and biological assay of chiral mutants of [Δ^4A6-A11]-dicarba insulin was embarked upon. The rationale behind this investigation was two-fold:

- To determine the synergistic effects of unnatural stereochemistry, in conjunction with dicarba replacement of the native cystine, on overall insulin structure and function.
- To develop synthetic and analytical skills pertinent to peptide chemistry, crucial for the remainder of candidature.

Work towards the synthesis and characterisation of six D-Cys-analogues of [Δ^4A6-A11]-dicarba insulin was thus carried out.

2.2 Results and Discussion

The first synthetic outcome was the synthesis of Fmoc-D-allylglycine **1** in sufficient quantity for subsequent peptide synthesis. Enzymatic resolution of the racemate was employed as the synthetic route to the D-enantiomer due to relative ease of handling and expediency. Commercially available racemic *N*-acetyl D,L-allylglycine **2** underwent stereoselective deacetylation by acylase I (*Aspergillus melleus*) liberating L-allylglycine as the free amine whilst retaining D-allyglycine as its *N*-acetylated derivative **3**. The *N*-acetyl D-allylglycine **3** was subsequently isolated through organic extraction (64% brsm) and deacetylated to give the amino acid salt **4**. The final protected amino acid **1** was obtained after Fmoc-protection in approx. 54% yield over three steps with 92% ee,

determined by comparison with the opposite enantiomer and the racemate by chiral HPLC (Scheme 2).

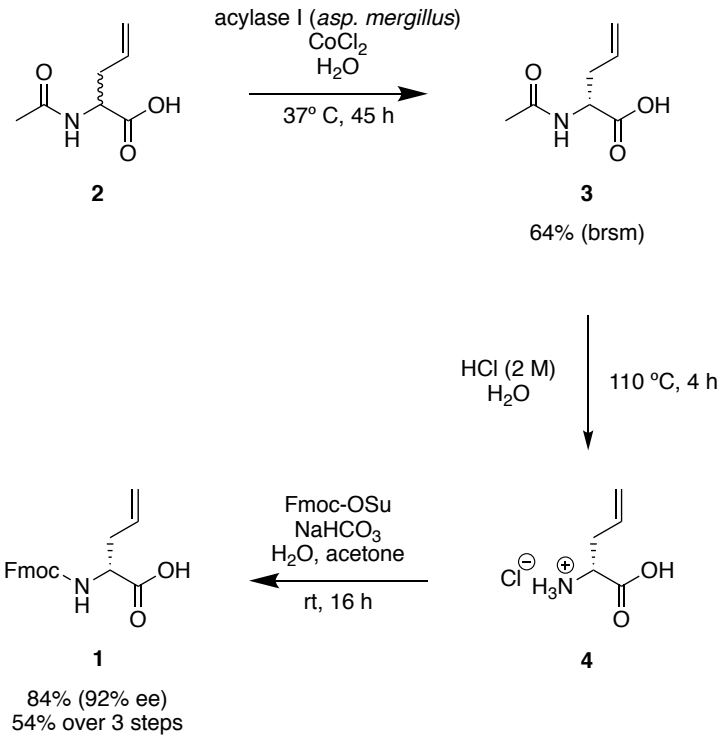

*Scheme 2 - Synthesis of Fmoc-D-allylglycine **1**.*

Automated and manual solid phase peptide synthesis (SPPS) methods were employed to synthesise *des*$_{A1\text{-}5}$-[A6-A11]-D-Agl-[A7]-Cys(^{t}Bu)-[A20]-Cys(Acm) human insulin A-chain **5** (Figure 14). The *N*-terminal residue (in this case D-Agl) was attached using manual SPPS and the hydrophobic *N*-terminal resides A1 to A5 were omitted to facilitate subsequent ring-closing metathesis (RCM).[90]

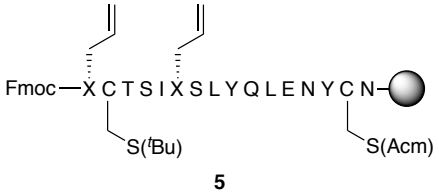

*Figure 14 - des**A1-5-[A6-A11]-D-Agl-human insulin A-chain **5**.*

The resin-bound peptide was treated with acetic anhydride solution to sequester any trace amine functionality as the acetamide. This was done to prevent any adverse coordination of peptidyl amines to the catalyst, which would diminish metathesis yield. Additionally, the resin was dried in a vacuum desiccator to remove traces of water for similar reasons. Ring-closing metathesis was carried out on-resin with Grubbs' 2nd Generation metathesis catalyst,[108] a chaotropic salt (LiCl) and microwave heating in an inert atmosphere (N_2), giving the desired cyclic species **6** as a pair of geometric isomers (Scheme 3). Chaotropic salts are often employed to disrupt aggregation and improve metathesis yield and form part of a standard on-resin protocol.[109] Small-scale cleavage and subsequent RP-HPLC analysis showed complete conversion to a pair of separable geometric isomers.

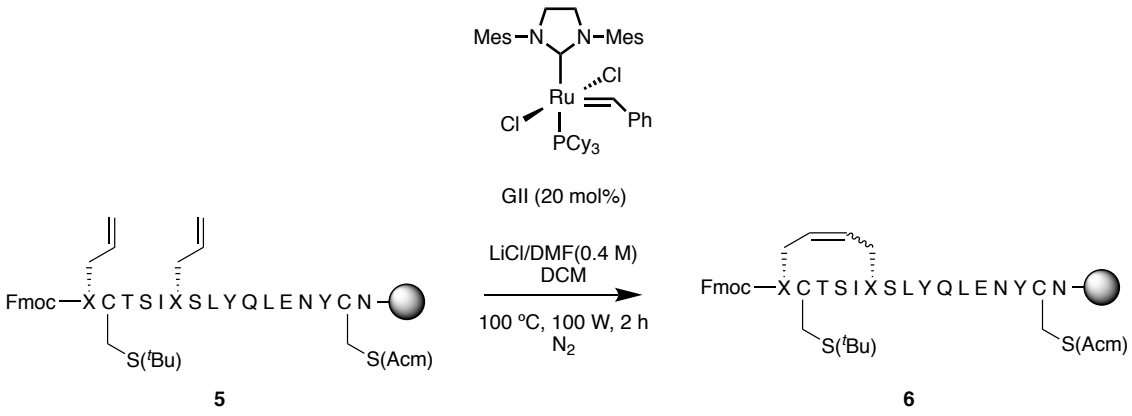

*Scheme 3 - RCM of insulin A-chain fragment **5**.*

The remaining residues (A1-A5) were coupled to the cyclic fragment using automated SPPS to give a complete, Cys-protected insulin A-chain analogue **7** that was subsequently cleaved from the resin (Scheme 4).

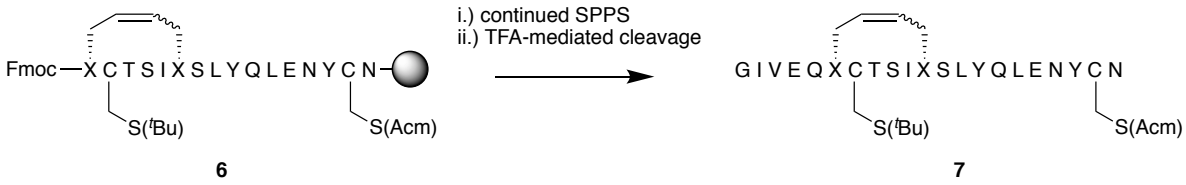

*Scheme 4 - Synthesis of complete, Cys-protected A-chain analogue **7** from cyclised resin-bound fragment **6**.*

Concerted removal of the A7 Cys(^{t}Bu) *tert*-butyl protecting group and reprotection as the *S*-pyridyl-disulfide (SPyr) was accomplished according to a procedure described by Büllesbach *et al.*[110] giving **8** (Scheme 5). The SPyr group was employed as an effective leaving group for subsequent attack by the free B7 cysteine thiol in downstream chain combination. The *E*- and *Z*-isomers of **8** were separated using preparative RP-HPLC to give separate conformers for prospective biological testing upon completion of the analogues, as discussed in Section 2.3.4.

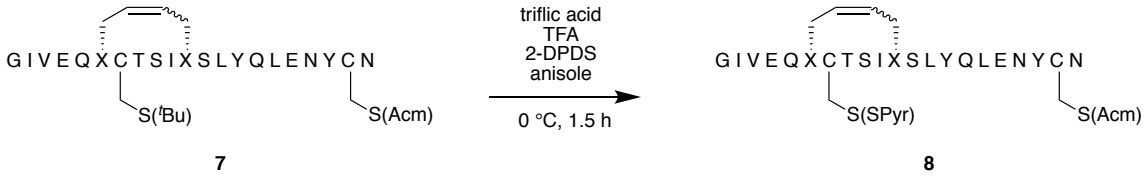

*Scheme 5 - Concerted removal of tert-butyl protecting group of **7** and reprotection as the S-pyridyl-disulfide (SPyr) **8**.*

Following separation, one isomer of the *S*-pyridyl A-chain **8** ('**8(I)**') was dissolved in an aqueous NH_4HCO_3 solution (50 mM), to which a half-equivalent (by mass) of [B19]-Cys(Acm) human insulin B-chain **9** was added (Scheme 6). The reaction progress was monitored by RP-HPLC. The actual peptide content of the *S*-pyridyl A-chain **8(I)** sample was shown to be much less than the sample's mass would suggest, as indicated by the presence of excess B-chain upon completion of the reaction. Upon reaction completion (ascertained by RP-HPLC), the reaction mixture was quenched and lyophilised to give the crude, monocyclic species **10(I)**.

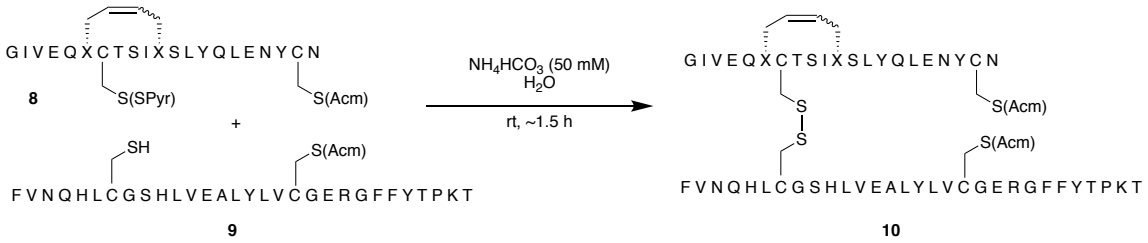

Scheme 6 - A-chain and B-chain combination.

The crude peptide **10(I)** was then subjected to an iodine oxidation procedure described by Lin *et al.*[111] (Scheme 7). Immediate purification by preparatory RP-HPLC followed precipitation of the crude peptide to give the target (D,D)-configured insulin analogues **11(I)** (after lyophilisation). Formation of **11(I)** was confirmed by analytical RP-HPLC and low-resolution mass spectrometry in the positive mode (electrospray) and the peptide subsequently purified by preparative scale RP-HPLC. The procedure was then repeated with the complementary A-chain isomer **8(II)** to give the complete target A-chain isomer and later the second isomeric target (D,D)-configured insulin **11(II)**.

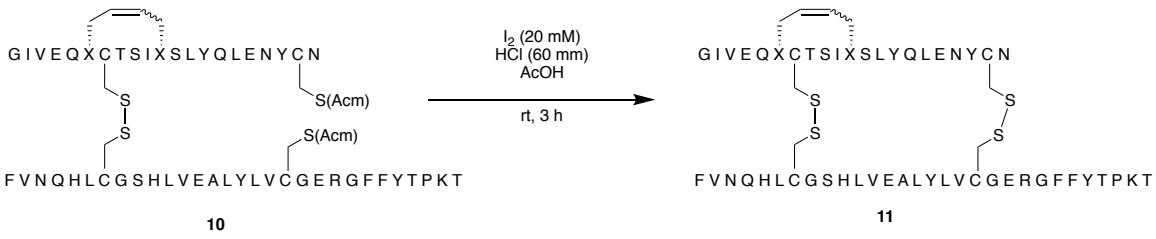

*Scheme 7 - Iodine oxidation of monocyclic insulin analogue precursor **10**.*

The (L,D)-configured dicarba analogues **12** (isomers I and II) (Figure 15) were prepared using procedures identical to those described for the (D,D) analogues (Schemes 3-7). The described methodology was also employed to synthesise the *cis*- and *trans*-(D,L) analogues **13** (isomers I and II) (Figure 15), proceeding successfully until the final iodine oxidation, which failed for both isomers despite multiple attempts. Consequently, these analogues could not be submitted for biological evaluation.

*Figure 15 - (L,D)-**12** and (D,L)-**13** configured insulin analogues.*

It was inferred that the inverted stereochemistry at the A6 C_α, in conjunction with native stereochemistry at A11, induced sufficient distortion of secondary structure to prevent formation of the bridge. Curiously, analysis of RP-HPLC fractions from the reaction mixture by mass spectrometry showed unreacted starting material, retaining the acetamidomethyl (Acm) protecting group. This was unexpected, as complete removal of this group in the highly oxidising reaction conditions was anticipated. Each reaction attempt employed freshly prepared iodine solutions. Hence, lack of reactivity of the precursors to isomers **13(I)** and **13(II)** is likely to be due to deleterious peptide conformation preventing site access and/or oxidative ring closure.

With four of the six desired chiral mutants in hand, samples of each peptide were submitted to the laboratory of Assoc. Prof. Briony Forbes (Flinders University) for biological assay (Figure 16).

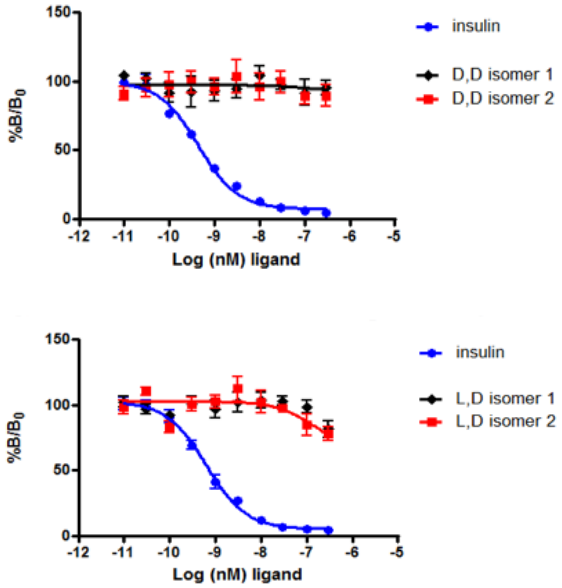

*Figure 16 – Results of binding assays conducted with (D,D)-configured dicarba insulin isomers **11** (left) and (L,D)-configured dicarba insulin isomers **12** (right). Courtesy of Forbes.*

Binding studies (Eu-labelled insulin displacement within immunocaptured IR-B) indicated negligible binding for all of the chiral mutants synthesised. A minor binding trend was observed of the L, D-configured analogues (Figure 16, lower), although this was still three orders of magnitude lower than that expressed by native insulin and only at the high extreme of the dosage concentration curve. Intriguingly, both geometric isomers of the L, D analogue displayed highly congruous if subtle binding, unlike the disparate activity of the L, L-configured analogues. This finding reflected the earlier results obtained by Sieber *et al.*[107] for chiral mutations of native insulin at the A6 and A11 positions. The comparable activity of the *cis* and *trans* isomers of each was unexpected and not consistent with observations of previously synthesised dicarba insulins.[95, 97] Structural identification of each geometric isomer (i.e. isomer I and II of **11** and **12**) can be achieved through NMR studies,[94] but as there was no distinction in activity between the chiral mutants this was not pursued. In light of this observation, further attempts at synthesis of the (D,L) analogues **13** were abandoned.

Synthesis and evaluation of these analogues demonstrated that retention of native stereochemistry at the C_α position of residue A11 is vital for bioactivity, regardless of the geometric connectivity at C_γ. Furthermore, the inability of the A6-A11-dicarba chiral mutants to bind reflects the exquisite sensitivity of the bridge to modification and reveals the dicarba bridge's inability to override this stereochemical preference. In the mutants where the constituent cysteines are replaced with serine,[98] the *trans*-dicarba analogue, native Cys-chiral mutants[53, 106-107] and the species described above, insulin receptor binding affinity is severely affected. This highlights how remarkable the activity of the L,L-configured *cis*-dicarba analogue (see Section 1.3) is within the canon of insulin's structural modification.[95, 97]

This investigation enabled the development of skills crucial to the execution of the work detailed in the following two chapters, principally peptide synthesis, homogeneous catalysis and analysis by high-performance liquid chromatography.

2.3 Experimental

2.3.1 Instrumentation

Proton nuclear magnetic resonance (^{1}H NMR) spectra were recorded on Bruker AVANCE I 300, AVANCE III 400 or AVANCE III 600 spectrometers operating at 300, 400 or 600 MHz respectively, as solutions in deuterated solvents as specified. Each resonance was assigned according to the following convention: Chemical shift; multiplicity; observed coupling constants (J = Hz) and number of protons. Chemical shifts (δ), measured in parts per million (ppm), are reported relative to the residual proton peak in the solvent used as specified. Multiplicities are denoted as singlet (s), doublet (d), triplet (t), multiplet (m) or prefixed broad (b), or a combination where necessary.

Carbon-13 nuclear magnetic resonance (^{13}C NMR) spectra were recorded on Bruker AVANCE I 300, AVANCE III 400 or AVANCE III 600 spectrometers operating at 75, 100 or 150 MHz respectively, as solutions in deuterated solvents as specified. Chemical shifts (δ), measured in parts per million (ppm), are reported relative to the residual proton peak in the solvent used as specified.

Low-resolution electrospray ionisation (ESI) mass spectra (LRMS) were recorded using either an Agilent ZQ instrument or a Micromass ZMD instrument as solutions in specified solvents. Spectra were recorded in the positive mode (ESI^+). High-resolution electrospray ionisation (ESI) mass spectra (HRMS) were recorded using an Agilent ESI-TOF instrument as solutions in specified solvents. Spectra were recorded in the positive mode (ESI^+) or negative mode (ESI^-).

Analytical thin layer chromatography (TLC) was performed on either plastic or aluminium plates coated with 0.25 mm of Merck silica gel 60 F_{254}. Column chromatography was carried out using Merck silica gel 60, 0.040-0.063 mm (230-400 mesh ASTM). Eluent mixtures are expressed as volume to volume ratios.

Chiral HPLC was performed using on an Agilent 1220 series instrument equipped with photodiode array (PDA) detection (controlled by ChemStation software) and an automated injector (100 μL loop volume). Experiments were carried out on a CHIRALPAK QN-AX column (4.6 mm x 150 mm, 5 μM) at a flow rate of 1.0 mL min^{-1}. The solvent system was 92:2:0.5 (v(mL):v(mL):w(g)); MeOH:AcOH:NH_4OAc.

Reverse phase high performance liquid chromatography (RP-HPLC) was performed on Agilent 1200 series instruments. For analytical experiments, the instrument was equipped with photodiode array (PDA) detection (controlled by ChemStation software) and a manual injection port (100 μL loop volume). In preparative examples, instruments

used multivariable wavelength (MVW) detection (controlled by ChemStation software) and an Agilent unit injector (2 mL loop volume). The solvent system used throughout this study (except where specified) was buffer A: 0.1% aqueous TFA; buffer B: 0.1% TFA in MeCN. Analytical experiments were performed on a Vydac C18 (4.6 x 250 mm, 5 μm) or an Agilent C18 (4.6 x 250 mm, 5 μm) analytical column, at a flow rate of 1.5 mL min^{-1}. Preparative RP-HPLC was performed on Vydac C18 (22 x 250 mm, 10 μm) preparative columns, at a flow rate of 10 mL min^{-1}. Linear gradients of 0.1% TFA in MeCN were employed as specified.

Microwave ring closing metathesis (RCM), manual microwave-assisted SPPS and other reactions were performed with a CEM Discover system fitted with the Benchmate option. Reactions were performed in 10 mL glass microwave vessels fitted with self-sealing PTFE caps or within a sealed glass pressure tube. Reactions were stirred with PTFE-coated magnetic stirrer beads. Reaction temperature was monitored continuously with a non-contact infrared sensor located below the microwave cavity floor and cooling was achieved where necessary with a continuous flow of compressed air.

Automated microwave-accelerated solid-phase peptide synthesis (SPPS) was performed with a CEM Liberty-Discover system. Unless indicated otherwise, all peptides were synthesised on a 0.1 mmol scale on Rink amide resin at 0.61 mmol/g loading (164 mg resin). Manual SPPS was performed in polypropylene Terumo syringes (5 or 10 mL) fitted with a polyethylene porous (20 μm) filter. Resin wash and filtering steps were aided by the use of a Visprep™ SPE DL 24-port model vacuum manifold. Coupling reactions and cleavage mixtures were shaken on a KS125 basic KA elliptical shaker at 400 revolutions per minute (rpm). Cleaved peptides were collected by centrifugation at a speed of 6,000 rpm, on a Hermle Z200A centrifuge or at a speed of 6,000 rpm on a TMC-1 mini centrifuge.

Lyophilisation of peptide samples was performed using a Christ Alpha 1-2 LD Plus freeze dryer. Melting points were determined using a navy blue and yellow Gallenkamp apparatus from the late 1970s before it was broken by an Honours student in 2018.

2.3.2 Solvents and Reagents

Acetone, acetonitrile (MeCN), concentrated hydrochloric acid (conc. HCl), dichloromethane (DCM), ethyl acetate (EtOAc), hexanes (petroleum ether), methanol (MeOH), tetrahydrofuran (THF), magnesium sulfate ($MgSO_4$), sodium chloride (NaCl), sodium bicarbonate ($NaHCO_3$), sodium hydroxide (NaOH) and potassium bisulphate ($KHSO_4$) were used as supplied by Merck. Anhydrous ('dry') THF was stored over potassium (K) mirror and distilled from K prior to use, or distilled from sodium (Na) and benzophenone prior to use. Anhydrous ('dry') DCM was distilled from calcium hydride (CaH_2) prior to use. Anhydrous ('dry') toluene was distilled from Na and benzophenone and stored over a K mirror. Common reagents were used as supplied by Sigma-Aldrich. Deuterated solvents were used as supplied by Merck.

Amino acids and other peptide reagents were supplied by Mimotopes and AusPep. Cys(Acm) B20 human insulin B-chain **9** was supplied by AusPep. Unless otherwise indicated, L-configured amino acids are used in all instances.

2.3.3 Synthetic Procedures

2.3.3.1 General automated SPPS procedure

The required amount of resin (164 mg, 0.1 mmol, 0.61 mmol/g) was added to a 50 mL self-standing centrifuge tube and suspended in approximately 10 mL of DCM:DMF (1:1) for approximately 60 minutes. The required Fmoc-protected amino acids (0.2 M in DMF), activator reagents (e.g. HATU, 0.5 M in DMF), activator base (DIPEA, 2 M in NMP) and deprotection reagent (piperidine, 20% v/v in DMF) were made up in the appropriate amounts as determined by the CEM PepDriver program immediately prior

to the commencement of the synthesis. The conditions for each automated synthesis step involving most amino acids are listed below (Table 4).

Table 3 - Parameters for automated SPPS reactions.

synthetic step	temperature	microwave power	time
initial deprotection	37°C	36 W	2 min
deprotection	75°C	45 W	10 min
pre-activation	25°C	0 W	2 min
coupling	75°C	25 W	10 min

Excepted from this protocol were arginine residues, which underwent an additional pre-activation and coupling step. Cysteine residues were coupled with an altered protocol employing lower temperatures (Table 3).

Table 4 - Modified SPPS reaction parameters for cysteine residues.

synthetic step	temperature	microwave power	time
initial deprotection	37°C	36 W	2 min
deprotection	75°C	45 W	10 min
pre-activation	25°C	0 W	2 min
coupling	50°C	25 W	10 min

Where the *C*-terminal amino acid of the synthesised peptide was an asparagine, the residue was installed by coupling C_α-COOH-protected aspartic acid to Rink amide resin *via* the aspartic acid's sidechain.

Unless stated otherwise, *N*-terminal residues underwent Fmoc-deprotection upon completion of all coupling steps. Upon completion of the synthesis, the resin either remained in the reaction vessel or was automatically transferred to the synthesiser's resin manifold.

The resin was suspended in DCM:DMF (approx. 1:1), transferred to a fritted syringe and subjected to aerial drying *via* vacuum filtration.

2.3.3.2 General manual SPPS procedure

To separate glass vials were added Fmoc-protected amino acid (4 equiv.) and HATU (4 equiv.) and each reagent was dissolved in a minimum volume of DMF. The solutions were combined, NMM (8 equiv.) added and the mixture added to a fritted syringe containing the resin-bound peptide. The suspension was shaken for 1.5-2 hours, drained, the resin washed with DMF (5x5 mL) and subjected to aerial drying *via* vacuum filtration.

2.3.3.3 General manual microwave-assisted SPPS procedure

To separate glass vials were added Fmoc-protected amino acid (4 equiv.) and HATU (4 equiv.) and each reagent dissolved in a minimum volume of DMF. The solutions were combined, NMM (8 equiv.) added and the mixture added to a microwave vessel containing a suspension of resin-bound peptide. The reaction mixture was stirred with microwave irradiation and heated for 5 minutes at 75 °C and 25 W, allowed to cool and the suspension transferred to a fritted syringe. The suspension was drained, the resin washed with DMF (5x5 mL) and subjected to aerial drying *via* vacuum filtration.

2.3.3.4 TNBS Test

To a small aliquot (~1 mg) of resin-bound peptide was added two drops of a 1% solution of 2,4,6-trinitrobenzene sulfonic acid (TNBS) in DMF followed by one drop of a 10% solution of DIPEA in DMF. Red colouration of resin indicates the presence of free amine functionality and consequently incomplete coupling of inbound Fmoc-protected amino acid residues. Conversely, colourless resin is indicative of a sufficient degree of coupling. The test is not applicable for *N*-terminal proline residues.

2.3.3.5 Fmoc deprotection

Resin-bound Fmoc-protected peptide was suspended in a 20% solution of piperidine in DMF of volume 1 mL or 4 mL for small- and full-scale reactions, respectively. The suspension was agitated for 15 minutes, drained, the resin washed with copious DMF and subjected to aerial drying *via* vacuum filtration.

2.3.3.6 Capping (*N*-terminal acetylation)

Resin-bound peptide was suspended in a capping solution (4 mL) (comprised of 94% DMF, 5% Ac_2O and 1% NMM). The suspension was agitated for 2 hours, drained, the resin washed with DMF (5x5 mL) and subjected to aerial drying *via* vacuum filtration.

2.3.3.7 TFA-mediated resin cleavage

Resin-bound peptide was suspended in a cleavage solution (comprised of 95% TFA, 2% TIPS, 2% H_2O and 1% thioanisole) of volume 1 mL or 20 mL for small- and full-scale cleavage, respectively. The reaction mixture was agitated at room temperature for between 1 and 4 hours then filtered through a fritted syringe. The filtrate was collected, concentrated under continuous N_2 flow, the residue diluted with cold Et_2O, the resulting suspension subjected to centrifugation and the ethereal layer decanted. Dilution, centrifugation and decantation were repeated to give the crude peptide as a solid.

2.3.3.8 General microwave-assisted on-resin RCM procedure

Prior to use, the resin-bound peptide was stored for a minimum of 16 hours in a vacuum desiccator containing indicating silica gel. The resin was transferred to a microwave vessel and GII (20 mol %) added. The vessel was then transferred to a dry box and dry deoxygenated DCM added (4 mL) followed by 6 drops of an 0.4 M solution of LiCl in dry, deoxygenated DMF. The vessel was sealed, removed from the dry box and stirred with microwave irradiation and heating for 2 hours at 100 °C and 100 W, allowed to cool

and the suspension transferred to a fritted syringe. The suspension was drained, the resin washed with DMF (5x5 mL) and subjected to aerial drying *via* vacuum filtration.

2.3.3.9 *N*-Ac-D-Agl-OH 3

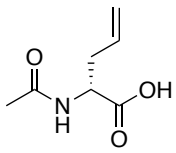

3

The amino acid derivative **3** was prepared according to a procedure described by Chenault *et al*..[112] To a 50 mL Falcon tube was added *N*-Acetyl D,L-allylglycine **2** (500 mg, 3.18 mmol, 1 equiv.), $CoCl_2.6H_2O$ (8.1 mg, 31.8 μmol, 0.01 equiv.) and deionised H_2O (16 mL). The resulting brown solution was basified to pH 8 with aqueous NaOH (2 M). Acylase I from *Aspergillus melleus* (132 mg, 39.6 U, 12.5 U per mmol of substrate) was added, the tube sealed and the reaction mixture stirred at 37° C for 45 hours, whereupon TLC of the reaction mixture (silica, 3:1:1 *n*-BuOH:H_2O:AcOH, $KMnO_4$ stain) revealed two spots of approx. equal intensity at R_f ~0.7 and ~0.3, the latter staining pink with ninhydrin. The reaction mixture was acidified (pH 4) with 1 M aqueous HCl, centrifuged (5000 rpm, 4 min) and concentrated under reduced pressure. The resulting off-white solid was suspended in the appropriate solvent system and purified by column chromatography (silica, 10% MeOH/DCM with 1% AcOH) to give **3** as a colourless solid upon addition of diethyl ether to the residue (0.160 mg, 64% brsm). Spectral data were in accordance with those of the opposite enantiomer in the literature.[113] ^{1}H-NMR (400 MHz, $CDCl_3$): δ 5.82-5.74 (m, 1H), 5.16-5.07 (m, 2H), 4.43 (t, *J* = 4.8 Hz, 1H), 2.63-2.40 (m, 2H), 1.98 (s, 3H); NH and OH not observed.

2.3.3.10 Fmoc-D-Agl-OH 1

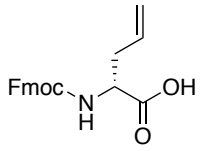

1

N-Acetyl D-allylglycine **3** (600 mg, 3.8 mmol, 1 equiv.) was dissolved in 2 M aqueous HCl (30 mL), heated to reflux (110 °C) and stirred for 4 hours, monitored by TLC (silica, 3:1:1 *n*-BuOH:H_2O:AcOH). The reaction mixture was then basified (pH 6) with 4 M aqueous LiOH and concentrated under reduced pressure. The residue was taken up in a solution of $NaHCO_3$ (1.28 g, 15.2 mmol, 4 equiv.) in H_2O (10 mL), to which was added a solution of Fmoc-OSu (1.41 g, 4.2 mmol, 1.1 equiv.) in acetone (10 mL). The reaction mixture was stirred at room temperature for 24 hours, acidified (pH 2) with 1 M aqueous HCl and the acetone removed under reduced pressure. The residue was extracted with DCM (3x65 mL). The combined organic extract was washed with 1 M aqueous HCl (2x60 mL), H_2O (60 mL) and brine (60 mL), dried ($MgSO_4$) and concentrated under reduced pressure to afford Fmoc-D-allylglycine **1** as a pale yellow solid (1.01 g, 84%). m.p. 127-128 °C (lit. 130-132 °C).[114] Chiral HPLC (Agilent: CHIRALPAK QN-AX column, 92:2:0.5 (v/v/w); MeOH:AcOH:NH_4OAc): t_R = 7.8 min (D-isomer, 96% total area); 11.6 min (L-isomer, 4% total area) – 92% ee. Fmoc-L-Agl-OH was used as a reference.

2.3.3.11 *des*$_{A1\text{-}5}$[A6,A11]-D-Agl-[A7]-Cys(^{t}Bu)-[A20]-Cys(Acm) human insulin A-chain 5

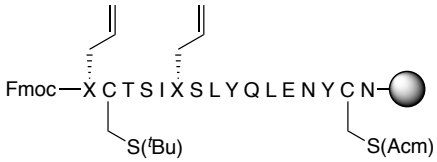

5

The resin-bound peptide **5** excluding *N*-terminal Agl residue A6 was prepared according to the general automated procedure outlined in Section 2.3.3.1. Agl A6 was attached according to the general manual microwave-assisted SPPS procedure outlined in Section 2.3.3.3 with the following quantities of reagents: HATU (114 mg, 0.3 mmol, 3 equiv.), Fmoc-D-allylglycine **1** (119 mg, 0.3 mmol, 3 equiv.), NMM (66 µL, 0.6 mmol, 6 equiv.) in DMF (4 mL). Where incomplete coupling was indicated by a positive TNBS test (Section 2.3.3.4), the manual coupling was repeated. Formation of **5** was subsequently verified by small-scale Fmoc deprotection and resin cleavage, RP-HPLC and LRMS. Mass spectrum (ESI+, MeCN:H_2O:TFA): *m/z* 987.0 $[M+2H]^{2+}$; ½($C_{87}H_{136}N_{20}O_{28}S_2$) requires 986.5. RP-HPLC (Agilent: Vydac C18 analytical column, 15 to 50% buffer B over 35 min): t_R = 20.7 min. The resin-bound peptide was subjected to the capping procedure outlined in Section 2.3.3.6 and stored overnight in a vacuum desiccator prior to RCM.

2.3.3.12 *des*$_{A1\text{-}5}$-[Δ^4A6-A11]-(D,D)-dicarba-[A7]-Cys(^{t}Bu)-[A20]-Cys(Acm) human insulin A-chain 6

6

Resin-bound peptide **5** was subjected to the general microwave-assisted on-resin RCM procedure outlined in Section 2.3.3.8 with the following quantities of reagents: GII (17

mg, 20 mol %), 0.4 M LiCl/DMF (~0.2 mL), DCM (4 mL). Formation of **6** as a pair of isomers (**6(I)** and **6(II)**) in a 2:1 ratio was subsequently verified by small-scale Fmoc deprotection and resin cleavage, RP-HPLC and LRMS. **6(I)**: Mass spectrum (ESI+, MeCN:H_2O:TFA): *m/z* 972.9 $[M+2H]^{2+}$; ½($C_{85}H_{132}N_{20}O_{28}S_2$) requires 972.4. RP-HPLC (Agilent: Vydac C18 analytical column, 15 to 50% buffer B over 35 min): t_R = 19.3 min. **6(II)**: Mass spectrum (ESI+, MeCN:H_2O:TFA): *m/z* 972.4 $[M+2H]^{2+}$; ½($C_{85}H_{132}N_{20}O_{28}S_2$) requires 972.4. RP-HPLC (Agilent: Vydac C18 analytical column, 15 to 50% buffer B over 35 min): t_R = 21.0 min.

2.3.3.13 [Δ^4A6-A11]-(D,D)-dicarba-[A7]-Cys(^{t}Bu)-[A20]-Cys(Acm) human insulin A-chain 7

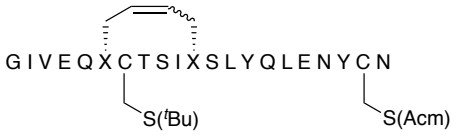

7

Peptide **7** was prepared from resin-bound **6** according to the general automated procedure outlined in Section 2.3.3.1. Formation of **7(I)** and **7(II)**) was subsequently verified by small-scale cleavage, RP-HPLC and LRMS. **7(I)**: Mass spectrum (ESI^+, MeCN:H_2O:TFA): *m/z* 824.3 $[M+3H]^{3+}$; ⅓($C_{108}H_{171}N_{26}O_{36}S_2$) requires 824.1. *m/z* 1236.1 $[M+2H]^{2+}$; ½($C_{108}H_{170}N_{26}O_{36}S_2$) requires 1235.6. RP-HPLC (Agilent: Vydac C18 analytical column, 15 to 50% buffer B over 35 min): t_R = 17.4 min. **7(II)** Mass spectrum (ESI^+, MeCN:H_2O:TFA): *m/z* 824.1 $[M+3H]^{3+}$; ⅓($C_{108}H_{171}N_{26}O_{36}S_2$) requires 824.1. 1236.3 $[M+2H]^{2+}$; ½($C_{108}H_{170}N_{26}O_{36}S_2$) requires 1235.6. RP-HPLC (Agilent: Vydac C18 analytical column, 15 to 50% buffer B over 35 min): t_R = 20.6 min. The resin was then subjected to TFA-mediated cleavage (Section 2.3.3.7), the residue dissolved in MeCN:H_2O (~1:5) and lyophilised to give the crude desired peptides **7(I)** and **7(II)** as an off-white solid (404 mg).

2.3.3.14 [Δ⁴A6-A11]-(D,D)-dicarba-[A7]-Cys(SPyr)-[A20]-Cys(Acm) human insulin A-chain 8

8

The concerted *tert*-butyl deprotection and *S*-pyridinyl protection at Cys A7 was executed according to the procedure described by Büllesbach *et al*..[110] To a solution of anisole:TFA (1:9, 6.5 mL) was added 2-dipyridyl disulfide (DPDS) (44.1 mg, 0.2 mmol, 2 equiv.) and the resulting solution cooled to 0 °C in an ice bath. To this solution was added lyophilised crude peptide **7** (404 mg) followed by a chilled solution of triflic acid:TFA (1:4, 6.5 mL). The resulting light brown solution was stirred at 0 °C for 1.5 hours upon which the solution was concentrated under a stream of N_2 and the crude peptide precipitated with chilled ether (35 mL). The suspension was centrifuged, the supernatant discarded, the precipitate resuspended and centrifuged in chilled ether (35 mL) a further two times. The crude peptide was then dissolved in MeCN:H_2O and lyophilised to give **8** as a brittle red gum. Formation of **8** as a pair of isomers **8(I)** and **8(II)** was subsequently verified by RP-HPLC and LRMS. **8(I)**: Mass spectrum (ESI^+, MeCN:H_2O:TFA): *m/z* 841.3 $[M+3H]^{3+}$; ⅓($C_{109}H_{163}N_{27}O_{36}S_3$) requires 841.7. RP-HPLC (Agilent: Vydac C18 analytical column, 15 to 50% buffer B over 35 min): t_R = 15.8 min. **8(II)** Mass spectrum (ESI^+, MeCN:H_2O:TFA): *m/z* 841.3 $[M+3H]^{3+}$; ⅓($C_{109}H_{163}N_{27}O_{36}S_3$) requires 841.2. RP-HPLC (Agilent: Vydac C18 analytical column, 15 to 50% buffer B over 35 min): t_R = 19.9 min. Peptide **8** was purified *via* preparative RP-HPLC (Agilent: Vydac C18 preparative column, 15 to 45% buffer B over 40 min) and selected fractions combined and lyophilised to give isomers **8(I)** and **8(II)**.

2.3.3.15 [Δ⁴A6-A11]-(D,D)-dicarba-[A20, B19]-Cys(Acm) human insulin 10

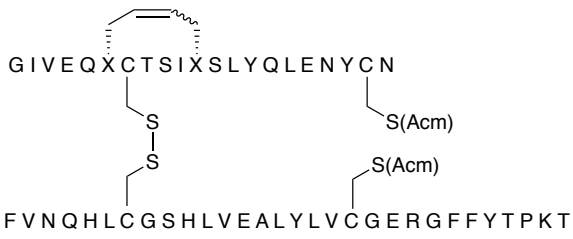

10

Combination of the A- and B-chain monomers was executed according to a modified version of a procedure originally described by Lin *et al*..[111] A single isomer (**I**) of the modified insulin A-chain **8** (~8 mg, ~3.2 μmol) was dissolved in 50 mM NH_4HCO_3 aqueous solution (5 mL). [B19]-Cys(Acm) human insulin B-chain **9** (5 mg, 1.6 μmol) was dissolved in MilliQ H_2O (8 mL) to give a cloudy solution, which was added dropwise to the solution of **8** and stirred for 1.5 hours with monitoring *via* RP-HPLC and MS. The reaction was quenched by addition of glacial AcOH to pH ~3 and the resulting solution lyophilised to give crude **10(I)** as a colourless solid. Mass spectrum (ESI^+, MeCN:H_2O:TFA): *m/z* 1479.4 $[M+4H]^{4+}$; ¼($C_{265}H_{400}N_{67}O_{79}S_4$) requires 1478.2. RP-HPLC (Agilent: Vydac C18 analytical column, 0 to 25% buffer B over 5 min then 25 to 50% buffer B over 30 min): t_R = 18.3 min. The process was repeated with the complementary isomer **10(II)**; Mass spectrum (ESI^+, MeCN:H_2O:TFA): *m/z* 1479.4 $[M+4H]^{4+}$; ¼($C_{265}H_{400}N_{67}O_{79}S_4$) requires 1478.2. RP-HPLC (Agilent: Vydac C18 analytical column, 0 to 25% buffer B over 5 min then 25 to 50% buffer B over 30 min): t_R = 18.0 min.

2.3.3.16 [Δ⁴A6-A11]-(D,D)-dicarba human insulin 11

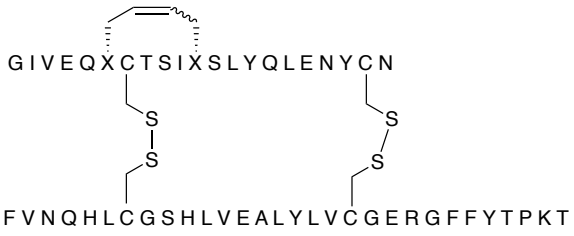

11

Oxidation of the insulin analogue precursor **10(I)** was executed according to a procedure described by Lin *et al*..[111] **10(I)** (2.5 μmol) was suspended in a 60 mM HCl aqueous solution (0.4 mL) followed by glacial AcOH (7.5 mL) to effect dissolution. A 20 mM solution of iodine in glacial acetic acid (7.5 mL) was added and the resulting solution stirred in darkness for 1 hour, exposed to light and stirred for a further 1.75 hours before being poured into chilled diethyl ether (2x35 mL). The resulting suspension was cooled to 0 °C, centrifuged (5000 rpm, 4 min), the supernatant discarded. The residue was suspended in MeCN (~0.5 mL) and 20 mM ascorbic acid aqueous solution (~0.5 mL) and purified by preparative RP-HPLC (Agilent: Vydac C18 preparative column, 0 to 30% buffer B over 5 min then 30 to 40% buffer B over 30 min): t_R = 16.1 min to give **11(I)** as a colourless solid (10.8 mg). RP-HPLC (Agilent): Vydac C18 analytical column, 0 to 25% buffer B over 5 min then 25 to 50% buffer B over 30 min: t_R = 16.4 min. Mass spectrum (ESI$^+$, MeCN:H_2O:TFA): *m/z* 1443.1 $[M+4H]^{4+}$; ¼($C_{259}H_{388}N_{65}O_{77}S_4$) requires 1442.2. *m/z* 1154.7 $[M+5H]^{5+}$; ⅕($C_{259}H_{389}N_{65}O_{77}S_4$) requires 1154.0.

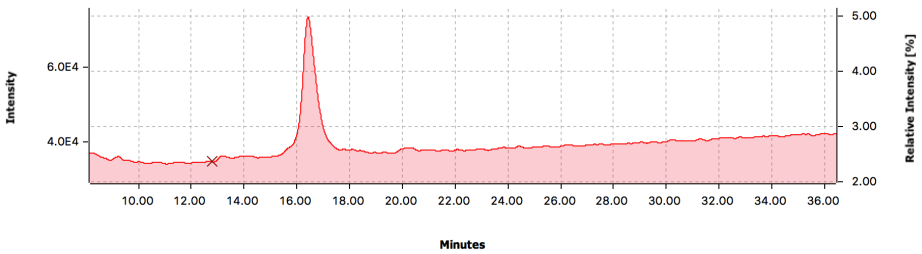

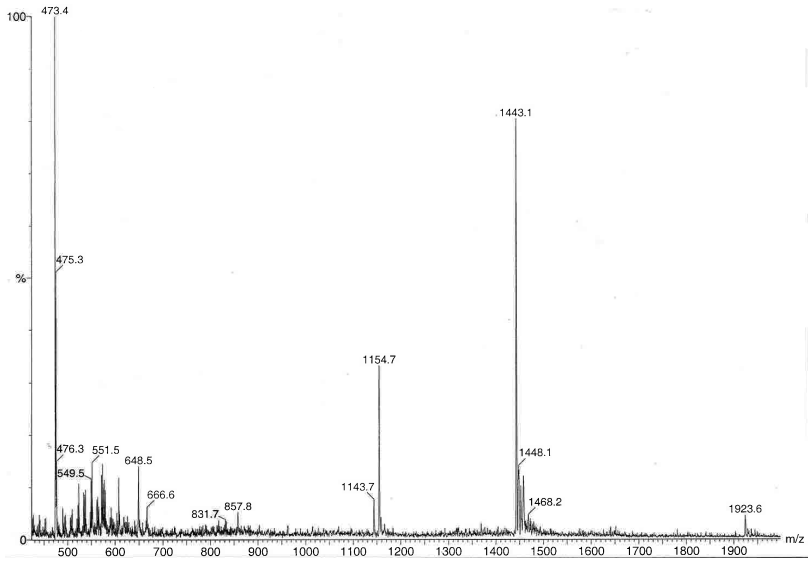

The process was repeated with the complementary isomer **11(II)**; RP-HPLC (Agilent): Vydac C18 analytical column, 0 to 25% buffer B over 5 min then 25 to 50% buffer B over 30 min: t_R = 17.9 min. Mass spectrum (ESI$^+$, MeCN:H_2O:TFA): *m/z* 1443.1 $[M+4H]^{4+}$; ¼($C_{259}H_{388}N_{65}O_{77}S_4$) requires 1442.2.

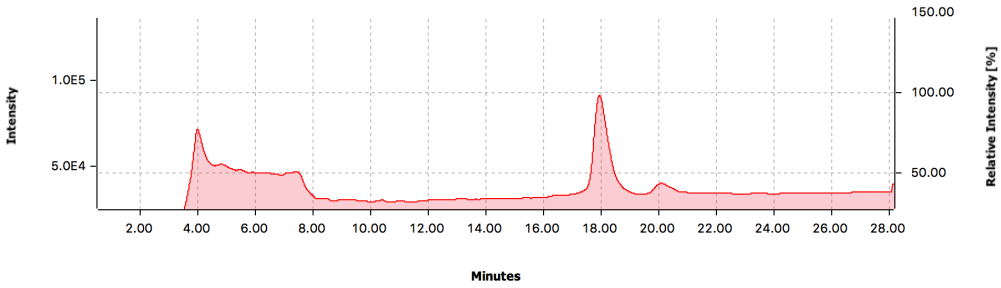

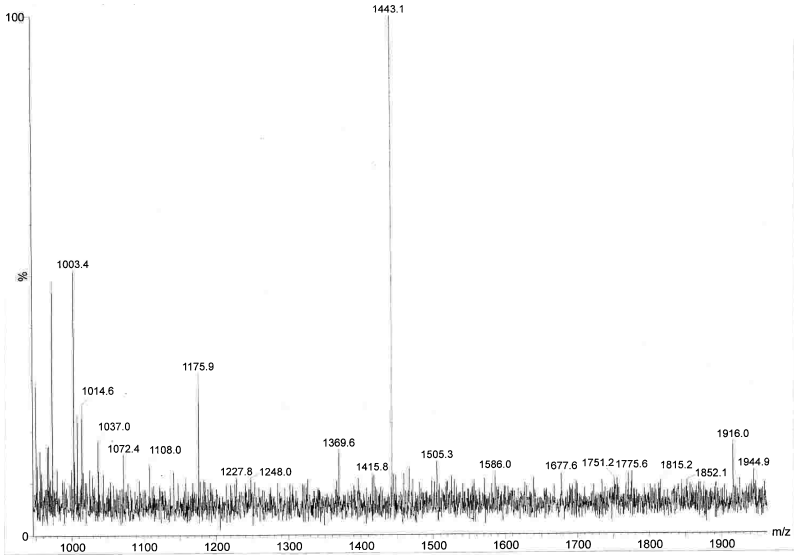

2.3.3.17 *des*$_{A1\text{-}5}$-[A6]-L-Agl-[A7]-Cys(^{t}Bu)-[A11]-D-Agl-[A20]-Cys(Acm) human insulin A-chain 14

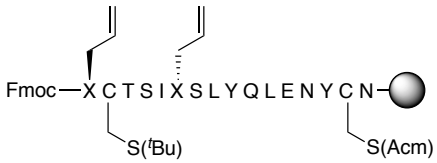

14

The resin-bound peptide **14** was prepared in an analogous fashion as described for **5** (see Section 2.3.3.11). Formation of **14** was subsequently verified by small-scale Fmoc deprotection and resin cleavage, RP-HPLC and LRMS. Mass spectrum (ESI^+, $MeCN:H_2O$:TFA): *m/z* 986.4 $[M+2H]^{2+}$; ½($C_{87}H_{136}N_{20}O_{28}S_2$) requires 986.5. RP-HPLC (Agilent: Vydac C18 analytical column, 15 to 50% buffer B over 35 min): t_R = 18.4 min.

2.3.3.18 *des*$_{A1-5}$-[Δ^4A6-A11]-(L,D)-dicarba-[A7]-Cys(^{t}Bu)-[A20]-Cys(Acm) human insulin A-chain 15

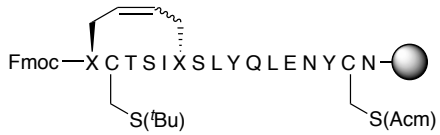

15

The resin-bound peptide **15** was prepared in an analogous fashion as described for **6** (see Section 2.3.3.12). Formation of **15** as a pair of isomers (**15(I)** and **15(II)**) in a 3:2 ratio was subsequently verified by small-scale Fmoc deprotection and resin cleavage, RP-HPLC and LRMS. **15(I)**: Mass spectrum (ESI$^+$, MeCN:H_2O:TFA): *m/z* 972.4 $[M+2H]^{2+}$; ½($C_{85}H_{132}N_{20}O_{28}S_2$) requires 972.4. RP-HPLC (Agilent: Vydac C18 analytical column, 15 to 50% buffer B over 35 min): t_R = 15.9 min. **15(II)**: Mass spectrum (ESI$^+$, MeCN:H_2O:TFA): *m/z* 972.8 $[M+2H]^{2+}$; ½($C_{85}H_{132}N_{20}O_{28}S_2$) requires 972.4. RP-HPLC (Agilent: Vydac C18 analytical column, 15 to 50% buffer B over 35 min): t_R = 17.4 min.

2.3.3.19 [Δ^4A6-A11]-(L,D)-dicarba-[A7]-Cys(^{t}Bu)-[A20]-Cys(Acm) human insulin A-chain 16

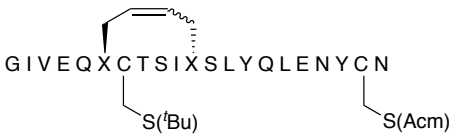

16

Peptide **16** was prepared in an analogous fashion as described for **7** (see Section 2.3.3.13). Formation of **16(I)** and **16(II)**) was subsequently verified by small-scale cleavage, RP-HPLC and LRMS. **16(I)**: Mass spectrum (ESI$^+$, MeCN:H_2O:TFA): *m/z* 824.3 $[M+3H]^{3+}$; ⅓($C_{108}H_{171}N_{26}O_{36}S_2$) requires 824.1. *m/z* 1236.1 $[M+2H]^{2+}$; ½($C_{108}H_{170}N_{26}O_{36}S_2$) requires 1235.6. RP-HPLC (Agilent: Vydac C18 analytical column, 15 to 50% buffer B over 35 min): t_R = 19.1 min. **16(II)** Mass spectrum (ESI$^+$,

MeCN:H_2O:TFA): *m/z* 824.1 $[M+3H]^{3+}$; ⅓($C_{108}H_{171}N_{26}O_{36}S_2$) requires 824.1. 1236.0 $[M+2H]^{2+}$; ½($C_{108}H_{170}N_{26}O_{36}S_2$) requires 1235.6. RP-HPLC (Agilent: Vydac C18 analytical column, 15 to 50% buffer B over 35 min): t_R = 19.6 min.

2.3.3.20 [Δ⁴A6-A11]-(L,D)-dicarba-[A7]-Cys(SPyr)-[A20]-Cys(Acm) human insulin A-chain 17

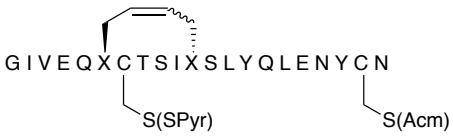

17

Peptide **17** was prepared in an analogous fashion as described for **8** (see Section 2.3.3.14). Formation of **17** as a pair of isomers **17(I)** and **17(II)** was subsequently verified by RP-HPLC and LRMS. **17(I)**: Mass spectrum (ESI^+, MeCN:H_2O:TFA): *m/z* 841.3 $[M+3H]^{3+}$; ⅓($C_{109}H_{163}N_{27}O_{36}S_3$) requires 841.2. RP-HPLC (Agilent: Vydac C18 analytical column, 15 to 50% buffer B over 35 min): t_R = 17.4 min. **17(II)** Mass spectrum (ESI^+, MeCN:H_2O:TFA): *m/z* 841.3 $[M+3H]^{3+}$; ⅓($C_{109}H_{163}N_{27}O_{36}S_3$) requires 841.2. RP-HPLC (Agilent: Vydac C18 analytical column, 15 to 50% buffer B over 35 min): t_R = 17.5 min. Peptide **17** was purified *via* preparative RP-HPLC (Agilent: Vydac C18 preparative column, 15 to 45% buffer B over 40 min) and selected fractions combined and lyophilised to give isomers **17(I)** (t_R = 20.6 min) and **17(II)** (t_R = 22.0 min).

2.3.3.21 [Δ⁴A6-A11]-(L,D)-dicarba-[A20, B19]-Cys(Acm) human insulin 18

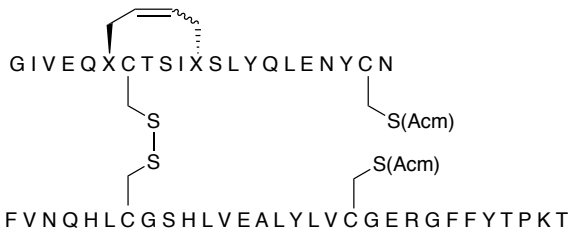

18

Peptide **18(I)** was prepared in an analogous fashion as described for **10(I)** (see Section 2.3.3.15). Mass spectrum (ESI⁺, MeCN:H_2O:TFA): *m/z* 1479.1 $[M+4H]^{4+}$; ¼($C_{265}H_{400}N_{67}O_{79}S_4$) requires 1478.2. RP-HPLC (Agilent: Vydac C18 analytical column, 0 to 25% buffer B over 5 min then 25 to 50% buffer B over 30 min): t_R = 17.9 min. The process was repeated with the complementary isomer **18(II)**; Mass spectrum (ESI⁺, MeCN:H_2O:TFA): *m/z* 1479.4 $[M+4H]^{4+}$; ¼($C_{265}H_{400}N_{67}O_{79}S_4$) requires 1478.2. RP-HPLC (Agilent: Vydac C18 analytical column, 0 to 25% buffer B over 5 min then 25 to 50% buffer B over 30 min): t_R = 18.0 min.

2.3.3.22 [Δ⁴A6-A11]-(L,D)-dicarba human insulin 12

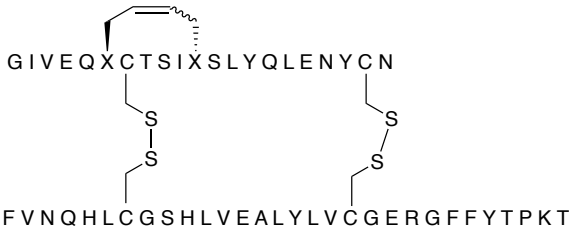

12

Peptide **12(I)** was prepared in an analogous fashion as described for **11** (see Section 2.3.3.16). Purification by preparative RP-HPLC (Agilent: Vydac C18 preparative column, 0 to 30% buffer B over 5 min then 30 to 40% buffer B over 30 min): t_R = 15.4 min gave **12(I)** as a colourless solid (0.1 mg). RP-HPLC (Agilent): Vydac C18 analytical column, 0 to 25% buffer B over 5 min then 25 to 50% buffer B over 30 min: t_R = 14.8 min. Mass spectrum (ESI⁺, MeCN:H_2O:TFA): *m/z* 1443.1 $[M+4H]^{4+}$;

¼($C_{259}H_{388}N_{65}O_{77}S_4$) requires 1442.2. *m/z* 1154.8 $[M+5H]^{5+}$; ⅕($C_{259}H_{389}N_{65}O_{77}S_4$) requires 1154.0

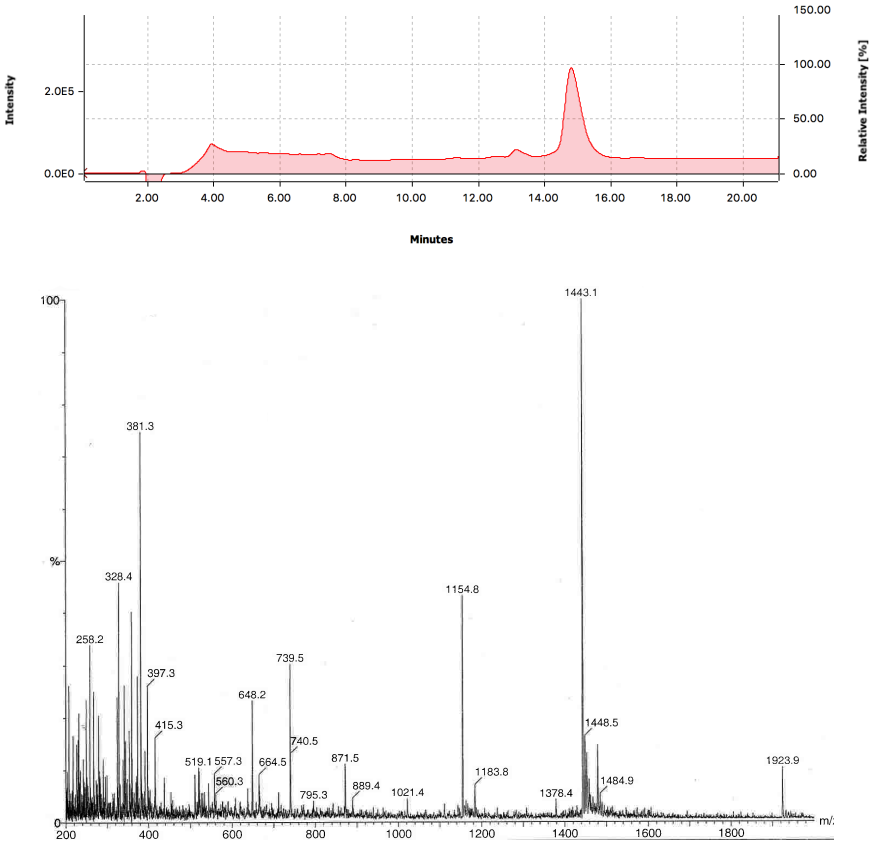

The process was repeated with the geometric isomer **12(II)**, giving the peptide as a white solid (0.5 mg); RP-HPLC (Agilent: Vydac C18 analytical column, 0 to 25% buffer B over 5 min then 25 to 50% buffer B over 30 min): t_R = 15.5 min. Mass spectrum (ESI^+, MeCN:H_2O:TFA): *m/z* 1443.1 $[M+4H]^{4+}$; ¼($C_{259}H_{388}N_{65}O_{77}S_4$) requires 1442.2. *m/z* 1154.9 $[M+5H]^{5+}$; ⅕($C_{259}H_{389}N_{65}O_{77}S_4$) requires 1154.0.

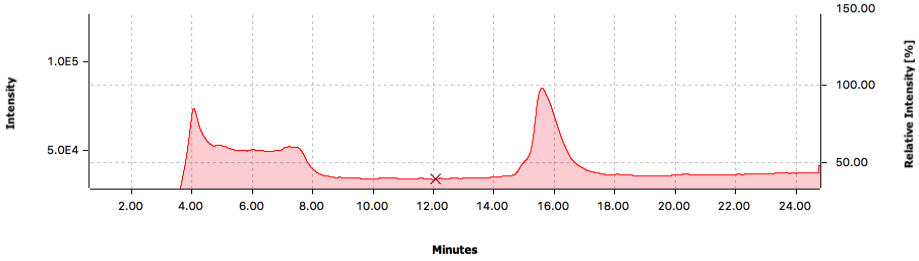

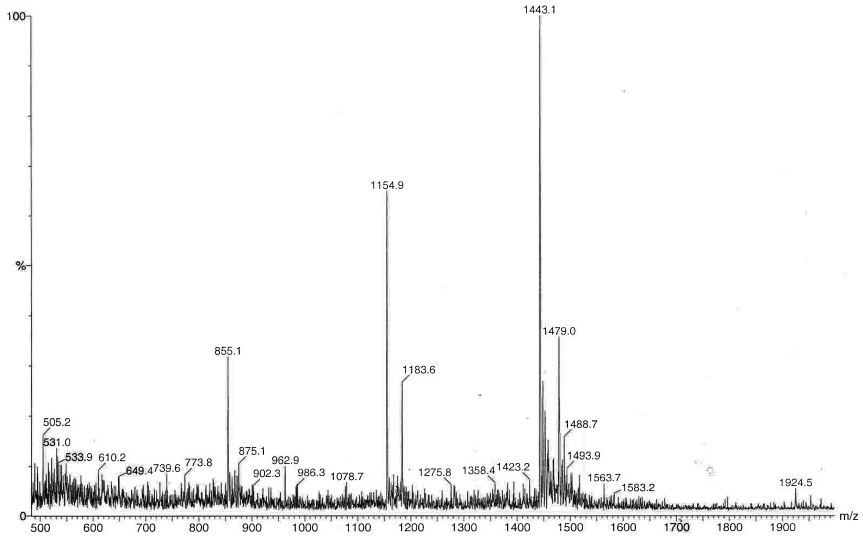

2.3.3.23 *des*$_{A1\text{-}5}$-[A6]-D-Agl-[A7]-Cys(^{t}Bu)-[A11]-L-Agl-[A20]-Cys(Acm) human insulin A-chain 19

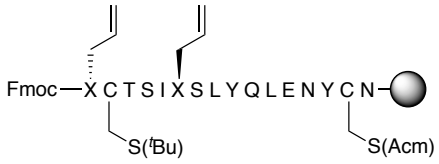

19

The resin-bound peptide **19** was prepared in an analogous fashion as described for **5** (see Section 2.3.3.11). Formation of **19** was subsequently verified by small-scale Fmoc deprotection and resin cleavage, RP-HPLC and LRMS. Mass spectrum (ESI^+, $MeCN:H_2O$:TFA): *m/z* 986.4 $[M+2H]^{2+}$; ½($C_{87}H_{136}N_{20}O_{28}S_2$) requires 986.5. RP-HPLC (Agilent: Vydac C18 analytical column, 15 to 50% buffer B over 35 min): t_R = 20.5 min.

2.3.3.24 *des*$_{A1\text{-}5}$-[Δ^{4}A6-A11]-(D,L)-dicarba-[A7]-Cys(^{t}Bu)-[A20]-Cys(Acm) human insulin A-chain 20

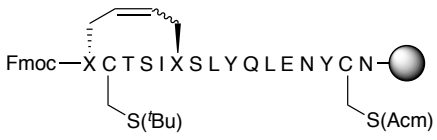

20

The resin-bound peptide **20** was prepared in an analogous fashion as described for **6** (see Section 2.3.3.12). Formation of **20** as a pair of isomers (**20(I)** and **20(II)**) in a 3:7 ratio was subsequently verified by small-scale Fmoc deprotection and resin cleavage, RP-HPLC and LRMS. **20(I)**: Mass spectrum (ESI$^+$, MeCN:H_2O:TFA): *m/z* 972.8 $[M+2H]^{2+}$; ½($C_{85}H_{132}N_{20}O_{28}S_2$) requires 972.4. RP-HPLC (Agilent: Vydac C18 analytical column, 15 to 50% buffer B over 35 min): t_R = 16.1 min. **20(II)**: Mass spectrum (ESI$^+$, MeCN:H_2O:TFA): *m/z* 973.8 $[M+2H]^{2+}$; ½($C_{85}H_{132}N_{20}O_{28}S_2$) requires 972.4. RP-HPLC (Agilent: Vydac C18 analytical column, 15 to 50% buffer B over 35 min): t_R = 18.4 min.

2.3.3.25 [Δ^{4}A6-A11]-(D,L)-dicarba-[A7]-Cys(^{t}Bu)-[A20]-Cys(Acm) human insulin A-chain 21

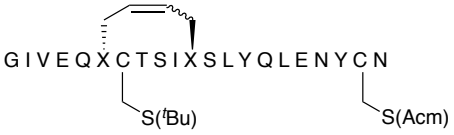

21

Peptide **21** was prepared in an analogous fashion as described for **7** (see Section 2.3.3.13). Formation of **21(I)** and **21(II)**) was subsequently verified by small-scale cleavage, RP-HPLC and LRMS. **21(I)**: Mass spectrum (ESI$^+$, MeCN:H_2O:TFA): *m/z* 824.2 $[M+3H]^{3+}$; ⅓($C_{108}H_{171}N_{26}O_{36}S_2$) requires 824.1. *m/z* 1235.9 $[M+2H]^{2+}$; ½($C_{108}H_{170}N_{26}O_{36}S_2$) requires 1235.6. RP-HPLC (Agilent: Vydac C18 analytical column, 15 to 50% buffer B over 35 min): t_R = 20.0 min. **21(II)** Mass spectrum (ESI$^+$,

MeCN:H_2O:TFA): *m/z* 824.3 $[M+3H]^{3+}$; ⅓($C_{108}H_{171}N_{26}O_{36}S_2$) requires 824.1. 1235.8 $[M+2H]^{2+}$; ½($C_{108}H_{170}N_{26}O_{36}S_2$) requires 1235.6. RP-HPLC (Agilent: Vydac C18 analytical column, 15 to 50% buffer B over 35 min): t_R = 20.4 min.

2.3.3.26 [Δ^4A6-A11]-(D,L)-dicarba-[A7]-Cys(SPyr)-[A20]-Cys(Acm) human insulin A-chain 22

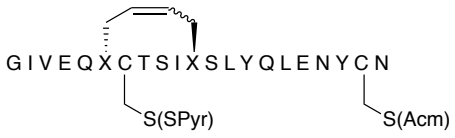

22

Peptide **22** was prepared in an analogous fashion as described for **8** (see Section 2.3.3.14). Formation of **22** as a pair of isomers **22(I)** and **22(II)** was subsequently verified by RP-HPLC and LRMS. **22(I)**: Mass spectrum (ESI^+, MeCN:H_2O:TFA): *m/z* 841.3 $[M+3H]^{3+}$; ⅓($C_{109}H_{163}N_{27}O_{36}S_3$) requires 841.2. RP-HPLC (Agilent: Vydac C18 analytical column, 15 to 50% buffer B over 35 min): t_R = 16.3 min. **22(II)** Mass spectrum (ESI^+, MeCN:H_2O:TFA): *m/z* 841.2 $[M+3H]^{3+}$; ⅓($C_{109}H_{163}N_{27}O_{36}S_3$) requires 841.2. RP-HPLC (Agilent: Vydac C18 analytical column, 15 to 50% buffer B over 35 min): t_R = 16.7 min. Peptide **22** was purified *via* preparative RP-HPLC (Agilent: Vydac C18 preparative column, 15 to 45% buffer B over 40 min) and selected fractions combined and lyophilised to give isomers **22(I)** (t_R = 23.9 min) and **22(II)** (t_R = 25.1 min).

2.3.3.27 [Δ⁴A6-A11]-(D,L)-dicarba-[A20, B19]-Cys(Acm) human insulin 23

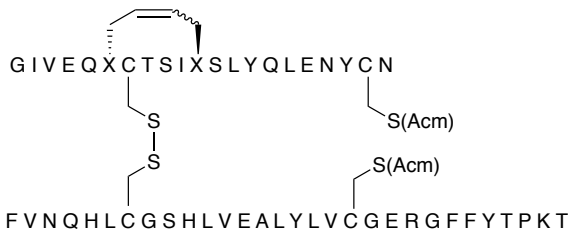

23

Peptide **23(I)** was prepared in an analogous fashion as to that described for **10** (see Section 2.3.3.15). **23(I)**: Mass spectrum (ESI^+, MeCN:H_2O:TFA): *m/z* 1479.0 $[M+4H]^{4+}$; ¼($C_{265}H_{400}N_{67}O_{79}S_4$) requires 1478.2. RP-HPLC (Agilent: Vydac C18 analytical column, 0 to 25% buffer B over 5 min then 25 to 50% buffer B over 30 min): t_R = 18.5 min. The process was repeated with the complementary isomer **23(II)**; Mass spectrum (ESI^+, MeCN:H_2O:TFA): *m/z* 1479.7 $[M+4H]^{4+}$; ¼($C_{265}H_{400}N_{67}O_{79}S_4$) requires 1478.2. RP-HPLC (Agilent: Vydac C18 analytical column, 0 to 25% buffer B over 5 min then 25 to 50% buffer B over 30 min): t_R = 18.4 min.

2.3.3.28 [Δ⁴A6-A11]-(D,L)-dicarba human insulin 13(I)

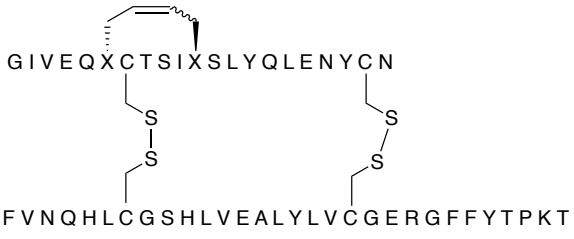

13

Peptide **13(I)** was prepared in an analogous fashion as to that described for **11** (see Section 2.3.3.16). Purification by preparative RP-HPLC (Agilent: Vydac C18 preparative column, 0 to 30% buffer B over 5 min then 30 to 40% buffer B over 30 min): t_R = 18.4 min gave **13(I)**, albeit in yield insufficient for further study. Mass spectrum (ESI^+, MeCN:H_2O:TFA): *m/z* 1443.1 $[M+4H]^{4+}$; ¼($C_{259}H_{388}N_{65}O_{77}S_4$) requires 1442.2.

Attempted synthesis of the geometric isomer **13(II)** returned only starting material with no conversion to the desired bicyclic species **13(II)**.

2.3.4 Insulin receptor competition binding assay

IR-B binding was measured as described by Denley *et al.*[115] Human IR isoform B (IR-B)[116] was solubilized from R$^-$IR-B cells. Cells were serum-starved for 4 h before lysis in lysis buffer (20 mM HEPES, 150 mM NaCl, 1.5 mM $MgCl_2$, 10% (v/v) glycerol, 1% (v/v) Triton X-100, 1 mM EGTA, and Roche cOmplete ULTRA protease inhibitors, pH 7.5) for 1 h at 4 °C. Lysates were centrifuged for 10 min at 2,200 × *g*, then 100 µL lysate was added per well to a white Greiner Lumitrac 600 96-well plate previously coated with anti-IR antibody 83-7 (250 ng/well in bicarbonate buffer pH 9.2).[117] Approximately 500,000 fluorescent counts of europium-labelled insulin (Eu-insulin, prepared in-house) was added to each well along with increasing concentrations of unlabelled competitor in a final volume of 100 µL and incubated for 16 h at 4 °C. Wells were washed four times with 20 mM Tris pH 7.4, 150 mM NaCl, and 0.1% (v / v) Tween 20 (TBST). Then 100 µL per well DELFIA enhancement solution (PerkinElmer Life Sciences) was added. After 10 min, time-resolved fluorescence was measured using 340 nm excitation and 612 nm emission filters with a BMG Lab Technologies Polarstar fluorometer (Mornington, Australia). Assays on insulin analogues were performed in triplicate.

3 Variation of A6-A11 dicarba bridge rigidity through synthesis of alkynyl- and *S*-allylcysteine-derived dicarba-insulins

3.1 Overview

Ring-closing alkyne metathesis (RCAM) can be employed to generate sp-hybridised dicarba-peptides *via* transformation of the butynylglycine (Bug)-containing precursors. Thereafter the alkynyl bridge can be selectively reduced to the *E*- or *Z*-olefin or fully reduced to the saturated analogue. RCAM has been shown to work orthogonally to RCM in some instances and with alkyne protecting groups (i.e. $CoCO_x$-complexation) in others, permitting facile, selective formation of both alkyne and alkene bridges within the same substrate.[118] It was thus envisioned that this process could be applied to butnylglycine-containing precursor **24** to give, downstream, the alkynyl-dicarba-containing insulin analogue **25** (Scheme 8). This strategy has been employed in the synthesis of a *bis*-dicarba analogue of the α-conotoxin Vc1.1.[93]

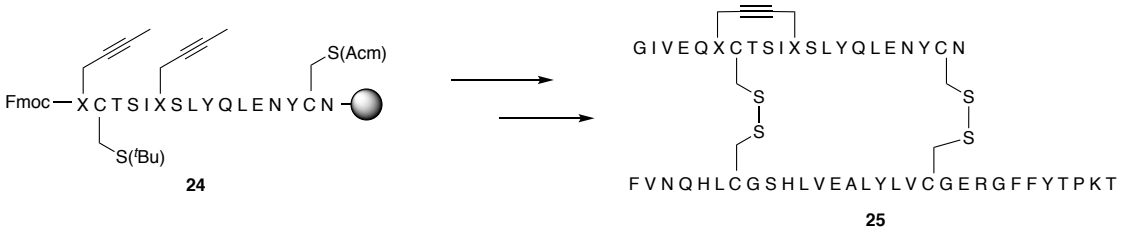

Scheme 8 - General scheme for synthetic inclusion of an alkyne intrachain bridge in human insulin.

The principal difficulty encountered with RCAM is the severe moisture and oxygen sensitivity of the canonical transition metal catalysts involved. Whilst catalysts such as Schrock's tungsten-alkylidyne catalyst **26**[119] and Fürstner's molybdenum complexes, e.g. **27**[120-121] (Figure 17) have demonstrated good functional group tolerance (requisite for use in a peptide context), difficulties in their handling have precluded ready deployment in dicarba peptide synthesis. Perhaps unsurprisingly, only a relatively small number of alkynyl dicarba-peptidomimetics have been reported.[122-125]

Initially, only small macrocycles, 4-7 residues in composition, could be constructed using this system, conducted in the liquid phase rather than on solid support.[126-127] Attention to RCAM on the solid phase remained sparse until recently, when a system described by Cromm *et al*. was employed in the synthesis of a GTPase Rab8 inhibitor analogue.[124-125] This analogue was synthesised using the tris(triphenylsilyloxy)molybdenum alkylidyne complex **27** developed by Fürstner[128] (Figure 17) and it demonstrated high affinity for its target GTPase.

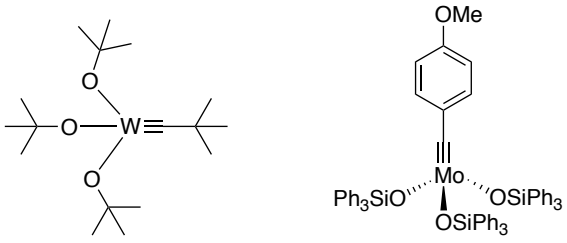

26 **27**

*Figure 17 - Catalysts commonly employed for RCAM; Schrock's tungsten-alkylidyne complex **26** and Fürstner's molybdenum-alkylidyne complex **27**.*

Synthesis of analogue **25** was to proceed in similar fashion to those described earlier in Chapter 2, however with two caveats – extensive drying of the resin-bound peptide and pseudoproline inclusion. An extensive resin-drying procedure (whereby water was repeatedly azeotropically removed from the peptidyl resin under reduced pressure) was developed and resulted in successful, reproducible cyclisation of an α-conotoxin Vc1.1 alkynyl dicarba-analogue.[96] Subsequent inclusion of a pseudoproline residue, designed to disrupt deleterious aggregation and orient the reacting alkyne termini into a favourable position, was foreseen to promote reticent RCAM where required.

In addition to the alkynyl analogue **25**, a linear sequence incorporating two allylated cysteine residues **28** was prepared to generate a pair of ring-closed *S*-allylcysteine analogues **29** (Scheme 9). It was considered that the larger macrocyclic moiety of the *S*-allylcysteine analogues would impart a beneficial conformational shift within the

structure if this flexibility was requisite.[129] Additionally, RCM of these analogues was expected to be facile given the propensity of the *S*-allyl moiety to readily undergo metathesis.[130] Conversely, it was anticipated that the smaller C-C distance of the alkyne compared with the *S*-allylcysteine analogues, as well the moiety's greater rigidity (conferred by its linear geometry) would lock insulin into a predominately inactive conformation, demonstrating that flexibility around the A6-A11 linkage is essential for insulin's activity.

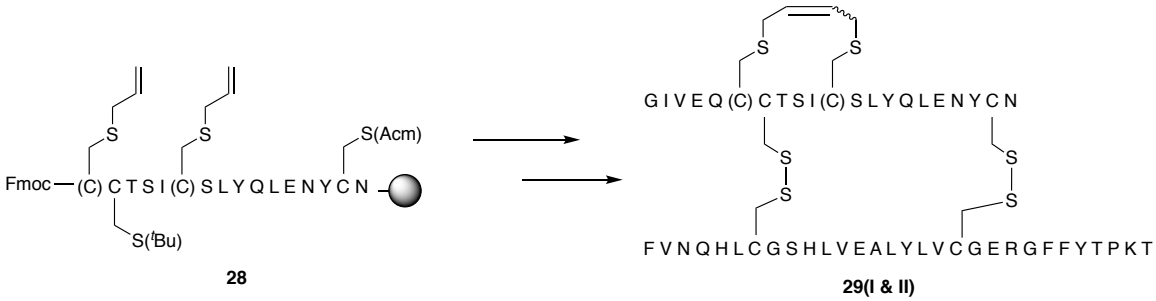

Scheme 9 - General scheme for synthetic inclusion of an S-allylcysteine-linked intrachain bridge in human insulin.

These strategies were thus used to determine the spatial range of the A6-A11 linkage required for a bioactive conformation.

3.2 Results and Discussion

With a protocol for on-resin RCAM in hand, attention turned to the synthesis of the requisite insulin A6-A11 dicarba peptidomimetic. The insulin A-chain sequence is substantially larger than that of the aforementioned GTPase Rab8 inhibitor[124] and the resulting macrocycle is more constrained. As such, we wished to use the resulting alkynyl linkage as a cystine bioisostere rather than as a stabilising hydrocarbon staple.

Synthesis of the target analogue **25** began in analogous fashion to the analogues described in Chapter 2. Truncated insulin A-chain **24** was synthesised *via* Fmoc-SPPS, employing HATU chemistry to generate the active esters *in situ*. L-Butynylglycine (Bug) was incorporated at the A6 and A11 positions and the Fmoc protecting group retained at the *N*-terminus (A6). The peptide-loaded resin was then suspended in dry THF and subjected to multiple cycles of azeotropic distillation before being placed under vacuum at 100 °C overnight. RCAM employing Schrock's catalyst **26** was then attempted on the dried resin-bound peptide. Despite multiple attempts under inert and dry conditions, the desired macrocycle could not be afforded using this approach. No formation of **30** was observed by small-scale cleavage and RP-HPLC analysis of the resin (Scheme 10).

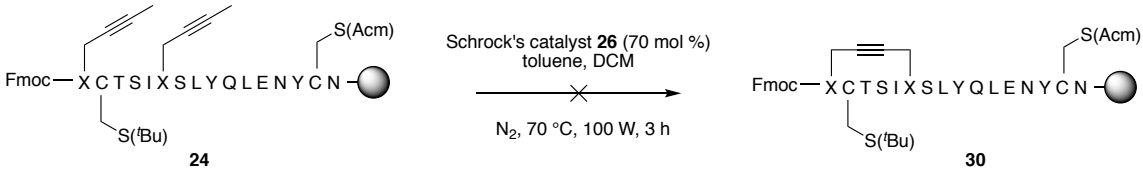

*Scheme 10 - Attempted synthesis of alkynyl-dicarba insulin A-chain fragment **30**.*

It was inferred that the reacting alkynyl termini may either not be sufficiently localised to permit macrocycle formation or deleterious aggregation may be occurring, hindering catalyst access to the substrate.[85] To alleviate both of these potential problems, it was envisioned that incorporation of the pseudoproline dipeptide Cys(*t*Bu)-Thr($\Psi^{Me,Me}$Pro)

(Figure 18, Fmoc-protected precursor **31** shown) would induce a backbone turn conducive to cyclisation. This strategy has been used successfully to promote RCM in reticent sequences.[88, 131] The placement of the pseudoproline dipeptide within the sequence was informed by the anticipated maximum turn radius as well as previous success in this approach with the alkenyl analogue.[88]

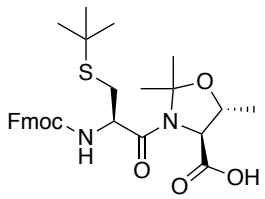

31

*Figure 18 - Fmoc-Cys(tBu)-Thr(ΨMe,MePro)-OH pseudoproline dipeptide derivative **31**.*

Synthesis of pseudoproline dipeptide **31** began with the activation of commercially available Fmoc-Cys(*t*Bu)-OH **32** by reaction with cyanuric fluoride **33** to give the target acyl fluoride **34** (Scheme 11). The acyl fluoride **34** was then coupled to threonine under basic aqueous conditions, giving the partially-protected dipeptide **35** in 67% yield over two steps. **35** then underwent microwave-assisted condensation on treatment with 2,2-dimethoxypropane in DCM to give the desired oxazolidine **31** in 59% yield (Scheme 11).

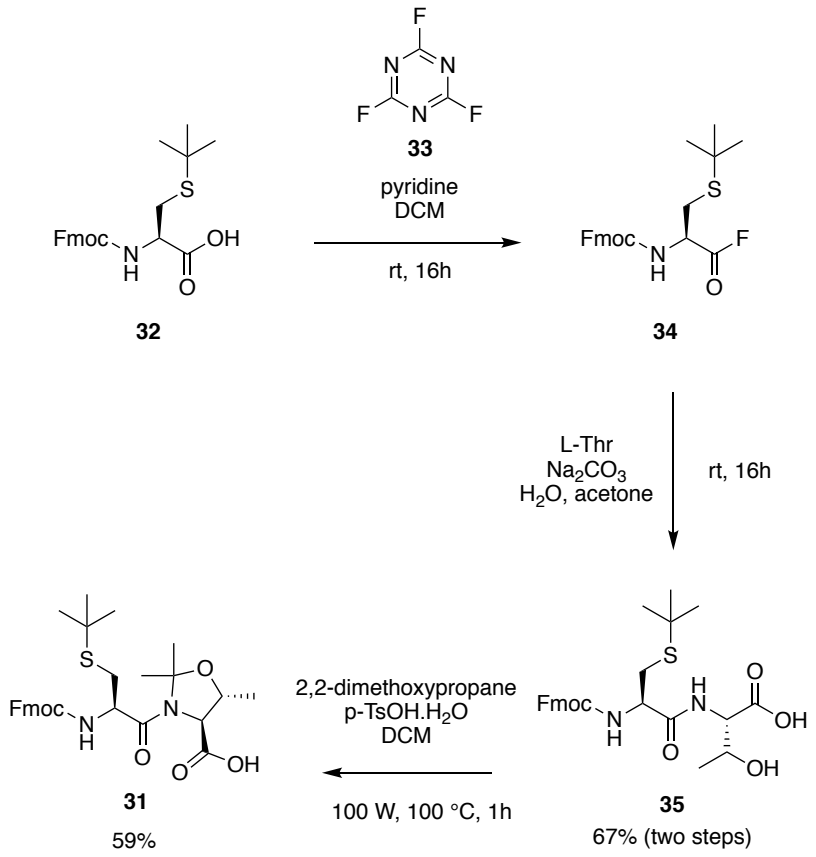

*Scheme 11 - Synthesis of Cys(tBu)-Thr($\Psi^{Me,Me}$Pro) dipeptide unit **31**.*

Coupling of the pseudoproline dipeptide **31** to the resin-bound sequence **36** proved to be difficult, ostensibly due to the increased steric bulk of the substituted oxazolidine and the difficulty encountered removing acetic acid from the final reaction product. Despite multiple microwave-assisted coupling cycles, an approximate maximum coupling yield (by RP-HPLC) of only 50% was accomplished (Scheme 12). Interestingly, small scale TFA cleavage of a resin-peptide aliquot did not result in complete ring-opening of the pseudoproline oxazolidine moiety to give Thr-deprotected peptide, such that the major product of the cleavage retained the intact oxazolidine (**37**). It was envisioned that downstream treatment with triflic acid would effect the transformation to the native threonine.

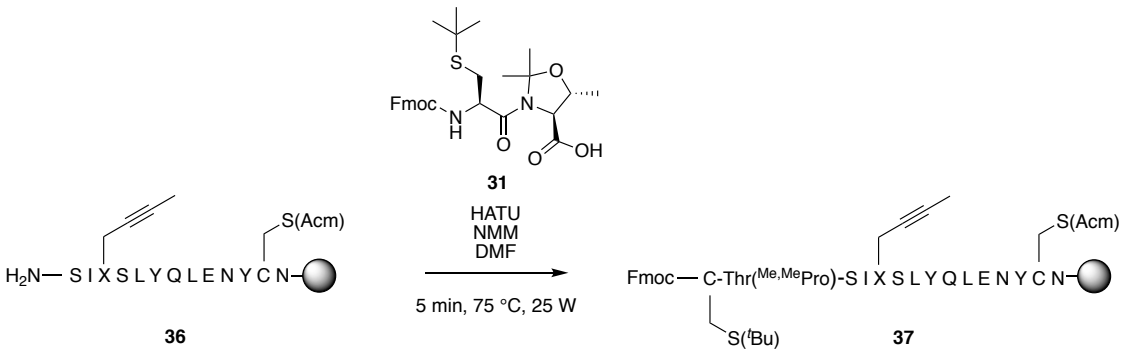

*Scheme 12 - Coupling of pseudoproline dipeptide **31** to butynylglycine-containing insulin A-chain precursor **36***

After Fmoc deprotection, an additional L-butynylglycine residue was coupled *via* microwave-assisted SPPS giving the desired pseudoproline-containing RCAM precursor sequence **38**. Resin-bound peptide **38** was then subjected to the aforementioned resin drying procedure. Gratifyingly, the pseudoproline-inclusive sequence underwent full conversion to the desired alkynyl macrocycle **39** determined by RP-HPLC and LRMS (Scheme 13).

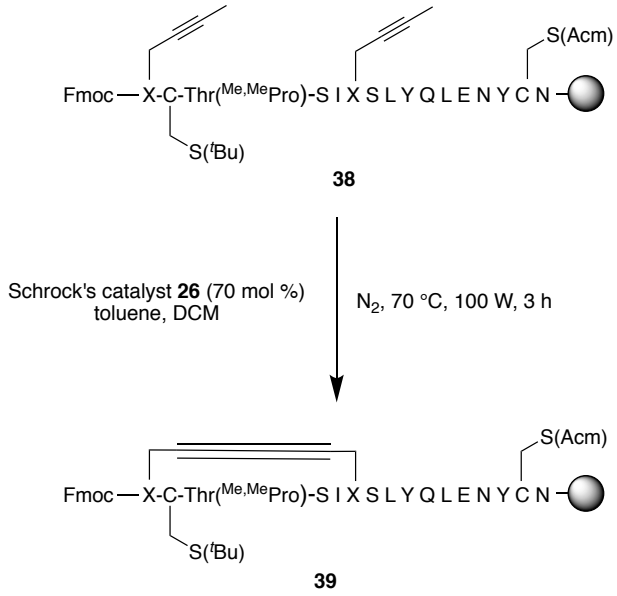

*Scheme 13 - RCAM of pseudoproline-containing alkynyl-dicarba insulin A-chain fragment **38***

Subsequent residues A1-A5 were appended to the *N*-terminus *via* automated SPPS and the complete insulin A-chain analogue cleaved from the resin with TFA and scavengers.

The crude peptide was then treated with triflic acid and DPDS, concertedly removing the *tert*-butyl protecting group from the A7 cysteine residue and giving the *S*-pyridyl derivative **40** (Scheme 14).

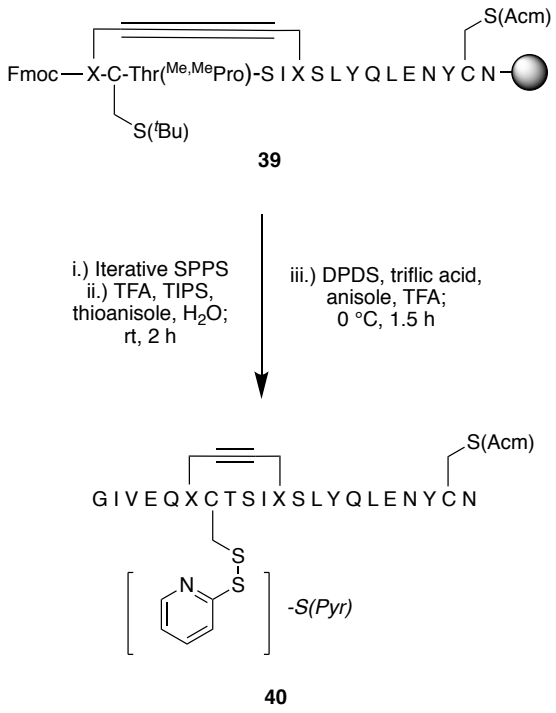

*Scheme 14 - Synthesis of alkynyl-dicarba insulin A-chain -SPyr derivative **40***

Importantly, this treatment facilitated full ring-opening of the reticent pseudoproline oxazolidine, giving the native threonine residue as indicated by analytical RP-HPLC and the correct mass identified in the mass spectrum. Prior to combination with human insulin B-chain, crude *S*-pyridinyl-protected peptide **40** was purified *via* preparative RP-HPLC, enabling removal of the truncated sequences arising from incomplete coupling of the pseudoproline dipeptide. Upon addition of an aqueous solution of human insulin B-chain **9** to the *S*-pyridyl derivative **40** in aqueous ammonium bicarbonate buffer (50 mM), the penultimate two-chain species **41** was formed and verified by RP-HPLC and LRMS (Scheme 15). All peptides thus formed were obtained in >90% purity after preparative HPLC.

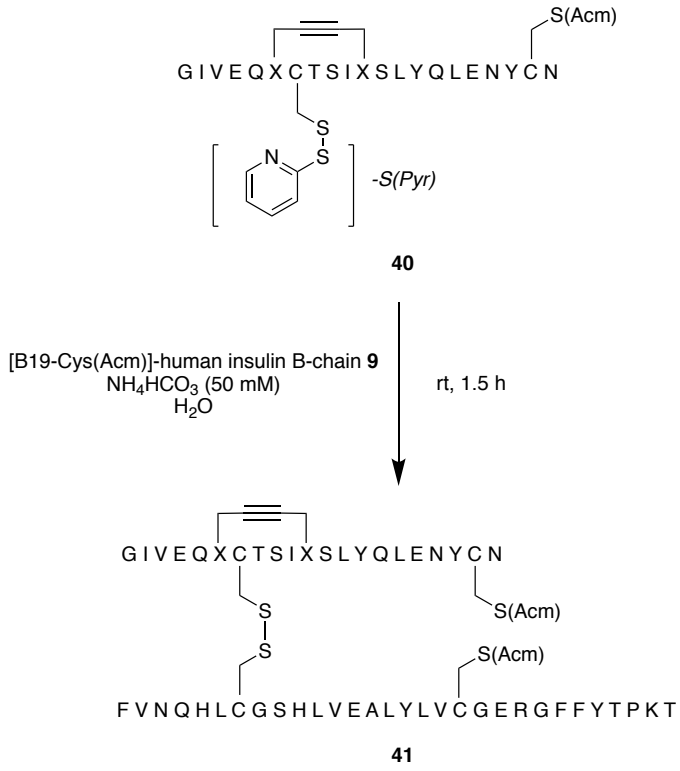

*Scheme 15 - Combination of alkynyl insulin A-chain-SPyr derivative **40** with B-chain **9***

The final A20-B19 linkage was formed *via* iodine-mediated oxidation in acetic acid, effecting removal of the Acm protecting group and subsequent formation of the interchain disulfide (Scheme 16). Chromatographic purification of the resulting complete insulin analogue **25** on a preparative scale proved challenging due to overlap of the elution time of the desired species with that of unreacted insulin B-chain. Despite attempted optimisation of elution conditions, the desired species could only be obtained through separation *via* an *analytical* RP-HPLC column, which provided sufficient separation resolution albeit with protracted processing. Ultimately, lyophilisation of the combined fractions gave the target peptide which was verified by LRMS.

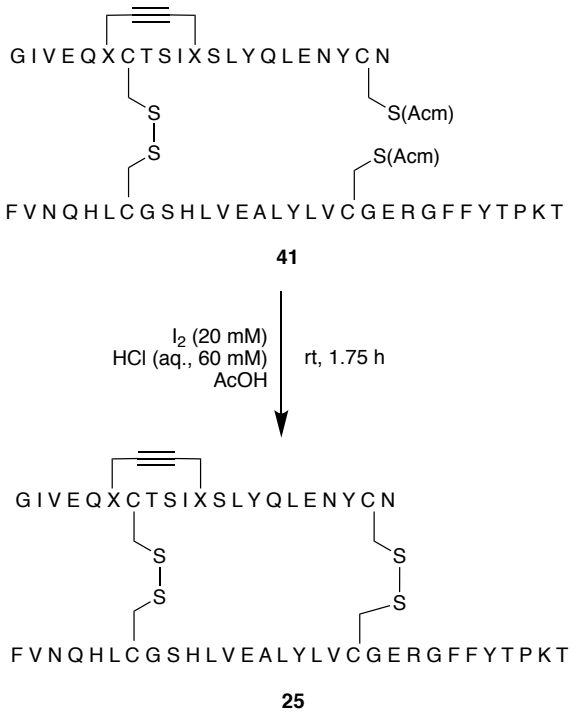

*Scheme 16 - I_2 mediated oxidation of dimeric precursor **41** to alkynyl insulin analogue **25***

Synthesis of the *S*-allyl cysteine analogues **29** was carried out in analogous fashion to that of the alkenyl-dicarba analogues **11**-**13**. Commercially available *S*-allyl cysteine was substituted in the A6 and A11 positions of precursor **28**. It should be noted that pseudoproline incorporation was not necessary for the synthesis of this analogue owing to the metathesis-promoting nature of coordinating *S*-allyl residues and larger ring size.[130, 132] RCM of **28** using Grubbs' 2nd Generation catalyst (GII) gave complete conversion to the desired carbocycle **42**. The remainder of the peptide was constructed in identical fashion to that of the alkynyl analogue **25**: After metathesis, the A-chain of **42** was extended and the full A-chain was activated and combined with the B-chain **9** to give **43**. Subsequent oxidation then yielded the target insulin construct **29** as a pair of geometric isomers (Scheme 17).

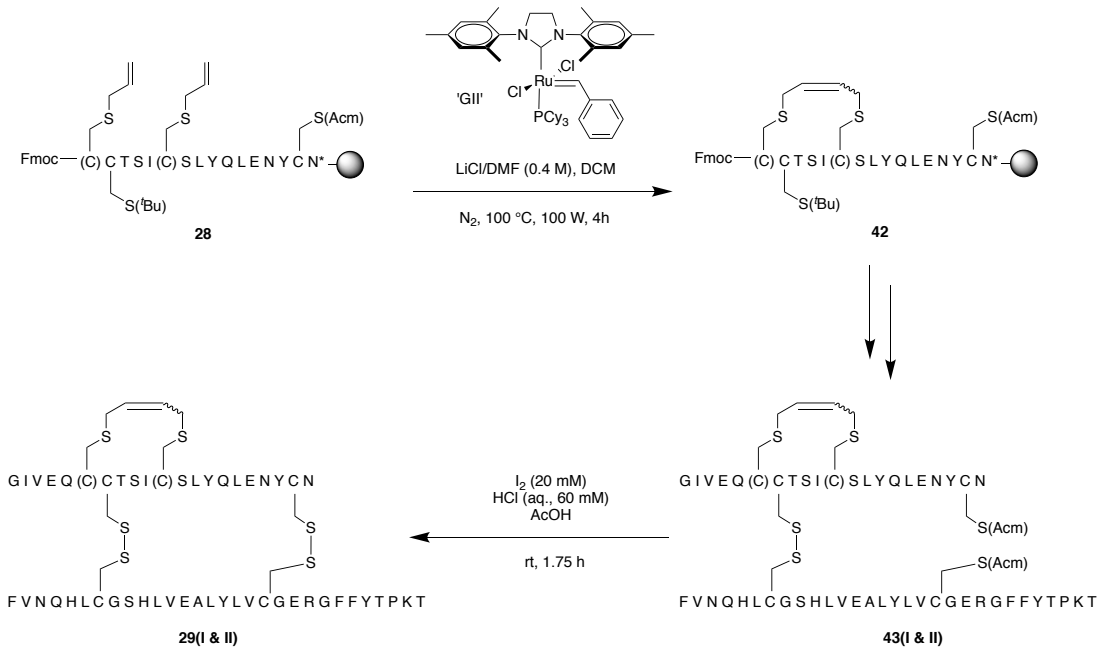

*Scheme 17 - Synthesis of S-allylcysteine-containing dicarba insulin analogues **29**.*

The capacity of the three insulin peptidomimetics **25**, **29(I)** and **29(II)** to act as ligands and displace human insulin from recombinant human insulin receptor isoform B (IR-B) was assessed in a competitive binding assay (Figure 19). Europium-labelled human insulin was displaced by native hINSL in a concentration dependent manner (IC_{50} 0.86 ± 0.10 nM).[95] Two dicarba analogues, A6-A11-[alkynyl-dicarba] **25** and *S*-allylcysteine-derived **29(II)**, also displaced [Eu]-insulin binding (Figure 19). While chemical modification of the native A6-All cystine bridge was tolerated in these analogues, there was an accompanying loss of affinity of ≳100 fold. The isomeric ring-expanded insulin isomer **29(I)** was inactive (Figure 19).

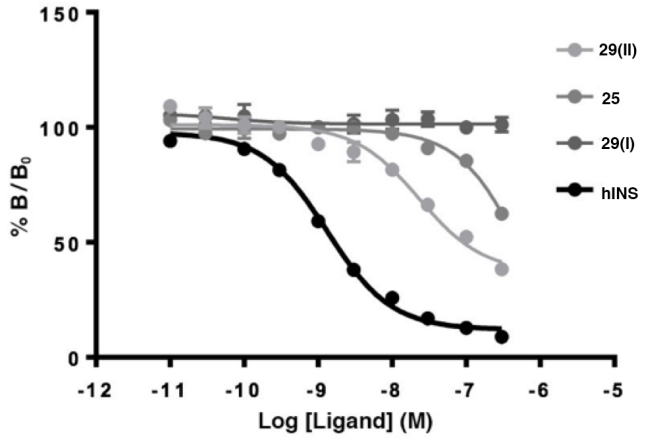

*Figure 19 - Binding affinity of human insulin (hINS) and synthetic analogues **25** and **29(I & II)** determined by displacement of Eu-labelled insulin from IR-B.*

These results highlight insulin's remarkable sensitivity to localised conformational change at the intrachain cystine bridge. Vast differences in activity are also observed with A6-A11-[alkene-dicarba] insulin geometric isomers synthesised by van Lierop *et al*.; the previously identified *cis*-isomer binds IR-B with similar affinity to native insulin (IC_{50} 0.75 ± 0.16 nM), whereas the *trans*-isomer has ~50-fold lower affinity (IC_{50} 40.4 ± 7.2 nM) for IR-B than native insulin.[95, 97] The ideal dihedral angle for disulfides is ± 90°, however deviation from this is widely encountered and such variation will affect redox activity and conformational stability. Native cystine bridges present with twenty different disulfide geometries where each of the five chi (χ) angles within the four atom bridging motif of Cα-**Cβ-Sγ-Sγ′-Cβ′**-Cα′ can be positive or negative.[61] Identifying insulin's bioactive A6-A11 cystine configuration, as opposed to its circulating and crystallographic conformation, and replacing it with bioisosteric functionality is highly challenging. Diaminosuberic acid analogues of the native cystine bridge possess comparable interatomic distance (Cα-Cβ-**Cγ-Cγ′**-Cβ′-Cα′) and polarity. The ease with which they can be generated, *via* metathesis and hydrogenation, coupled with their varying hybridisation sp-sp^2-sp^3 (Cγ≡Cγ′, Cγ=Cγ′, Cγ-Cγ′ respectively), geometry and

conformational flexibility, facilitates restriction of conformational mobility and assists with affirming structure-activity relationships.

The analogues **25**, **29(I)** and **29(II)** clearly demonstrate that simple tethering of the side-chains at the A6 and A11 positions is not sufficient to ensure activity; the native cysteine residues are clearly performing an important role in facilitating a bioactive conformation. Though the aforementioned *cis*/*trans* isomers of A6-A11-alkenyl dicarba insulin possess geometries that may be considered extreme when applied to their disulfide counterparts, they are still conceivably within the realm of possibility for highly-strained native peptides. However, this work demonstrates the limits to which these parameters can be pushed, towards high constraint and rigidity or towards the flexibility offered by a relatively large macrocycle, and the consequences of doing so. In addition, the difficulty of the chemistry associated with the generation of the *sp*-hybridised dicarba linkage is illustrated; measures to encourage the crucial metathesis step must be taken into account when designing syntheses of alkynyl-dicarba peptidomimetics.

Conclusions

RCAM represents a viable method for the solid phase synthesis of alkynyl peptidomimetics. Rigorous drying procedures and judicious sequence inclusion of turn-inducing pseudoproline residues facilitate tungsten-alkylidyne metathesis of alkynyl residues. With regards to insulin's structure-activity relationship, the alkynyl analogue **25** and ring-closed *S*-allyl cysteine analogues **29(I)** and **(II)** possess reduced receptor binding affinity akin to the previously discussed *trans*-configured alkenyl analogue (see Section 1.3), in stark contrast to the high activity of the *cis*-configured alkenyl analogue.[95, 97] This observation highlights the often-overlooked role of the hormone's A6-A11 *S*-*S* linkage in modulating insulin's biological activity. This region is thus shown

to be highly sensitive to modification and must be adequately considered in the future development of modified insulins for pharmaceutical applications.

3.3 Experimental

3.3.1 Synthetic Procedures

3.3.1.1 Microwave-assisted on-resin RCAM

Resin-bound peptide (0.1 mmol) was stored for a minimum of 16 hours in an evacuated desiccator containing indicating silica gel. The resin was transferred to a flame-dried Carius tube then placed under N_2. The resin was then suspended in dry THF (2 mL), heated to 40 °C and the THF evaporated under reduced pressure without stirring. This process was repeated twice more, then the resin heated to 100 °C under vacuum (~100 mTorr) for at least 16 hours without stirring. The tube was then backfilled with N_2, allowed to cool and transferred to a drybox (N_2). A standard solution (50 mg/mL) of Schrock's catalyst **26** in dry toluene (0.66 mL, 70 mol %) was added, followed by dry DCM (4 mL). The tube was sealed, removed from the dry box and stirred with constant microwave irradiation (100 W) and heating (70 °C maintained with cooling) for 3 hours. The suspension was allowed to cool then was transferred to a fritted syringe. The suspension was drained, the resin washed with DMF (5x5 mL) and subjected to aerial drying *via* vacuum filtration.

3.3.1.2 Fmoc-L-Cys(ᵗBu)-F 34

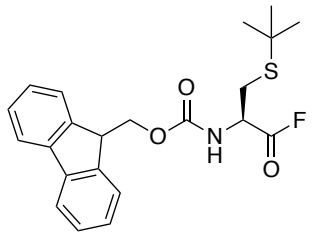

34

Acyl fluoride **34** was prepared according to a procedure described by Carpino *et al.*.[133] To a solution of Fmoc-Cys(ᵗBu)-OH **32** (1.20 g, 3.00 mmol, 1 equiv.) in 23 mL dry DCM was added pyridine (122 µL, 1.6 mmol, 0.53 equiv.) followed by cyanuric fluoride **33** (330 µL, 3.9 mmol, 1.3 equiv.). Formation of an off-white precipitate was observed after

approx. 30 minutes. The resulting mixture was stirred overnight at room temperature before being diluted with deionised H_2O (~25 mL). The phases were separated and the organic phase was dried ($MgSO_4$), filtered and concentrated under reduced pressure to give **34** as a yellow gum (1.10 g). Crude **34** was used in the next synthetic step without purification. Spectral data for **34** were consistent with the literature.[91] ^{1}H-NMR (400 MHz, $CDCl_3$): δ 7.77 (d, *J* = 7.6 Hz, 2H), 7.59 (d, *J* = 7.6 Hz, 2H), 7.41 (t, *J* = 7.2 Hz, 2H), 7.32 (t, *J* = 7.4 Hz, 2H), 5.70 (d, *J* = 8 Hz, NH), 4.82 (m, 1H), 4.44 (m, 2H), 4.24 (t, *J* = 6.8 Hz, 1H), 3.05 (d, *J* = 4 Hz, 2H), 1.34 (s, 9H). ^{13}C-NMR (150 MHz, $CDCl_3$): δ 162.8, 153.7, 143.8, 141.4, 127.9, 127.2, 125.1, 120.1, 67.7, 53.0, 47.1, 42.8, 30.9, 30.0.

3.3.1.3 Fmoc-L-Cys(*t*Bu)-L-Thr-OH 35

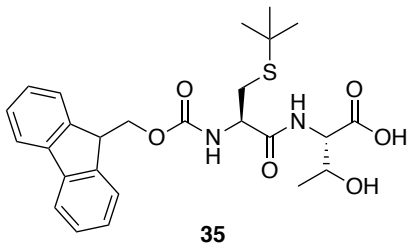

35

The partially-protected dipeptide **35** was prepared according to a procedure described by Wohr *et al*..[134] To a stirred solution of Fmoc-Cys(*t*Bu)-F **34** (1.10 g, 2.7 mmol, 1 equiv.) in acetone (50 mL) was added a solution of L-threonine (978 mg, 8.2 mmol, 3 equiv.) in 10% w/v aqueous Na_2CO_3 (11 mL). Formation of a colourless precipitate was observed after approx. 10 minutes. The resulting mixture was stirred overnight at room temperature. The acetone was then removed under reduced pressure, EtOAc (~20 mL) added and the solution acidified to pH ~2 with 1 M aqueous HCl. The phases were then separated and the aqueous phase was extracted with EtOAc (3x80 mL). The combined organic extract was washed with brine (~100 mL), dried ($MgSO_4$), filtered and concentrated under reduced pressure to give a yellow gum (1.46 g). Purification by column chromatography (silica, 1:1:0.1:0.05 EtOAc:petroleum ether:MeOH:AcOH)

gave the desired compound **35** as a pale yellow foam (1.00 g, 67% over two steps). Spectral data were consistent with those in the literature.[91] ^{1}H-NMR (400 MHz, $CDCl_3$): δ 7.74 (d, *J* = 7.2 Hz, 2H), 7.58 (d, 6.8 Hz, 2H), 7.42-7.37 (m, 4H), 7.27 (t, *J* = 5.6 Hz, 2H), 5.87 (d, *J* = 6.4 Hz, NH), 4.62 (d, *J* = 8.4 Hz, 1H), 4.50 (bm, 1H), 4.43 (m, 2H), 4.36 (m, 1H), 4.22 (t, *J* = 7.2 Hz, 1H), 2.99-2.85 (m, 2H), 1.29 (s, 9H), 1.21 (d, *J* = 6.4 Hz, 3H). ^{13}C-NMR (150 MHz, $CDCl_3$): δ 173.5, 171.5, 156.6, 143.7, 141.4, 127.9, 127.3, 125.3, 120.1, 68.4, 67.8, 57.7, 54.7, 47.2, 43.1, 31.0, 20.7, 19.6.

3.3.1.4 Fmoc-L-Cys(*t*Bu)-L-Thr(Ψ^{Me,Me}Pro)-OH 31

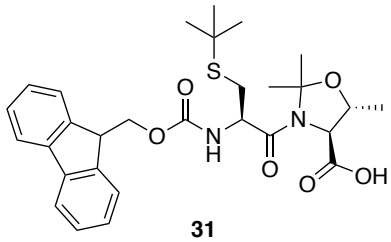

31

Fmoc-Cyst(*t*Bu)-Thr-OH **35** (519 mg, 1.0 mmol, 1 equiv.) was dissolved in 6 mL of dry DCM in a 10 mL microwave tube to which was then added *p*-TsOH monohydrate (21 mg, 0.11 mmol, 11 mol %) and 2,2-dimethoxypropane (1.04 g, 1.2 mL, 10 mmol, 10 equiv.). The vessel was then sealed and heated to 100 °C with microwave irradiation (100 W) for 1 h. The reaction mixture was then allowed to cool, diluted with deionised H_2O (6 mL), the phases separated and the organic phase concentrated under reduced pressure to give a brown oil (660 mg). Purification *via* column chromatography (silica, 1:1:0.1:0.05 EtOAc:petroleum ether:MeOH:AcOH) gave the desired compound **31** as a pale yellow foam (330 mg, 59%). Spectral data were consistent with those in the literature.[91] ^{1}H-NMR (400 MHz, $CDCl_3$): δ 7.70 (d, *J* = 7.5 Hz, 2H), 7.51 (dd, *J* = 13.1, 7.5 Hz, 2H), 7.39-7.30 (m, 2H), 7.30-7.19 (m, 2H), 6.12 (d, *J* = 8.7 Hz, NH), 4.45 (bd, *J* = 6.4 Hz, 1H), 4.41-4.29 (m, 2H), 4.25 (bd, *J* = 7.3 Hz 2H), 4.10 (t, *J* = 7.3 Hz, 1H), 2.72-2.83 (m, 2H), 1.70 (s, 3H), 1.58 (s, 3H), 1.46 (d, *J* = 6 Hz, 3H), 1.29 (s, 9H); OH not

observed. ^{13}C-NMR (150 MHz, $CDCL_3$): δ 172.8, 168.8, 156.2, 144.0, 141.4, 127.9, 127.2, 125.3, 120.1, 97.6, 75.2, 67.7, 66.5, 53.8, 47.1, 43.2, 31.0, 26.4, 23.9, 19.9.

3.3.1.5 *des*$_{A1\text{-}5}$-[A6,A11]-Bug-[A7]-Cys(^{t}Bu)-[A8]-Thr(Ψ^{Me,Me}Pro)-[A20]-Cys(Acm) human insulin A-chain 38

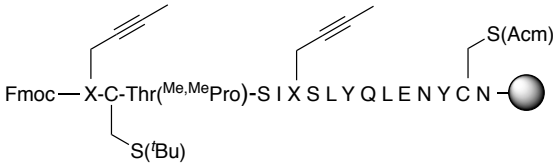

38

The resin-bound peptide **38** excluding the three *N*-terminal residues was prepared on an 0.1 mmol scale according to the general automated procedure outlined in Section 2.3.3.1. Fmoc-Cys(^{t}Bu)-Thr(Ψ^{Me,Me}Pro)-OH **31** was attached according to the general manual microwave-assisted SPPS procedure outlined in Section 2.3.3.3 with the following quantities of reagents: Fmoc-Cys(^{t}Bu)-Thr(Ψ^{Me,Me}Pro)-OH **31** (162 mg, 0.3 mmol, 3 equiv.), HATU (114 mg, 0.3 mmol, 3 equiv.), NMM (66 μL, 0.6 mmol, 6 equiv.) in DMF (4 mL). Successful coupling was subsequently verified by small-scale Fmoc deprotection and resin cleavage, RP-HPLC and LRMS. RP-HPLC (Agilent: Vydac C18 analytical column, 15 to 50% buffer B over 35 min): t_R = 22.3 min. Mass spectrum (ESI$^+$, MeCN:H_2O:TFA): *m/z* 964.7 $[M+2H]^{2+}$, ½($C_{86}H_{132}N_{19}O_{27}S_2$) requires 963.9. Fmoc-L-butynylglycine was then attached according to the general manual microwave-assisted SPPS procedure outlined in Section 2.3.3.3 with the following quantities of reagents: Fmoc-Bug-OH (109 mg, 0.3 mmol, 3 equiv.), HATU (119 mg, 0.3 mmol, 3 equiv.), NMM (66 μL, 0.6 mmol, 6 equiv.) in DMF (4 mL). Formation of **38** (with ring-opening of the pseudoproline residue) was subsequently verified by small-scale Fmoc deprotection and resin cleavage, RP-HPLC and LRMS. RP-HPLC (Agilent: Vydac C18 analytical column, 15 to 50% buffer B over 35 min): t_R = 19.1 min. Mass spectrum (ESI$^+$, MeCN:H_2O:TFA): *m/z* 998.4 $[M+2H]^{2+}$; ½($C_{89}H_{136}N_{20}O_{28}S_2$) requires 998.5.

3.3.1.6 *des*$_{A1-5}$-[Δ^4-alkynyl-A6-A11]-dicarba-[A7]-Cys(^{t}Bu)-[A8]-Thr($\Psi^{Me,Me}$Pro)-[A20]-Cys(Acm) human insulin A-chain 39

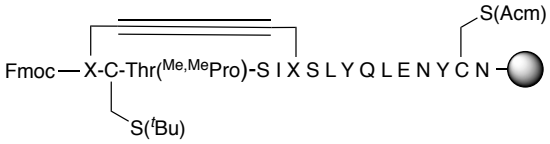

39

The resin-bound peptide **38** was subjected to the general RCAM procedure outlined in Section 3.3.1.1 using the following amounts of reagents: Schrock's catalyst **26** (33 mg, 0.66 mL of a 50 mg/mL solution in dry toluene, 70 mol %), dry DCM (4 mL). Full conversion to **39** from starting material was subsequently verified by small-scale Fmoc deprotection and resin cleavage, RP-HPLC and LRMS. RP-HPLC (Agilent: Vydac C18 analytical column, 15 to 50% buffer B over 35 min): t_R = 22.6 min. Mass spectrum (ESI$^+$, MeCN:H_2O:TFA): *m/z* 991.6 $[M+2H]^{2+}$, ½($C_{88}H_{134}N_{20}O_{28}S_2$) requires 991.5.

3.3.1.7 [Δ^4–alkynyl-A6-A11]-dicarba-[A7]-Cys(^{t}Bu)-[A20]-Cys(Acm) human insulin A-chain 44

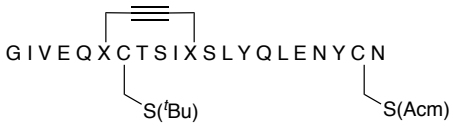

44

Peptide **44** was prepared from resin-bound **39** according to the general automated procedure outlined in Section 2.3.3.1. Formation of **44** was subsequently verified by small-scale cleavage, RP-HPLC and LRMS. RP-HPLC (Agilent: Vydac C18 analytical column, 15 to 50% buffer B over 35 min): t_R = 21.5 min. Mass spectrum (ESI$^+$, MeCN:H_2O:TFA): *m/z* 822.3 $[M+3H]^{3+}$, ⅓($C_{108}H_{169}N_{26}O_{36}S_2$) requires 823.4 (data not shown). The product was detected in the resultant mixture with the pseudoproline oxazolidine moiety intact: RP-HPLC (Agilent: Vydac C18 analytical column, 15 to 50% buffer B over 35 min): t_R = 23.9 min. Mass spectrum (ESI$^+$, MeCN:H_2O:TFA): *m/z* 837.0

[M+3H]$^{3+}$, ⅓($C_{111}H_{173}N_{26}O_{36}S_2$) requires 836.7; *m/z* 1254.9 [M+2H]$^{2+}$, ½($C_{111}H_{172}N_{26}O_{36}S_2$) requires 1254.6. The resin was then subjected to Fmoc deprotection and TFA-mediated resin cleavage (Sections 2.3.3.5 and 2.3.3.7, respectively), the residue dissolved in MeCN:H_2O (~1:5) and lyophilised to give the desired crude peptide as a off-white solid.

3.3.1.8 [Δ^4–alkynyl-A6-A11]-dicarba-[A7]-Cys(SPyr)-[A20]-Cys(Acm) human insulin A-chain 40

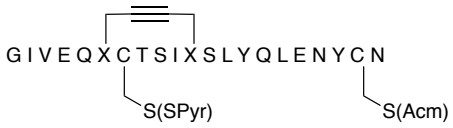

40

The concerted *tert*-butyl deprotection and *S*-pyridinyl protection at Cys A7 was executed according to the procedure described by Büllesbach and Schwabe.[110] To a solution of anisole:TFA (1:9, 6.5 mL) was added 2,2'-dipyridyldisulfide (44.1 mg, 0.2 mmol, 2 equiv.) and the resulting solution cooled to 0 °C in an ice bath. To this solution was added lyophilised crude peptide **44** (0.1 mmol) followed by a chilled solution of triflic acid:TFA (1:4, 6.5 mL). The resulting light brown solution was stirred at 0 °C for 1.5 hours upon which the solution was concentrated under a stream of N_2 and the crude peptide precipitated with chilled ether (30 mL). The suspension was centrifuged, the supernatant discarded, and the precipitate resuspended and centrifuged in chilled ether (30 mL) a further two times. The crude peptide was then dissolved in MeCN:H_2O (1:1) and lyophilised to give **40** as a red solid (305 mg). Formation of **40** was subsequently verified by RP-HPLC and LRMS. RP-HPLC (Agilent: Vydac C18 analytical column, 15 to 50% buffer B over 35 min): t_R = 18.0 min. Mass spectrum (ESI$^+$, MeCN:H_2O:TFA): *m/z* 841.0 [M+3H]$^{3+}$, ⅓($C_{109}H_{164}N_{27}O_{36}S_3$) requires 841.0; *m/z* 1261.4 [M+2H]$^{2+}$, ½($C_{109}H_{163}N_{27}O_{36}S_3$) requires 1261.1. Peptide **40** was purified *via* preparative RP-HPLC (Agilent: Vydac C18 preparative column, 15 to 45% buffer B over

40 min) and selected fractions combined and lyophilised to give **40** (t_R = 22.1 min) which was analysed by RP-HPLC and LRMS. RP-HPLC (Agilent: Vydac C18 analytical column, 15 to 50% buffer B over 35 min): t_R = 18.2 min. Mass spectrum (ESI^+, MeCN:H_2O:TFA): *m/z* 1261.8 $[M+2H]^{2+}$, ½($C_{109}H_{163}N_{27}O_{36}S_3$) requires 1261.1; *m/z* 841.4 $[M+3H]^{3+}$, ⅓($C_{109}H_{164}N_{27}O_{36}S_3$) requires 841.0.

3.3.1.9 [Δ^4–alkynyl-A6-A11]-dicarba-[A20, B19]-Cys(Acm) human insulin 41

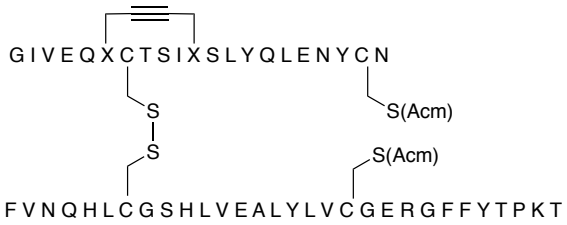

41

Combination of the A- and B-chain monomers was executed according to a modified version of a procedure originally described by Lin *et al.*.[111] Peptide **40** (1.1 mg, ~0.44 μmol) was dissolved in 50 mM aqueous NH_4HCO_3 (1 mL). [B19]-Cys(Acm) human insulin B-chain **9** (0.83 mg, 0.24 μmol) was dissolved in MilliQ H_2O (1 mL) and added dropwise to the solution of **40**. The reaction mixture was stirred at room temperature with monitoring *via* RP-HPLC and LRMS. After 1.5 hours, additional [B19]-Cys(Acm) human insulin B-chain **9** (0.50 mg, 0.14 μmol) dissolved in MilliQ H_2O (0.5 mL) was added to the reaction mixture. The reaction was stirred for an additional 2.75 hours then quenched by addition of glacial AcOH to pH ~2 and the resulting solution lyophilised to give crude **41** as a colourless solid (3.4 mg). RP-HPLC (Agilent: Vydac C18 analytical column, 0 to 25% buffer B over 5 min then 25 to 50% buffer B over 30 min): t_R = 18.0 min. Mass spectrum (ESI^+, MeCN:H_2O:TFA): *m/z* 1479.4 $[M+4H]^{4+}$, ¼($C_{265}H_{399}N_{67}O_{79}S_4$) requires 1478.0.

3.3.1.10 [Δ⁴-alkynyl-A6-A11]-dicarba human insulin 25

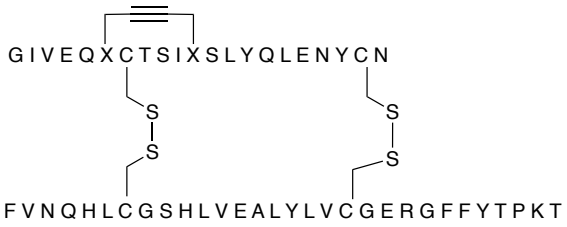

25

Oxidation of the insulin analogue precursor **41** was executed according to a procedure described by Lin *et al*..[111] Crude **41** (3.4 mg) was suspended in a 60 mM aqueous HCl solution (80 μL) followed by glacial AcOH (1.32 mL) to affect dissolution. A 20 mM solution of iodine in glacial acetic acid (1.32 mL) was added and the resulting solution stirred in darkness for 1.5 hours, exposed to light and stirred for a further 0.5 hours before being poured into chilled Et_2O (2x30 mL). The resulting suspension was cooled to 0 °C, centrifuged (5000 rpm, 4 min), the supernatant discarded. The residue was suspended in MeCN (~0.5 mL) and 20 mM ascorbic acid aqueous solution (~0.5 mL) and purified by preparative RP-HPLC (Agilent: Vydac C18 preparative column, 0 to 30% buffer B over 5 min then 30 to 40% buffer B over 30 min): t_R = 15.6 min to give crude **25** as a colourless solid. Mass spectrum (ESI^+, MeCN:H_2O:TFA): *m/z* 1442.7 $[M+4H]^{4+}$, ¼($C_{259}H_{383}N_{65}O_{77}S_4$) requires 1441.9. The crude peptide **25** was then subjected to further purification *via* analytical-scale RP-HPLC (Agilent: Vydac C18 analytical column, 0 to 30% buffer B over 5 min then 30 to 40% buffer B over 30 min): t_R = 15.4 min to give **25** as a colourless solid; RP-HPLC (Agilent: Vydac C4 analytical column at T 40 °C, 25 → 31% buffer B over 5 min then 31→ 50% buffer B over 16 min, flow rate 0.5 mL min^{-1}): t_R = 12.8 min. Buffer A: 0.1% Aqueous TFA; Buffer B: 0.08% TFA in MeCN:H_2O, 80:20. Mass spectrum (ESI^+, MeCN:H_2O:TFA): *m/z* 1442.7 $[M+4H]^{4+}$, ¼($C_{259}H_{383}N_{65}O_{77}S_4$) requires 1441.9.

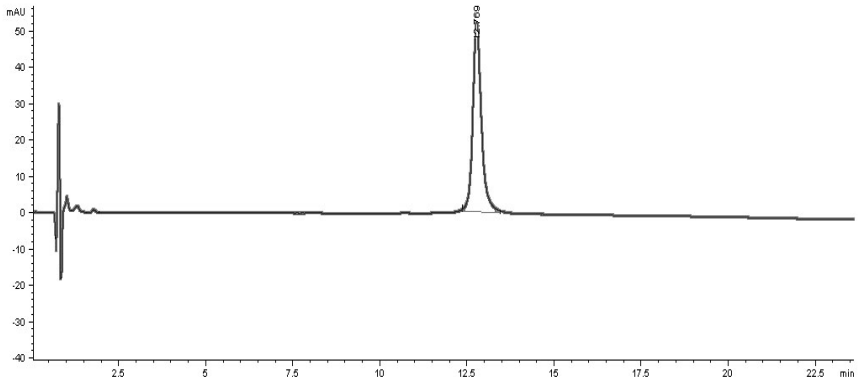
mAU
50
40
30
20
10
0
-10
-20
-30
-40
2.5
5
7.5
10
12.5
15
17.5
20
22.5
min

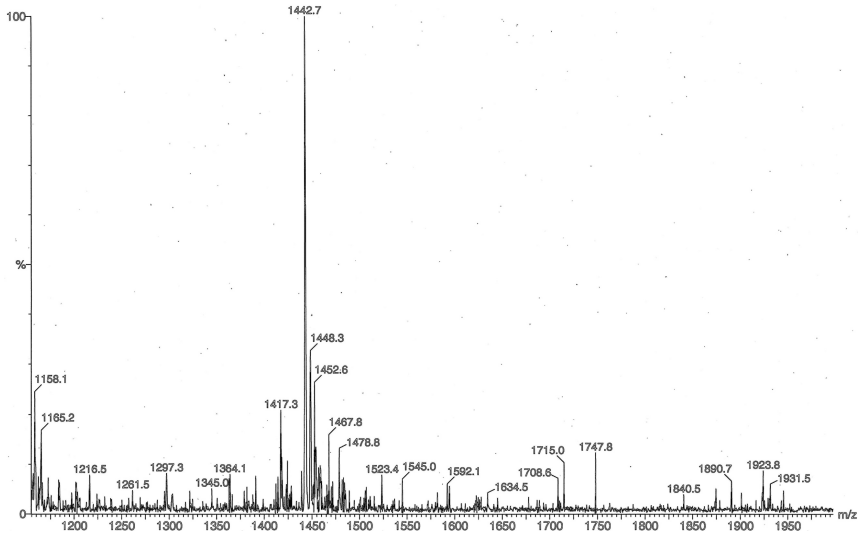
100
%
0
1442.7
1448.3
1452.6
1158.1
1165.2
1417.3
1467.8
1478.8
1216.5
1297.3
1364.1
1261.5
1345.0
1523.4
1545.0
1592.1
1708.6
1634.5
1715.0
1747.8
1890.7
1923.8
1931.5
1840.5
1200
1250
1300
1350
1400
1450
1500
1550
1600
1650
1700
1750
1800
1850
1900
1950
m/z

3.3.1.11 *des*$_{A1\text{-}5}$-[A6,A11]-Sac-[A7]-Cys(^{t}Bu)-[A20]-Cys(Acm) human insulin A chain 28

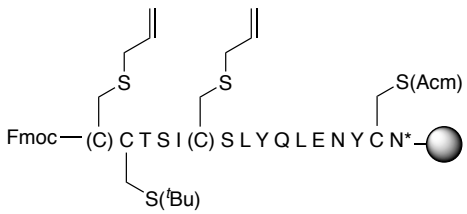

28

The resin-bound peptide **28** was prepared on a 0.1 mmol scale according to the general automated procedure outlined in Section 2.3.3.1. Formation of **28** was subsequently verified by small-scale Fmoc deprotection and resin cleavage, RP-HPLC and LRMS. RP-HPLC (Agilent: Vydac C18 analytical column, 15 → 50% buffer B over 35 min): t_R = 21.6 min. Mass spectrum (ESI$^+$, MeCN:H_2O:TFA): *m/z* 1032.6 $[M + 2H]^{2+}$, ½($C_{89}H_{140}N_{20}O_{28}S_4$) requires 1032.4. The resin-bound peptide was subjected to the capping procedure outlined in Section 2.3.3.6 and stored overnight in a vacuum desiccator prior to RCM.

3.3.1.12 *des*$_{A1\text{-}5}$-[$\Delta^{2'}$Sac-A6-A11]-dicarba-[A7]-Cys(^{t}Bu)-[A20]-Cys(Acm) human insulin A chain 42

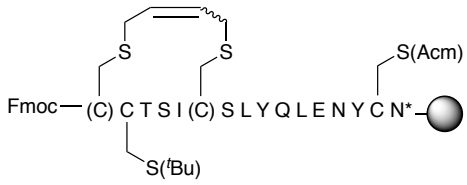

42

Resin-bound peptide **28** was subjected to the general microwave-assisted on-resin RCM procedure outlined in Section 2.3.3.8 with the following quantities of reagents: GII (17 mg, 20 mol %), 0.4 M LiCl/DMF (~0.2 mL), DCM (4 mL) and extension of reaction time to 4 hours. **42** was obtained as a pair of isomers (**42(I)** and **42(II)**) in a 5:1 ratio with ~95% conversion from starting material, verified by small-scale Fmoc deprotection and

resin cleavage, RP-HPLC and LRMS. **42(I)**: RP-HPLC (Agilent: Vydac C18 analytical column, 15 to 50% buffer B over 35 min): t_R = 18.6 min. Mass spectrum (ESI^+, MeCN:H_2O:TFA): *m/z* 1019.0 $[M+2H]^{2+}$, ½($C_{87}H_{136}N_{20}O_{28}S_4$) requires 1018.4; 1358.3 $[2M+3H]^{3+}$, ⅓($C_{174}H_{275}N_{40}O_{56}S_8$) requires 1357.6. **42(II)**: RP-HPLC (Agilent: Vydac C18 analytical column, 15 to 50% buffer B over 35 min): t_R = 19.4 min. Mass spectrum (ESI^+, MeCN:H_2O:TFA): *m/z* 1019.0 $[M+2H]^{2+}$, ½($C_{87}H_{136}N_{20}O_{28}S_4$) requires 1018.4.

3.3.1.13 [$\Delta^{2'}$Sac-A6-A11]-dicarba-[A7]-Cys(^{t}Bu)-[A20]-Cys(Acm) human insulin A-chain 45

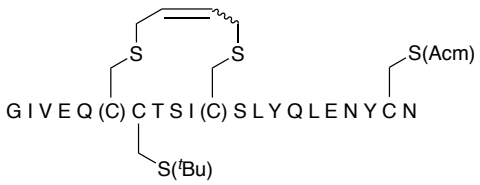

45

Peptide **45** was prepared from resin-bound **42** according to the general automated procedure outlined in Section 2.3.3.1. Formation of **45(I)** and **45(II)** was subsequently verified by small-scale cleavage, RP-HPLC and LRMS. **45(I)**: RP-HPLC (Agilent: Vydac C18 analytical column, 15 to 50% buffer B over 35 min): t_R = 20.1 min. Mass spectrum (ESI$^+$, MeCN:H_2O:TFA): *m/z* 855.4 $[M+3H]^{3+}$, ⅓($C_{110}H_{175}N_{26}O_{36}S_4$) requires 854.7; *m/z* 1282.2 $[M+2H]^{2+}$, ½($C_{110}H_{174}N_{26}O_{36}S_4$) requires 1281.6; *m/z* 1709.6 [2M + 3H]$^{3+}$, ⅓($C_{220}H_{347}N_{52}O_{72}S_8$) requires 1709.6. **45(II)** RP-HPLC (Agilent: Vydac C18 analytical column, 15 to 50% buffer B over 35 min): t_R = 20.4 min. Mass spectrum (ESI$^+$, MeCN:H_2O:TFA): *m/z* 855.0 $[M+3H]^{3+}$, ⅓($C_{110}H_{175}N_{26}O_{36}S_4$) requires 854.7; 1282.0 $[M+2H]^{2+}$, ½($C_{110}H_{174}N_{26}O_{36}S_4$) requires 1281.6. The resin was then subjected to Fmoc deprotection and TFA-mediated resin cleavage (Sections 2.3.3.5 and 2.3.3.7, respectively), the residue dissolved in MeCN:H_2O (~1:5) and lyophilised to give a mixture of the crude desired peptides **45(I)** and **45(II)** as an off-white solid (283 mg).

3.3.1.14 [Δ²'Sac-A6-A11]-dicarba-[A7]-Cys(SPyr)-[A20]-Cys(Acm) human insulin A chain 46

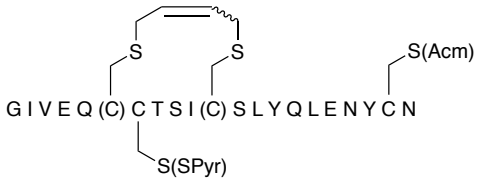

46

The concerted *tert*-butyl deprotection and *S*-pyridinyl protection at Cys A7 was executed according to the procedure described by Büllesbach *et al.*.[110] To a solution of anisole:TFA

(1:9, 7.2 mL) was added 2-dipyridyldisulfide (121 mg, 0.55 mmol, 5.5 equiv.) and the resulting solution cooled to 0 °C in an ice bath. To this solution was added lyophilised crude peptide **45** (283 mg) followed by a chilled solution of triflic acid:TFA (1:4, 7.2 mL). The resulting light brown solution was stirred at 0 °C for 1.5 hours after which the solution was concentrated under a stream of N_2 and the crude peptide precipitated with chilled ether (35 mL). The suspension was centrifuged, the supernatant discarded, and the precipitate resuspended and centrifuged in chilled ether (35 mL) a further two times. The crude peptide was then dissolved in MeCN:H_2O (1:1) and lyophilised to give **46** as a red solid. Formation of **46** as a pair of isomers **46(I)** and **46(II)** in a 4:1 ratio was subsequently verified by RP-HPLC and LRMS. **46(I)**: RP-HPLC (Agilent: Vydac C18 analytical column, 15 to 50% buffer B over 35 min): t_R = 19.0 min. Mass spectrum (ESI$^+$, MeCN:H_2O:TFA): *m/z* 872.6 $[M+3H]^{3+}$, ⅓($C_{111}H_{170}N_{27}O_{36}S_5$) requires 872.4; *m/z* 1308.7 $[M + 2H]^{2+}$, ½($C_{111}H_{169}N_{27}O_{36}S_5$) requires 1308.0. **46(II):** RP-HPLC (Agilent: Vydac C18 analytical column, 15 to 50% buffer B over 35 min): t_R = 19.5 min. Mass spectrum (ESI$^+$, MeCN:H_2O:TFA): *m/z* 872.6 $[M+3H]^{3+}$, ⅓($C_{111}H_{170}N_{27}O_{36}S_5$) requires 872.4; 1308.7 $[M+2H]^{2+}$, ½($C_{111}H_{169}N_{27}O_{36}S_5$) requires 1308.0; 1744.9 $[2M + 3H]^{3+}$, ⅓($C_{222}H_{337}N_{54}O_{72}S_{10}$) requires 1743.7. Peptide **46**

was purified *via* preparative RP-HPLC (Agilent: Vydac C18 preparative column, 15 to 45% buffer B over 40 min, t_R = 25.5 and 26.0 min) and selected fractions combined and lyophilised to give isomers **46(I)** and **46(II)** in >85% purity.

3.3.1.15 [Δ²'Sac-A6-A11]-dicarba-[A20, B19]-Cys(Acm) human insulin 43

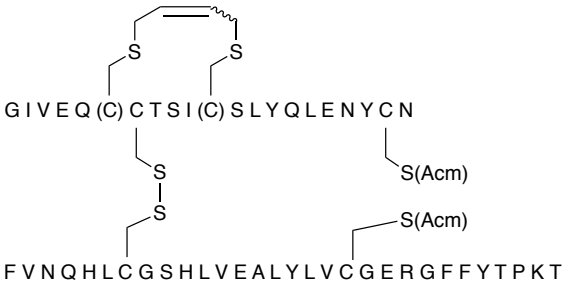

43

Combination of the A- and B-chain monomers was executed according to a modified version of a procedure originally described by Lin *et al.*.[111] **43(I)**: The modified insulin A-chain **46(I)** (2.5 mg, 0.96 μmol crude) was dissolved in 50 mM aqueous NH_4HCO_3 (2 mL). [B19]-Cys(Acm) human insulin B-chain **9** (1.3 mg, 0.37 μmol) was dissolved in MilliQ H_2O (4 mL) and added dropwise to the solution of **46(I)**. The mixture was stirred for 0.75 hours with monitoring *via* RP-HPLC and MS. The reaction was quenched by addition of glacial AcOH and the resulting solution lyophilised to give a pale yellow solid (17.2 mg). Formation of **43(I)** was verified by RP-HPLC and MS. RP-HPLC (Agilent: Vydac C18 analytical column, 0 to 25% buffer B over 5 min then 25 to 50% buffer B over 30 min): t_R = 18.8 min. Mass spectrum (ESI^+, MeCN:H_2O:TFA): *m/z* 1202.2 $[M+5H]^{5+}$; ⅕($C_{267}H_{406}N_{67}O_{79}S_6$) requires 1201.4; 1502.4 $[M + 4H]^{4+}$, ¼($C_{267}H_{405}N_{67}O_{79}S_6$) requires 1501.4. **43(II)**: The modified insulin A-chain **46(II)** (5.1 mg, 2.0 μmol crude) was dissolved in 50 mM aqueous NH_4HCO_3 (5 mL). [B19]-Cys(Acm) human insulin B-chain **9** (3.6 mg, 1.0 μmol) was dissolved in MilliQ H_2O (8 mL) and added dropwise to the solution of **46(II)**. The mixture was stirred for 0.75 hours with monitoring *via* RP-HPLC and MS. The reaction was quenched by addition of glacial

AcOH and the resulting solution lyophilised to give a pale yellow solid (13.8 mg). Formation of **43(II)** was verified by RP-HPLC and MS. RP-HPLC (Agilent: Vydac C18 analytical column, 0 to 25% buffer B over 5 min then 25 to 50% buffer B over 30 min): t_R = 19.3 min. Mass spectrum (ESI$^+$, MeCN:H_2O:TFA): *m/z* 1202.4 $[M+5H]^{5+}$, $\frac{1}{5}(C_{267}H_{406}N_{67}O_{79}S_6)$ requires 1201.4; 1502.1 $[M + 4H]^{4+}$, $\frac{1}{4}(C_{267}H_{405}N_{67}O_{79}S_6)$ requires 1501.4.

3.3.1.16 [Δ^4'Sac-A6-A11]-dicarba human insulin 29

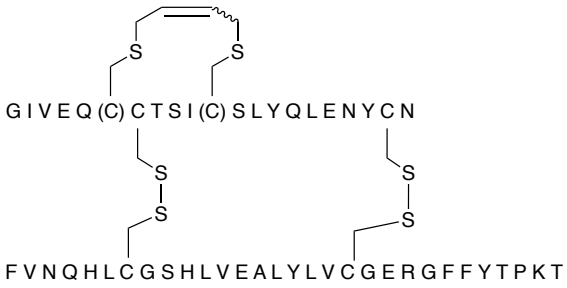

29

Oxidation of the insulin analogue precursors **43(I)** and **43(II)** was executed according to a procedure described by Lin *et al*..[111] **29(I): 43(I)** (17.2 mg crude) was suspended in a 60 mM aqueous HCl solution (0.45 mL) followed by glacial AcOH (4.8 mL) to effect dissolution. A 10 mM solution of iodine in glacial acetic acid (6.3 mL) was added and the resulting solution stirred in darkness for 1 hour, exposed to light and stirred for a further 1.75 hours before being poured into chilled diethyl ether (35 mL). The resulting suspension was cooled to 0 °C, centrifuged (5000 rpm, 5 min), and the supernatant discarded – a process that was repeated twice with fresh diethyl ether (2x35 mL). The residue was suspended in MeCN (~0.5 mL) and 20 mM ascorbic acid aqueous solution (1 mL) to quench excess iodine before it was purified by preparative RP-HPLC (Agilent: Vydac C18 preparative column, 0 to 30% buffer B over 5 min then 30 to 40% buffer B over 60 min): t_R = 17.3 min to give **29(I)** as a colourless solid (33.8 μg as determined by standardisation against human IGF-1) in >90% purity.

RP-HPLC (Agilent: Vydac C4 analytical column at T 40 °C, 25 → 31% buffer B over 5 min then 31→ 50% buffer B over 16 min, flow rate 0.5 mL min^{-1}): t_R = 13.3 min. Buffer A: 0.1% Aqueous TFA; Buffer B: 0.08% TFA in MeCN:H_2O, 80:20. HRMS (ESI^+, MeCN:H_2O:TFA): m/z 1173.15 $[M+5H]^{5+}$, ⅕($C_{261}H_{394}N_{65}O_{77}S_6$) requires 1172.54; 1466.43 $[M+4H]^{4+}$, ¼($C_{261}H_{393}N_{65}O_{77}S_6$) requires 1465.42; 1954.58 $[M + 3H]^{3+}$, ⅓($C_{261}H_{392}N_{65}O_{77}S_6$) requires 1953.56.

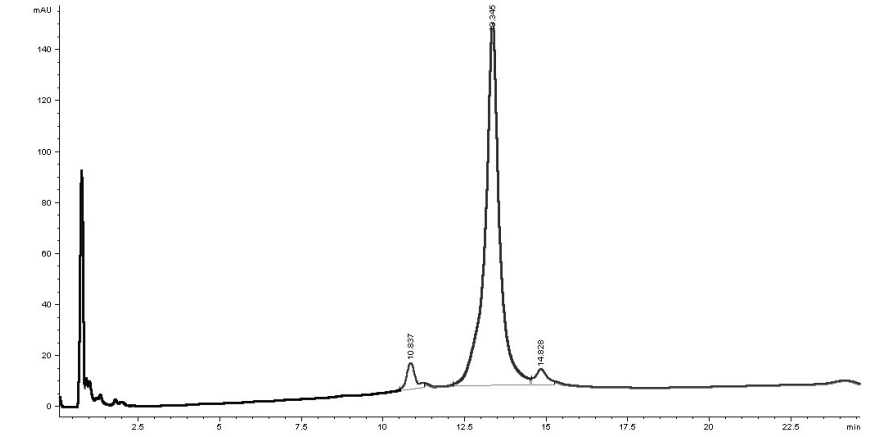

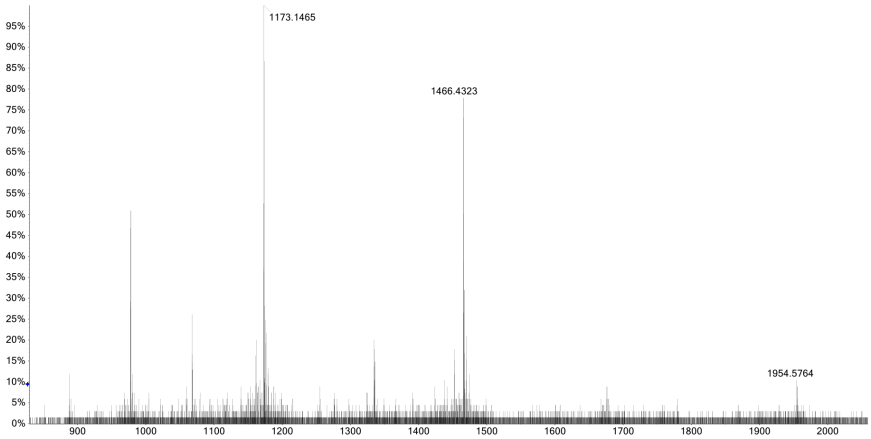

29(II): 43(II) (crude 13.8 mg) was suspended in a 60 mM aqueous HCl (0.9 mL) followed by glacial AcOH (9.5 mL) to affect dissolution. A 10 mM solution of iodine in glacial acetic acid (12.6 mL) was added and the resulting solution stirred in darkness for 1 hour, exposed to light and stirred for a further 1.75 hours before being poured into chilled diethyl ether (3x35 mL). The resulting suspension was cooled to 0 °C, centrifuged

(5000 rpm, 5 min), and the supernatant discarded – a process that was repeated twice with fresh diethyl ether (2x35 mL). The residue was suspended in MeCN (~0.5 mL) and 20 mM ascorbic acid aqueous solution (1 mL) to quench excess iodine before it was purified by preparative RP-HPLC (Agilent: Vydac C18 preparative column, 0 to 30% buffer B over 5 min then 30 to 40% buffer B over 60 min): t_R = 22.3 min to give **29(II)** as a colourless solid (0.91 mg as determined by standardisation against human IGF-1) in >99% purity. RP-HPLC (Agilent: Vydac C4 analytical column at T 40 °C, 25 → 31% buffer B over 5 min then 31→ 50% buffer B over 16 min, flow rate 0.5 mL min^{-1}): t_R = 13.1 min. Buffer A: 0.1% Aqueous TFA; Buffer B: 0.08% TFA in MeCN:H_2O, 80:20. Mass spectrum (ESI^+, MeCN:H_2O:TFA): *m/z* 1173.4 $[M + 5H]^{5+}$, ⅕($C_{261}H_{394}N_{65}O_{77}S_6$) requires 1172.5; 1466.5 $[M + 4H]^{4+}$, ¼($C_{261}H_{393}N_{65}O_{77}S_6$) requires 1465.4; 1955.4 $[M + 3H]^{3+}$, ⅓($C_{261}H_{392}N_{65}O_{77}S_6$) requires 1953.6.

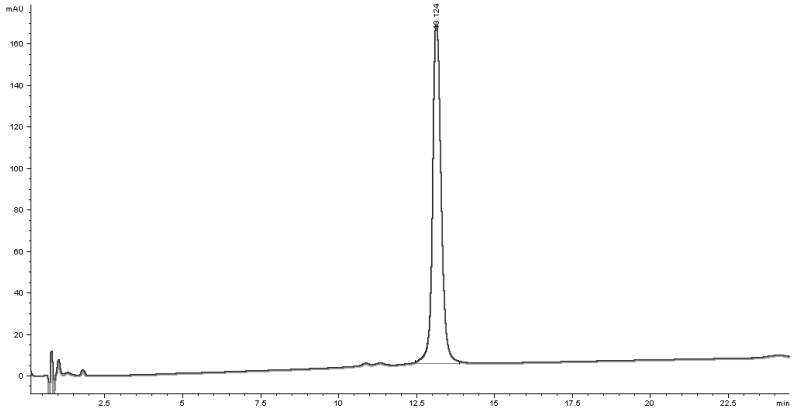

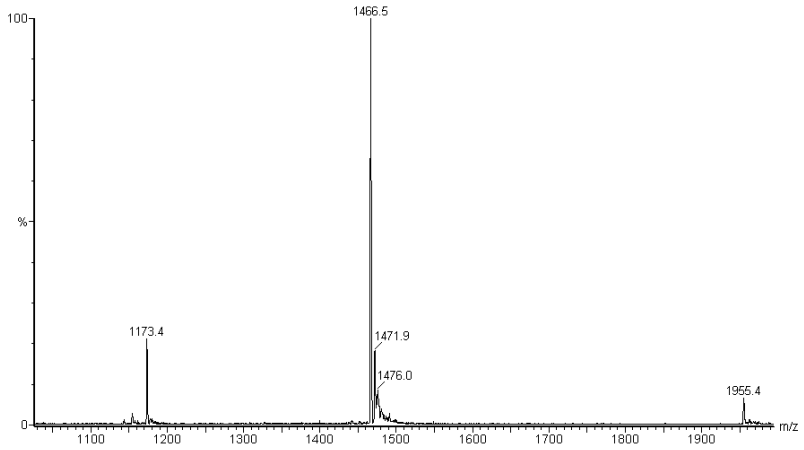
1466.5
100
%
1173.4
1471.9
1476.0
1955.4
0
1100
1200
1300
1400
1500
1600
1700
1800
1900
m/z

4 Towards an interchain insulin dicarba peptidomimetic: Strategies for enabling a biomimetic synthesis

4.1 Overview

Spurred by the exciting developments stemming from [A6-A11]-dicarba insulin, attention was turned to the construction of interchain dicarba-analogues of insulin (systematic replacement of the A7-B7 and A20-B19 disulfides) to further probe their role in insulin structure, function and potential allostery. It was hypothesized that the conformational switch undergone by the A6-A11 disulfide may be induced by a *second* conformational switch conveyed by the A7-B7 bridge, which would ostensibly transmit conformational distortion encountered in the B-chain. Given that the 'protective hinge' mechanism of the B-chain *C*-terminus has been recently elucidated,[32] this may be a potential mechanism for allosteric transmission to the A-chain. Variation of the rigidity and geometry of the A7-B7 bridge could be used to evaluate this hypothesis.

The inclusion of two or more dicarba bridges in insulin could potentially improve stability and/or selectivity whilst maintaining optimal binding affinity and activity at the insulin receptor. The regioselective formation of dicarba bridges in peptides has been a longstanding interest in the Robinson group.[85] This may be accomplished by exploiting the differing reactivities of prenylglycine and allylglycine moieties (Type III and Type I olefins, respectively)[135] in olefin metathesis to give only the desired product. Installation of a prenylglycine residue at the A6 and A11 positions would enable formation of the intrachain bridge pending conversion to the crotylglycine after full reduction of the interchain linkage. This strategy has been successfully employed in the synthesis of dicarba analogues of the α-conotoxin Rg1A.[85]

Attempts at direct cross metathesis (CM) between resin-bound A-chain and protected allylglycine residues failed to yield the desired cross metathesis product and resulted exclusively in homodimerisation of the allylglycine derivatives. Inclusion of a pseudoproline, established to encourage metathesis by disrupting aggregation,[88] failed to improve this result. An *O*-acyl isopeptide analogue, a moiety known for the disruption of chain aggregation, also failed to undergo metathesis. Ultimately, a number of truncated species designed to eliminate aggregation also failed to undergo metathesis. Finally, CM of a heavily truncated species (Fmoc-QAXTS-resin, X = L-allylglycine (L-Agl)) gave near-complete conversion to the cross product (with Bz/Ac-L-Agl-OMe) when extended microwave heating was employed (4 hours). The obstinate nature of this approach lead to the exploration of a chain linker-based strategy.

The intramolecular nature of the RCM reaction, in a very general sense, predisposes its substrates for relatively facile conversion to cyclised products. This is in contrast to the equivalent CM reaction, which due to its trimolecular nature is less statistically feasible by comparison. Difficulties in the case above stem not only from aggregation of the resin-bound substrate but also the statistical difficulty of sufficiently localising the reacting olefin termini amidst a very large and flexible molecular framework. Use of a single-chain precursor improves the feasibility of metathesis by converting an intermolecular CM reaction to a more favourable intramolecular RCM reaction (Scheme 18).

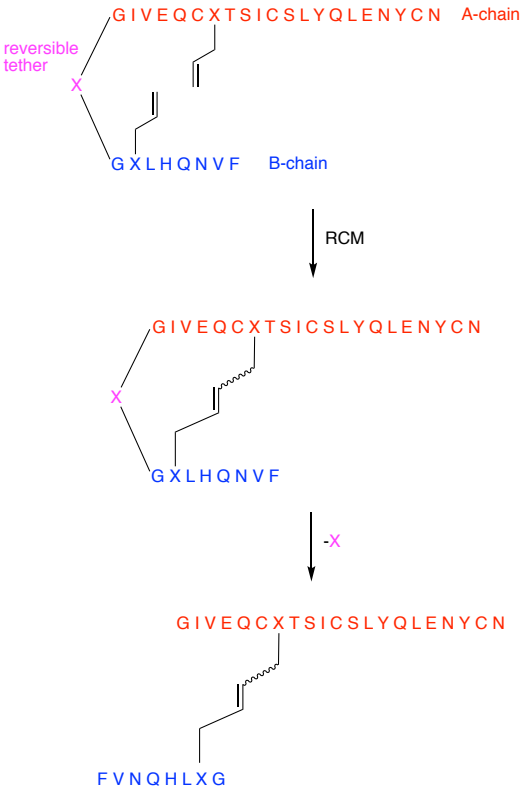

Scheme 18 - A tethered single-chain precursor strategy for the construction of interchain dicarba bridges in insulin. Adapted from van Lierop.[136]

van Lierop and Robinson explored the use of a photochemically labile HnB tether (Figure 20) to facilitate RCM of a single chain dicarba insulin precursor. However, despite successful RCM of substrates modelling this strategy, the tether was highly susceptible to hydrolysis under the reaction conditions used, leading to complex mixtures of reaction products. Improved tether moieties are thus required for the development of this strategy.

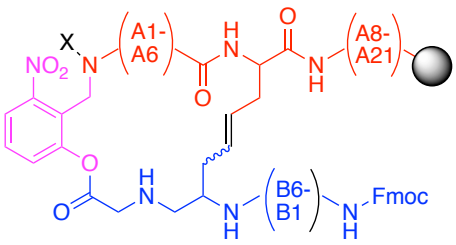

Figure 20 - 'Tethered' cyclic single-chain precursor. HnB linker is shown in pink. Adapted from van Lierop.[136]

It was a primary aim of this project to extend upon the work of van Lierop and Robinson and complete the synthesis of the interchain dicarba-insulin analogues [A7-B7]-dicarba

insulin and [A20-B19]-dicarba insulin. However, rather than redesign of the photochemically labile tether, an approach mimicking the biosynthesis of insulin was embarked upon due to its widespread use in both industry and small-scale research.[137-143]

Early studies on the conversion of proinsulin to insulin *in vitro* revealed the action of trypsin and carboxypeptidase B generated the same products as C-peptide cleavage in biosynthesis.[140] These enzymes were later employed in the recombinant synthesis of 'miniproinsulin', a proinsulin analogue with a heavily truncated C-peptide that retained the correct folding of its native forebear.[143] These conditions were also the basis of an industrial-scale recombinant synthesis patented by Frank *et al*.[141-142] and are currently *de rigeur* in commercial insulin production.[138] More recently, this biomimetic methodology formed the basis of an insulin lispro synthesis involving an oxime-forming ligation.[138] An alternate enzymatic strategy employing lysine-specific *Acromobacter lyticus* protease (ALP) has been developed by Tofteng *et al*. for the production of *des*-B30 insulin analogues.[139] However, the limited commercial availability of this enzyme compared to that of trypsin and carboxypeptidase B disfavours this approach for general experimentation.

The C-peptide is the least conserved region of proinsulin amongst different species.[144] It is bookended by a pair of basic dipeptides (Arg-Arg) which are considered to be the recognition sites for endopeptidases *in vivo* (Figure 21). Engineering of the interstitial residues that comprise C-peptide analogues often aim for greater folding efficiency and solubility. The C-peptide mimic sequence employed by Chang *et al*. (B-Chain-RRYPGDVKR-A-chain) is designed with a turn-forming sequence, stabilised by the anticipated charge interaction between the Arg and Asp side chains.[143] Thim *et al*. demonstrated that efficient expression of an insulin-like peptide in yeast could be

effected by joining the A- and B-chains together with a single dibasic sequence and that the interstitial C-peptide residues were generally redundant for correct folding, albeit conferring total resistance to enzymatic digestion.[145]

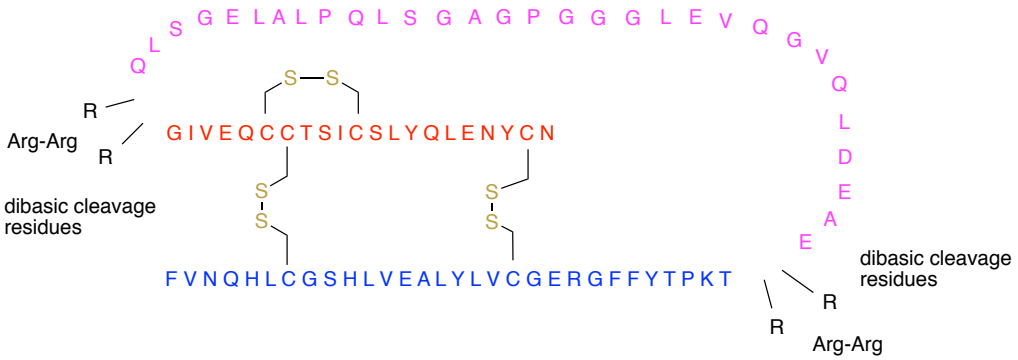

Figure 21 - Action on dibasic sites by endopeptidases in the conversion of proinsulin to insulin.

However, for the synthesis embarked upon in this work, mimicry of native folding is not relevant; the primary sequence provides the necessary regioselective metathesis-driven ligation, a process performed on-resin where microwave heating and chaotropic agents are employed to avoid deleterious aggregation and structural impediments to the reaction. The linker sequence is relevant to the synthesis at hand only in that solubility must be retained in aqueous media, enabling enzymatic digestion, and that the interstitial residues favour selective digestion at the dibasic sites. Hence, minimal, turn-inducing, enzymatically cleavable tether sequences were explored for the RCM of a single chain precursor. Post cyclisation, enzymatic digestion was investigated to give the desired interchain dicarba analogue.

It was anticipated that the truncated interchain insulins generated by this strategy may have the remainder of their sequences joined by traditional fragment condensation or *via* more modern ligation chemistries. Some ligation techniques that were considered included classical native chemical ligation (NCL),[146] selenocysteine-to-serine ligation,[147] aldehyde capture ligation[148] and oxazetidine ligation.[149] However, a novel intramolecular

fragment condensation was ultimately conceived, as it lacked the residue-specific limitations of the aforementioned techniques. Unfortunately, due to time constraints, this aspect of the synthesis is awaiting development investigation.

Through the synthesis of interchain dicarba insulin analogues we hope to attain powerful tools for the structural exploration of insulin and other peptides. The research in this Chapter focused on the design and development of reproducible methodology to achieve the formation of interchain dicarba-bridges between two peptide sequences. If successful, this new chemistry will complement our established RCM protocol for intrachain bridges and permit new investigations into insulin's structure-activity relationship.

4.2 Results and Discussion

4.2.1 Model sequence construction and evaluation of RCM protocol

To ascertain the validity of the enzymatic cleavage protocol and the effectiveness of RCM, a fragment of human insulin A-chain (*des*$_{A11\text{-}21}$-human insulin A-chain; GIVEQCCTSI) was chosen as a preliminary model sequence. Truncating the chain's *C*-terminus at residue 11 enabled sufficient representation of the full chain whilst reducing the likelihood of synthetic complications associated with increased chain length. Cys A7 was replaced with an L-Agl residue and Cys A6 was protected with the ^{t}Bu protecting group.

To expedite synthesis, the enzymatically-cleaved tether sequence was designed to be as small as possible whilst remaining viable with respect to digestion. A minimised sequence based upon that of a recombinant 'miniproinsulin' described by Chang *et al*.[143] was used as it incorporated a turn-inducing proline residue, useful for promoting RCM and disrupting deleterious peptide aggregation. This sequence included pairs of basic residues (RR and KR) for site-specific cleavage by trypsin and carboxypeptidase B alongside a central proline, giving a full tether of RRPKR. This is the shortest sequence expected to yield the desired result. Residues flanking the central proline found in Chang's linker were omitted as their function (facilitating native folding) is redundant in this application. Finally, an *N*-terminal Agl-Gly dipeptide was included in the sequence to complete the RCM precursor (Figure 22). The glycine residue enables downstream ligation flexibility as protocols that may induce *C*-terminal racemisation may be used (i.e. solution phase fragment condensation).[150]

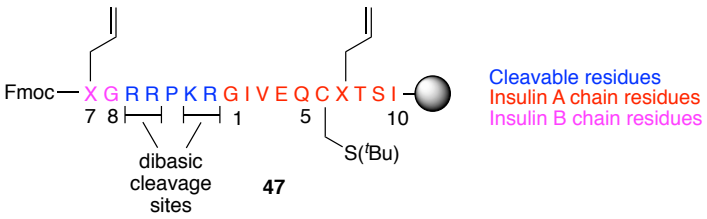

*Figure 22 - Schematic of enzymatically-cleavable tether model peptide **47**.*

Synthesis of the initial model sequence **47** *via* automated and manual SPPS afforded the linear peptide in good purity as assessed by small-scale deprotection, cleavage, RP-HPLC and MS. The resin-bound peptide was treated with acetic anhydride to negate any trace amine functionality that may be detrimental to catalysis and dried overnight in a vacuum desiccator. Attempted RCM using a standard procedure (20 mol % catalyst loading – see Section 2.3.3.8) failed to yield the desired cyclised peptide **48** and only the starting peptide was recovered (Scheme 19).

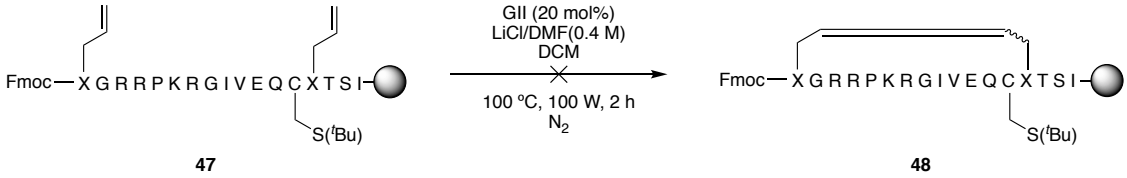

*Scheme 19 - Attempted RCM of the enzymatically-cleavable tether model peptide **47**.*

Increasing the catalyst loading to 50 mol % similarly failed to give the desired cyclised species **48**. In light of this outcome, the steric bulk of the protected guanidine groups of the interstitial cleavage residues, in combination with the substantial distance between reacting olefin termini, was suspected of hindering bridge formation. To assess this possibility, a truncated sequence **49** was synthesised, omitting the basic cleavage residues and reducing the distance between the reacting olefins. Disappointingly, this species similarly failed to undergo metathesis to yield the desired cyclised product **50** (Scheme 20).

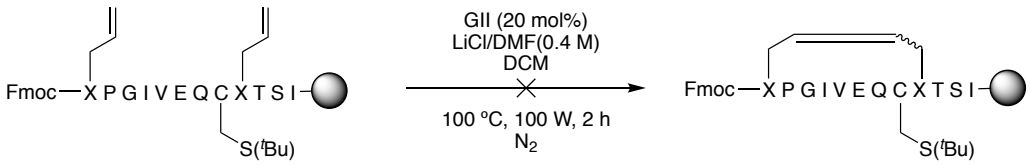

*Scheme 20 - Attempted RCM of the truncated model peptide **49**.*

Reasons for this failure were not immediately apparent. We first examined the influence of the sterically-bulky *tert*-butyl protecting group adjacent to the Agl A7 residue.[†] Despite successful use of this protecting group adjacent to Agl residues in previous syntheses of dicarba-insulins (see Chapter 2), the combination of this group and larger ring size could conceivably impede the RCM reaction. In the event that this was confirmed, a number of viable protecting groups for use at Cys A6 position[151] could be considered to achieve successful synthesis. To ascertain whether the Cys A6 was an impediment to metathesis, the analogous Ala-substituted model peptide **51** was synthesised. Regrettably, this species also failed to undergo metathesis to the desired cyclic species **52** under standard conditions (Scheme 21).

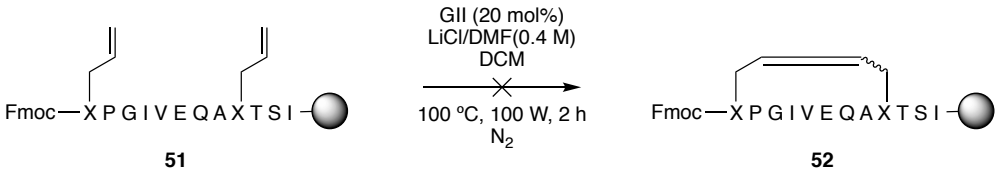

*Scheme 21 - Attempted RCM of Ala-substituted truncated model peptide **51**.*

Revision of the primary sequence of the tether was thus deemed necessary to assess synthetic viability of the tether approach. Val A3 was thus substituted with a Pro residue and the *N*-terminal Agl coupled directly to Gly A1. It was anticipated that this would not only maximise the influence of the induced turn but would also disrupt the hydrophobic

[†] To avoid confusion, residues are numbered according to A- and B-chain location. For example, allylyglycine residues are located at positions 1 and 9 in peptide **49**, but described as Agl B7 and Agl A7 respectively. On cross metathesis, these residues will form the A7-B7 bridge.

GIVEQ sequence thought to participate in deleterious aggregation. Peptide **53** was thus synthesised using automated and manual techniques and Cys A6 was accordingly reinstated in the sequence. Gratifyingly, standard RCM conditions gave complete conversion to the cyclic peptide **54** (Scheme 22).

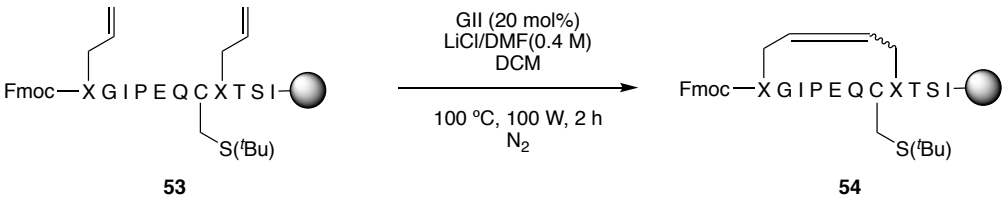

53 54

*Scheme 22 - RCM of [A3]-Pro substituted truncated model peptide **53**.*

With this encouraging result, a mutant incorporating the original desired basic cleavage residues was synthesised and subjected to RCM under identical conditions. Quantitative conversion to the cyclic peptide **56** was also achieved (Scheme 23).

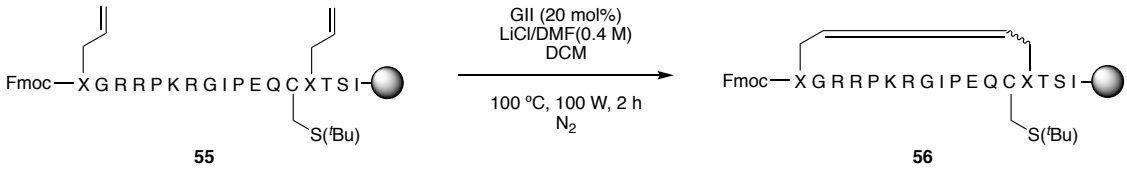

55 56

Scheme 23 - RCM of [A3]-Pro substituted model peptide 55.

Success of RCM following inclusion of a non-native Pro A3 mutation points to possible aggregation of the hydrophobic A1-A3 region as a cause for non-viable metathesis. In addition, possible steric clash between the branched alkyl sidechains of Val A3 and Ile A2 may inhibit the conformational flexibility required to form the requisite dicarba bridge, defeating the use of chaotropic agents and microwave heating for aggregation disruption during the metathesis reaction. Unfortunately, the *N*-terminal residues of the insulin A-chain are amongst the most conserved residues within insulins of all species, indicating their importance for biological function.[1] Substitutions at Val A3 have resulted in analogues with exceptionally low binding affinity and biological activity; mutation of

Val A3 to a Leu residue (insulin Wakayama), a similarly branched amino acid, resulted in 100-fold loss in binding affinity and inability to stimulate glucose uptake.[105] It was therefore highly unlikely that a Val → Pro mutation at A3 would be well tolerated. Nevertheless, the effect of the Pro A3 mutation on the binding and biological activity of insulin was examined through the synthesis and assay of [A3]-Pro-[Δ^4A6-A11]-dicarba human insulin **57** (Figure 23). This synthesis was executed according to a synthetic route similar to that described for the chiral mutants of [Δ^4A6-A11]-dicarba human insulin (see Sections 4.3.1.13-4.3.1.18 for synthetic procedures).

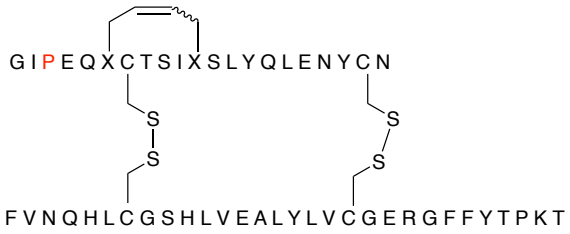

57

*Figure 23 - [A3]-Pro-[Δ⁴A6-A11]-dicarba insulin **57**.*

A binding assay was performed by collaborators at Flinders University to assess the viability of such a dramatic mutation at a highly conserved residue. As expected, neither isomer of the [A3]-Pro insulin demonstrated appreciable binding.

With the desired ring-closed model **56** in hand, the resin-bound peptide was subjected to continued automated SPPS to append B-chain residues B1-B6 to the *N*-terminus. Analysis of the resulting peptide by small-scale deprotection, cleavage, RP-HPLC and MS showed the formation of the truncated pyroglutamate species **58** as the dominant product (Figure 24), resulting from premature cyclisation of the glutamine. Despite the omission of the *N*-terminal residues, the peptide **58** was cleaved, purified, and used as a model in subsequent preliminary enzymatic digestion studies.

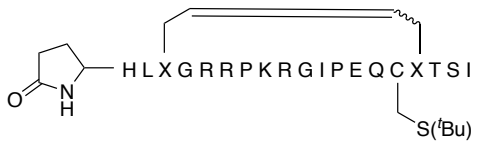

58

*Figure 24 - Truncated pyroglutamate species **58**.*

The procedure for enzymatic digestion of **58** was derived from conditions developed by Given and coworkers thought to mimic C-peptide cleavage during insulin biosynthesis.[152] Carboxypeptidase B and trypsin were added to a solution of **58** in tris-HCl buffer and shaken at 22 °C for 8 hours with regular monitoring. Aliquots were taken at regular intervals, quenched with glacial acetic acid and injected into an RP-HPLC instrument to monitor the distribution of products. It became apparent that the digestion occurred very rapidly, with cleavage products observed immediately after addition of the enzyme solutions (Scheme 24).

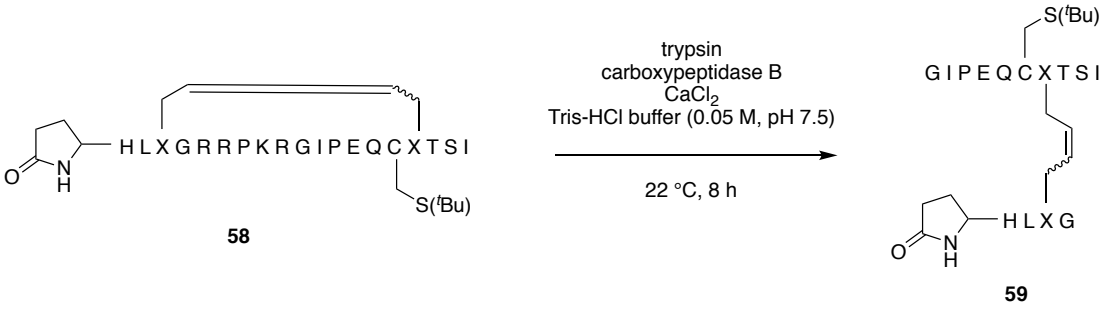

58 59

*Scheme 24 - Digestion of truncated single-chain insulin **58**.*

Promisingly, the desired digestion product **59** was identified within the chromatogram by mass spectrometry, and found to constitute the greatest proportion of the product distribution. However, many deletion products (predominately -Gly) resulting from over-digestion of the peptide were also observed, causing a broadened set of overlapping peaks in the chromatogram. It was surmised that further optimisation of the digestion protocol was required, for instance by modifying the buffer composition, in order to

suppress the over-digestion and maximise the product obtained. This is crucial in the context of the final [A7-B7]-dicarba insulin synthesis, as the numerous on-resin transformations are expected to diminish the yield of the desired material and certainly require purification prior to and after digestion. However, further development of the digestion was postponed until a more representative analogue was furnished downstream so as to avoid premature optimisation.

With the verification of the enzymatic digestion protocol and identification of Val A3 as the 'problem' residue retarding metathesis, attention then turned to the development of a novel method of aggregation disruption that would permit formation of the A7-B7 dicarba bridge. Traditional reversible pseudoproline residues could not be used, as none of these could revert to the problematic *N*-terminal aliphatic sidechains upon cleavage. Investigation into the use of α,β-dehydroamino acid residues as aggregation-disrupting turn inducers was thus undertaken with the aim of permitting the crucial A7-B7 ring closure.

4.2.2 Dehydroamino acids as turn-inducing deaggregators for enabling on-resin RCM

An analogous method of aggregation/conformation disruption was consequently investigated, employing an α,β-dehydrovaline (Dhv) residue in place of the native Val A3. It was anticipated that this residue would induce a turn and favour cyclisation owing to the preference of Dhv derivative-containing peptides to adopt *cis*-amide configurations at their *N*-termini.[153] After RCM, the residue could then be stereoselectively reduced to the native L-Val residue by way of hydrogenation with the appropriate chiral Rh(I)-phosphine catalyst (Scheme 25).[154-155]

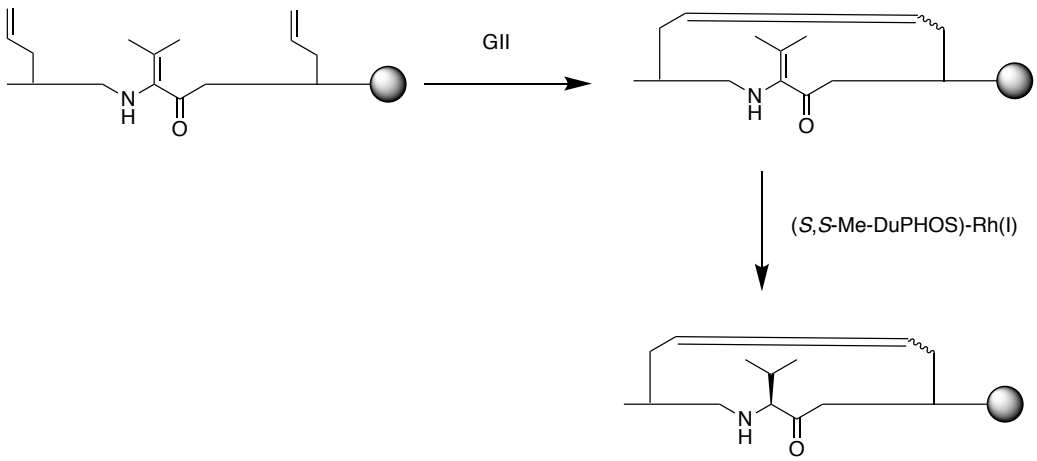

Scheme 25 - General scheme of dehydro-residue inclusion for facilitation of RCM on-resin.

α,β-Dehydroamino acids are analogous to canonical α-amino acids, albeit unsaturated at the α- and β-carbons and thus readily classified as enamides. Although naturally occurring, their biosynthesis is largely limited to fungi and bacteria.[156-157] α,β-Dehydroamino acids are well documented in the literature, with numerous reviews showcasing their synthesis and appearance in natural products.[156-159]

The concept of using dehydroamino acids as turn-inducing residues was prompted by an examination of the literature concerning the unique conformational properties they bestow upon naturally-occurring peptides and peptide-like compounds. It was universally acknowledged that the presence of a dehydroamino acid caused a 'stiffening' of backbone conformation, owing to the rigidity conferred by the planarity of the sp^2 hybridised carbon pair in conjunction with the adjacent amides.[159] Though this may seem counterintuitive with regards to a process (RCM) that requires some backbone flexibility, if the degree of conformational freedom can be limited to a small subset of potential conformations that include favourable orientation of the reacting olefin termini, RCM conversion is likely to be improved rather than diminished. The likelihood of favourable orientation is suspected to be quite sequence dependent, and formed the focal point of this investigation.

Additionally, dehydroamino acids are known to induce β-turns. Gupta and Chauhan demonstrated through small molecule studies that singly-substituted β-branched dehydroamino acids such as dehydrophenylalanine and dehydroleucine encourage formation of β-turns where the dehydroamino acid occupies the $i + 2$ position of the turn; non-branched dehydroalanine, on the other hand, supported an inverse γ-turn.[160] It was thus inferred that additional β-branching, encountered with doubly-substituted β-branched dehydroamino acids such as dehydrovaline and dehydroisoleucine, may further reinforce the β-turn motif by limiting conformational mobility. This is analogous to the action of the previously-discussed pseudoprolines, which also induce a β-turn by virtue of their tendency to adopt a *cis* conformation at their *N*-terminal amide.[161] Indeed, it has been demonstrated that singly β-substituted *N*-methyl dehydroamino acids preferentially induce a *cis*-amide conformation at the *N*-terminal residue,[153] making them (and non-methylated analogues) excellent candidates for turn-inducing aggregation disruption.

Whilst this investigation was underway a similar strategy was published, pre-empting our approach in the literature but nevertheless verifying its validity. Le and coworkers employed α,β-dehydrophenylalanine as a 'traceless turn-inducer' for the synthesis of the cyclic pentapeptide dichotomin E.[162] The α,β–dehydrophenylalanine residue was stereoselectively hydrogenated to the required enantiomer using a rhodium(I)-DuanPHOS[163] system (Scheme 26).

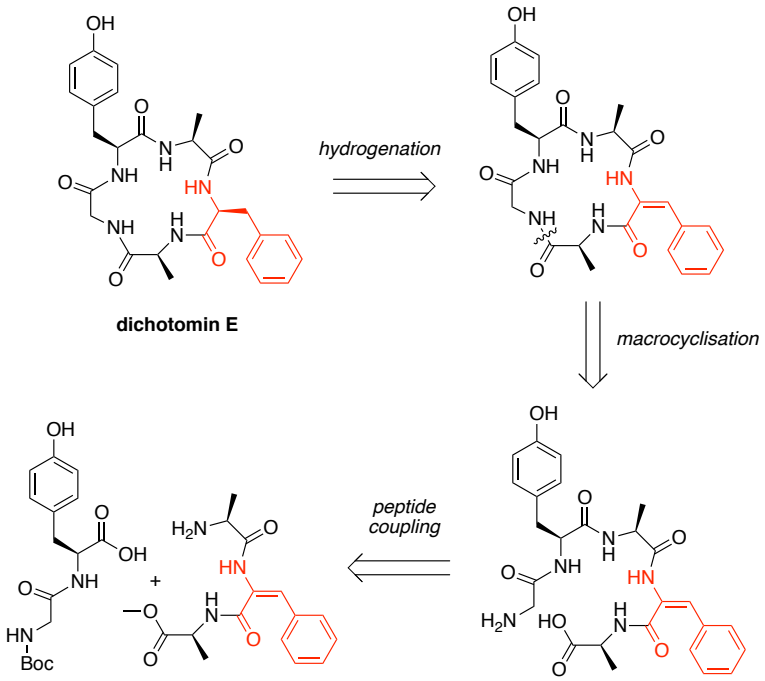

Scheme 26 - Retrosynthetic scheme for the synthesis of dichotomin E by Le and coworkers.[162]

However, Le and coworkers' implementation differs from our aims in two aspects. Firstly, no provision for variously functionalised dehydro-sidechains is made, as no particulars are given for the synthesis of the β-hydroxyphenylalanine dehydration precursor in the paper.[162] Secondly, the dichotomin E synthesis inclusive of the cyclisation is conducted off-resin, thus complicating purification. We sought to address these limitations in our synthetic investigation.

Preliminary inquiry into the commercial availability of dehydro-precursors lead to the purchase of Fmoc-dehydrovaline **60**, which was readily coupled to a fragment of the truncated sequence **61**, giving **62** (Scheme 27). However, subsequent deprotection (giving **63**) and exposure to an activated amino acid residue failed to couple the Ile residue at the *N*-terminus despite repeated attempts (including the standard HATU protocol, the symmetric anhydride method and the use of an acyl fluoride). This was attributed to the ostensible lack of nucleophilicity of the amine owing to enamine-imine tautomerism (**63** and **64**, respectively, Scheme 27).[164]

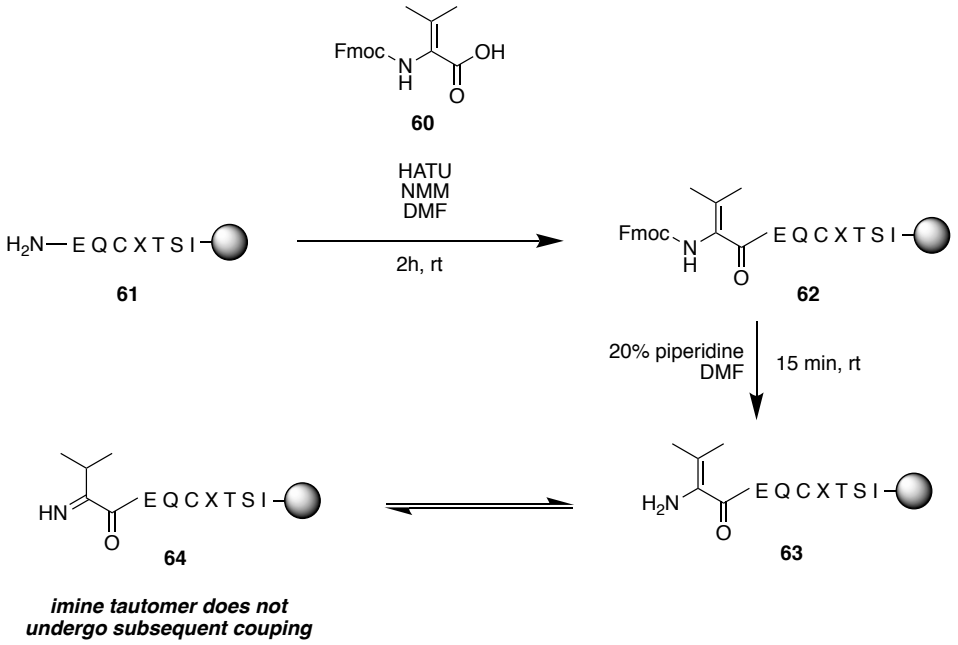

Scheme 27 - Attempted coupling of dehydrovaline via SPPS.

An alternative method of insertion was envisioned, synthesising the Fmoc-Ile-Dhv as a preformed dipeptide cassette, bypassing the on-resin imine tautomerism. After reviewing the literature, the shortest route to the desired isoleucine-dehydrovaline dipeptide was found to be the direct condensation of a carboxamide with an α-ketoacid, originally described by Makowski and coworkers (Scheme 28).[165-166] As this route had not been extensively revisited in the literature, we sought to evaluate its performance for the expedited synthesis of the desired dehydro species and improve on any shortcomings that had prevented it from becoming a more widely used route.

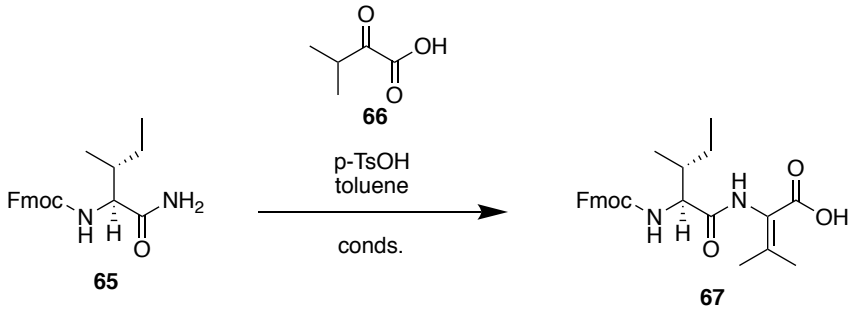

*Scheme 28 - Condensation of Fmoc-isoleucyl carboxamide **65** with α-ketoisovaleric acid **66** as per Makowski et al.*[165-166]

The Fmoc-isoleucyl carboxamide **65** was synthesised in 60% yield from commercially available Fmoc-isoleucine **68** using the method of Pozdnev, which had been shown to be compatible with Fmoc-amino acids and to give moderately high yields (Scheme 29).[167]

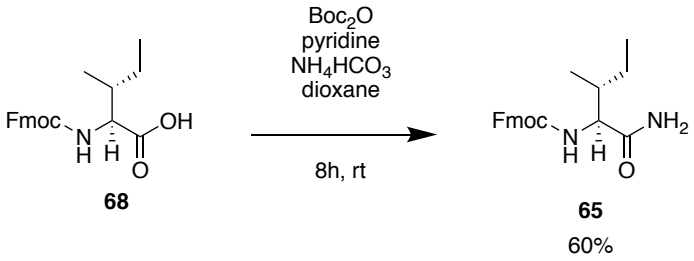

*Scheme 29 - Synthesis of Fmoc-isoleucyl carboxamide **67** from commercially available Fmoc-isoleucine **68**.*

Subsequent attempts at condensing the Fmoc-isoleucyl carboxamide **65** with the sodium salt of 2-oxo-3-methyl butanoic acid were not fruitful, though reprotonating the salt to the acid **66** and using it as such gave much improved results. A higher-running TLC spot was observed after refluxing with a Dean-Stark trap in toluene (with catalytic *p*TsOH) for 24 hours, with significant consumption of the starting amide. Interestingly, the major product of this transformation was not the desired dipeptide **67** but the azlactone **69** (Scheme 30). Additionally, the isoleucyl C_α position appeared to have epimerised, giving a pair of chromatographically-inseparable diastereomers in a 1:1 ratio by ^{1}H NMR spectroscopy.

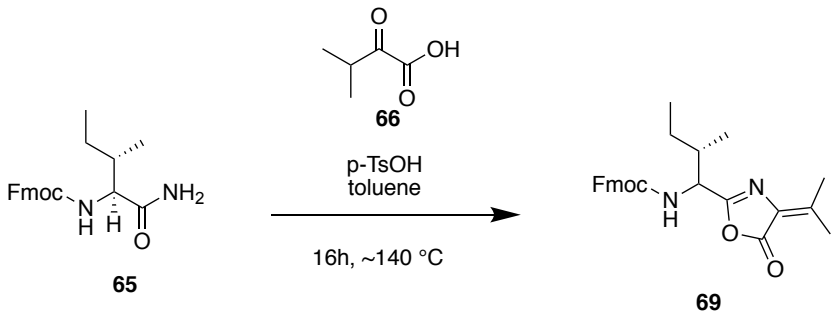

*Scheme 30 - Synthesis of dehydro-dipeptide azlactone **69**.*

The generation of an azlactone in lieu of dipeptide **67** is not necessarily problematic for the remainder of the synthesis. Jiang *et al*. recently reported the use of azlactone 'dipeptide' units akin to **69** for the SPPS inclusion of dehydrovaline residues, making use of facile ring-opening of the azlactone moiety in the presence of an amine.[168] However, the authors note that an Fmoc protecting group on the *N*-terminal of the dipeptide-azlactone unit is not compatible with their strategy due to unspecified decomposition (likely lability of the group in the presence of DMAP). Indeed in our hands, attempts to heat (with microwave irradiation) the Fmoc-Ile-Dhv azlactone **69** in the presence of peptidyl resin did not result in coupling. However, success was achieved with the orthogonally-cleaved Alloc-protecting group.[168]

Despite the undesirable epimerisation of the isoleucine, it was considered pertinent to verify the viability of the dehydro strategy as an RCM-enhancement method; hence resolution of the epimerisation issue was postponed. Synthesis of the Alloc analogue of the dehydrodipeptide commenced with *N*-terminal acylation of L-isoleucine **70** with allylchloroformate **71** to the allyloxycarbamate **72**, followed by conversion to the carboxamide **73** *via* the previously employed route (Scheme 31).

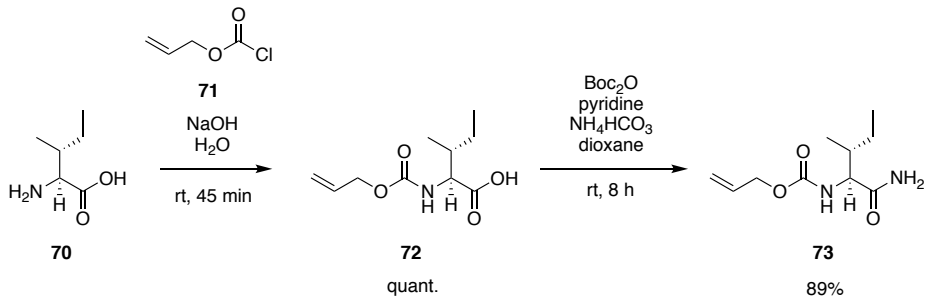

*Scheme 31 - Synthesis of Alloc-protected isoleucyl carboxamide **73**.*

Condensation of the *N*-protected carboxamide **73** with 2-oxo-3-methyl butanoic acid **66** under the previously used conditions afforded the expected azlactone species **74** in 60% yield (Scheme 32). Interestingly, upon leaving the crude product exposed to air for six hours, the formation of a colourless solid was observed, which was later confirmed as the dipeptide **75** by mass spectrometry. Both the azlactone **74** and dipeptide **75** are soluble in methanol, though only the former is soluble in DCM, allowing ready separation by filtration.

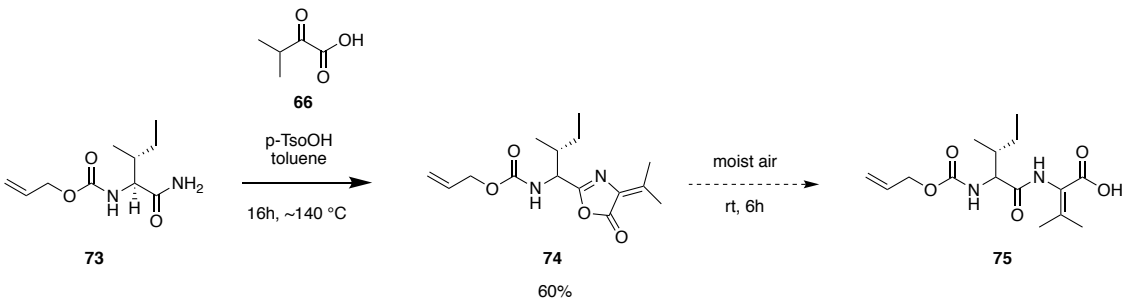

*Scheme 32 - Synthesis of Alloc-protected dipeptide-azlactone **74** and subsequent decomposition to protected dipeptide **75**.*

Gratifyingly, coupling of **74** to resin-bound peptide fragment **61** using Jiang and coworkers' conditions gave the desired Alloc-protected dehydropeptide chain Alloc-IΔVEQCXTSI **76** in 85% conversion (Scheme 33).

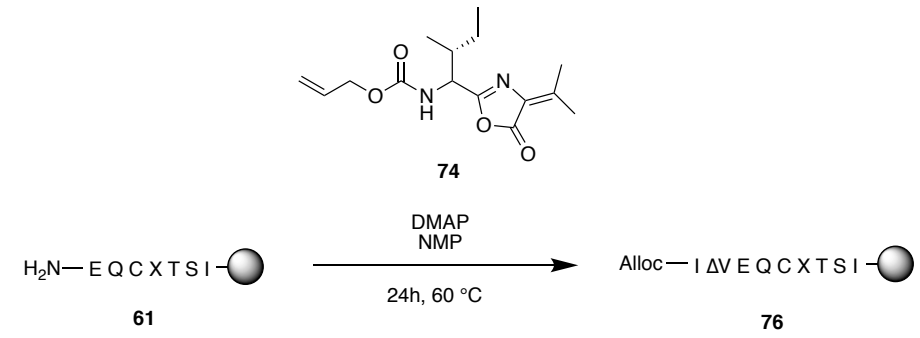

*Scheme 33 - Coupling of dipeptide-azlactone **74** to insulin fragment **61** under Jiang* et al. *conditions.*[168]

The removal of the Alloc protecting group from the model peptide **76** was not as facile as expected, with the standard conditions employed by Jiang *et al.*[168] for this transformation on-resin yielding neglible deprotection (Scheme 34).

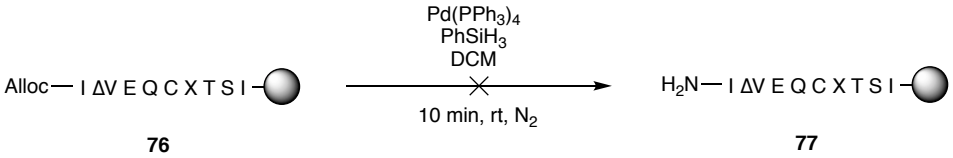

*Scheme 34 - Attempted Alloc-deprotection of dehydrovaline-containing insulin fragment **78**.*

Reviewing recent literature regarding the use of this protecting group in SPPS, an effective method was found employing microwave irradiation to expedite the removal of the group (Scheme 35).[169] Interestingly, this method can be performed in air, as the deprotection occurs faster than decomposition of the sensitive palladium complex.

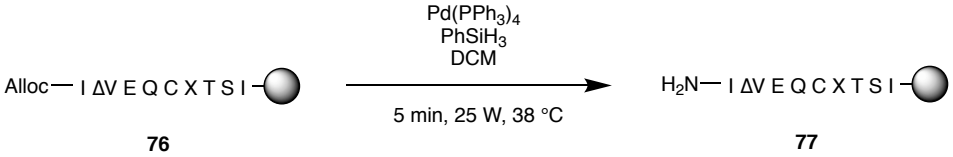

*Scheme 35 - Microwave-enhanced Alloc-deprotection of sequence **76**.*

The desired deprotected species **77** was obtained in 80% conversion from the Alloc-protected starting material. The remaining residues were coupled using standard

SPPS protocol to give the complete, resin-bound, Fmoc-protected RCM substrate **78**. Alas, initial attempts to cyclise this species under standard RCM conditions did not give the requisite carbocyle. Troubleshooting pointed to the presence of ~20% *N*-allyloxycarbonyl starting material remaining from the initial Alloc-deprotection. Allyl carbamates have been known to be troublesome substrates in metathesis reactions, particularly in the context of peptides, ostensibly due to coordination to the catalyst and consequent deactivation.[170] A subsequent synthesis of the precursor **77** involved repetition of the Alloc-deprotection step a further two times, effectively eliminating traces of the Alloc-protected starting material. It should be noted that performing the microwave deprotection reaction under an inert atmosphere did not improve the yield, necessitating repetition.

RCM was then performed on the newly synthesised precursor **78**. Gratifyingly, the desired macrocycle **79** was obtained with >90% conversion, tentatively verifying the efficacy of the dehydro-residue inclusion strategy for enabling RCM on a reticent substrate (Scheme 36).

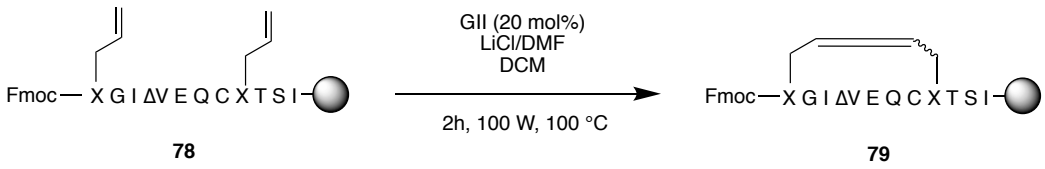

*Scheme 36 - RCM of dehydrovaline-containing insulin fragment **78**.*

The approach was also verified by RCM of the longer substrate **80**, which included in its sequence the basic residues required for downstream enzymatic digestion, giving complete conversion to the desired ring-closed peptide **81** (Scheme 37).

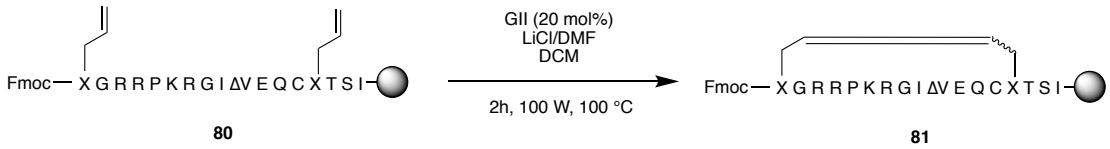

80 **81**

*Scheme 37 - RCM of dehydrovaline-containing extended insulin fragment **80**.*

The resin-bound, ring-closed species **79** was then subjected to initial asymmetric hydrogenation using [(*S*,*S*)-Me-DuPHOS-Rh(I)-COD]BF_4 under 60 psi of hydrogen in 10% MeOH in DCM (Scheme 38). The suspension was stirred for 24 hours, after which an aliquot was cleaved and assessed by RP-HPLC and mass spectrometry. Promisingly, the resultant mass spectrum indicated hydrogenation of the substrate giving **82**. However, this material co-eluted with unreacted material **79** which could not be separated from the desired **82**. This was likely due to the presence of stereoisomers arising from the non-stereoselective RCM (*E*- and *Z*- isomers), the epimerised isoleucine residue, and the indeterminate selectivity of the asymmetric hydrogenation.

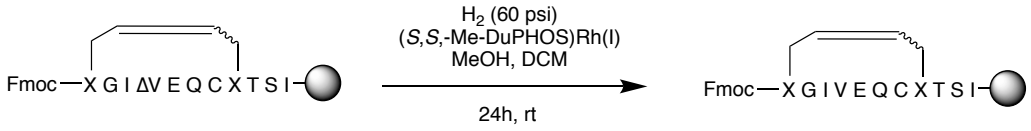

79 **82**

*Scheme 38 - Asymmetric hydrogenation of dehydrovaline-containing insulin fragment **79**.*

With preliminary confirmation of the RCM-inducing capability of the dehydrovaline residue, attention then turned to an optimised synthesis of precursor azlactone **74** with a view to eliminate the detrimental epimerisation encountered in the direct condensation route. The conditions to effect the condensation are relatively harsh, involving high temperatures (~140 °C) and a strong acid catalyst (*p*TsOH). Epimerisation presumably involves reversible, acid-catalysed isomerisation of the desired, enantiopure azlactone **83** to the oxazolidinone **84**, resulting in loss of the stereochemistry at the adjacent amino acid α-carbon giving the racemic azlactone **74** (Scheme 39).

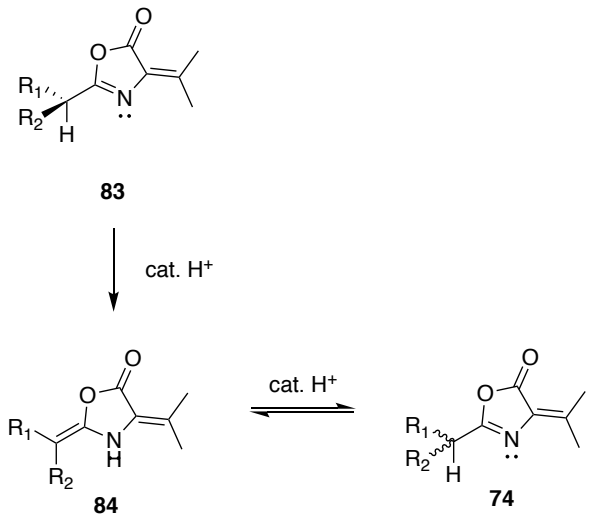

Scheme 39 - Azlactone isomerisation resulting in epimerisation.

Several attempts were made to optimise the condensation, as summarised in Table 5. The use of pyridinium *p*-toluenesulfonate (PPTS) as a weaker acidic catalyst resulted only in slightly diminished yield, as did the use of benzene and lower reflux temperatures (Table 5). Halting the reaction after 90 minutes gave the azlactone product in only 4% yield with subsequent NMR spectroscopic analysis revealing 30% epimerisation to the unwanted diastereomer, suggesting that the epimerisation process occurs rapidly relative to product formation. Fortuitously, the formation of diastereoisomeric products *via* this condensation route alerted us to the inherent epimerisation problem which may have otherwise gone unnoticed (by us and others) until insertion into a sequence.

Table 5 – Attempted optimisation of reaction conditions.

solvent	additive	temperature	yield	>10% racemisation?
toluene	PTSA	140 °C	**60%**	Y
benzene	PTSA	120 °C	53%	Y
toluene	PPTS	140 °C	56%	Y
toluene	none	140 °C	37%	Y

Microwave heating was not feasible given the transparency of the azeotrope-forming solvents such as toluene to microwaves. Though THF forms an azeotrope with water, the miscibility of these solvents meant that this combination was not applicable to the Dean-Stark method. Molecular sieves were also employed, not for water removal but as

a microwave absorbant. This enabled sufficient heating of the solvents used, but proved impractical as the finely divided sieves caused frothing of the solvent within the Dean-Stark trap. Additional microwave reactions employing chemical water scavengers (trimethylsilyl chloride and 2,2-dimethoxypropane) gave only intractable products that could not be converted to the desired azlactone.

The contemporary synthesis of Jiang *et al.*[168] was an obvious route to the desired azlactone, avoiding capricious couplings demonstrated in other recent syntheses of dehydroamino acids.[171] However, we wished to avoid the use of (toxic) osmium tetroxide as an oxidant early in the route, as well as the subsequent high-pressure hydrogenolysis of the Cbz protecting group. In light of this, the development of a novel synthetic route was embarked upon. The late-stage deprotection and dehydration of the Jiang *et al*. route were to be retained, as these were high yielding transformations requiring only mild conditions and known to retain stereochemistry at the *N*-terminal amino acid α-carbon. It was decided that an aldol condensation could be employed to generate the required β-hydroxyl group from a glycine derivative, enabling diverse sidechains to be installed simply by employing a suitable aldehyde or ketone (Scheme 40).

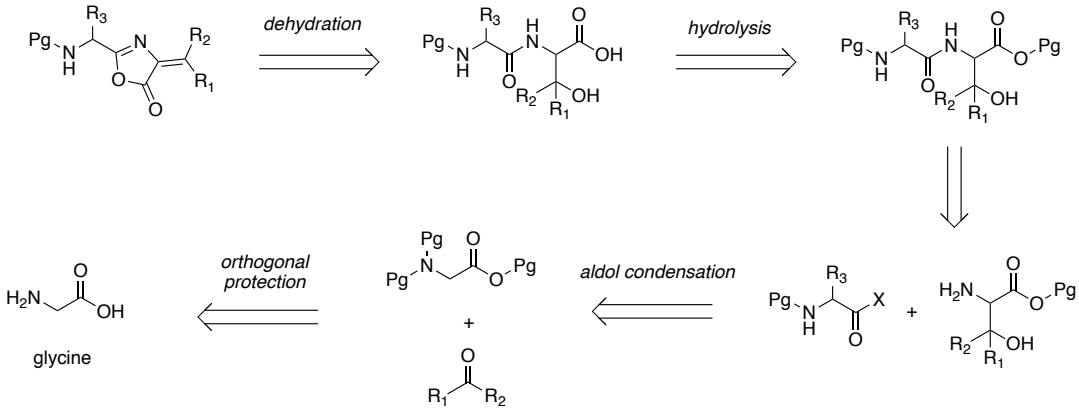

Scheme 40 – Retrosynthetic schematic of proposed general azlactone route.

Key to enabling this transformation is the selection of orthogonal protecting groups for the glycine-derived enolate precursor. A history of group work in this area lead to the identification of the 'stabase' protecting group. Relatively little-used, the stabase group is a pair of silylaza- moieties joined by an ethyl backbone, with the remaining silyl valences terminated with methyl substituents.[172] Its resistance to strong bases such as LDA and its lability in weak acid make it ideal for the protection of primary amines in the aldol condensation, a task for which it was originally conceived.[172] Additionally, prior work within the Robinson group has demonstrated that stabase can be displaced with acylating agents, enabling a one-pot, tandem deprotection/acylation sequence (i.e. transprotection).[173-174]

The stabase-protected glycine derivative can be synthesised in a single step from commercially available ethyl glycinate hydrochloride **85** and 1,2-bis(chlorodimethylsilyl)ethane **86**.[172] This was accomplished as per the literature procedure, although the extreme acid sensitivity of the stabase-adduct caused problems during the synthesis; for optimal yield, any sources of acidic proton must be avoided, and moisture ideally kept to a minimum. Use of dry and base-washed solvents as well as an inert atmosphere during the preparation of the stabase glycine derivative **87** enabled its synthesis in 91% yield (Scheme 41).

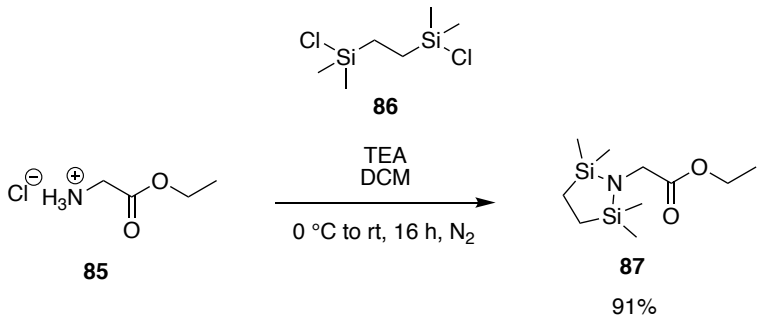

*Scheme 41 - Synthesis of stabase-ethyl glycinate adduct **87**.*

The synthesis of the *N*-terminal acylating agent, an activated isoleucine derivative, was subsequently investigated. The carboxylic acid was chosen to be activated as the acyl fluoride. Acyl fluorides, in particular those derived from *N*-protected amino acids, are known to chemoselectively acylate amines while displaying only minimal reactivity towards oxygen nucleophiles.[133] This is advantageous in preserving the β-hydroxyl group installed in the downstream aldol condensation during amine transprotection. Additionally, the affinity of silicon for fluoride is well established, particularly in the context of protecting group removal,[175] which was anticipated to facilitate the downstream transprotection. The amine of the inbound *N*-terminal isoleucine was to be protected as the Alloc-derivative, in accordance with the work of Jiang and coworkers.[168]

Accordingly, the protected isoleucyl acid fluoride **88** was synthesised from **72** in high yield (91%), employing cyanuric fluoride **33** as the fluorinating agent (Scheme 42).

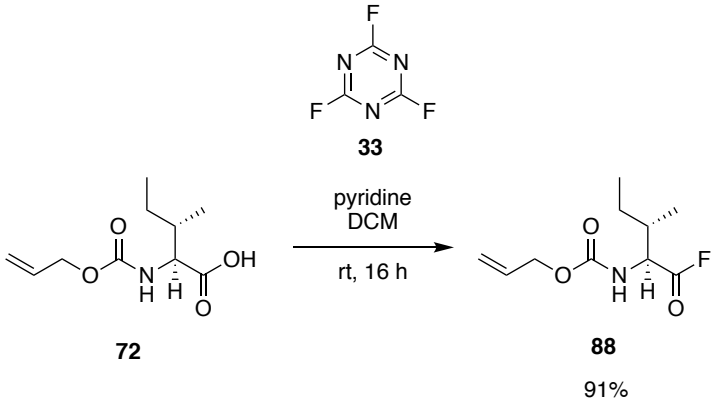

*Scheme 42 - Synthesis of Alloc-isoleucyl acid fluoride **88**.*

With the constituent halves of the required dipeptide in hand, the key aldol condensation-transprotection tandem synthesis was investigated. The reaction methodology involved addition of neat stabase-ethyl glycinate adduct **87** to a solution of freshly prepared lithium diisoproylamide (LDA) in THF at -78 °C, a period of stirring followed by addition of excess acetone. The aldol product **89** could then be telescoped to

the subsequent transprotection reaction by addition of acyl fluoride **88** to the residue containing crude **89**. This tandem sequence, comprised of four consecutive reaction processes, would ultimately furnish a facile pseudo-one pot method for the synthesis of β-hydroxy-substituted protected dipeptides such as the target **90**.

Initial attempts at generating the enolate **91** by reaction of stabase-ethyl glycinate adduct **87** with LDA were unsuccessful, as the final post-acylation product obtained was that of an orthogonally protected isoleucine-glycine dipeptide as opposed to the desired β-hydroxy species **90**. It was postulated that the steric bulk of the dimethylsilyl components of the stabase group may be hindering the approach of LDA, itself a bulky species, preventing deprotonation. Allowing the reaction mixture to warm to -30 °C as well as extension of reaction time alleviated this issue (Scheme 43).

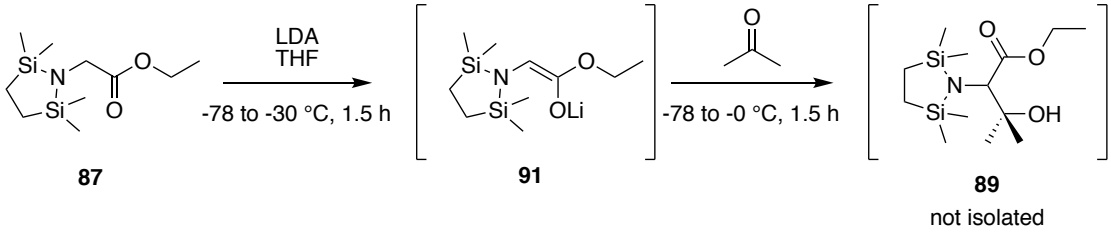

*Scheme 43 - Synthesis of protected β-hydroxyvaline derivative **89**.*

Addition of the acyl fluoride **88** to crude **89** gave a complex mixture of products. Isolation of these compounds revealed the presence of the desired protected dipeptide **90**, as well as the partially-deprotected species **92** and its silanol analogue **93** (Scheme 44). These azasilyl compounds were found to be relatively stable and amenable to complete characterisation. It was discovered that treatment of **92** and **93** with ethanolic HCl liberated the reticent stabase remnants, giving the desired dipeptide **90**. Subsequent preparations of **90** and derivatives included treatment with ethanolic HCl as part of the workup procedure, resulting in attainment of **90** in 75% yield, after purification (Scheme 44).

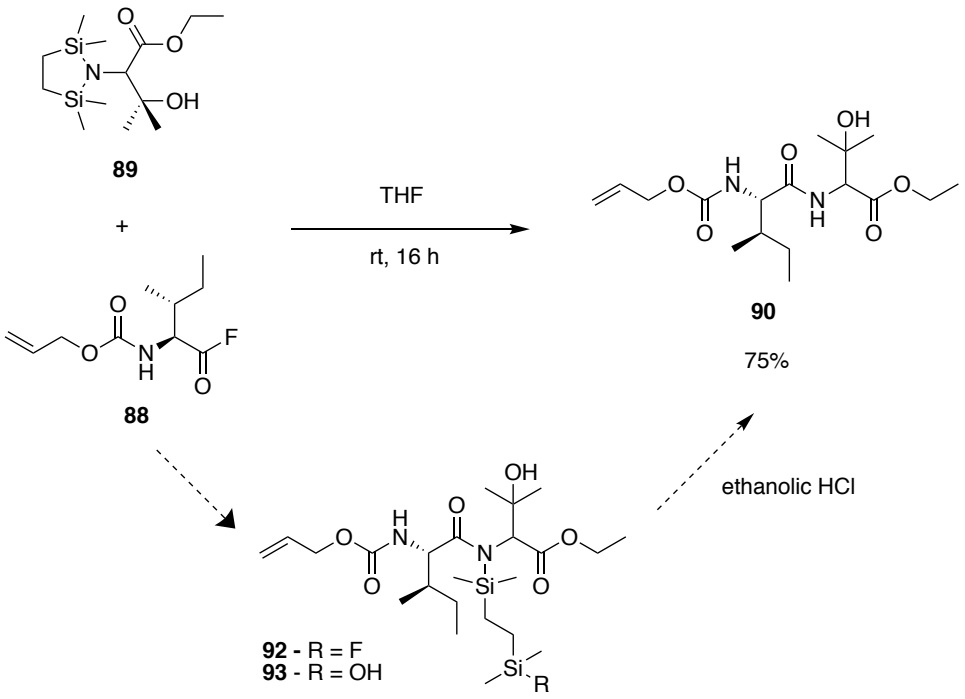

*Scheme 44 - Transprotection furnishing β-hydroxy valine dipeptide **90**.*

With the desired protected azlactone precursor dipeptide **90** in hand, attention turned to completion of the synthesis using the methodology of Jiang *et al.*.[168] Selective hydrolysis of the ethyl ester **90** to the free acid **94** was accomplished in 90% yield with the use of $LiOH.H_2O$ in a $^tBuOH:H_2O$ solvent system (Scheme 45).

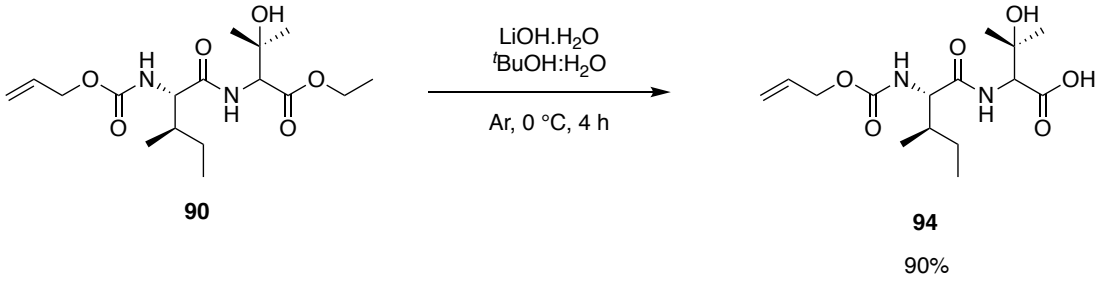

*Scheme 45 - Hydrolysis of ester **90** to give the azlactone precursor **94**.*

Cyclisation of the free acid **94** to the azlactone **83** through dehydration was then carried out, employing acetic anhydride as the dehydrating agent and sodium acetate as base.

Heating at 50 °C in an inert atmosphere furnished the desired azlactone **83** in 81% yield (Scheme 46).

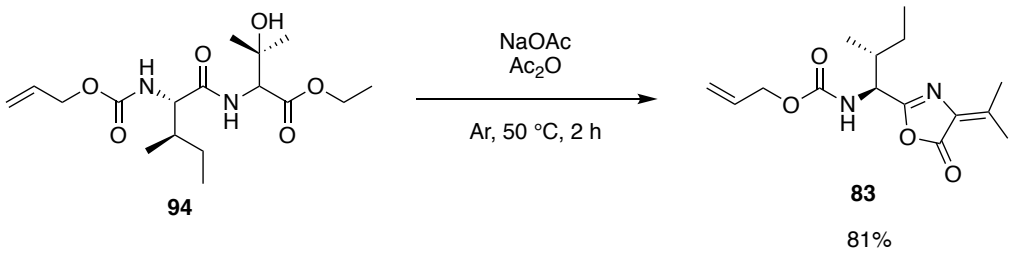

*Scheme 46 - Dehydration of **97** to azlactone **85**.*

Gratifyingly, analysis of the product by ^{1}H NMR spectroscopy and comparison with the spectrum previously obtained for the diastereomeric pair **74** (Scheme 39) revealed stereochemical purity in the newer product, as demonstrated by the absence of the undesired resonance at 4.72 ppm (Figure 25).

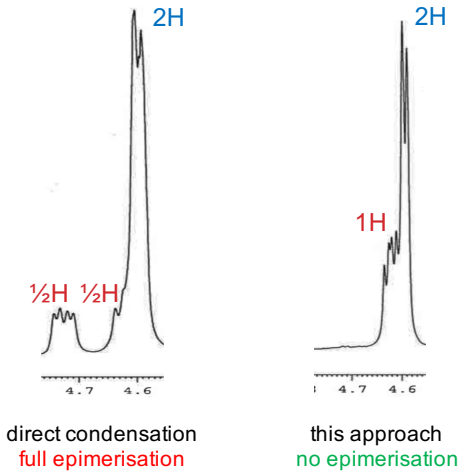

*Figure 25 - Convergence of α-carbon methine proton resonances (right) of azlactone **83**, indicating diastereomeric purity retained in the revised synthesis, compared with that of racemic azlactone **74** (left).*

In order to quantify the efficacy of the turn-inducing strategy in an RCM context, a quartet of experiments were embarked upon using a dicarba analogue of the human growth factor fragment AOD 9604 ('dicarba-AOD 9604') **95** (Figure 26). This species is known to be a difficult species to ring close by RCM, and thus proved an excellent test

substrate to quantify the viability of the strategy without the additional synthetic complications associated with target insulin derivative **96** (e.g. longer chain length, the necessity of repeated arginine couplings, etc.).

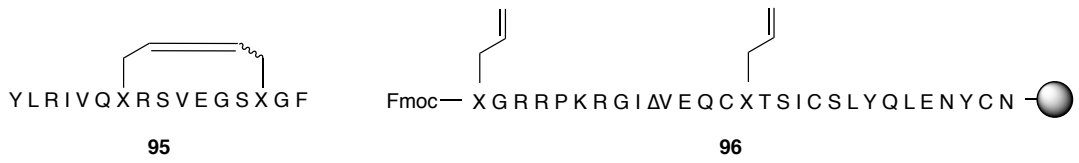

*Figure 26 - Dicarba-AOD 9604 **95** and extended single-chain insulin fragment **96**.*

Previous attempts at the synthesis of this dicarba peptide had demonstrated that a turn-inducing residue, in those cases a serine-derived pseudoproline, is essential to effect ring closing metathesis on the full sequence.[88] It was envisioned that a dehydrovaline residue could be used as a convenient replacement for the pseudoproline. Accordingly, a serine-dehydrovaline dipeptide precursor azlactone **97** was synthesised using the methodology developed for the synthesis of the isoleucine-dehydrovaline azlactone **83** (Scheme 47). The *tert*-butyl ether moiety used in protection of the serine sidechain was well-tolerated, except in the initial Alloc-protection reaction whereby its higher than expected lability during the subsequent acidic workup resulted in a diminished yield. Nevertheless, sufficient quantity of **98** was obtained in order to progress with the synthesis. Future syntheses of Alloc-protected *N*-terminal amino acids with acid-labile sidechain protecting groups should, in this context, should consider a revised workup method.

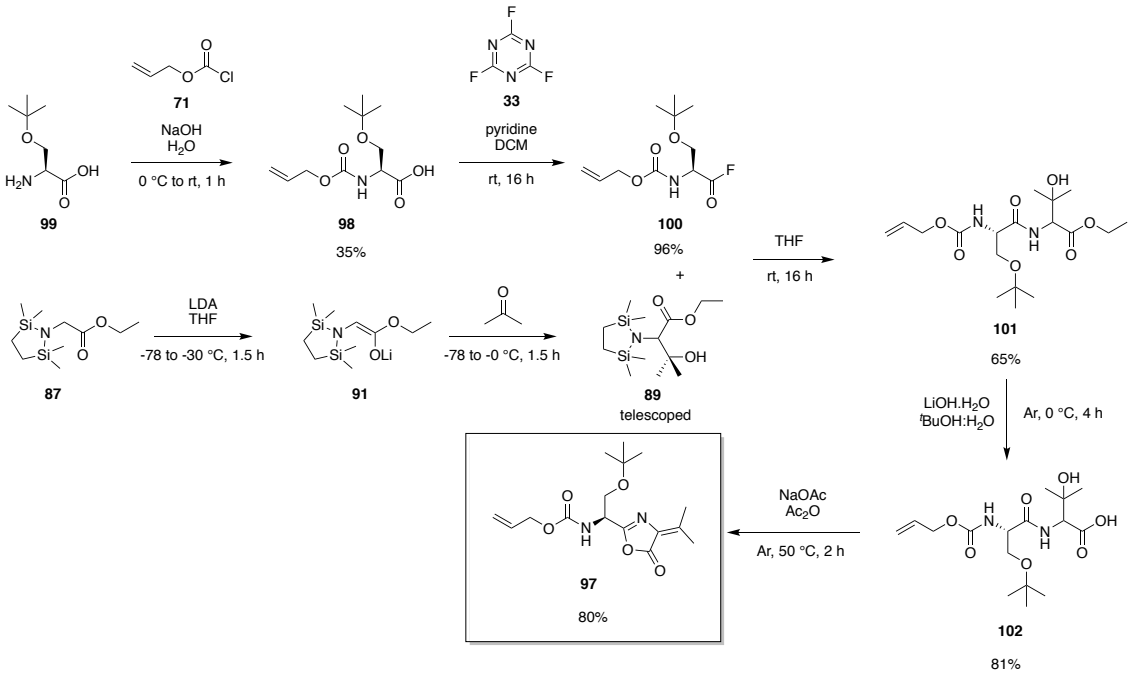

*Scheme 47 - Synthesis of Ser(O^{t}Bu)-Dhv azlactone **97**.*

The obtained azlactone **97** was then coupled to the dicarba-AOD9604 fragment **103** using the previously employed protocol (Scheme 48).

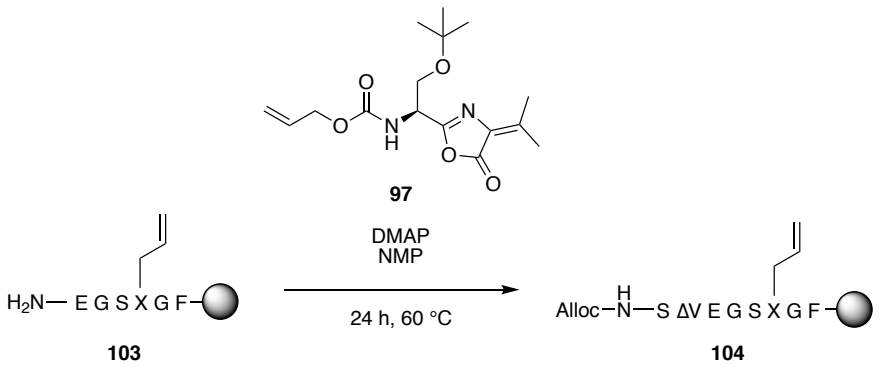

*Scheme 48 - Coupling of azlactone **97** to dicarba-AOD9604 fragment **103**.*

Unlike the previous synthesis of insulin fragment **77**, Alloc-deprotection of **104** was facile and accomplished in a single step (Scheme 49). This may suggest that the extent of Alloc-deprotection is sequence-dependent, an observation not covered readily in the literature.

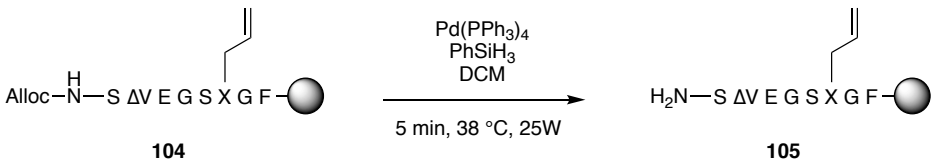

*Scheme 49 - Alloc deprotection of dicarba-AOD9604 fragment **104**.*

The resin was then divided to enable two sets of experiments – RCM of the whole sequence, including *N*-terminal residues 1-6 (i.e. peptide **106**), and RCM of a truncated ten residue sequence terminating at the second allylglycine residue (i.e. **107**). This second 'interrupted' approach, whereby the six *N*-terminal residues of the final sequence are omitted, has been known to improve RCM yields compared with metathesis of a complete resin-bound sequence.[90] The missing residues are appended after metathesis. This strategy was not known at the time of the original reported AOD synthesis and it was thus of interest to see its effect on this otherwise reticent sequence.

Both species **106** and **107** were synthesised from **105** *via* manual and automated SPPS and subjected to RCM (Scheme 50). Concurrently, the non-dehydrovaline-containing species **108** and **109** were also synthesised and subjected to an identical RCM procedure as controls (Scheme 50).

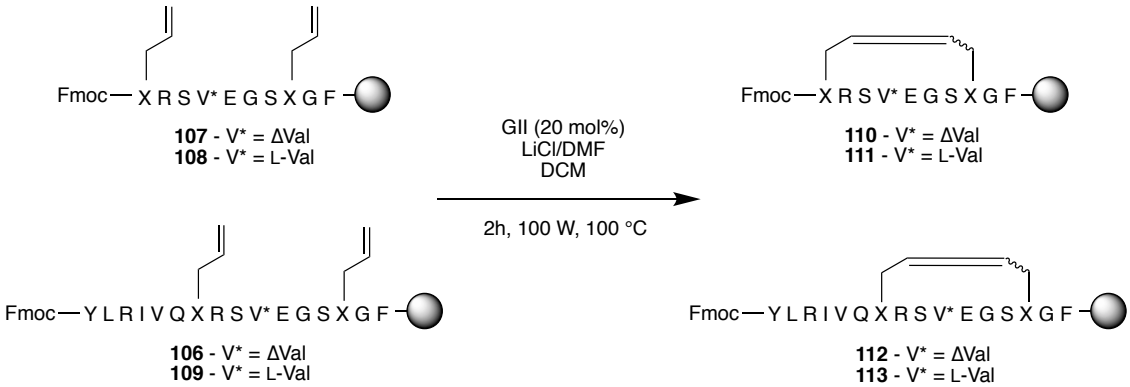

Scheme 50 - RCM of dehydrovaline- and L-valine-containing dicarba-AOD9604 derivatives.

Conversions were then calculated from the distribution of products following small-scale deprotection, cleavage, RP-HPLC and mass spectrometry. Contrary to expectations, species **109** including *N*-terminal residues and the 'native' L-valine gave 20% conversion to the ring-closed product **113** using this protocol, as opposed to the negligible conversion previously reported (despite the use of significantly elongated reaction times (10 h) and increased catalyst loading (24 mol%)).[88] It had been noted during development of the previously discussed RCAM protocol (see Section 3.3.1.1) that stirring of a peptide resin suspension at elevated temperatures for extended periods of time physically degrades the resin, preventing quantitative recovery of the bound peptide after cleavage. The shorter reaction times used in this experiment (Scheme 50) may have resulted in the improved conversion.

As expected, omission of the *N*-terminal residues 1-6 resulted in enhanced metathesis conversion, resulting in 40% conversion of **108** (containing L-valine) to ring-closed product **111**. More gratifyingly, inclusion of the dehydrovaline residue resulted in improved conversion to the ring-closed product in both the full sequence **112** and truncated case **110**, of 56% and 79% respectively. Comparative conversions are listed below (Table 6).

*Table 6 - RCM conversions for products **110-113**.*

	L-valine	**dehydrovaline**
full sequence	20% (**113**)	56% (**112**)
truncated sequence	40% (**111**)	79% (**110**)

These results indicate a quantitative (at least two-fold) improvement in RCM conversion attributable to dehydrovaline inclusion, and unequivocally confirm the viability of the dehydro methodology in promotion of ring-closure as an alternative to pseudoproline

inclusion. The final aspect of the methodology requiring verification was the asymmetric hydrogenation of resin-bound **110** or **112**, selectively reducing the dehydrovaline to the native L-valine.

Whilst other forms of asymmetric catalysis on solid-supports are well-documented in the literature, there are relatively few specific examples of asymmetric hydrogenation.[176-177] An early example was demonstrated by Ojima *et al*. whereby an Fmoc-protected, dehydrophenylalanine-containing tripeptide bound to Wang resin was stereoselectively hydrogenated using Rh(diPAMP) and Rh(Ph-CAPP) catalysts.[178] Doi *et al*. later extended upon this methodology in a combinatorial context by synthesising a dehydroalanine-containing precursor peptide using an on-resin Mizoroki-Heck reaction, followed by Rh(DuPHOS)-catalysed asymmetric hydrogenation to give the desired stereochemistry at the alanine residue.[155]

It should be noted that these prior literature syntheses employed much higher H_2 pressures (150 psi vs. 55-60 psi) and catalyst loadings (50 mol % vs. 1.6 mol %) than that previously trialled for the hydrogenation of insulin fragment **79** (Scheme 38). Owing to the apparent success of the latter strategy, initial conditions to further assess the viability of on-resin asymmetric hydrogenation were chosen judiciously. Resin-bound **110** was subjected to the procedure formerly employed for the reduction of insulin model fragment **79**. Once again, [(*S*,*S*)-Me-DuPHOS-Rh(I)-COD]BF_4 was employed as catalyst and a MeOH/DCM mixture as solvent, giving the reduced peptide in 30% conversion from starting material, determined by RP-HPLC and LRMS (Scheme 51).

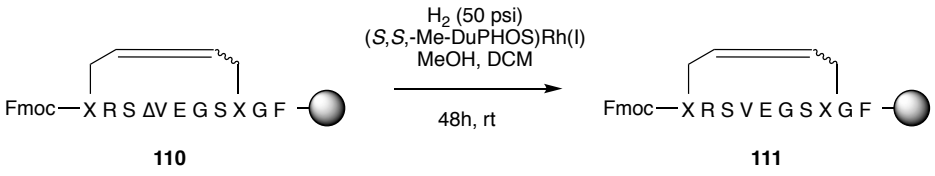

*Scheme 51 - Asymmetric hydrogenation of resin-bound dicarba-AOD9604 fragment **110**.*

The diminished conversion observed in this reaction is of some concern, given the necessity of high-yielding transformations in peptide total synthesis. Repeating the reaction with identical conditions on the same batch of resin gave no improvement and the conversion remained at 30%. Given the precedent of forcing conditions for the transformation on-resin, higher pressures, catalyst loadings and solvent optimisation may be required for this transformation to achieve desired quantitative conversion.

Asymmetrically hydrogenated **111** and an authentic sequence prepared *via* RCM of an L-Val-containing linear sequence **108** were subsequently found to coelute under RP-HPLC conditions. No isomeric peaks were identified in the chromatogram of asymmetrically hydrogenated **111**, suggesting that the process singly installed the native L-stereochemistry. Future unequivocal assignment of stereochemistry would involve synthesis and ring-closure of the D-Val-containing analogue of **111** and subsequent comparison of RP-HPLC retention times with those of the L-configured RCM product and the asymmetrically hydrogenated product, however this was not investigated due to time constraints.

4.2.3 Synthesis of [Δ^4A7-B7]-dicarba-insulin sequence inclusive of truncated C-peptide residues

After tractable verification of the dehydro methodology, attention returned to the synthesis of the interchain dicarba insulin. Numerous attempts at the synthesis of the Agl A7 insulin A-chain fragment **114** were made, however significant deletions were encountered after couping of the Agl A7 residue in each case. The Glu A4-Gln A5-Cys(^{t}Bu) A6 *N*-terminal tripeptide sequence proved difficult to append, ostensibly due to deleterious chain aggregation. An attempt was made to synthesise an Fmoc-Agl-($\Psi^{Me,Me}$Pro)Thr-OH dipeptide to alleviate the aggregation, though this particular compound proved extremely difficult to isolate from an Fmoc-Agl-OH

hydrolysis product and was consequently abandoned. An optimised automated, repeated coupling method was instead developed and applied to the three difficult residues, enabling synthesis of A-chain derivative **114** in sufficiently high purity. It was anticipated that, pending successful coupling of the isoleucine-dehydrovaline azlactone **83**, subsequent couplings would be facilitated by the proposed aggregation-disrupting effects of the dehydrovaline. Accordingly, **83** was coupled to the Agl A7 containing sequence **114** with complete conversion to the desired peptide **115** (Scheme 52).

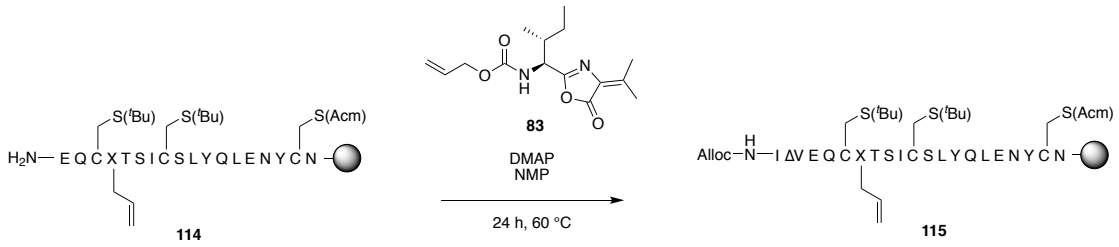

*Scheme 52 - Coupling of Alloc-isoleucine-dehydrovaline azlactone **83** to [A7]-Agl insulin A chain sequence **114**.*

The Alloc-protected species **115** was then deprotected using the microwave protocol developed by Wilson *et al*..[179] Unlike the truncated Agl A7-insulin A-chain sequence **76**, deprotection proceeded quantitatively in one iteration (Scheme 53).

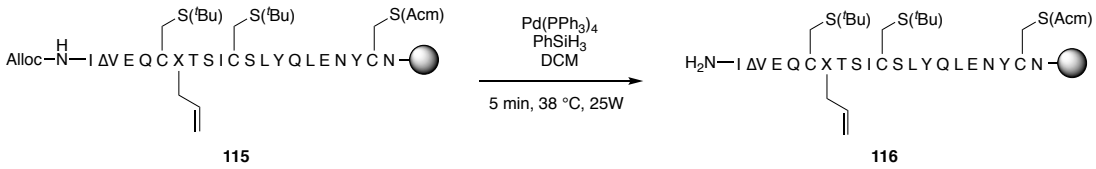

*Scheme 53 - Alloc deprotection of [A3]-Dhv-[A7]-Agl insulin A-chain sequence **115**.*

Initial attempts at coupling the 'C-peptide' sequence GRRPKRG (including Gly A1 and Gly B8) to **116** using automated methods failed, giving multiple deletion products despite the employment of double-couplings for each residue. Eventually the complete peptide **117** was obtained *via* repeated manual couplings (Section 2.3.3.2). Regrettably, when subjected to the standard RCM protocol described in Section 2.3.3.8, subsequent

small-scale Fmoc-deprotection, cleavage and analysis by RP-HPLC and MS showed complete decomposition of both starting material and, if formed, product **118** (Scheme 54).

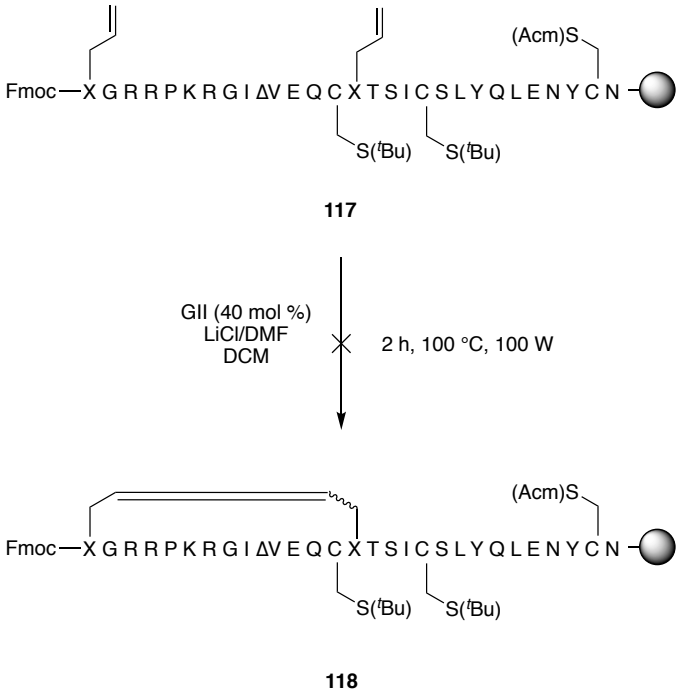

*Scheme 54 - Attempted RCM of sequence **117** including A-chain, tether and B-chain residues.*

Completion of intermediate **118** is requisite for the success of this strategy. However, due to time constraints, resynthesis of **117** was not possible. Future success of this approach will require further optimisation.

4.3 Conclusions

Despite the failure of the final RCM reaction (Scheme 54), the synthetic strategy explored in this final chapter may yet provide a viable toolkit for the construction of the elusive interchain dicarba-insulin. The individual elements of this strategy have been demonstrated as proof-of-concept and, pending optimisation, may conceivably be deployed in a revision of this synthesis. These elements include:

- Enzymatic liberation of the tether sequence -RRPKR-, giving the interchain-dicarba-linked species **59** (Scheme 24, page 111).
- A novel synthesis of dehydroamino acids such as **83** and **97.**
- Quantitative improvement of RCM yield in peptides by the use of aforementioned dehydroamino acids as reversible turn-inducers.

Though the enzymatic digestion protocol afforded the desired two-chain dicarba-linked species **59** as the dominant product, the transformation was not adequately selective, giving several byproducts with sequence deletions. However, it is anticipated that systematic optimisation of digestion conditions, including the use of cofactors, will ameliorate this and give high performance akin to the use of these enzymes in industrial production of insulin pharmaceuticals.

The dehydroamino acid synthesis used to generate **83** and **97** has multiple advantages over existing routes. An extremely diverse range of dehydro-sidechain groups are possible, including those proteinogenic and non-canonical, simply by employing the appropriate ketone or aldehyde. This is an improvement upon the synthesis of Jiang *et al*.,[168] wherein the dehydro-sidechain-containing starting material is a relatively more synthetically complex (and thus presumably less commercially accessible) δ-functionalised α,β-unsaturated ester. Additionally, the use of highly toxic reagents (OsO_4) and high pressures (650 psi H_2) are eliminated. The novel concerted deprotection/acylation 'transprotection' sequence is also highly amenable to rapid and facile synthesis, requiring only the addition of the protected aldol product and the *N*-terminal activated amino acid derivative with no other coupling or deblocking reagents.

Indeed, it is conceivable that coupled with an appropriate on-resin stereoselective hydrogenation method, non-proteinogenic amino acids in their dehydro form could be

installed within a peptide sequence and selectively reduced to their *S*- or *R*-configured forms, allowing for combinatorial diversity.

Potential extension of this chemistry might involve:

- Inclusion in the insulin sequence to permit turn induction, as previously verified in the model sequences **78** and **80** employing the racemic azlactone **74**;
- Applying the synthesis to azlactones containing varied *N*-terminal amino acid residues, including those with protected polar side-chain functionalities;
- Asymmetric hydrogenation of the dehydrovaline species on-resin and evaluation of the stereoselectivity of the transformation (possible due to the elimination of diastereomer formation in the new dehydro synthesis); and
- Exploration of selective dehydration to give *E*- or *Z*-configured dehydroamino acids with non-symmetric geminal substituents.

The primary obstacle impeding this synthesis at present is the difficult RCM of the final precursor **117**. Optimisation of the final sequence may involve incorporation of another aggregation-disrupting species, such as a pseudoproline or *N*-protected amino acid residue, to discourage aggregation if it is the cause of the failed metathesis. Alternatively, resins with optimised swelling characteristics may be employed in later syntheses to enable better chain access for the catalyst.

The chemistries developed in the course of this project thus open up exciting avenues for further development. The distinct biological and chemical challenges presented by insulin and its derivatives ensures that it will remain a perennial subject of innovative research for years to come.

4.4 Experimental

4.4.1 Synthetic Procedures

4.4.1.1 Fmoc-Agl-Pro-*des*$_{A11-21}$-[A6]-Cys(^{t}Bu)-[A7]-Agl human insulin A-chain 49

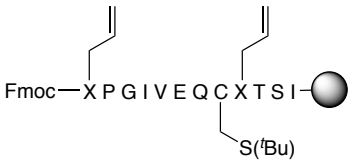

49

The resin-bound peptide **49** excluding the *N*-terminal Agl and Pro residues was prepared on a 0.125 mmol scale according to the general automated procedure outlined in Section 2.3.3.1. Formation of **49** excluding the *N*-terminal Agl and Pro residues was subsequently verified by small-scale Fmoc deprotection and resin cleavage, RP-HPLC and LRMS. Mass spectrum (ESI$^+$, MeCN:H_2O:TFA): *m/z* 1101.6 $[M+H]^+$; $C_{48}H_{83}N_{11}O_{16}S$ requires 1101.6. RP-HPLC (Agilent: Vydac C18 analytical column, 15 to 50% buffer B over 35 min): t_R = 17.8 min. L-Pro was attached according to the general manual SPPS procedure outlined in Section 2.3.3.2 with the following quantities of reagents: HATU (192 mg, 0.5 mmol, 4 equiv.), Fmoc-L-proline (170 mg, 0.5 mmol, 4 equiv.), NMM (110 µL, 1.0 mmol, 8 equiv.) in DMF (4 mL). L-Agl was attached according to the general manual SPPS procedure with the following quantities of reagents: HATU (192 mg, 0.5 mmol, 4 equiv.), Fmoc-L-allylglycine (170 mg, 0.5 mmol, 4 equiv.), NMM (110 µL, 1.0 mmol, 8 equiv.) in DMF (4 mL). Where incomplete coupling was indicated by a positive TNBS test (Section 2.3.3.4), the manual coupling was repeated. Formation of **49** was subsequently verified by small-scale Fmoc deprotection and resin cleavage, RP-HPLC and LRMS. Mass spectrum (ESI$^+$, MeCN:H_2O:TFA): *m/z* 1295.5 $[M+H]^+$; $C_{58}H_{97}N_{13}O_{18}S$ requires 1295.7. RP-HPLC (Agilent: Vydac C18 analytical column, 15 to 50% buffer B over 35 min): t_R = 19.6 min. The resin-bound peptide was subjected to

the capping procedure outlined in Section 2.3.3.6 and stored overnight in a vacuum desiccator prior to RCM.

4.4.1.2 Fmoc-[Δ⁴Agl-A7]-dicarba-Pro-*des*$_{A11-21}$-[A6]-Cys(ᵗBu)- human insulin A-chain 50

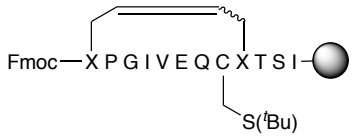

50

Resin-bound peptide **49** was subjected to the general microwave-assisted on-resin RCM procedure outlined in Section 2.3.3.8 with the following quantities of reagents: GII (17 mg, 20 mol %), 0.4 M LiCl/DMF (~0.2 mL), DCM (1.6 mL). Analysis of the resin-bound peptide by RP-HPLC and MS following small-scale Fmoc deprotection and resin cleavage showed only the presence of starting material. Repetition of the RCM reaction under similar conditions to those above (GII (17.5 mg, 20 mol %), 0.4 M LiCl/DMF (~0.2 mL), DCM (4 mL)) resulted in formation of **50** with 6% conversion. Mass spectrum (ESI^+, MeCN:H_2O:TFA): *m/z* 1267.7 $[M+H]^+$; $C_{56}H_{93}N_{13}O_{18}S$ requires 1267.7. RP-HPLC (Agilent: Vydac C18 analytical column, 15 to 50% buffer B over 35 min): t_R = 17.1 min.

4.4.1.3 Fmoc-Agl-Gly-Arg-Arg-Pro-Lys-Arg-*des*$_{A11-21}$-[A6]-Cys(ᵗBu)-[A7]-Agl human insulin A-chain 47

47

The resin-bound peptide **47** excluding the *N*-terminal Agl residue was prepared on an 0.125 mmol scale according to the general automated procedure outlined in Section

2.3.3.1. Formation of **47** excluding the *N*-terminal Agl residue was subsequently verified by small-scale Fmoc deprotection and resin cleavage, RP-HPLC and LRMS. Mass spectrum (ESI^+, MeCN:H_2O:TFA): *m/z* 926.8 $[M+2H]^{2+}$; ½($C_{79}H_{141}N_{27}O_{22}S$) requires 927.0. RP-HPLC (Agilent: Vydac C18 analytical column, 15 to 50% buffer B over 35 min): t_R = 15.6 min. L-Agl was attached according to the general manual SPPS procedure outlined in Section 2.3.3.2 with the following quantities of reagents: HATU (191 mg, 0.5 mmol, 4 equiv.), Fmoc-L-allylglycine (171 mg, 0.5 mmol, 4 equiv.), NMM (110 µL, 1.0 mmol, 8 equiv.) in DMF (4 mL). Formation of **47** was subsequently verified by small-scale Fmoc deprotection and resin cleavage, RP-HPLC and LRMS. Mass spectrum (ESI^+, MeCN:H_2O:TFA): *m/z* 975.3 $[M+2H]^{2+}$; ½($C_{84}H_{148}N_{28}O_{23}S$) requires 975.6. RP-HPLC (Agilent: Vydac C18 analytical column, 15 to 50% buffer B over 35 min): t_R = 15.7 min. The resin-bound peptide was subjected to the capping procedure outlined in Section 2.3.3.6 and stored overnight in a vacuum desiccator prior to RCM.

4.4.1.4 Attempted synthesis of Fmoc-[[Δ⁴Agl-A7]-dicarba]-Gly-Arg-Arg-Pro-Lys-Arg-*des*$_{A11\text{-}21}$-[A6]-Cys(ᵗBu) human insulin A-chain 48

48

Resin-bound peptide **47** was subjected to the general microwave-assisted on-resin RCM procedure outlined in Section 2.3.3.8 with the following quantities of reagents: GII (19 mg, 23 mol %), 0.4 M LiCl/DMF (~0.2 mL), DCM (4 mL). Analysis of the resin-bound peptide by RP-HPLC and MS following small-scale Fmoc deprotection and resin cleavage showed only the presence of starting material. Repetition of the RCM reaction with increased catalyst loading similarly failed to yield **48** (GII (43 mg, 50 mol %), 0.4 M LiCl/DMF (~0.2 mL), DCM (4 mL)) determined by analysis of the resin-bound

peptide by RP-HPLC and MS following small-scale Fmoc deprotection and resin cleavage.

4.4.1.5 Fmoc-Agl-Pro-*des*$_{A11\text{-}21}$-[A6]-Ala-[A7]-Agl human insulin A-chain 51

51

The resin-bound peptide **51** excluding the *N*-terminal Agl residue was prepared on an 0.1 mmol scale according to the general automated procedure outlined in Section 2.3.3.1. Formation of **51,** excluding the *N*-terminal Agl residue, was verified by small-scale Fmoc deprotection and resin cleavage, RP-HPLC and LRMS. Mass spectrum (ESI^+, MeCN:H_2O:TFA): *m/z* 1110.6 $[M+H]^+$; $C_{49}H_{82}N_{12}O_{17}$ requires 1110.6. RP-HPLC (Agilent: Vydac C18 analytical column, 15 to 50% buffer B over 35 min): t_R = 11.3 min. L-Agl was attached according to the general manual SPPS procedure outlined in Section 2.3.3.2 with the following quantities of reagents: HATU (143 mg, 0.4 mmol, 4 equiv.), Fmoc-L-allylglycine (135 mg, 0.4 mmol, 4 equiv.), NMM (110 µL, 1.0 mmol, 8 equiv.) in DMF (4 mL). Formation of **51** was subsequently verified by small-scale Fmoc deprotection and resin cleavage, RP-HPLC and LRMS. Mass spectrum (ESI^+, MeCN:H_2O:TFA): *m/z* 1207.5 $[M+H]^+$; ($C_{54}H_{89}N_{13}O_{18}$) requires 1207.6. RP-HPLC (Agilent: Vydac C18 analytical column, 15 to 50% buffer B over 35 min): t_R = 12.9 min. The resin-bound peptide was subjected to the capping procedure outlined in Section 2.3.3.6 and stored overnight in a vacuum desiccator prior to RCM.

4.4.1.6 Attempted synthesis of Fmoc-[Δ⁴Agl-A7]-dicarba-Pro-*des*$_{A11-21}$-[A6]-Ala human insulin A-chain 52

52

Resin-bound peptide **51** was subjected to the general microwave-assisted on-resin RCM procedure outlined in Section 2.3.3.8 with the following quantities of reagents: GII (22 mg, 26 mol %), 0.4 M LiCl/DMF (~0.2 mL), DCM (4 mL). Analysis of the resin-bound peptide by RP-HPLC and MS following small-scale Fmoc deprotection and resin cleavage showed only the presence of starting material.

4.4.1.7 Fmoc-Agl-*des*$_{A11-21}$-[A3]-Pro-[A6]-Cys(^{t}Bu)-[A7]-Agl human insulin A-chain 53

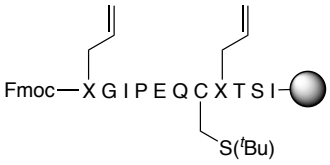

53

The resin-bound peptide **53** excluding the *N*-terminal Agl residue was prepared on an 0.1 mmol scale according to the general automated procedure outlined in Section 2.3.3.1. Formation of **53** excluding the *N*-terminal Agl residue was subsequently verified by small-scale Fmoc deprotection and resin cleavage, RP-HPLC and LRMS. Mass spectrum (ESI$^+$, MeCN:H_2O:TFA): *m/z* 1100.3 $[M+H]^+$; $C_{48}H_{81}N_{11}O_{16}S$ requires 1100.6. RP-HPLC (Agilent: Vydac C18 analytical column, 15 to 50% buffer B over 35 min): t_R = 12.5 min. L-Agl was attached according to the general manual SPPS procedure outlined in Section 2.3.3.2 with the following quantities of reagents: HATU (143 mg, 0.4 mmol, 4 equiv.), Fmoc-L-allylglycine (135 mg, 0.4 mmol, 4 equiv.), NMM (110 μL, 1.0 mmol, 8 equiv.) in DMF (4 mL). The resin-bound peptide was subjected to

the capping procedure outlined in Section 2.3.3.6 and stored overnight in a vacuum desiccator prior to RCM.

4.4.1.8 Fmoc-[Δ⁴Agl-A7]-dicarba-*des*$_{A11-21}$-[A3]-Pro-[A6]-Cys(ᵗBu) human insulin A-chain 54

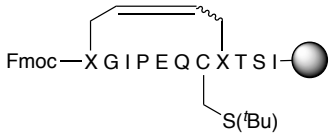

54

Resin-bound peptide **53** was subjected to the general microwave-assisted on-resin RCM procedure outlined in Section 2.3.3.8 with the following quantities of reagents: GII (19 mg, 22 mol %), 0.4 M LiCl/DMF (~0.2 mL), DCM (4 mL). Formation of **54** as a pair of isomers (**54(I)** and **54(II)**) was subsequently verified by small-scale Fmoc deprotection and resin cleavage, RP-HPLC and LRMS. **54(I)**: Mass spectrum (ESI$^+$, MeCN:H_2O:TFA): *m/z* 1168.5 $[M+H]^+$; ($C_{51}H_{84}N_{12}O_{17}S$) requires 1169.6. 584.9 $[M+2H]^{2+}$; ½($C_{51}H_{84}N_{12}O_{17}S$) requires 585.3. RP-HPLC (Agilent: Vydac C18 analytical column, 15 to 50% buffer B over 35 min): t_R = 10.8 min.

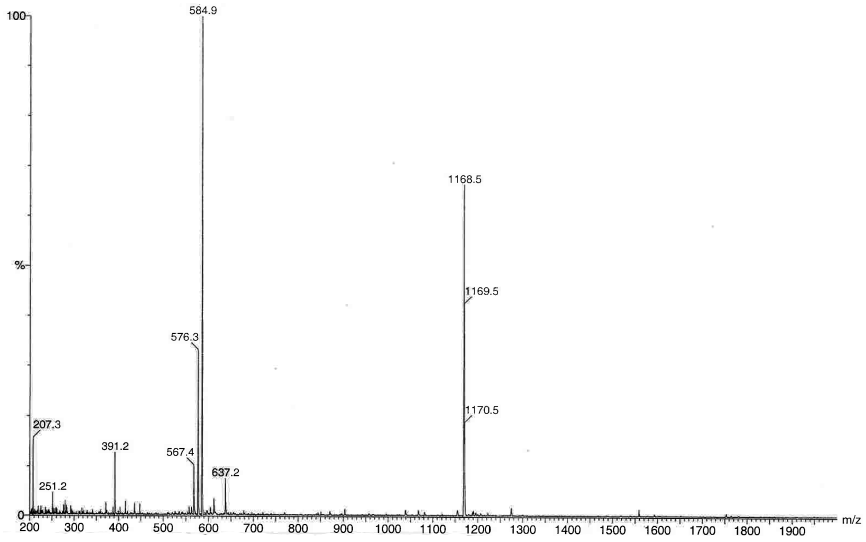

54(II): Mass spectrum (ESI^+, MeCN:H_2O:TFA): *m/z* 1168.5 $[M+H]^+$; ($C_{51}H_{84}N_{12}O_{17}S$) requires 1169.6. 584.9 $[M+2H]^{2+}$; ½($C_{51}H_{84}N_{12}O_{17}S$) requires 585.3. RP-HPLC (Agilent: Vydac C18 analytical column, 15 to 50% buffer B over 35 min): t_R = 11.1 min.

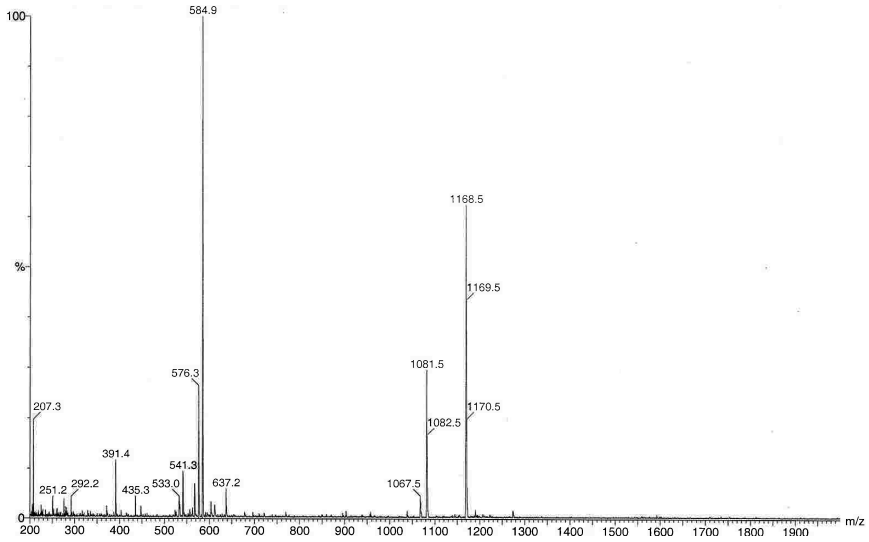

4.4.1.9 Fmoc-Agl-Gly-Arg-Arg-Pro-Lys-Arg-*des*$_{A11\text{-}21}$-[A3]-Pro-[A6]-Cys(^{t}Bu)-[A7]-Agl human insulin A-chain 55

55

The resin-bound peptide **55** excluding the *N*-terminal Agl residue was prepared on an 0.1 mmol scale *via* the general automated procedure outlined in Section 2.3.3.1.

L-Agl was attached according to the general manual SPPS procedure outlined in Section 2.3.3.2 with the following quantities of reagents: HATU (191 mg, 0.5 mmol, 4 equiv.), Fmoc-L-allylglycine (171 mg, 0.5 mmol, 4 equiv.), NMM (110 µL, 1.0 mmol, 8 equiv.) in DMF (4 mL). Formation of **55** was subsequently verified by small-scale Fmoc deprotection and resin cleavage, RP-HPLC and LRMS. Mass spectrum (ESI^+, MeCN:H_2O:TFA): *m/z* 650.1 $[M+3H]^{3+}$; ⅓($C_{84}H_{146}N_{28}O_{23}S$) requires 650.0. 974.8

$[M+2H]^{2+}$; ½($C_{84}H_{146}N_{28}O_{23}S$) requires 974.5. RP-HPLC (Agilent: Vydac C18 analytical column, 15 to 50% buffer B over 35 min): t_R = 11.3 min. The resin-bound peptide was subjected to the capping procedure outlined in Section 2.3.3.6 and stored overnight in a vacuum desiccator prior to RCM.

4.4.1.10 Fmoc-[Δ^4Agl-A7]-dicarba-Gly-Arg-Arg-Pro-Lys-Arg-*des*$_{A11\text{-}21}$-[A3]-Pro-[A6]-Cys(^{t}Bu) human insulin A-chain 56

56

Resin-bound peptide **55** was subjected to the general microwave-assisted on-resin RCM procedure outlined in Section 2.3.3.8 with the following quantities of reagents: GII (19 mg, 23 mol %), 0.4 M LiCl/DMF (~0.2 mL), DCM (4 mL). Formation of **56** as a pair of isomers (**56(I)** and **56(II)**) was subsequently verified by small-scale Fmoc deprotection and resin cleavage, RP-HPLC and LRMS. **56(I)**: Mass spectrum (ESI^+, MeCN:H_2O:TFA): *m/z* 960.7 $[M+2H]^{2+}$; ½($C_{82}H_{142}N_{28}O_{23}S$) requires 960.5. RP-HPLC (Agilent: Vydac C18 analytical column, 15 to 50% buffer B over 35 min): t_R = 8.6 min.

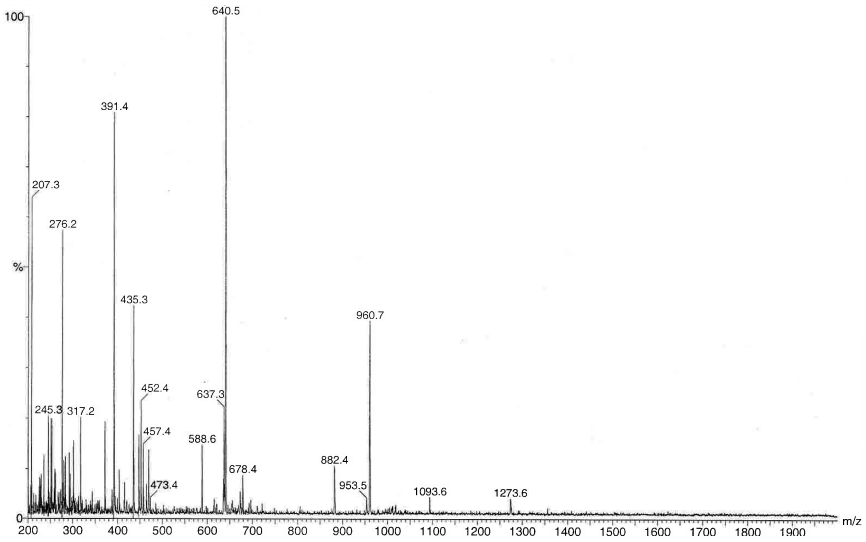

56(II): Mass spectrum (ESI^+, MeCN:H_2O:TFA): *m/z* 960.3 $[M+2H]^{2+}$; ½($C_{82}H_{142}N_{28}O_{23}S$) requires 960.5. RP-HPLC (Agilent: Vydac C18 analytical column, 15 to 50% buffer B over 35 min): t_R = 9.0 min.

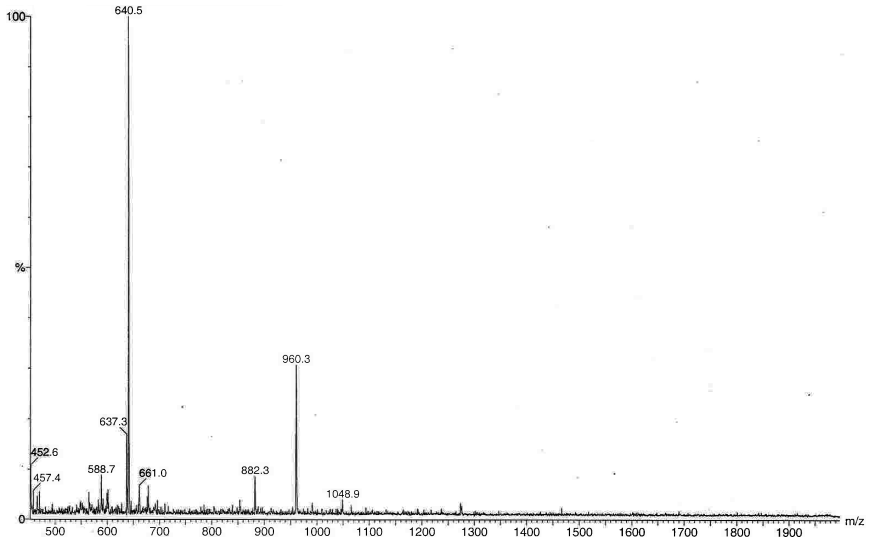

4.4.1.11 Attempted synthesis of Phe-Val-Asn-Gln-His-Leu-[Δ⁴Agl-A7]-dicarba-Gly-Arg-Arg-Pro-Lys-Arg- *des*$_{A11-21}$-[A3]-Pro-[A6]-Cys(*t*Bu) human insulin A-chain 119 (leading to 58)

119

Synthesis of peptide **119** from resin-bound **56** was attempted according to the general automated procedure outlined in Section 2.3.3.1. Formation of the truncated pyroglutamate species Glp-His-Leu-[[Δ⁴Agl-A7]-dicarba]-Gly-Arg-Arg-Pro-Lys-Arg-*des*$_{A11-21}$-[A3]-Pro-[A6]-Cys(*t*Bu) human insulin A-chain **58** as a mixture of isomers was subsequently observed as the dominant product by small-scale cleavage, RP-HPLC and LRMS.

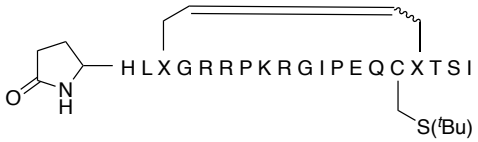

58

Mass spectrum (ESI$^+$, MeCN:H_2O:TFA): *m/z* 760.9 $[M+3H]^{3+}$; ⅓($C_{99}H_{165}N_{33}O_{27}S$) requires 761.1. 1140.6 $[M+2H]^{2+}$; ½($C_{99}H_{165}N_{33}O_{27}S$) requires 1141.1. RP-HPLC (Agilent: Vydac C18 analytical column, 15 to 50% buffer B over 35 min): t_R = 10.6 min. The resin was then subjected to TFA-mediated cleavage, the residue dissolved in MeCN:H_2O (~1:5) and lyophilised to give the peptide as an off-white solid (96 mg). The peptide was then purified *via* preparative RP-HPLC (Agilent: Vydac C18 preparative column, 15 to 50% buffer B over 45 min) and selected fractions combined and lyophilised to give **58** as a colourless solid, comprised of mixed isomers (mass spectrum of crude and post-purification chromatogram shown below).

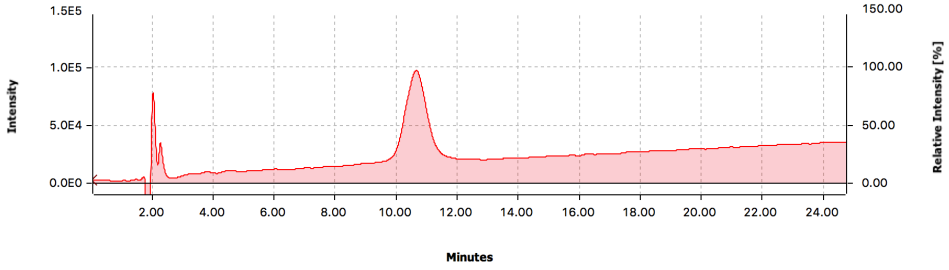
Intensity
1.5E5
1.0E5
5.0E4
0.0E0
150.00
100.00
50.00
0.00
Relative Intensity [%]
2.00
4.00
6.00
8.00
10.00
12.00
14.00
16.00
18.00
20.00
22.00
24.00
Minutes

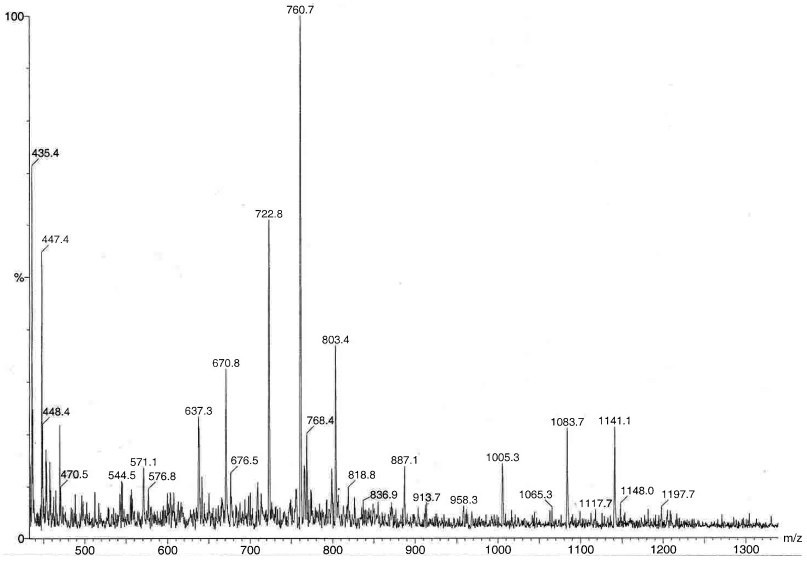
100
%
0
760.7
435.4
722.8
447.4
803.4
670.8
448.4
637.3
768.4
1083.7
1141.1
571.1
676.5
887.1
1005.3
470.5
544.5
576.8
818.8
836.9
913.7
958.3
1065.3
1117.7
1148.0
1197.7
500
600
700
800
900
1000
1100
1200
1300
m/z

4.4.1.12 *des*$_{A11\text{-}21,B1\text{-}3,B9\text{-}30}$-[A3]-Pro-[$\Delta^4$A7-B7]-dicarba-[A6]-Cys(^{t}Bu) human insulin 59

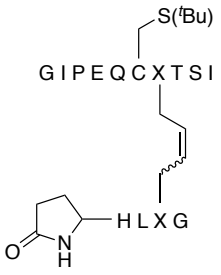

59

Enzymatic digestion of **58** was carried out according to a modified version of a procedure originally described by Given *et al.*[152] **58** (1.7 mg) was dissolved in Tris-HCl buffer (1.5 mL, 0.05 M, pH 7.5) containing Ca^{2+} (5 µM, as chloride) and warmed to 22 °C in a temperature-controlled elliptical shaker. Solutions of carboxypeptidase B (168 µL, 1 g/L) and then trypsin (8.5 µL, 1 g/L) were then added and the solution incubated with shaking at 22 °C for 8 hours. 50 µL aliquots of the reaction mixture were taken at regular intervals, diluted with 50 µL glacial acetic acid and injected directly into an RP-HPLC instrument for monitoring. At the end of the digestion duration, the reaction mixture was lyophilised to give crude **59** as a colourless powder (13.4 mg). Mass spectrum (ESI^+, MeCN:H_2O:TFA): *m/z* 802.7 $[M+2H]^{2+}$; ½($C_{70}H_{114}N_{19}O_{22}S$) requires 802.9. RP-HPLC (Agilent: Vydac C18 analytical column, 15 to 50% buffer B over 35 min): t_R = 10.3 min.

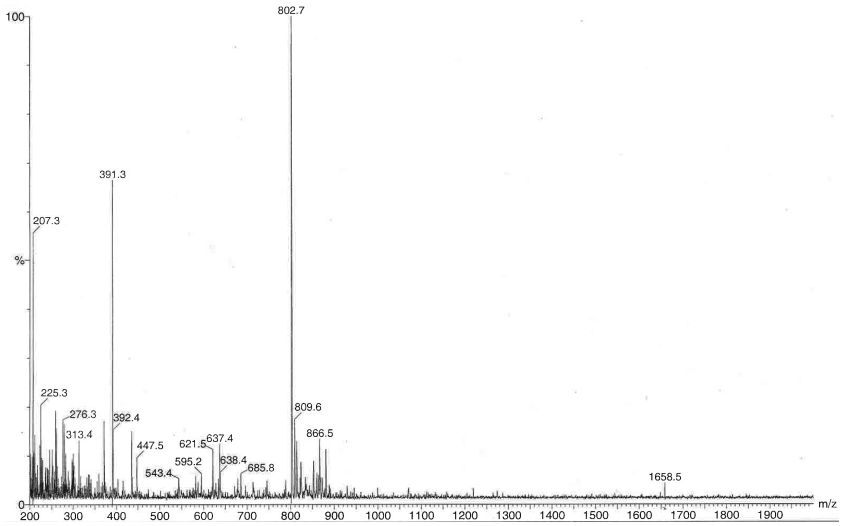

4.4.1.13 *des*$_{A1\text{-}5}$-[A6,A11]-Agl-[A7]-Cys(^{t}Bu)-[A20]-Cys(Acm) human insulin A-chain 120

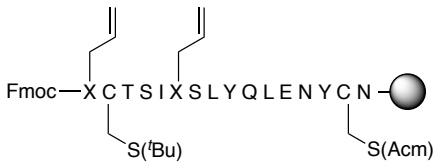

120

The resin-bound peptide **120** excluding *N*-terminal Agl residue A6 was prepared according to the general automated procedure outlined in Section 2.3.3.1. Formation of **120** excluding *N*-terminal Agl residue A6 was subsequently verified by small-scale Fmoc deprotection and resin cleavage, RP-HPLC and LRMS. Mass spectrum (ESI^+, MeCN:H_2O:TFA): *m/z* 938.2 $[M+2H]^{2+}$; ½($C_{82}H_{127}N_{19}O_{27}S_2$) requires 937.9. RP-HPLC (Agilent: Vydac C18 analytical column, 15 to 50% buffer B over 35 min): t_R = 17.1 min. Fmoc-L-Agl A6 was attached according to the general manual microwave-assisted SPPS procedure outlined in Section 2.3.3.3 with the following quantities of reagents: HATU (114 mg, 0.3 mmol, 3 equiv.), Fmoc-L-allylglycine (119 mg, 0.3 mmol, 3 equiv.), NMM (66 μL, 0.6 mmol, 6 equiv.) in DMF (4 mL). The resin-bound peptide was subjected to

the capping procedure outlined in Section 2.3.3.6 and stored overnight in a vacuum desiccator prior to RCM.

4.4.1.14 *des*$_{A1\text{-}5}$-[Δ^4A6-A11]-dicarba-[A7]-Cys(^{t}Bu)-[A20]-Cys(Acm) human insulin A-chain 121

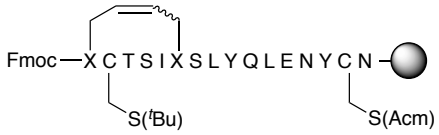

121

Resin-bound peptide **120** was subjected to the general microwave-assisted on-resin RCM procedure outlined in Section 2.3.3.8 with the following quantities of reagents: GII (18 mg, 21 mol %), 0.4 M LiCl/DMF (~0.2 mL), DCM (4 mL). Formation of **121** as a pair of isomers (**121(I)** and **121(II)**) in a 7:3 ratio was subsequently verified by small-scale Fmoc deprotection and resin cleavage, RP-HPLC and LRMS. **121(I)**: Mass spectrum (ESI$^+$, MeCN:H_2O:TFA): *m/z* 973.1 $[M+2H]^{2+}$; ½($C_{85}H_{132}N_{20}O_{28}S_2$) requires 972.4. RP-HPLC (Agilent: Vydac C18 analytical column, 15 to 50% buffer B over 35 min): t_R = 17.3 min. **121(II)**: Mass spectrum (ESI$^+$, MeCN:H_2O:TFA): *m/z* 973.1 $[M+2H]^{2+}$; ½($C_{85}H_{132}N_{20}O_{28}S_2$) requires 972.4. RP-HPLC (Agilent: Vydac C18 analytical column, 15 to 50% buffer B over 35 min): t_R = 17.7 min.

4.4.1.15 [A3]-Pro-[Δ^4A6-A11]-dicarba-[A7]-Cys(^{t}Bu)-[A20]-Cys(Acm) human insulin A-chain 122

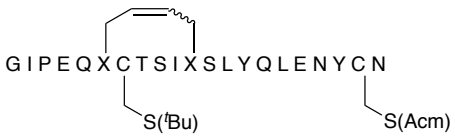

122

Peptide **122** was prepared from resin-bound **121** according to the general automated procedure outlined in Section 2.3.3.1. Formation of **122(I)** and **122(II)** was verified by small-scale cleavage, RP-HPLC and LRMS. **122(I)**: Mass spectrum (ESI$^+$,

MeCN:H_2O:TFA): *m/z* 823.9 $[M+3H]^{3+}$; ⅓($C_{108}H_{166}N_{26}O_{36}S_2$) requires 823.4. 1235.3 $[M+2H]^{2+}$; ½($C_{108}H_{166}N_{26}O_{36}S_2$) requires 1234.6. RP-HPLC (Agilent: Vydac C18 analytical column, 15 to 50% buffer B over 35 min): t_R = 17.7 min. **122(II)** Mass spectrum (ESI^+, MeCN:H_2O:TFA): *m/z* 823.6 $[M+3H]^{3+}$; ⅓($C_{108}H_{166}N_{26}O_{36}S_2$) requires 823.4. *m/z* 1235.1 $[M+2H]^{2+}$; ½($C_{108}H_{166}N_{26}O_{36}S_2$) requires 1234.6. RP-HPLC (Agilent: Vydac C18 analytical column, 15 to 50% buffer B over 35 min): t_R = 18.1 min. The resin was then subjected to TFA-mediated cleavage, the residue dissolved in MeCN:H_2O (~1:5) and lyophilised to give the desired peptides **122(I)** and **122(II)** as an off-white solid (181 mg).

4.4.1.16 [A3]-Pro-[Δ⁴A6-A11]-dicarba-[A7]-Cys(SPyr)-[A20]-Cys(Acm) human insulin A-chain 123

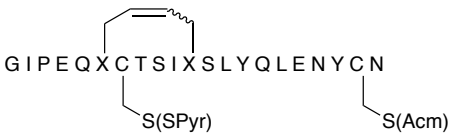

123

The concerted *tert*-butyl deprotection and *S*-pyridinyl protection at Cys A7 was executed according to the procedure described by Büllesbach *et al*..[110] To a solution of anisole:TFA (1:9, 4.8 mL) was added 2-dipyridyl disulfide (DPDS) (34 mg, 0.2 mmol, 2 equiv.) and the resulting solution cooled to 0 °C in an ice bath. To this solution was added lyophilised peptide **122** (181 mg) followed by a chilled solution of triflic acid:TFA (1:4, 4.8 mL). The resulting light brown solution was stirred at 0 °C for 1.5 hours upon which the solution was concentrated under a stream of N_2 and the crude peptide precipitated with chilled ether (35 mL). The suspension was centrifuged, the supernatant discarded, the precipitate resuspended and centrifuged in chilled ether (35 mL) a further two times. The crude peptide was then dissolved in MeCN:H_2O and lyophilised to give **123** as a brittle red gum (278 mg). Formation of **123** as a pair of isomers **123(I)** and **123(II)** was subsequently verified by small-scale cleavage, RP-HPLC and LRMS.

123(I): Mass spectrum (ESI^+, MeCN:H_2O:TFA): *m/z* 841.4 $[M+3H]^{3+}$; ⅓($C_{109}H_{161}N_{27}O_{36}S_3$) requires 841.0. *m/z* 1261.6 $[M+2H]^{2+}$; ½($C_{109}H_{161}N_{27}O_{36}S_3$) requires 1261.0. RP-HPLC (Agilent: Vydac C18 analytical column, 15 to 50% buffer B over 35 min): t_R = 16.4 min. **123(II)** Mass spectrum (ESI^+, MeCN:H_2O:TFA): *m/z* 841.6 $[M+3H]^{3+}$; ⅓($C_{109}H_{161}N_{27}O_{36}S_3$) requires 841.0. 1261.6 $[M+2H]^{2+}$; ½($C_{109}H_{161}N_{27}O_{36}S_3$) requires 1261.0. RP-HPLC (Agilent: Vydac C18 analytical column, 15 to 50% buffer B over 35 min): t_R = 16.4 min. Peptide **123** was purified *via* preparative RP-HPLC (Agilent: Vydac C18 preparative column, 15 to 50% buffer B over 45 min) and selected fractions combined and lyophilised to give **123** as a mixture of isomers (146 mg).

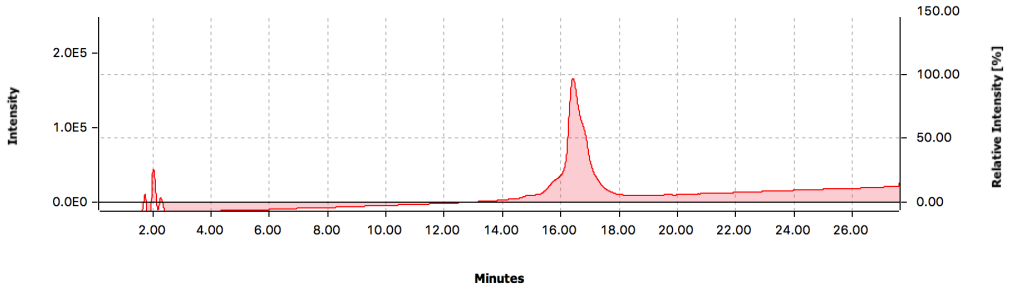

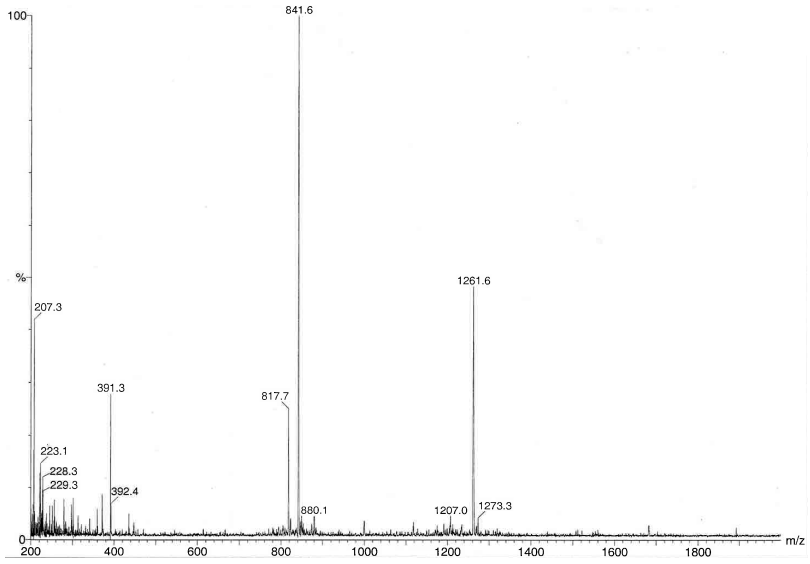

4.4.1.17 [A3]-Pro-[Δ⁴A6-A11]-dicarba-[A20, B19]-Cys(Acm) human insulin 124

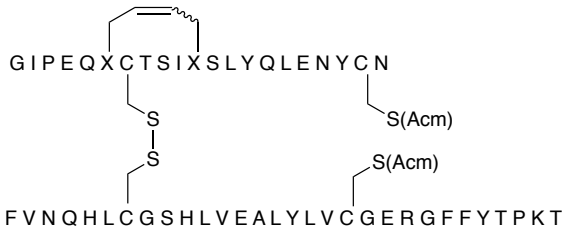

124

Combination of the A- and B-chain monomers was executed according to a modified version of a procedure originally described by Lin *et al.*[111] A portion of the combined modified insulin A-chain **123** (containing both isomers **123(I)** and **123(II)**) (9.8 mg, 3.9 μmol) was dissolved in 50 mM aqueous NH_4HCO_3 (6 mL). [B19]-Cys(Acm) human insulin B-chain **9** (6.2 mg, 1.6 μmol) was dissolved in MilliQ H_2O (8 mL) to give a cloudy solution, which was added dropwise to the solution of **123** and stirred for 1.5 hours (at pH ~8) with monitoring *via* RP-HPLC and MS. The reaction was quenched by acidification to pH ~3 (glacial AcOH) and the resulting solution lyophilised to give crude **124** as a colourless solid (14.8 mg). **124(I)**: Mass spectrum (ESI^+, MeCN:H_2O:TFA): *m/z* 1478.9 $[M+4H]^{4+}$; ¼($C_{265}H_{395}N_{67}O_{79}S_4$) requires 1477.9. RP-HPLC (Agilent: Vydac C18 analytical column, 0 to 25% buffer B over 5 min then 25 to 50% buffer B over 30 min): t_R = 18.4 min. **124(II)**: Mass spectrum (ESI^+, MeCN:H_2O:TFA): *m/z* 1479.2 $[M+4H]^{4+}$; ¼($C_{265}H_{395}N_{67}O_{79}S_4$) requires 1477.9. RP-HPLC (Agilent: Vydac C18 analytical column, 0 to 25% buffer B over 5 min then 25 to 50% buffer B over 30 min): t_R = 18.7 min.

4.4.1.18 [A3]-Pro-[Δ⁴A6-A11]-dicarba human insulin 57

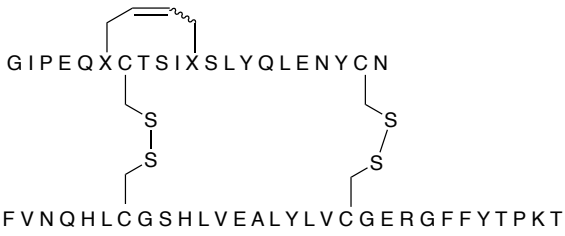

57

Oxidation of the insulin analogue precursors **124(I)** and **124(II)** was executed according to a procedure described by Lin *et al*..[111] **124** (14.8 mg) was suspended in a 60 mM aqueous HCl solution (0.4 mL) followed by glacial AcOH (6 mL) to effect dissolution. A 10 mM solution of iodine in glacial acetic acid (6 mL) was added and the resulting solution stirred in darkness for 2 hours, exposed to light and stirred for a further 1 hour before being poured into chilled diethyl ether (2x35 mL). The resulting suspension was cooled to 0 °C, centrifuged (5000 rpm, 5 min), and the supernatant discarded. The residue was suspended in MeCN (~0.5 mL) and 20 mM ascorbic acid aqueous solution (1 mL) to quench excess iodine before it was purified by preparative RP-HPLC (Agilent: Vydac C18 preparative column, 0 to 30% buffer B over 5 min then 30 to 40% buffer B over 60 min): t_R = 16.8 min to give **57(I)** as a colourless solid (275 μg as determined by standardisation against human IGF-1) in >99% purity. RP-HPLC (Agilent: Vydac C4 analytical column at T 40 °C, 25 → 31% buffer B over 5 min then 31→ 50% buffer B over 16 min, flow rate 0.5 mL min^{-1}): t_R = 12.5 min. Buffer A: 0.1% Aqueous TFA; Buffer B: 0.08% TFA in MeCN:H_2O, 80:20. Mass spectrum (ESI^+, MeCN:H_2O:TFA): *m/z* 1154.5 $[M+5H]^{5+}$, ⅕($C_{260}H_{390}N_{65}O_{77}S_4$) requires 1156.5. *m/z* 1443.1 $[M+4H]^{4+}$, ¼($C_{260}H_{389}N_{65}O_{77}S_4$) requires 1445.4 (mass spectrum below obtained prior to final purification).

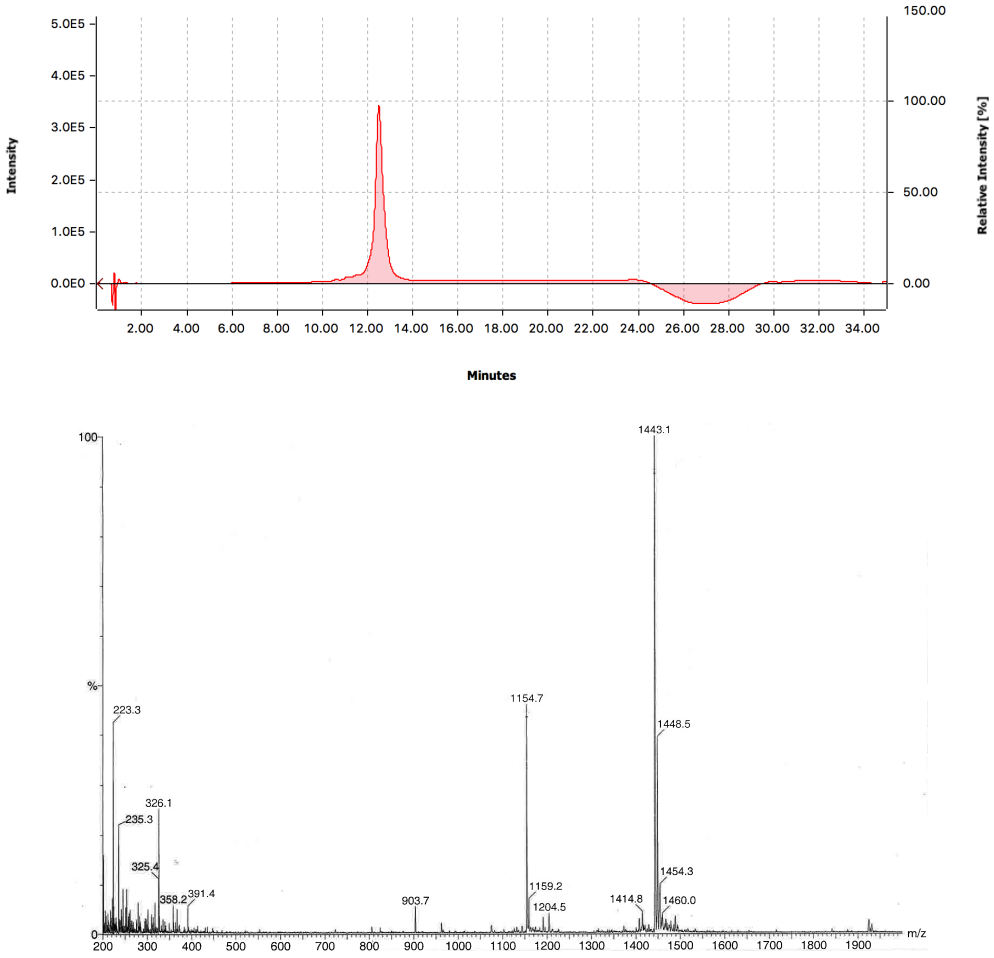

57(II): Preparative RP-HPLC (Agilent: Vydac C18 preparative column, 0 to 30% buffer B over 5 min then 30 to 40% buffer B over 60 min): t_R = 19.4 min gave **57(II)** as a colourless solid (857 µg as determined by standardisation against human IGF-1) in >90% purity. RP-HPLC (Agilent: Vydac C4 analytical column at T 40 °C, 25 → 31% buffer B over 5 min then 31→ 50% buffer B over 16 min, flow rate 0.5 mL min^{-1}): t_R = 14.0 min. Buffer A: 0.1% Aqueous TFA; Buffer B: 0.08% TFA in MeCN:H_2O, 80:20. LRMS (ESI^+, MeCN:H_2O:TFA): m/z 1154.0 $[M+5H]^{5+}$, ⅕($C_{260}H_{390}N_{65}O_{77}S_4$) requires 1156.5; 1442.7 $[M+4H]^{4+}$, ¼($C_{260}H_{389}N_{65}O_{77}S_4$) requires 1445.4 (mass spectrum below obtained prior to final purification).

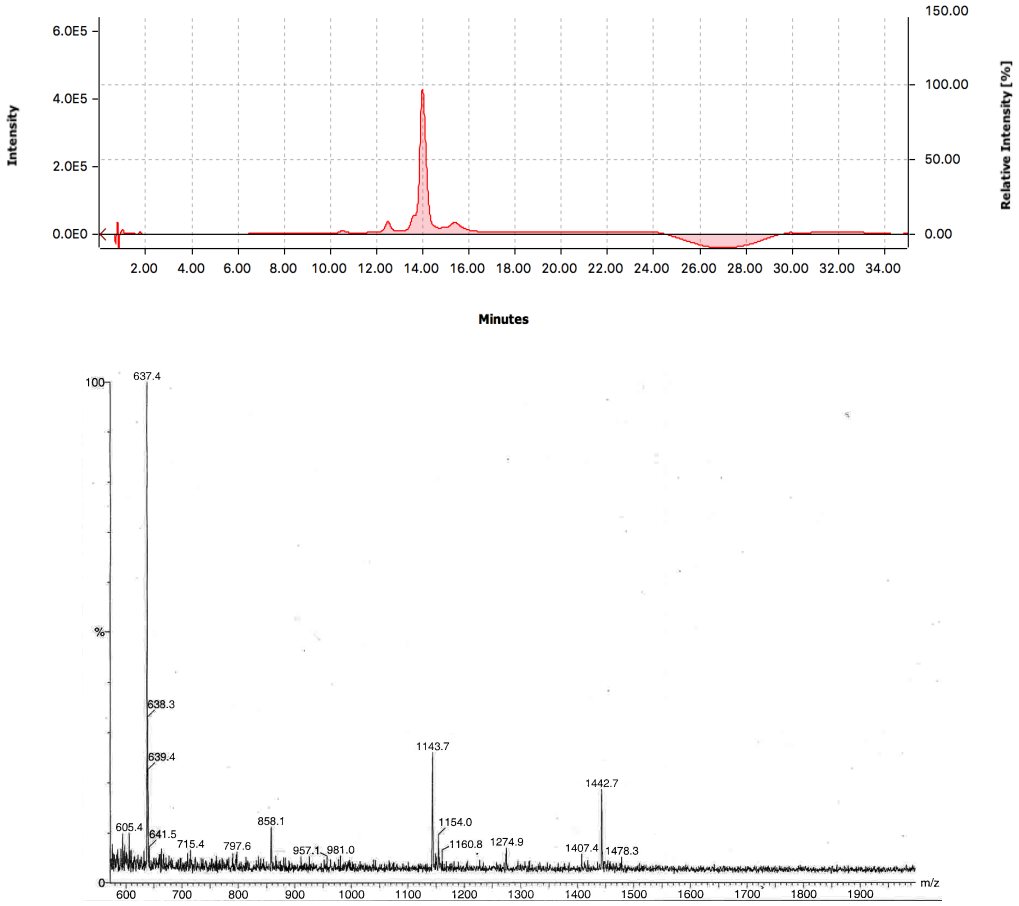

4.4.1.19 Fmoc-Ile-NH_2 65

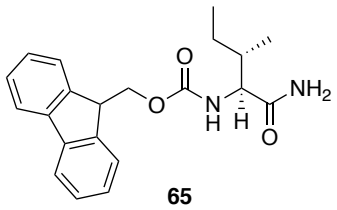

65

The protected carboxamide **65** was prepared according to a procedure described by Pozdnev.[167] To a stirred solution of Fmoc-L-isoleucine **68** (500 mg, 1.4 mmol, 1 equiv.) in dioxane (5 mL) was added pyridine (70 µL) then di-*tert*-butyl dicarbonate (400 mg, 1.8 mmol, 1.3 equiv.), the solution stirred for 10 minutes, then ammonium bicarbonate (141 mg, 1.8 mmol, 1.3 equiv.) was added. The resulting solution was stirred overnight at room temperature to give a pink suspension. The suspended solid was filtered off,

washed with H_2O (2x30 mL), 5% v/v H_2SO_4 aqueous solution (30 mL), then H_2O (30 mL), resuspended in H_2O and lyophilised to give **65** as a colourless solid (294 mg, 60% m.p. 170.2-172.5). ν_{max} (FTIR): 3300w, 1296w, 2964w, 1655s, 1531s, 1449m, 1304m, 1250s, 1120m, 1078m, 1030s, 978w, 733s. ^{1}H-NMR (400 MHz, MeOD): δ 7.80 (d, *J* = 7.6 Hz, 2H), 7.67 (t, *J* = 6 Hz, 2H), 7.39 (t, *J* = 7.2 Hz, 2H), 7.31 (t, *J* = 7.2 Hz, 2H), 4.46-4.35 (m, 2H), 4.23 (t, *J* = 6.8 Hz, 1H), 3.96 (d, *J* = 7.2 Hz), 1.81-1.49 (dm, 2H), 1.20-1.13 (m, 1H), 0.97-0.89 (m, 6H). ^{13}C-NMR (150 MHz, $CDCl_3$): δ 173.8, 156.5, 144.3, 141.2, 128.1, 127.5, 125.8, 120.6, 66.1, 59.5, 47.1, 36.7, 24.8, 16.0, 11.5. Mass spectrum (ESI$^+$, MeOH): *m/z* 375.2 $[M+Na]^+$; $C_{21}H_{24}N_2O_3Na$ requires 375.2.

4.4.1.20 Fmoc-Ile-Dhv azlactone 69

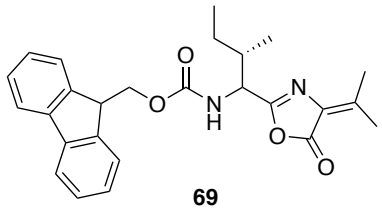

69

The azlactone **69** was prepared according to a modified version of a procedure originally described by Makowski *et al.*[165] To a round-bottomed flask containing 3-methyl-2-oxobutanoic acid **66** (420 mg, 3.6 mmol, 2.5 equiv.) was added Fmoc-L-isoleucine carboxamide **65** (500 mg, 1.4 mmol, 1 equiv.), *p*-toluenesulfonic acid (27 mg, 11 mol %) and dry toluene (100 mL). The resulting suspension was stirred at reflux for 24 hours, with water removed by use of a Dean-Stark apparatus. All solids dissolved upon reaching reflux. The solution was then cooled, concentrated under reduced pressure and redissolved in EtOAc (50 mL). The resulting suspension was then washed with H_2O (2x50 mL) and the organic layer dried ($MgSO_4$) then concentrated under reduced pressure to give a finely divided solid interspersed with a yellow gum. The yellow gum was dissolved in DCM, the suspension filtered and the filtrate concentrated

under reduced pressure (620 mg), then purified by column chromatography (silica; 3:1:0.1:0.05 petroleum ether:EtOAc:MeOH:AcOH)[a] to give **69** as a pale yellow oil (292 mg, 48%). ^{1}H-NMR (400 MHz, $CDCl_3$): δ 7.77 (d, *J* = 7.2 Hz, 2H), 7.61 (m, 2H), 7.40 (t, *J* = 7.2 Hz, 2H), 7.31 (t, *J* = 7.6 Hz, 2H), 5.30 (dd, *J* = 9.6 Hz, 14.4 Hz, 1H), 4.78-4.63 (dm, 1H), 4.47-4.43 (m, 2H), 4.27-4.23 (m, 1H), 2.35 (s, 3H), 2.26 (s, 3H), 1.99-1.46 (dm, 2H), 1.23-1.18 (m, 1H), 0.99-0.89 (m, 6H). ^{13}C-NMR (150 MHz, $CDCl_3$): δ 165.1, 162.7, 156.4/156.1, 154.9, 144.0, 141.5, 130.1, 127.9, 127.2, 125.2, 120.2, 67.3, 54.6, 47.4, 38.1, 26.3, 24.9, 23.0, 19.9, 11.6. Mass spectrum (ESI$^+$, MeOH): *m/z* 433.2123 $[M+H]^+$; $C_{26}H_{30}N_2O_4$ requires 433.2127.

4.4.1.21 Alloc-Ile-OH 72

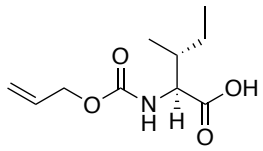

72

To a stirred solution of L-isoleucine **70** (3.00 g, 22.9 mmol, 1 equiv.) in 2 M NaOH aqueous solution (15 mL) at 0 °C was added a solution of allyl chloroformate **71** (3.18 g, 26.3 mmol, 1.15 equiv.) in 2 M NaOH aqueous solution (15 mL) dropwise. The resulting solution was allowed to warm to room temperature and stirred for 50 minutes then acidified to pH 1 with conc. HCl, resulting in precipitation of a colourless solid. The suspension was extracted with EtOAc (3x80 mL), the combined organic extract dried ($MgSO_4$) and concentrated under reduced pressure to give **72** as a pale yellow oil (4.88g, quant.) Spectral data were in accordance with those in the literature.[180]

4.4.1.22 Alloc-Ile-NH_2 73

[a] In later syntheses of similar azlactones, it was found that omission of acetic acid from the chromatography eluent improved recovery of the desired material.

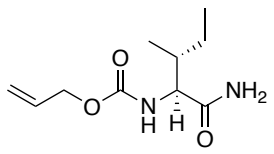

73

The protected carboxamide **73** was prepared according to a procedure described by Pozdnev.[167] To a stirred solution of Alloc-L-isoleucine **72** (5.08 g, 23 mmol, 1 equiv.) in dioxane (5 mL) was added pyridine (1.15 mL) then di-*tert*-butyl dicarbonate (6.53 g, 6.9 mL, 30 mmol, 1.3 equiv.), the solution stirred for 5 minutes, then ammonium bicarbonate (2.29 g, 29 mmol, 1.26 equiv.) was added. The resulting solution was stirred for 22 hours at room temperature, giving a colourless precipitate. The suspension was diluted with H_2O (50 mL) and extracted with EtOAc (3x150 mL). The combined organic extracts were washed with brine, dried ($MgSO_4$) and concentrated under reduced pressure to give **73** as a pale pink solid (4.41 g, 89%, m.p. 172.6-173.7 °C). ν_{max} (FTIR): 3383m, 3315m, 3201w, 2933w, 2876w, 1656s, 1541s, 1419m, 1301m, 1243s, 1127m, 1039m, 974m, 930m, 775w. ^{1}H-NMR (400 MHz, MeOD): δ 5.99-5.89 (m, 1H), 5.34-5.33 (dm, 1H), 5.21-5.17 (dm, 1H), 4.55 (m, 2H), 3.97 (d, J = 7.2 Hz, 1H), 1.83-1.51 (dm, 2H), 1.24-1.13 (m, 1H), 0.96 (d, J = 6.8 Hz, 3H), 0.92 (t, J = 7.6 Hz, 3H). ^{13}C-NMR (150 MHz, $CDCl_3$): δ 177.0, 158.5, 134.4, 117.6, 66.6, 60.9, 38.2, 25.7, 16.0, 11.6. Mass spectrum (ESI$^+$, MeOH): *m/z* 215.1393 $[M+H]^+$; $C_{10}H_{19}N_2O_3$ requires 215.1396.

4.4.1.23 Alloc-Ile-Dhv azlactone 74

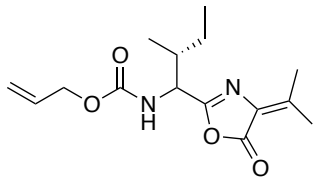

74

The azlactone **74** was prepared according to a modified version of a procedure originally described by Makowski *et al*.[165] To a round-bottomed flask containing 3-methyl-2-oxobutanoic acid **66** (339 mg, 2.92 mmol, 2.5 equiv.) was added Alloc-L-isoleucyl carboxamide **73** (250 mg, 1.17 mmol, 1 equiv.), *p*-toluenesulfonic acid (22 mg, 11 mol %) and dry toluene (60 mL). The resulting suspension was stirred at reflux for 51 hours, with water removed by use of a Dean-Stark apparatus. All solids dissolved upon reaching reflux. The solution was then cooled, concentrated under reduced pressure and redissolved in EtOAc (50 mL). The resulting suspension was then washed with H_2O (2x50 mL), brine (50 mL), the organic layer dried ($MgSO_4$) then concentrated under reduced pressure to give a finely divided solid interspersed with an orange oil. The oil was dissolved in DCM, the suspension filtered and the filtrate concentrated under reduced pressure (141 mg), then purified by column chromatography (silica; 4:1:0.1 petroleum ether:EtOAc:MeOH) to give **74** as a pale yellow oil (84 mg, 24%). ν_{max} (FTIR): 3329w, 2965w, 2931w, 2878w, 1793m, 1719s, 1672s, 1508m, 1458w, 1369w, 1222s, 1155s, 1089s, 1040s, 879s, 776s. ^{1}H-NMR (400 MHz, $CDCl_3$): δ 5.94-5.90 (m, 1H), 5.33 (d, J = 17.2 Hz, 1H), 5.23 (d, J = 10.4 Hz, 1H), 4.74-4.71 (m, 0.5H), 4.64-4.59 (overlapping m, 0.5H), 4.60 (d, J = 4.4 Hz, 2H), 2.34 (s, 3H), 2.25 (s, 3H), 1.96-1.93 (m, 1H), 1.55-1.20 (dm, 2H), 0.98-0.89 (m, 6H). Mass spectrum (ESI^+, MeOH): *m/z* 295.1658 $[M+H]^+$; $C_{15}H_{23}N_2O_4$ requires 295.1658.

4.4.1.24 *des*$_{A1\text{-}3,A11\text{-}21}$-[A6]-Cys(^{t}Bu)-[A7]-Agl human insulin A-chain 61

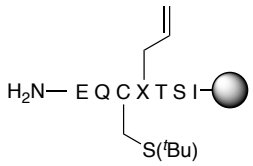

61

The resin-bound peptide **61** was prepared on a 0.1 mmol scale according to the general automated procedure outlined in Section 2.3.3.1. Formation of **61** was subsequently verified by small-scale Fmoc deprotection and resin cleavage, RP-HPLC and LRMS. Mass spectrum (ESI+, MeCN:H_2O:TFA): *m/z* 833.3 $[M+H]+$; $C_{35}H_{61}N_8O_{13}S$ requires 833.4. RP-HPLC (Agilent: Vydac C18 analytical column, 15 to 50% buffer B over 35 min): t_R = 7.5 min.

4.4.1.25 Alloc-*des*$_{A1,A11\text{-}21}$-[A2]-D/L-Ile-[A3]-Dhv-[A6]-Cys(^{t}Bu)-[A7]-Agl human insulin A-chain 76

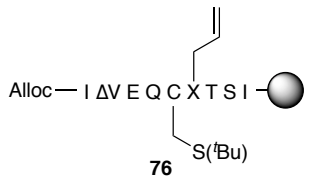

76

76 was synthesised according to a procedure described by Jiang *et al*..[168] Resin-bound **61** (0.05 mmol) was suspended in a solution of **74** (74 mg, 0.25 mmol, 5 equiv.) and DMAP (13 mg, 0.11 mmol, 2.2 equiv.) in NMP (0.75 mL) and stirred at 60 °C for 24 hours. The resin was then filtered from the reaction mixture and washed with DMF (5x5 mL) and DCM (1x5 mL). Formation of **76** as a pair of isomers was verified by small-scale cleavage, RP-HPLC and LRMS. **76(I)**: Mass spectrum (ESI^+, MeCN:H_2O:TFA): *m/z* 1127.6 $[M+H]^+$; $C_{50}H_{83}N_{10}O_{17}S$ requires 1127.6. RP-HPLC (Agilent: Vydac C18 analytical column, 5 to 100% buffer B over 30 min): t_R = 25.9 min. **76(II)**: Mass spectrum (ESI^+, MeCN:H_2O:TFA): *m/z* 1127.6 $[M+H]^+$; $C_{50}H_{83}N_{10}O_{17}S$ requires 1127.6.

RP-HPLC (Agilent: Vydac C18 analytical column, 5 to 100% buffer B over 30 min): t_R = 26.9 min.

4.4.1.26 *des*$_{A1,A11\text{-}21}$-[A2]-D/L-Ile-[A3]-Dhv-[A6]-Cys(^{t}Bu)-[A7]-Agl human insulin A-chain 77

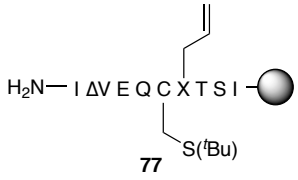

77

77 was prepared according to a procedure described by Wilson *et al*.[179] In a drybox (N_2), resin-bound **76** (0.1 mmol) was suspended in a minimal volume of dry DCM (~2 mL) in a microwave tube, to which was added tetrakis(triphenylphosphine)palladium(0) (30 mg, 25 μmol, 0.25 equiv) then phenylsilane (162 mg, 190 μL, 1.5 mmol, 15 equiv.) The vessel was sealed and immediately subjected to heating by microwave irradiation (25 watts) for 5 minutes at 38 °C to give a black suspension. The resin was then filtered from the reaction mixture and rinsed with DCM (5x5 mL). The process was repeated a further two times, omitting use of the drybox. Formation of **77** as a pair of isomers was verified by small-scale cleavage, RP-HPLC and HRMS. **77(I)**: Mass spectrum (ESI^+, MeCN:H_2O:TFA): *m/z* 1042.6 $[M+H]^+$; $C_{46}H_{79}N_{10}O_{15}S$ requires 1042.5. RP-HPLC (Agilent: Vydac C18 analytical column, 15 to 50% buffer B over 35 min): t_R = 13.7 min. **77(II)**: Mass spectrum (ESI^+, MeCN:H_2O:TFA): *m/z* 1042.6 $[M+H]^+$; $C_{46}H_{79}N_{10}O_{15}S$ requires 1042.5. RP-HPLC (Agilent: Vydac C18 analytical column, 5 to 100% buffer B over 30 min): t_R = 20.6 min.

4.4.1.27 Fmoc-Agl-*des*$_{A11\text{-}21}$-[A2]-D/L-Ile-[A3]-Dhv-[A6]-Cys(^{t}Bu)-[A7]-Agl human insulin A-chain 78

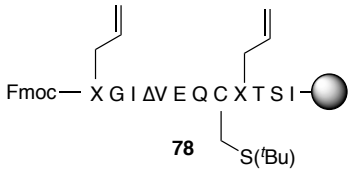

The resin-bound peptide **78** was prepared from **77** on a 0.05 mmol scale. Fmoc-Gly was attached on a 0.1 mmol scale according to the general microwave-assisted manual SPPS procedure outlined in Section 2.3.3.3 with the following quantities of reagents: HATU (152 mg, 0.4 mmol, 4 equiv.), Fmoc-L-Gly-OH (119 mg, 0.4 mmol, 4 equiv.), NMM (88 µL, 0.8 mmol, 8 equiv.) in DMF (4 mL). The resin was then deprotected according to the general procedure outlined in Section 2.3.3.5. The resin was then divided into two lots and Fmoc-L-Agl was attached on a 0.05 mmol scale according to the general microwave-assisted manual SPPS procedure outlined in Section 2.3.3.3 with the following quantities of reagents: HATU (85 mg, 0.2 mmol, 4 equiv.), Fmoc-L-Agl-OH (74 mg, 0.2 mmol, 4 equiv.), NMM (44 µL, 0.4 mmol, 8 equiv.) in DMF (4 mL). This coupling was subsequently repeated. Formation of **78** *sans* Fmoc was subsequently verified by small-scale Fmoc deprotection and resin cleavage, RP-HPLC and LRMS. Mass spectrum (ESI$^+$, MeCN:H_2O:TFA): *m/z* 1196.8 $[M+H]^+$; $C_{53}H_{90}N_{13}O_{16}S$ requires 1196.6. *m/z* 599.0 $[M+2H]^{2+}$; ½($C_{53}H_{91}N_{13}O_{16}S$) requires 598.8. RP-HPLC (Agilent: Vydac C18 analytical column, 15 to 50% buffer B over 35 min): t_R = 19.7 min. The resin-bound peptide was subjected to the capping procedure outlined in Section 2.3.3.6 and stored overnight in a vacuum desiccator prior to RCM.

4.4.1.28 Fmoc-[Δ⁴Agl-A7]-dicarba-*des*$_{A11-21}$-[A3]-Dhv-[A6]-Cys(ᵗBu) human insulin A-chain 79

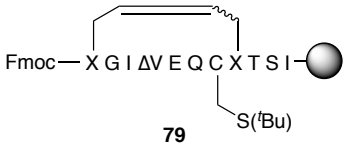

79

Resin-bound peptide **78** was subjected to the general microwave-assisted on-resin RCM procedure outlined in Section 2.3.3.8 with the following quantities of reagents: GII (8.9 mg, 21 mol %), 0.4 M LiCl/DMF (~0.1 mL), DCM (2 mL). Formation of **79** as a pair of isomers (**79(I)** and **79(II)**) with 78% conversion from starting material was subsequently verified by small-scale Fmoc deprotection and resin cleavage, RP-HPLC and LRMS (below). **79(I)**: Mass spectrum (ESI^+, MeCN:H_2O:TFA): *m/z* 1168.8 $[M+H]^+$; ($C_{51}H_{86}N_{13}O_{16}S$) requires 1168.6. *m/z* 585.0 $[M+2H]^{2+}$; ½($C_{51}H_{87}N_{13}O_{16}S$) requires 584.9. RP-HPLC (Agilent: Vydac C18 analytical column, 15 to 50% buffer B over 35 min): t_R = 10.4 min.

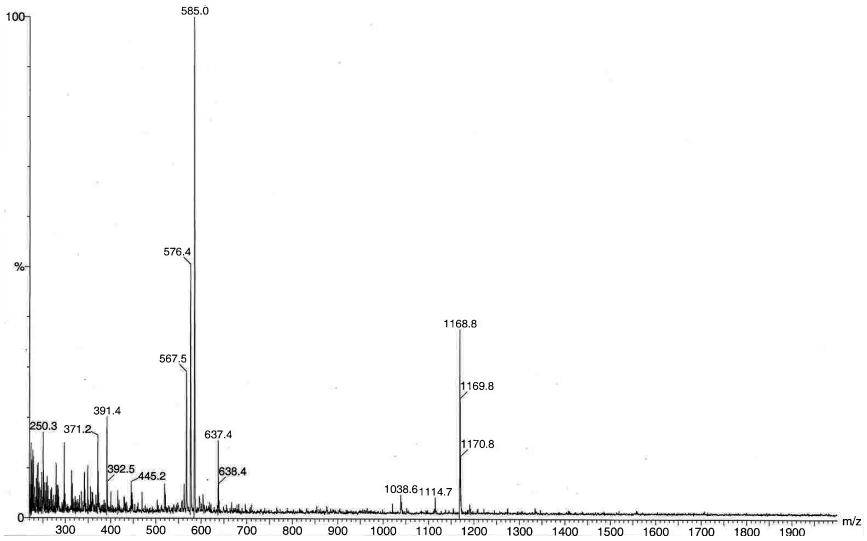

79(II): Mass spectrum (ESI^+, MeCN:H_2O:TFA): *m/z* 1168.8 $[M+H]^+$; ($C_{51}H_{86}N_{13}O_{16}S$) requires 1168.6. *m/z* 584.9 $[M+2H]^{2+}$; ½($C_{51}H_{87}N_{13}O_{16}S$) requires 584.9. RP-HPLC (Agilent: Vydac C18 analytical column, 15 to 50% buffer B over 35 min): t_R = 10.9 min.

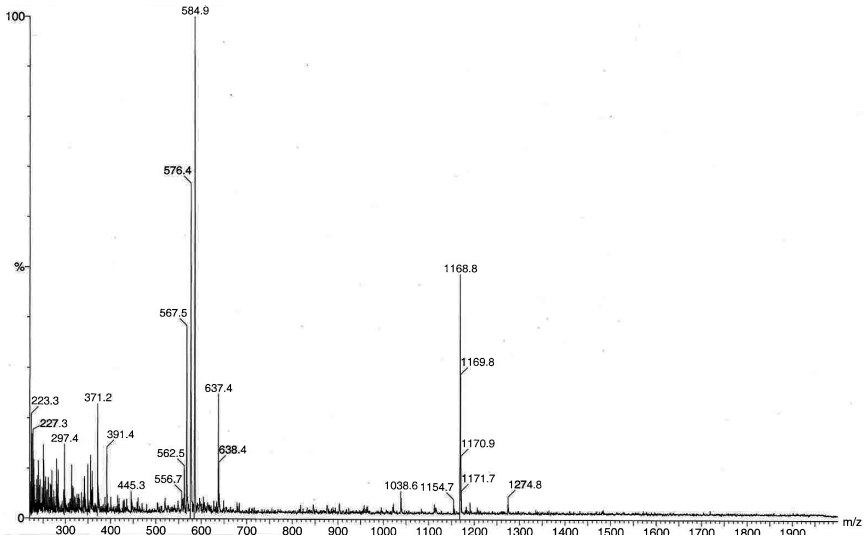

4.4.1.29 Fmoc-[Δ⁴Agl-A7]-dicarba-*des*$_{A11\text{-}21}$-[A6]-Cys(ᵗBu) human insulin A-chain 82

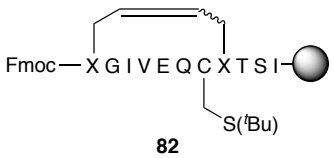

82

In a drybox (N_2), resin-bound **79** was suspended in 10% v/v degassed MeOH in dry DCM (2 mL) in a Fischer-Porter tube, to which was added [(*S*,*S*)-Me-DuPHOS-Rh(I)-COD]BF_4 (1 mg, ~1.6 mol %) and the vessel sealed. The vessel was then pressurised with H_2 (60 psi) and stirred at room temperature for 24 hours. The vessel was then vented to atmosphere, the resin filtered from the suspension and washed with DCM (5x5mL). Formation of **82** *sans* Fmoc was subsequently verified by small-scale Fmoc deprotection and resin cleavage, RP-HPLC and LRMS. Mass spectrum (ESI^+, MeCN:H_2O:TFA): *m/z* 1171.1 $[M+H]^+$; $C_{51}H_{88}N_{13}O_{16}S$ requires 1170.6. *m/z* 586.0 $[M+2H]^{2+}$; ½($C_{51}H_{88}N_{13}O_{16}S$) requires 585.8. RP-HPLC (Agilent: Vydac C18 analytical column, 15 to 50% buffer B over 35 min): t_R = 11.3 min (crude mass spectrum shown below).

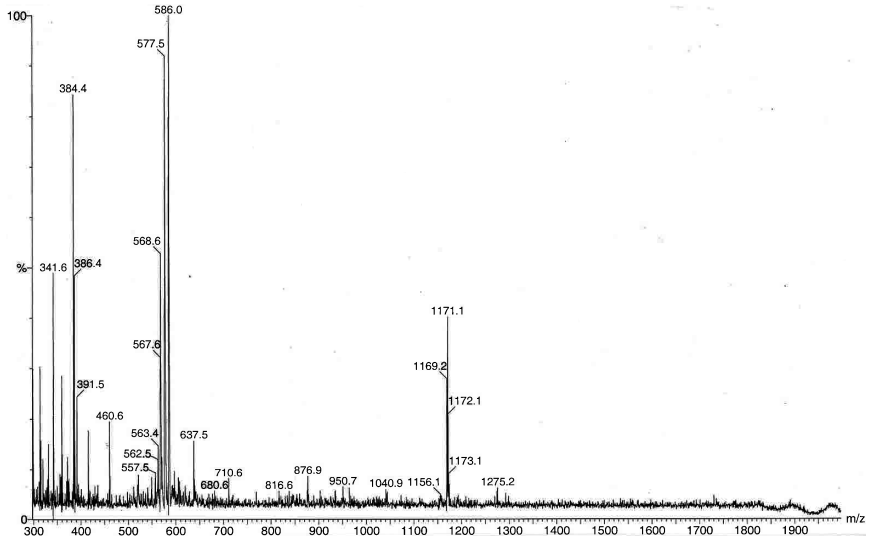

4.4.1.30 Fmoc-Agl-Arg-Arg-Pro-Lys-Arg-*des*$_{A11\text{-}21}$-[A2]-D/L-Ile-[A3]-Dhv-[A6]-Cys(^{t}Bu)-[A7]-Agl human insulin A-chain 80

80

The resin-bound peptide **80** excluding *N*-terminal Agl residue A6 was prepared from **77** on a 0.05 mmol scale according to the general automated procedure outlined in Section 2.3.3.1. Fmoc-L-Agl was attached on a 0.1 mmol scale according to the general microwave-assisted manual SPPS procedure outlined in Section 2.3.3.3 with the following quantities of reagents: HATU (76 mg, 0.2 mmol, 4 equiv.), Fmoc-L-Agl-OH (67 mg, 0.2 mmol, 4 equiv.), NMM (44 μL, 0.4 mmol, 8 equiv.) in DMF (4 mL). Formation of **82** as a pair of isomers (**82(I)** and **82(II)** *sans* Fmoc was subsequently verified by small-scale Fmoc deprotection and resin cleavage, RP-HPLC and LRMS. **82(I)**: Mass spectrum (ESI$^+$, MeCN:H_2O:TFA): *m/z* 974.8 $[M+2H]^{2+}$; ½($C_{84}H_{147}N_{29}O_{22}S$) requires 974.1. *m/z* 650.0 $[M+3H]^{3+}$; ⅓($C_{84}H_{150}N_{29}O_{22}S$) requires 649.7. RP-HPLC (Agilent: Vydac C18 analytical column, 15 to 50% buffer B over

35 min): t_R = 16.5 min. **82(II)**: Mass spectrum (ESI$^+$, MeCN:H_2O:TFA): *m/z* 974.5 $[M+2H]^{2+}$; ½($C_{84}H_{147}N_{29}O_{22}S$) requires 974.1. *m/z* 650.1 $[M+3H]^{3+}$; ⅓($C_{84}H_{149}N_{29}O_{22}S$) requires 649.7. RP-HPLC (Agilent: Vydac C18 analytical column, 15 to 50% buffer B over 35 min): t_R = 17.6 min. The resin-bound peptide was subjected to the capping procedure outlined in Section 2.3.3.6 and stored overnight in a vacuum desiccator prior to RCM.

4.4.1.31 Fmoc-[Δ^{4}Agl-A7]-dicarba-Arg-Arg-Pro-Lys-Arg-*des$_{A11\text{-}21}$*-[A2]-D/L-Ile-[A3]-Dhv-[A6]-Cys(^{t}Bu)-[A7]-Agl human insulin A-chain 81

81

Resin-bound peptide **80** was subjected to the general microwave-assisted on-resin RCM procedure outlined in Section 2.3.3.8 with the following quantities of reagents: GII (8.9 mg, 21 mol %), 0.4 M LiCl/DMF (~0.1 mL), DCM (2 mL). Formation of **81** as a pair of isomers (**81(I)** and **81(II)**) with 78% conversion was subsequently verified by small-scale Fmoc deprotection and resin cleavage, RP-HPLC and LRMS. **81(I)** and **81(II)**: Mass spectrum (ESI$^+$, MeCN:H_2O:TFA): *m/z* 960.4 $[M+2H]^{2+}$; ½($C_{82}H_{145}N_{29}O_{22}S$) requires 960.0. *m/z* 640.7 $[M+3H]^{3+}$; ⅓($C_{82}H_{146}N_{29}O_{22}S$) requires 640.4. RP-HPLC (Agilent: Vydac C18 analytical column, 15 to 50% buffer B over 35 min): t_R = 13.0 min.

4.4.1.32 Stabase-Gly-OEt 87

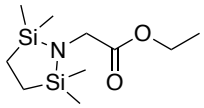

87

To a stirred suspension of glycine ethyl ester hydrochloride **85** (2.63 g, 19.3 mmol, 1 equiv.) in dry DCM (20 mL) under N_2 was added triethylamine (7.9 mL, 56.4 mmol, 3 equiv.) and stirred for 15 minutes at 0 °C. A solution of 1,2-bis(chlorodimethylsilyl)ethane **86** (4.06 g, 19.3 mmol, 1 equiv.) in dry DCM (10 mL) was then added dropwise to the stirred suspension *via* plastic syringe. The resulting colourless suspension was stirred under N_2 at 0 °C for 5 minutes, then left to warm to room temperature and stirred overnight. Dry petroleum ether (100 mL) was then added to the suspension and stirred for 15 minutes, the suspension filtered through a glass sinter and the filtrate concentrated under reduced pressure. The residue was then taken up in dry petroleum ether (50 mL), again filtered through a glass sinter and concentrated under reduced pressure to give **87** as a colourless oil (4.22 g, 91%).[b] ^{1}H NMR (400 MHz, $CDCl_3$): δ 4.12 (q, J = 7.2 Hz, 2H), 3.50 (s, 2H), 1.25 (t, J = 7.2 Hz), 0.73 (s, 2H), 0.05 (s, 12H).[c]

[b] In instances of this preparation where impurities were identified by ^{1}H NMR, the crude product was purified by Kugelrohr distillation (50-60 °C, ~0.2 Torr).

[c] Owing to the lability of the Stabase protecting group in acidic media, NMR spectra of these compounds were measured in $CDCl_3$ stored over K_2CO_3 so as to remove trace HCl from the solvent.

4.4.1.33 Alloc-Ile-F 88

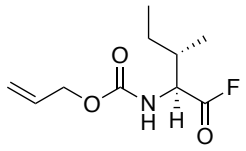

88

To a stirred solution of **72** (702 mg, 3.26 mmol, 1 equiv.) in dry DCM (3 mL) was added pyridine (258 mg, 263 µL, 3.26 mmol, 1 equiv.) then cyanuric fluoride **33** (441 mg, 263 µL, 3.26 mmol, 1 equiv.) The resulting solution was stirred at room temperature for 16 hours, with a colourless precipitate appearing after 30 minutes. The suspension was then diluted with deionised H_2O (5 mL) to dissolve the precipitate, the organic layer quickly separated and concentrated under reduced pressure to give a **88** as a pale yellow oil (642 mg, 91%).^{1}H NMR (400 MHz, $CDCl_3$): δ 5.97-5.87 (m, 2H), 5.33 (dd, *J* = 1.2 Hz, 17.2 Hz, 1H), 5.27-5.23 (m, 1H), 5.12 (bd, *J* = 7.2 Hz, 1H), 4.6 (d, *J* = 5.6 Hz, 2H), 4.51 (dd, 4.8 Hz, 8.4 Hz, 1H), 1.99-1.97 (m, 1H), 1.53-1.43 (m, 1H), 1.31-1.20 (m, 1H), 1.03 (d, *J* = 6.8 Hz, 3H), 0.96 (t, *J* = 7.6 Hz, 3H). Mass spectrum (ESI$^+$, MeOH): *m/z* 230.2 $[M(OMe)+H]^+$; $C_{11}H_{20}NO_4$ requires 230.1. *m/z* 252.2 $[M(OMe)+Na]^+$; $C_{11}H_{19}NO_4Na$ requires 252.1.[d]

[d] Acyl fluorides were observed as the methyl ester (OMe) derivative owing to *in situ* reaction with the carrier solvent.

4.4.1.34 Stabase-(β-OH)Val-OEt 89

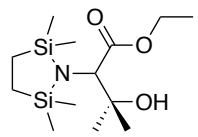

89

To a stirred solution of freshly prepared solution of lithium diisopropylamide (273 mg, 2.5 mmol, 1.1 equiv.) in dry THF (5 mL) at -78 °C under N_2 was added neat **87** (569 mg, 2.3 mmol, 1 equiv.) and the resulting yellow solution allowed to warm to -30 °C with stirring over 1.5 hours. The solution was then cooled back to -78 °C, dry acetone (1 mL) added and allowed to warm to 0 °C over 2 hours. The reaction mixture was then quenched with saturated aqueous NH_4Cl solution (10 mL), concentrated under reduced pressure and the resulting mixture extracted with EtOAc (3x30 mL). The combined organic extracts were dried (Na_2SO_4) and concentrated under reduced pressure to give crude **89** as a yellow oil (878 mg). The crude **89** was used in subsequent reactions without purification.

4.4.1.35 Alloc-Ile-(β-OH)Val-OEt 90

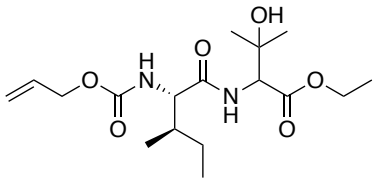

90

To a stirred solution of crude **89** (878 mg) in dry THF (5 mL) was added a solution of **88** (503 mg, 2.3 mmol, 1 equiv.) in dry THF (5 mL) dropwise and stirred for 16 hours. The resulting purple solution was concentrated under reduced pressure and the residue taken up in absolute EtOH (5 mL), to which was added ethanolic HCl (5 mL). The resulting solution was stirred at room temperature for 1 hour, or until the disappearance of

higher-running species in TLC (silica, 2:1 petroleum ether:EtOAc). The solution was concentrated under reduced pressure and the residue purified by column chromatography (silica, 2:1:0.1 petroleum ether:EtOAc:MeOH) to give **90** as a brown oil (619 mg, 1.7 mmol, 75%). ν_{max} (FTIR): 3315bw, 2968w, 2937m, 2878w, 1708s, 1655s, 1523s, 1465m, 1374s, 1332m, 1235s, 1210s, 1156m, 1138m, 1097m, 1035s, 995m, 931m, 862w, 777w cm^{-1}. ^{1}H NMR (600 MHz, $CDCl_3$): δ 6.83-6.81 (m, NH), 5.95-5.85 (m, 1H), 5.40-5.38 (m, OH), 5.29 (dd, J = 17.2; 3.2, 1H), 5.20 (d, J = 9.2 Hz, 1H), 4.56 (bs, 1H), 4.52-4.48 (m, 1H), 4.27-4.18 (m, 1H), 4.15-4.07 (m, 1H), 2.90-2.81 (m, 1H), 1.94-1.84 (m, 1H), 1.55-1.46 (m, 1H), 1.31-1.24 (m, 9H), 1.21-1.12 (m, 1H), 0.97-0.88 (m, 6H). ^{13}C NMR (100 MHz, $CDCl_3$): δ 171.7, 171.3, 156.3, 132.7, 118.0, 72.0, 66.1, 61.8, 60.1, 59.9, 37.7, 26.9, 24.7, 15.8, 14.2, 11.6. Mass spectrum (ESI^+, MeOH): *m/z* 359.2178 $[M+H]^+$; $C_{17}H_{31}N_2O_6$ requires 359.2182.

4.4.1.36 Alloc-Ile-(β-OH)Val-OH 94

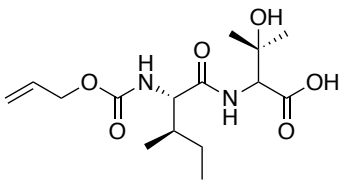

94

94 was synthesised according to a procedure described by Jiang *et al*.[168] To a stirred solution of **90** (752 mg, 2.1 mmol, 1 equiv.) in ^{t}BuOH:H_2O (8.5 mL, 3:1) at 0 °C under Ar was added LiOH.H_2O (449 mg, 10.7 mmol, 5.1 equiv.) *via* solid addition tube and the resulting solution stirred at 0 °C for 4 hours, or until the disappearance of starting material by TLC (silica, 10% MeOH in DCM, 1% AcOH). The solution was extracted with EtOAc (3x40 mL), dried (Na_2SO_4) and concentrated under reduced pressure to give **94** as a pink solid (604 mg, 1.9 mmol, 90%). **94** was deemed of sufficient purity by TLC that it was used telescopically in subsequent reactions, as per the Jiang *et al*. protocol.[168] ^{1}H NMR (400 MHz, $CDCl_3$): δ 5.94-5.84 (m, 1H), 5.60-5.59 (m, 1H), 5.30 (d, J = 16.8 Hz, 1H), 5.22 (m, 1H), 4.56 (d, J = 4.4 Hz, 1H), 4.27 (m, 1H), 4.18-4.15 (m, 1H), 1.88-1.85 (m, 1H), 1.56-1.52 (m, 1H), 1.28-1.24 (m, 6H), 1.03-0.87 (m, 6H). Mass spectrum (ESI^+, MeOH): *m/z* 353.3 $[M+H]^+$; $C_{15}H_{26}N_2O_6Na$ requires 353.2.

4.4.1.37 Alloc-Ile-Dhv azlactone 83

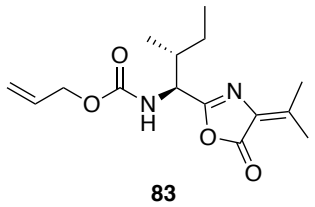

83

83 was synthesised according to a procedure described by Jiang *et al.*[168] To a stirred solution of **94** (604 mg, 1.9 mmol, 1 equiv.) in acetic anhydride (12 mL) at 50 °C under Ar was added sodium acetate (255 mg, 3.11 mmol, 1.7 equiv.) and the resulting solution stirred at 50 °C for 2 hours, or until the disappearance of starting material by TLC (silica, 2:1:0.1 petroleum ether:EtOAc;MeOH). The solution was diluted with deionised H_2O (6 mL), extracted with EtOAc (3x40 mL), the combined organic extracts washed with 10% Na_2CO_3 aqueous solution (40 mL), brine (40 mL), dried (Na_2SO_4) and concentrated under reduced pressure to give **83** as a brown oil (456 mg, 81%). ^{1}H NMR (600 MHz, $CDCl_3$): δ 5.95-5.90 (m, 1H), 5.33 (d, *J* = 11.6 Hz, 1H), 5.29 (d, *J* = 6 Hz, 1H), 5.23 (d, *J* = 6.8 Hz), 4.62 (dd, *J* = 3.6 Hz, 6 Hz, 1H), 4.59 (d, *J* = 4 Hz, 2H), 2.34 (s, 3H), 2.25 (s, 3H), 1.94-1.93 (m, 1H), 1.51-1.47 (m, 1H), 1.23-1.18 (m, 1H), 0.96 (d, *J* = 4.4 Hz, 3H), 0.93 (t, *J* = 4.8 Hz, 3H). ^{13}C NMR (150 MHz, $CDCl_3$): δ 165.1, 162.3, 155.9, 154.9, 132.7, 130.2, 66.1, 54.5, 38.2, 24.9, 23.0, 19.9, 15.5, 11.6. Mass spectrum (ESI$^+$, MeOH): *m/z* 295.3 $[M+H]^+$; $C_{15}H_{23}N_2O_4$ requires 295.2; 317.2 $[M+Na]^+$; $C_{15}H_{22}N_2O_4Na$ requires 317.2.

4.4.1.38 Alloc-Ser(O^{t}Bu)-OH 98

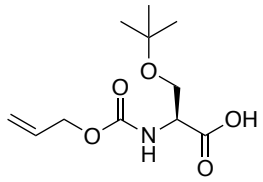

98

To a stirred solution of *O*-(*tert*-butyl)-L-serine **99** (1.5 g, 9.3 mmol, 1 equiv.) in 2 M NaOH aqueous solution (10 mL) at 0 °C was added a solution of allyl chloroformate **71** (1.29 g, 10.7 mmol, 1.15 equiv.) in 2 M NaOH aqueous solution (10 mL) dropwise. The resulting solution was allowed to warm to room temperature and stirred overnight, then acidified to pH 1 with conc. HCl, resulting in precipitation of a colourless solid. The suspension was extracted with EtOAc (3x80 mL), the combined organic extract dried ($MgSO_4$) and concentrated under reduced pressure to give **98** as a colourless oil (793 mg, 35%). Spectral data were in accordance with those in the literature.[181]

4.4.1.39 Alloc-Ser(O^{t}Bu)-F 100

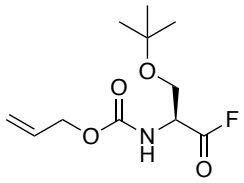

100

To a stirred solution of **98** (793 mg, 3.23 mmol, 1 equiv.) in dry DCM (5 mL) was added pyridine (255 mg, 260 µL, 3.23 mmol, 1 equiv.) then cyanuric fluoride **33** (437 mg, 278 µL, 3.23 mmol, 1 equiv.) The resulting solution was stirred at room temperature for 16 hours, with a colourless precipitate appearing after 30 minutes. The suspension was then diluted with deionised H_2O (5 mL) to dissolve the precipitate, the organic layer quickly separated and concentrated under reduced pressure to give a **100** as a pale yellow oil (763 mg, 96%). ν_{max} (FTIR): 3447w, 3328w, 2976m, 1852s, 1719s, 1508s, 1365m,

1283m, 1255m, 1192s, 1092s, 1057s, 984m, 932m, 776m cm^{-1}. ^{1}H NMR (400 MHz, $CDCl_3$): δ 5.98-5.89 (m, 1H), 5.59 (d, *J* = 7.6 Hz, 1H), 5.34 (d, *J* = 17.2 Hz, 1H), 5.25 (d, *J* = 10.4 Hz, 1H), 4.67-4.62 (m, 1H), 4.62 (d, *J* = 5.2 Hz, 2H), 3.89 & 3.61 (abd, *J* = 9.2 Hz, 2H), 1.18 (s, 9H). ^{13}C NMR (150 MHz, $CDCl_3$): δ 162.6, 155.9, 132.4, 118.4, 74.3, 66.4, 61.2, 54.2, 27.3.

4.4.1.40 Alloc-Ser(O′Bu)-(β-OH)Val-OEt 101

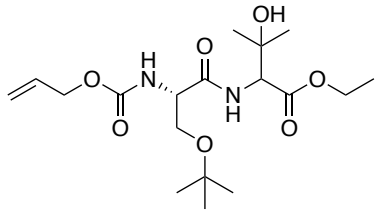

101

To a stirred solution of crude **89** (~1.28 mmol) in dry THF (5 mL) was added a solution of **100** (317 mg, 1.28 mmol, 1 equiv.) in dry THF (5 mL) dropwise and stirred for 16 hours. The resulting purple solution was concentrated under reduced pressure and the residue taken up in absolute EtOH (5 mL), to which was added ethanolic HCl (5 mL). The resulting solution was stirred at room temperature for 1 hour, or until the disappearance of higher-running species in TLC (silica, 2:1 petroleum ether:EtOAc). The solution was concentrated under reduced pressure and the residue purified by column chromatography (silica, 2:1:0.1 petroleum ether:EtOAc:MeOH) to give **101** as a brown oil (321 mg, 0.83 mmol, 65 %). ν_{max} (FTIR): 3411w, 2976m, 2937w, 2877w, 1726s, 1664s, 1499s, 1365m, 1332m, 1194s, 1094s, 1037s, 929m, 873m, 777m cm^{-1}. ^{1}H NMR (400 MHz, $CDCl_3$): δ 5.95-5.87 (m, 1H), 5.67 (bs, 1H), 5.32 (d, *J* = 16 Hz, 1H), 5.23 (d, *J* = 12 Hz, 1H), 4.59 (d, *J* = 8 Hz, 2H), 4.55 & 4.51 (abd, *J* = 8 Hz, 1H), 4.29-4.18 (m, 3H), 3.86-3.81 & 3.45-3.38 (abm, 2H), 1.30 (t, *J* = 8 Hz, 3H), 1.28-1.24 (m, 6H), 1.21 (d, 9H). ^{13}C NMR (150 MHz, $CDCl_3$): δ 171.3, 170.6, 156.1, 132.7, 118.2, 74.6, 74.4,

72.2, 66.1, 61.8, 60.1, 54.8, 27.5, 26.5, 14.3. Mass spectrum (ESI^+, MeOH): *m/z* 389.2276 $[M+H]^+$; $C_{18}H_{33}N_2O_7$ requires 389.2288.

4.4.1.41 Alloc-Ser(O^{t}Bu)-(β-OH)Val-OH 102

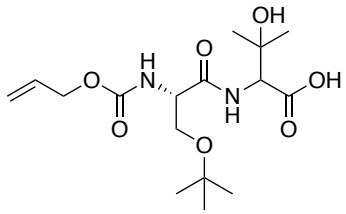

102

102 was synthesised according to a procedure described by Jiang *et al*..[168] To a stirred solution of **101** (320 mg, 0.82 mmol, 1 equiv.) in ^{t}BuOH:H_2O (4.5 mL, 3:1) at 0 °C under Ar was added LiOH.H_2O (173 mg, 4.12 mmol, 5.1 equiv.) *via* solid addition tube and the resulting solution stirred at 0 °C for 2 hours, or until the disappearance of starting material by TLC (silica, 10% MeOH in DCM, 1% AcOH). The solution was extracted with EtOAc (3x50 mL), dried (Na_2SO_4) and concentrated under reduced pressure to give **102** as a pink solid (244 mg, 0.66 mmol, 81%). **102** was deemed of sufficient purity by TLC that it was used telescopically in subsequent reactions, as per the Jiang *et al*. protocol.[168] Mass spectrum (ESI^+, MeOH): *m/z* 383.1098 $[M+H]^+$; $C_{16}H_{28}N_2O_7Na$ requires 383.1794.

4.4.1.42 Alloc-Ser(OtBu)-Dhv azlactone 97

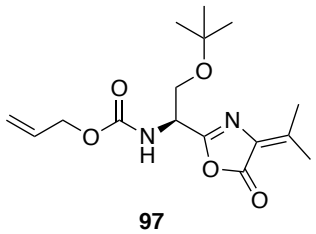

97

97 was synthesised according to a procedure described by Jiang and Castle.[168] To a stirred solution of **102** (239 mg, 0.66 mmol, 1 equiv.) in acetic anhydride (5 mL) at 50 °C under Ar was added sodium acetate (92 mg, 1.13 mmol, 1.7 equiv.) and the resulting solution stirred at 50 °C for 2 hours, or until the disappearance of starting material by TLC (silica, 2:1:0.1 petroleum ether:EtOAc;MeOH). The solution was diluted with deionised H_2O (10 mL), extracted with EtOAc (3x40 mL), the combined organic extracts washed with 10% Na_2CO_3 aqueous solution (40 mL), brine (40 mL), dried (Na_2SO_4) and concentrated under reduced pressure to give **97** as a brown oil (172 mg, 80%). ν_{max} (FTIR): 3442w, 2975w, 2935w, 2875w, 1792m, 1725s, 1674s, 1508m, 1364m, 1193s, 1156s, 1096m, 1056m, 994m, 874s, 776m cm^{-1}. ^1H NMR (400 MHz, $CDCl_3$): δ 5.99-5.87 (m, 1H), 5.62 (d, J = 8 Hz, 1H), 5.35 (d, J = 20 Hz, 1H), 5.23 (d, J = 12 Hz, 1H), 4.77-4.75 (m, 1H), 4.62-4.60 (m, 2H), 3.84 & 3.66 (abdd, J = 12 Hz & 4 Hz, 2H), 2.34 (s, 3H), 2.24 (s, 3H), 1.14 (s, 9H). Mass spectrum (ESI^+, MeOH): *m/z* 325.1734 $[M+H]^+$; $C_{16}H_{25}N_2O_5$ requires 325.1763.

4.4.1.43 *des*$_{1-10}$-[14]-Agl AOD9604 103

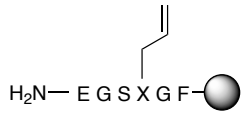

103

Peptide **103** was prepared according to the general automated procedure outlined in Section 2.3.3.1. Formation of **103** was verified by small-scale cleavage, RP-HPLC and LRMS. Mass spectrum (ESI$^+$, MeCN:H_2O:TFA): *m/z* 593.1 $[M+H]^+$; $C_{26}H_{37}N_6O_{10}$ requires 593.3. RP-HPLC (Agilent: Agilent C18 analytical column, 5 to 100% buffer B over 30 min): t_R = 11.2 min.

4.4.1.44 Alloc-*des*$_{1-8}$-[10]-Dhv-[14]-Agl AOD9604 104

104

104 was synthesised according to a procedure described by Jiang *et al*..[168] Resin-bound **103** (0.1 mmol), having been swelled for 96 hours in DCM/DMF (5 mL, 1:1) was suspended in NMP (4.5 mL), to which was added DMAP (8.7 mg, 0.07 mmol, 0.7 equiv.) The suspension was transferred to a round-bottom flask containing **97** (157 mg, 0.48 mmol, 4.8 equiv.) and stirred at 60 °C for 24 hours. The resin was then filtered from the reaction mixture and washed with DMF (5x5 mL) and DCM (1x5 mL). Formation of **104** was verified by small-scale cleavage, RP-HPLC and HRMS. Mass spectrum (ESI$^-$, MeCN:H_2O:TFA): *m/z* 859.3476 $[M-H]^-$; $C_{38}H_{51}N_8O_{15}$ requires 859.3474. RP-HPLC (Agilent: Agilent C18 analytical column, 5 to 100% buffer B over 30 min): t_R = 12.6 min.

4.4.1.45 *des*$_{1\text{-}8}$-[10]-Dhv-[14]-Agl AOD9604 105

105

105 was prepared according to a procedure described by Wilson *et al.*[179] Resin-bound **104** (0.1 mmol) was suspended in a minimal volume of dry DCM (~1 mL) to which was added phenylsilane (54 mg, 62 µL, 0.5 mmol, 5 equiv.) and left to stand for 5 minutes. Tetrakis(triphenylphosphine)palladium(0) (31 mg, 25 µmol, 0.25 equiv) was then added and the suspension immediately subjected to heating by microwave irradiation (25 watts) for 5 minutes at 38 °C to give a black suspension. The resin was then filtered from the reaction mixture and rinsed with DCM (5x5 mL). Formation of **105** was verified by small-scale cleavage, RP-HPLC and LRMS. Mass spectrum (ESI^+, MeCN:H_2O:TFA): *m/z* 777.2 $[M+H]^+$; $C_{34}H_{49}N_8O_{13}$ requires 777.3. RP-HPLC (Agilent: Agilent C18 analytical column, 10 to 40% buffer B over 30 min): t_R = 15.1 min.

4.4.1.46 Fmoc-[7, 14]-Agl-[10]-Dhv AOD9604 106

106

The resin-bound peptide **106** excluding the *N*-terminal Tyr residue was prepared from **105** on a 0.05 mmol scale according to the general automated procedure outlined in Section 2.3.3.1. Fmoc-L-Tyr was attached according to the general manual SPPS procedure outlined in Section 2.3.3.2 with the following quantities of reagents: HATU (153 mg, 0.4 mmol, 8 equiv.), Fmoc-L-(*O*-tBu)tyrosine-OH (193 mg, 0.4 mmol, 8 equiv.), NMM (88 µL, 0.8 mmol, 16 equiv.) in DMF (4 mL). Formation of **106** *sans* Fmoc was subsequently verified by small-scale Fmoc deprotection and resin cleavage,

RP-HPLC and LRMS. Mass spectrum (ESI^+, MeCN:H_2O:TFA): *m/z* 902.1 $[M+2H]^{2+}$; $C_{82}H_{127}N_{23}O_{23}$ requires 902.0. RP-HPLC (Agilent: Agilent C18 analytical column, 10 to 40% buffer B over 30 min): t_R = 21.7 min. The resin-bound peptide was subjected to the capping procedure outlined in Section 2.3.3.6 and stored overnight in a vacuum desiccator prior to RCM.

4.4.1.47 Fmoc-[7, 14]-Agl AOD9604 109

109

The resin-bound peptide **109** excluding the *N*-terminal Tyr residue was prepared on a 0.05 mmol scale according to the general automated procedure outlined in Section 2.3.3.1. Fmoc-L-Tyr was attached according to the general manual SPPS procedure outlined in Section 2.3.3.2 with the following quantities of reagents: HATU (154 mg, 0.4 mmol, 4 equiv.), Fmoc-L-(*O*-tBu)tyrosine-OH (203 mg, 0.4 mmol, 4 equiv.), NMM (88 μL, 0.8 mmol, 8 equiv.) in DMF (4 mL). Formation of **109** *sans* Fmoc was subsequently verified by small-scale Fmoc deprotection and resin cleavage, RP-HPLC and LRMS. Mass spectrum (ESI^+, MeCN:H_2O:TFA): *m/z* 903.2 $[M+2H]^{2+}$; $C_{82}H_{129}N_{23}O_{23}$ requires 903.0. RP-HPLC (Agilent: Agilent C18 analytical column, 10 to 40% buffer B over 30 min): t_R = 22.0 min. The resin-bound peptide was subjected to the capping procedure outlined in Section 2.3.3.6 and stored overnight in a vacuum desiccator prior to RCM.

4.4.1.48 *des*$_{1\text{-}6}$-[7,14]-Agl-[10]-Dhv AOD9604 107

107

The resin-bound peptide **107** was prepared from **105** on a 0.05 mmol scale. L-Arg was attached according to the general manual SPPS procedure outlined in Section 2.3.3.2 with the following quantities of reagents: HATU (154 mg, 0.4 mmol, 8 equiv.), Fmoc-L-Arg(Pbf)-OH (266 mg, 0.4 mmol, 8 equiv.), NMM (88 µL, 0.8 mmol, 16 equiv.) in DMF (4 mL). The resin was then deprotected according to the general procedure outlined in Section 2.3.3.5. Fmoc-L-Agl was attached according to the general manual SPPS procedure outlined in Section 2.3.3.2 with the following quantities of reagents: HATU (152 mg, 0.4 mmol, 8 equiv.), Fmoc-L-Agl-OH (135 mg, 0.4 mmol, 8 equiv.), NMM (88 µL, 0.8 mmol, 16 equiv.) in DMF (4 mL). Formation of **107** *sans* Fmoc was subsequently verified by small-scale Fmoc deprotection and resin cleavage, RP-HPLC and LRMS. Mass spectrum (ESI^+, MeCN:H_2O:TFA): *m/z* 1030.4 $[M+H]^+$; $C_{45}H_{68}N_{13}O_{15}$ requires 1030.5. *m/z* 515.8 $[M+2H]^{2+}$; ½($C_{45}H_{69}N_{13}O_{15}$) requires 515.7. RP-HPLC (Agilent: Agilent C18 analytical column, 10 to 40% buffer B over 30 min): t_R = 15.5 min. The resin-bound peptide was subjected to the capping procedure outlined in Section 2.3.3.6 and stored overnight in a vacuum desiccator prior to RCM.

4.4.1.49 *des*$_{1\text{-}6}$-[7,14]-Agl AOD9604 108

108

The resin-bound peptide **108** excluding the *N*-terminal Agl residue was synthesised on a 0.1 mmol scale according to the general automated procedure outlined in Section 2.3.3.1. Fmoc-L-Agl was attached according to the general manual SPPS procedure outlined in Section 2.3.3.2 with the following quantities of reagents: HATU (153 mg, 0.4 mmol, 4 equiv.), Fmoc-L-Agl-OH (143 mg, 0.4 mmol, 4 equiv.), NMM (88 μL, 0.8 mmol, 8 equiv.) in DMF (4 mL). Formation of **108** *sans* Fmoc was subsequently verified by small-scale Fmoc deprotection and resin cleavage, RP-HPLC and LRMS. Mass spectrum (ESI^+, MeCN:H_2O:TFA): *m/z* 1032.3 $[M+H]^+$; $C_{45}H_{70}N_{13}O_{15}$ requires 1032.5. *m/z* 516.8 $[M+2H]^{2+}$; ½($C_{45}H_{70}N_{13}O_{15}$) requires 516.8. RP-HPLC (Agilent: Agilent C18 analytical column, 10 to 40% buffer B over 30 min): t_R = 15.1 min. The resin-bound peptide was subjected to the capping procedure outlined in Section 2.3.3.6 and stored overnight in a vacuum desiccator prior to RCM.

4.4.1.50 Fmoc-[Δ^{4}7-14]-dicarba-[10]-Dhv AOD9604 112

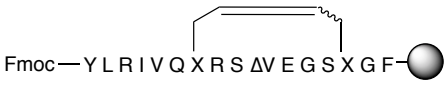

112

Resin-bound peptide **106** was subjected to the general microwave-assisted on-resin RCM procedure outlined in Section 2.3.3.8 with the following quantities of reagents: GII (9.1 mg, 21 mol %), 0.4 M LiCl/DMF (~0.1 mL), DCM (2 mL). Formation of **112** as an inseparable mixture of isomers with 56% conversion from starting material **106** was subsequently verified by small-scale Fmoc deprotection and resin cleavage, RP-HPLC

and LRMS. Mass spectrum (ESI^+, MeCN:H_2O:TFA): *m/z* 888.0 $[M+2H]^{2+}$; ½($C_{80}H_{125}N_{23}O_{23}$) requires 888.0. RP-HPLC (Agilent: Agilent C18 analytical column, 10 to 40% buffer B over 30 min): t_R = 19.7 min.

4.4.1.51 Fmoc-[Δ⁴7-14]-dicarba AOD9604 113

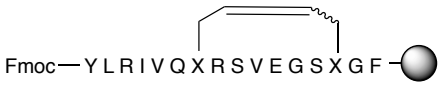

113

Resin-bound peptide **109** was subjected to the general microwave-assisted on-resin RCM procedure outlined in Section 2.3.3.8 with the following quantities of reagents: GII (17.7 mg, 21 mol %), 0.4 M LiCl/DMF (~0.2 mL), DCM (4 mL). Formation of **113** as an inseparable mixture of isomers with 20% conversion from starting material **109** was subsequently verified by small-scale Fmoc deprotection and resin cleavage, RP-HPLC and LRMS. Mass spectrum (ESI^+, MeCN:H_2O:TFA): *m/z* 889.2 $[M+2H]^{2+}$; ½($C_{80}H_{127}N_{23}O_{23}$) requires 889.0. RP-HPLC (Agilent: Agilent C18 analytical column, 10 to 40% buffer B over 30 min): t_R = 20.2 min.

4.4.1.52 Fmoc-*des*$_{1-6}$-[Δ⁴7,14]-dicarba-[10]-Dhv AOD9604 110

110

Resin-bound peptide **107** was subjected to the general microwave-assisted on-resin RCM procedure outlined in Section 2.3.3.8 with the following quantities of reagents: GII (8.7 mg, 21 mol %), 0.4 M LiCl/DMF (~0.1 mL), DCM (2 mL). Formation of **110** as a pair of isomers **110 (I)** and **110(II)** in a 3:5 ratio with 79% conversion from starting material **107** was subsequently verified by small-scale cleavage, RP-HPLC and LRMS (below).

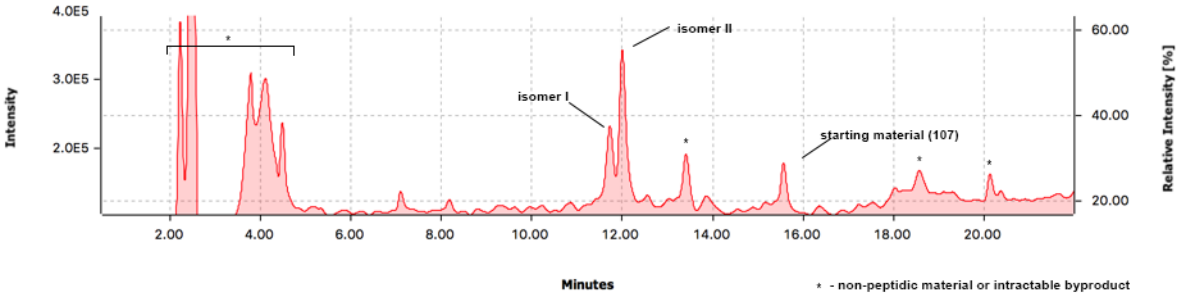

110(I): Mass spectrum (ESI$^+$, MeCN:H_2O:TFA): *m/z* 1003.5 $[M+H]^+$; $C_{43}H_{64}N_{13}O_{15}$ requires 1002.5. 501.7 $[M+2H]^{2+}$; ½($C_{43}H_{65}N_{13}O_{15}$) requires 501.7. RP-HPLC (Agilent: Agilent C18 analytical column, 10 to 40% buffer B over 30 min): t_R = 11.7 min.

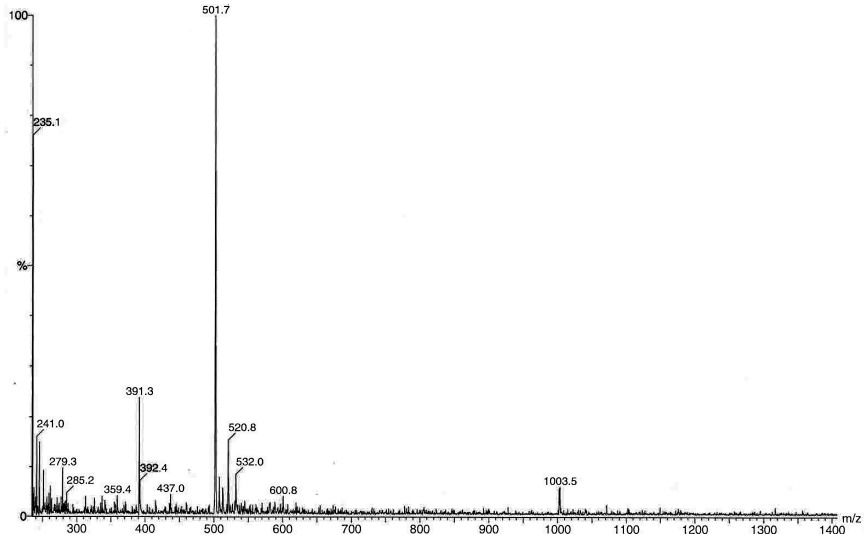

110(II) Mass spectrum (ESI$^+$, MeCN:H_2O:TFA): *m/z* 1002.4 $[M+H]^+$; $C_{43}H_{64}N_{13}O_{15}$ requires 1002.5. 501.9 $[M+2H]^{2+}$; ½($C_{43}H_{65}N_{13}O_{15}$) requires 501.7. RP-HPLC (Agilent: Agilent C18 analytical column, 10 to 40% buffer B over 30 min): t_R = 12.0 min.

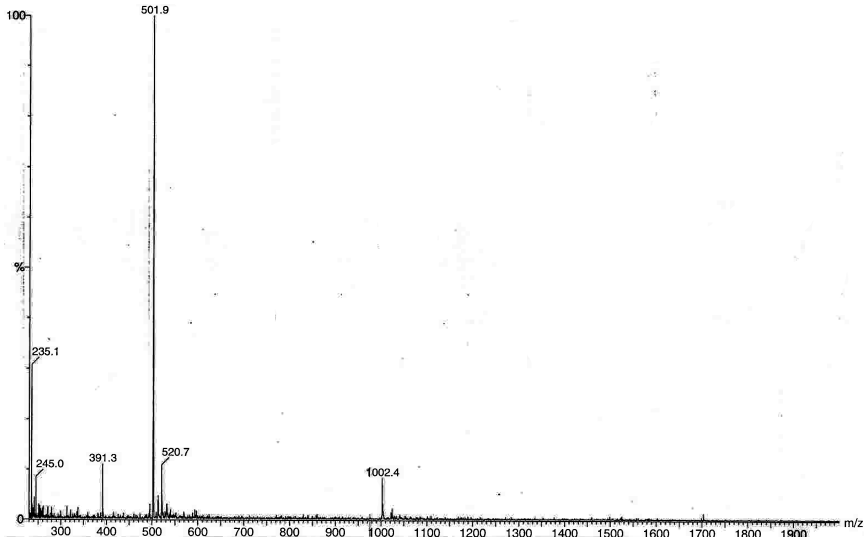

4.4.1.53 Fmoc-*des*$_{1\text{-}6}$-[Δ^{4}7,14]-dicarba AOD9604 (direct synthesis) 111

111

Resin-bound peptide **108** was subjected to the general microwave-assisted on-resin RCM procedure outlined in Section 2.3.3.8 with the following quantities of reagents: GII (18.8 mg, 22 mol %), 0.4 M LiCl/DMF (~0.2 mL), DCM (4 mL). Formation of **111** as a pair of isomers **111(I)** and **111(II)** in a 3:5 ratio with 40% conversion from starting material **108** was subsequently verified by small-scale cleavage, RP-HPLC and LRMS. **111(I)**: Mass spectrum (ESI^+, MeCN:H_2O:TFA): *m/z* 1004.5 $[M+H]^+$; $C_{43}H_{66}N_{13}O_{15}$ requires 1004.5. 502.9 $[M+2H]^{2+}$; ½($C_{43}H_{67}N_{13}O_{15}$) requires 502.8. RP-HPLC (Agilent: Agilent C18 analytical column, 10 to 40% buffer B over 30 min): t_R = 7.6 min.

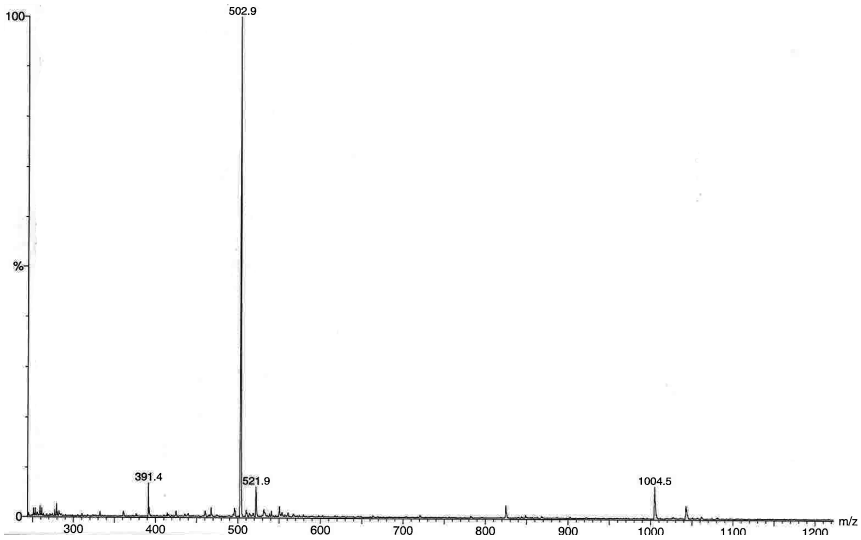

111(II) Mass spectrum (ESI$^+$, MeCN:H_2O:TFA): *m/z* 1004.3 $[M+H]^+$; $C_{43}H_{66}N_{13}O_{15}$ requires 1004.5. 502.8 $[M+2H]^{2+}$; ½($C_{43}H_{67}N_{13}O_{15}$) requires 502.8. RP-HPLC (Agilent: Agilent C18 analytical column, 10 to 40% buffer B over 30 min): t_R = 11.6 min.

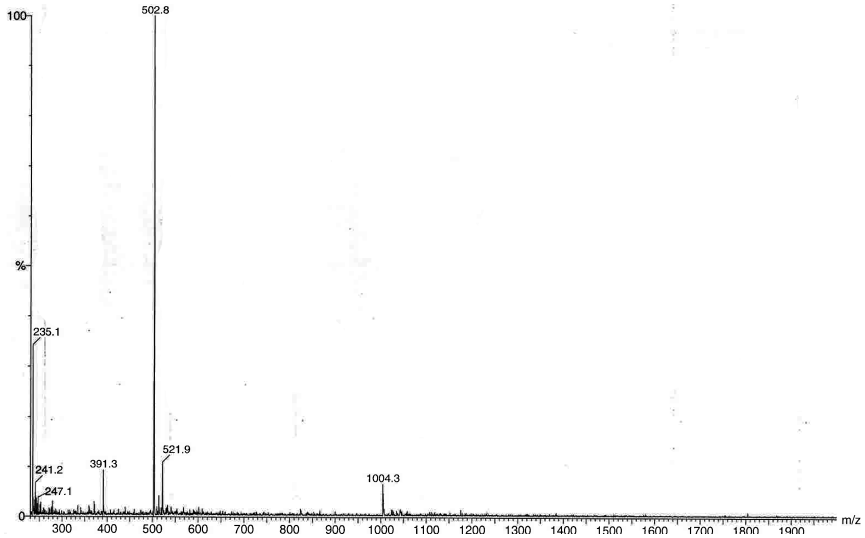

4.4.1.54 Fmoc-*des*$_{1\text{-}6}$-[$\Delta^4$7,14]-dicarba AOD9604 (*via* asymmetric hydrogenation) **111**

111

In a drybox (N_2), resin-bound **110** was suspended in 10% v/v degassed MeOH in dry degassed DCM (5 mL) in a Fischer-Porter tube, to which was added [(*S*,*S*)-Me-DuPHOS-Rh(I)-COD]BF_4 (1 mg) and the vessel sealed. The vessel was then pressurised with H_2 (50 psi) and stirred slowly at room temperature for 48 hours. The vessel was then vented to atmosphere, the resin filtered from the suspension and washed with DCM (5x5mL). Formation of **111** with 30% conversion, *sans* Fmoc, was subsequently verified by small-scale Fmoc deprotection and resin cleavage, RP-HPLC and LRMS. Mass spectrum (ESI$^+$, MeCN:H_2O:TFA): *m/z* 1004.4 $[M+H]^+$; $C_{43}H_{66}N_{13}O_{15}$ requires 1004.5. *m/z* 502.9 $[M+2H]^{2+}$; ½($C_{43}H_{67}N_{13}O_{15}$) requires 502.7. RP-HPLC (Agilent: Agilent C18 analytical column, 10 to 40% buffer B over 30 min): t_R = 6.8 min.

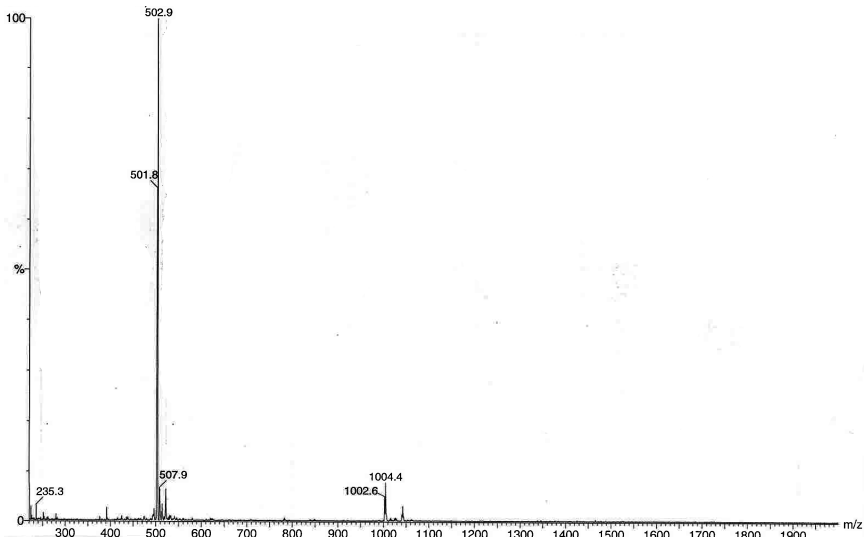

4.4.1.55 *des*$_{A1-3}$-[A7]-Cys(*t*Bu)-[A20]-Cys(Acm) human insulin A-chain 114

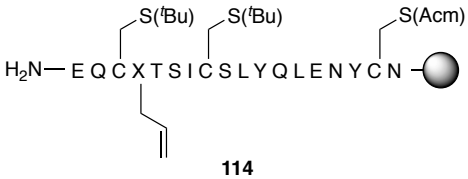

114

The resin-bound peptide **114** was prepared according to the general automated procedure outlined in Section 2.3.3.1. Formation of **114** was subsequently verified by small-scale Fmoc deprotection and resin cleavage, RP-HPLC and LRMS. Mass spectrum (ESI$^+$, MeCN:H_2O:TFA): *m/z* 1121.3 $[M+2H]^{2+}$; ½($C_{93}H_{147}N_{23}O_{33}S_4$) requires 1121.0. RP-HPLC (Agilent: Agilent C18 analytical column, 15 to 50% buffer B over 35 min): t_R = 17.2 min.

4.4.1.56 Alloc-*des*$_{A1}$-[A3]-Dhv-[A6, A11]-Cys(*t*Bu)-[A20]-Cys(Acm) human insulin A-chain 115

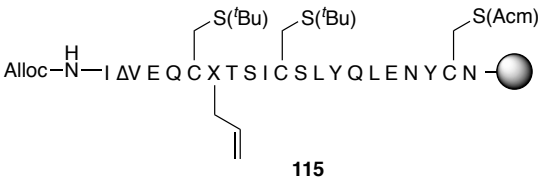

115

115 was synthesised according to a modified version of a procedure originally described by Jiang *et al*.[168] Resin-bound **114** (0.1 mmol) was suspended in a solution of **83** (174 mg, 0.59 mmol, 6 equiv.) and DMAP (6.6 mg, 0.05 mmol, 0.5 equiv.) in NMP (5 mL) and stirred at 60 °C under N_2 for 24 hours, then in air for a further 48 hours, the last 24 hours with no heating or stirring. The resin was then filtered from the reaction mixture and washed with DMF (5x5 mL) and DCM (1x5 mL). Formation of **115** was verified by small-scale cleavage, RP-HPLC and HRMS. Mass spectrum (ESI+, MeCN:H_2O:TFA): m/z 1267.8 [M+H]+; ½($C_{108}H_{167}N_{25}O_{37}S_4$) requires 1268.0. RP-HPLC (Agilent: Agilent C18 analytical column, 15 to 50% buffer B over 35 min): t_R = 22.4 min.

4.4.1.57 *des*$_{A1}$-[A3]-Dhv-[A7]-Cys(*t*Bu)-[A20]-Cys(Acm) human insulin A-chain 116

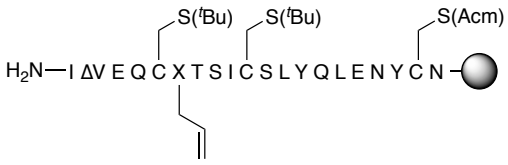

116

116 was prepared according to a procedure described by Wilson *et al.*[179] Resin-bound **115** (0.1 mmol) was suspended in a minimal volume of dry DCM (2 mL) to which was added phenylsilane (54 mg, 62 µL, 0.5 mmol, 5 equiv.) and left to stand for 5 minutes. Tetrakis(triphenylphosphine)palladium(0) (31 mg, 25 µmol, 0.25 equiv) was then added and the suspension immediately subjected to heating by microwave irradiation (25 watts) for 5 minutes at 38 °C to give a black suspension. The resin was then filtered from the reaction mixture and rinsed with DCM (5x5 mL). Formation of **116** was verified by small-scale cleavage, RP-HPLC and LRMS. Mass spectrum (ESI$^+$, MeCN:H_2O:TFA): *m/z* 1226.8 $[M+2H]^{2+}$; ½($C_{104}H_{165}N_{25}O_{35}S_4$) requires 1226.8. RP-HPLC (Agilent: Agilent C18 analytical column, 15 to 50% buffer B over 35 min): t_R = 20.5 min.

4.4.1.58 *des*$_{B1\text{-}B6,B9\text{-}B30}$-[B7]-Agl-Arg-Arg-Pro-Lys-Arg-[A3]-Dhv-[A6, A11]-Cys(*t*Bu)-[A7]-Agl-[A20]-Cys(Acm) human insulin 117

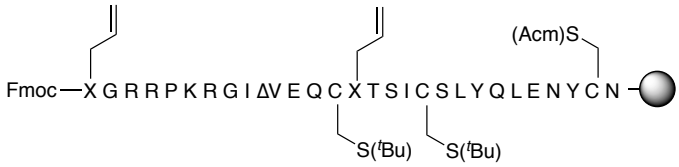

117

117 was prepared from **116** using repeated iterations of the manual SPPS procedure described in Section 2.3.3.2, albeit using 8 molar equivalents of each amino acid and HATU as well as 16 molar equivalents of NMM for each coupling. Formation of **117** was verified by small-scale cleavage, RP-HPLC and LRMS. Mass spectrum (ESI$^+$,

MeCN:H_2O:TFA): *m/z* 852.7 $[M+4H]^{4+}$; ¼($C_{148}H_{245}N_{43}O_{43}S_3$) requires 852.2. *m/z* 1136.6 $[M+3H]^{3+}$; ⅓($C_{148}H_{244}N_{43}O_{43}S_3$) requires 1135.9. RP-HPLC (Agilent: Agilent C18 analytical column, 5 to 100% buffer B over 30 min): t_R = 18.3 min. The resin-bound peptide was subjected to the capping procedure outlined in Section 2.3.3.6 and stored overnight in a vacuum desiccator prior to RCM.

4.4.1.59 Attempted synthesis of *des$_{B1\text{-}B6,B9\text{-}B30}$*-[B7]-Agl-Arg-Arg-Pro-Lys-Arg-[A3]-Dhv-[A6-A11]-Cys(^{t}Bu)-[A7]-Agl-[A20]-Cys(Acm) human insulin **118**

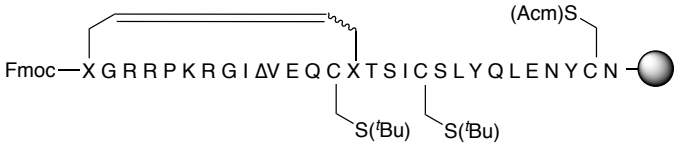

118

Resin-bound peptide **117** was subjected to the general microwave-assisted on-resin RCM procedure outlined in Section 2.3.3.8 with the following quantities of reagents: GII (34 mg, 40 mol %), 0.4 M LiCl/DMF (~0.2 mL), DCM (4 mL). Analysis of the resin-bound peptide by RP-HPLC and MS following small-scale Fmoc deprotection and resin cleavage showed only intractable byproducts with no evidence of either starting material **117** or product **118**, suggesting decomposition.

5 References

1. Mayer, J. P.; Zhang, F.; DiMarchi, R. D., Insulin structure and function. *Peptide Science* **2007,** *88* (5), 687-713.
2. Cutfield, J.; Cutfield, S.; Dodson, E.; Dodson, G.; Emdin, S.; Reynolds, C., Structure and biological activity of hagfish insulin. *Journal of molecular biology* **1979,** *132* (1), 85-100.
3. Muggeo, M.; Van Obberghen, E.; Kahn, C. v.; Roth, J.; Ginsberg, B.; De Meyts, P.; Emdin, S.; Falkmer, S., The insulin receptor and insulin of the Atlantic hagfish: extraordinary conservation of binding specificity and negative cooperativity in the most primitive vertebrate. *Diabetes* **1979,** *28* (3), 175-181.
4. Conlon, J. M., Evolution of the insulin molecule: insights into structure-activity and phylogenetic relationships. *Peptides* **2001,** *22* (7), 1183-1193.
5. Karamitsos, D. T., The story of insulin discovery. *Diabetes research and clinical practice* **2011,** *93*, S2-S8.
6. Banting, F.; Best, C. H.; Collip, J. B.; Campbell, W. R.; Fletcher, A. A., Pancreatic extracts in the treatment of diabetes mellitus. *Canadian Medical Association Journal* **1922,** *12* (3), 141.
7. Ward, C. W.; Lawrence, M. C., Landmarks in insulin research. *Frontiers in endocrinology* **2011,** *2*.
8. Saltiel, A. R.; Kahn, C. R., Insulin signalling and the regulation of glucose and lipid metabolism. *Nature* **2001,** *414* (6865), 799-806.
9. Steiner, D. F., Adventures with insulin in the islets of Langerhans. *Journal of Biological Chemistry* **2011,** *286* (20), 17399-17421.
10. Steiner, D. F.; Cunningham, D.; Spigelman, L.; Aten, B., Insulin biosynthesis: evidence for a precursor. *Science* **1967,** *157* (3789), 697-700.
11. Steiner, D.; Chan, S.; Welsh, J.; Kwok, S., Structure and evolution of the insulin gene. *Annual review of genetics* **1985,** *19* (1), 463-484.
12. Metzler, D. E., *Biochemistry: The Chemical Reactions of Living Cells*. Academic Press: 2003.
13. Steiner, D.; Clark, J.; Nolan, C.; Rubenstein, A.; Margoliash, E.; Aten, B.; Oyer, P., Proinsulin and the biosynthesis of insulin. *Recent progress in hormone research* **1969,** *25*, 207.
14. Adams, M. J.; Blundell, T.; Dodson, E.; Dodson, G.; Vijayan, M.; Baker, E.; Harding, M.; Hodgkin, D.; Rimmer, B.; Sheat, S., Structure of rhombohedral 2 zinc insulin crystals. *Nature* **1969,** *224* (5218), 491-495.
15. Dunn, M. F., Zinc–ligand interactions modulate assembly and stability of the insulin hexamer–a review. *Biometals* **2005,** *18* (4), 295-303.
16. Ciszak, E.; Smith, G. D., Crystallographic evidence for dual coordination around zinc in the T3R3 human insulin hexamer. *Biochemistry* **1994,** *33* (6), 1512-7.
17. O'donoghue, S. I.; Chang, X.; Abseher, R.; Nilges, M.; Led, J. J., Unraveling the symmetry ambiguity in a hexamer: calculation of the R6 human insulin structure. *Journal of biomolecular NMR* **2000,** *16* (2), 93-108.
18. Pettersen, E. F.; Goddard, T. D.; Huang, C. C.; Couch, G. S.; Greenblatt, D. M.; Meng, E. C.; Ferrin, T. E., UCSF Chimera—a visualization system for exploratory research and analysis. *Journal of computational chemistry* **2004,** *25* (13), 1605-1612.
19. Pandyarajan, V.; Weiss, M. A., Design of Non-Standard Insulin Analogs for the Treatment of Diabetes Mellitus. *Curr Diab Rep* **2012,** *12* (6), 697-704.
20. DiMarchi, R.; Chance, R.; Long, H.; Shields, J.; Slieker, L., Preparation of an insulin with improved pharmacokinetics relative to human insulin through consideration of structural homology with insulin-like growth factor I. *Hormone Research in Paediatrics* **1994,** *41* (Suppl. 2), 93-96.

21. Heinemann, L.; Heise, T.; Jorgensen, L.; Starke, A., Action profile of the rapid acting insulin analogue: human insulin B28Asp. *Diabetic medicine* **1993,** *10* (6), 535-539.
22. Walsh, G., Therapeutic insulins and their large-scale manufacture. *Applied Microbiology and Biotechnology* **2005,** *67* (2), 151-159.
23. Shabanpoor, F.; Separovic, F.; Wade, J. D., The human insulin superfamily of polypeptide hormones. *Vitamins & Hormones* **2009,** *80*, 1-31.
24. Weinstein, D.; Simon, M.; Yehezkel, E.; Laron, Z.; Werner, H., Insulin analogues display IGF-I-like mitogenic and anti-apoptotic activities in cultured cancer cells. *Diabetes/metabolism research and reviews* **2009,** *25* (1), 41-49.
25. Ish-Shalom, D.; Christoffersen, C.; Vorwerk, P.; Sacerdoti-Sierra, N.; Shymko, R.; Naor, D.; De Meyts, P., Mitogenic properties of insulin and insulin analogues mediated by the insulin receptor. *Diabetologia* **1997,** *40* (2), S25-S31.
26. De Meyts, P., Insulin and its receptor: structure, function and evolution. *BioEssays* **2004,** *26* (12), 1351-1362.
27. Menting, J. G.; Whittaker, J.; Margetts, M. B.; Whittaker, L. J.; Kong, G. K.-W.; Smith, B. J.; Watson, C. J.; Žáková, L.; Kletvíková, E.; Jiráček, J., How insulin engages its primary binding site on the insulin receptor. *Nature* **2013,** *493* (7431), 241-245.
28. Scapin, G.; Dandey, V. P.; Zhang, Z.; Prosise, W.; Hruza, A.; Kelly, T.; Mayhood, T.; Strickland, C.; Potter, C. S.; Carragher, B., Structure of the insulin receptor–insulin complex by single-particle cryo-EM analysis. *Nature* **2018,** *556* (7699), 122.
29. Schaffer, L., A model for insulin binding to the insulin receptor. *European Journal of Biochemistry* **1994,** *221* (3), 1127-1132.
30. Ward, C. W.; Lawrence, M. C., Ligand-induced activation of the insulin receptor: a multi-step process involving structural changes in both the ligand and the receptor. *Bioessays* **2009,** *31* (4), 422-434.
31. Gammeltoft, S., Insulin receptors: binding kinetics and structure-function relationship of insulin. *Physiological reviews* **1984,** *64* (4), 1321-1378.
32. Menting, J. G.; Yang, Y.; Chan, S. J.; Phillips, N. B.; Smith, B. J.; Whittaker, J.; Wickramasinghe, N. P.; Whittaker, L. J.; Pandyarajan, V.; Wan, Z.-l., Protective hinge in insulin opens to enable its receptor engagement. *Proceedings of the National Academy of Sciences* **2014,** *111* (33), E3395-E3404.
33. Ward, C. W.; Menting, J. G.; Lawrence, M. C., The insulin receptor changes conformation in unforeseen ways on ligand binding: sharpening the picture of insulin receptor activation. *Bioessays* **2013,** *35* (11), 945-954.
34. Hua, Q.; Weiss, M. A., Comparative 2D NMR studies of human insulin and despentapeptide insulin: sequential resonance assignment and implications for protein dynamics and receptor recognition. *Biochemistry* **1991,** *30* (22), 5505-5515.
35. Shoelson, S. E.; Lu, Z. X.; Parlautan, L.; Lynch, C. S.; Weiss, M. A., Mutations at the dimer, hexamer, and receptor-binding surfaces of insulin independently affect insulin-insulin and insulin-receptor interactions. *Biochemistry* **1992,** *31* (6), 1757-1767.
36. Fávero-Retto, M. P.; Palmieri, L. C.; Souza, T. A.; Almeida, F. C.; Lima, L. M. T., Structural meta-analysis of regular human insulin in pharmaceutical formulations. *European Journal of Pharmaceutics and Biopharmaceutics* **2013,** *85* (3), 1112-1121.
37. Shoelson, S.; Fickova, M.; Haneda, M.; Nahum, A.; Musso, G.; Kaiser, E.; Rubenstein, A.; Tager, H., Identification of a mutant human insulin predicted to contain a serine-for-phenylalanine substitution. *Proceedings of the National Academy of Sciences* **1983,** *80* (24), 7390-7394.
38. Shoelson, S.; Polonsky, K.; Zeidler, A.; Rubenstein, A.; Tager, H., Human insulin B24 (Phe----Ser). Secretion and metabolic clearance of the abnormal insulin in man and in a dog model. *Journal of Clinical Investigation* **1984,** *73* (5), 1351.

39. Mirmira, R.; Tager, H., Role of the phenylalanine B24 side chain in directing insulin interaction with its receptor. Importance of main chain conformation. *Journal of Biological Chemistry* **1989,** *264* (11), 6349-6354.
40. Shoelson, S.; Haneda, M.; Blix, P.; Nanjo, A.; Sanke, T.; Inouye, K.; Steiner, D.; Rubenstein, A.; Tager, H., Three mutant insulins in man. *Nature* **1983,** *302* (5908), 540-543.
41. Xu, B.; Huang, K.; Chu, Y.-C.; Hu, S.-Q.; Nakagawa, S.; Wang, S.; Wang, R.-Y.; Whittaker, J.; Katsoyannis, P. G.; Weiss, M. A., Decoding the cryptic active conformation of a protein by synthetic photoscanning insulin inserts a detachable arm between receptor domains. *Journal of Biological Chemistry* **2009,** *284* (21), 14597-14608.
42. Hua, Q. X.; Shoelson, S. E.; Kochoyan, M.; Weiss, M. A., Receptor binding redefined by a structural switch in a mutant human insulin. **1991**.
43. Nakagawa, S. H.; Tager, H., Role of the phenylalanine B25 side chain in directing insulin interaction with its receptor. Steric and conformational effects. *Journal of Biological Chemistry* **1986,** *261* (16), 7332-7341.
44. Mirmira, R. G.; Tager, H. S., Disposition of the phenylalanine B25 side chain during insulin-receptor and insulin-insulin interactions. *Biochemistry* **1991,** *30* (33), 8222-8229.
45. Quan, B.; Smiley, D. L.; Gelfanov, V. M.; DiMarchi, R. D., Site Specific Introduction of Unnatural Amino Acids at Sites Critical to Insulin Receptor Recognition and Biological Activity. In *Understanding Biology Using Peptides*, Springer: 2006; pp 311-312.
46. Young, J. D.; Carpenter, F. H., Isolation and characterization of products formed by the action of trypsin on insulin. *Journal of Biological Chemistry* **1961,** *236* (3), 743-748.
47. Katsoyannis, P. G.; Zalut, C.; Harris, A.; Meyer, R. J., Analogs of insulin. I. Synthesis of destripeptide B28-30 bovine insulin and destripeptide B28-30 procine (human) insulin. *Biochemistry* **1971,** *10* (21), 3884-3889.
48. Katsoyannis, P. G.; Ginos, J.; Cosmatos, A.; Schwartz, G., Synthesis of destetrapeptide B27-30 human (porcine) insulin. Biologically active insulin analog. *Journal of the American Chemical Society* **1973,** *95* (19), 6427-6434.
49. Katsoyannis, P. G.; Ginos, J.; Schwartz, G. P.; Cosmatos, A., Synthesis of a biologically active truncated insulin. Des (pentapeptide B 26–30) human (porcine) insulin. *Journal of the Chemical Society, Perkin Transactions 1* **1974**, 1311-1317.
50. Vinther, T. N.; Norrman, M.; Ribel, U.; Huus, K.; Schlein, M.; Steensgaard, D. B.; Pedersen, T. Å.; Pettersson, I.; Ludvigsen, S.; Kjeldsen, T., Insulin analog with additional disulfide bond has increased stability and preserved activity. *Protein Science* **2013,** *22* (3), 296-305.
51. Chang, S.-G.; Choi, K.-D.; Jang, S.-H.; Shin, H.-C., Role of disulfide bonds in the structure and activity of human insulin. *Molecules and cells* **2003,** *16* (3), 323-330.
52. Guo, Z.-Y.; Jia, X.-Y.; Feng, Y.-M., Replacement of the interchain disulfide bridge-forming amino acids A7 and B7 by glutamate impairs the structure and activity of insulin. *Biological chemistry* **2004,** *385* (12), 1171-1175.
53. Märki, F.; De Gasparo, M.; Eisler, K.; Kamber, B.; Riniker, B.; Rittel, W.; Sieber, P., Synthesis and biological activity of seventeen analogues of human insulin. *Hoppe-Seyler´s Zeitschrift für physiologische Chemie* **1979,** *360* (2), 1619-1632.
54. Clark, S.; Harrison, L., Disulfide exchange between insulin and its receptor. A possible post-binding step in insulin action. *Journal of Biological Chemistry* **1983,** *258* (19), 11434-11437.

55. Videnov, G.; Stoev, S.; Brandenburg, D., Synthesis of A7, B7-Dicarbainsulin, an Analogue with a Noncleavable Bond Between A-and B-Chain. II. Synthesis of the A-Chain Segments. *Biological Chemistry Hoppe-Seyler* **1989,** *370* (2), 1103-1112.
56. Kurouski, D.; Washington, J.; Ozbil, M.; Prabhakar, R.; Shekhtman, A.; Lednev, I. K., Disulfide bridges remain intact while native insulin converts into amyloid fibrils. *PloS one* **2012,** *7* (6), e36989.
57. Li, Y.; Gong, H.; Sun, Y.; Yan, J.; Cheng, B.; Zhang, X.; Huang, J.; Yu, M.; Guo, Y.; Zheng, L., Dissecting the role of disulfide bonds on the amyloid formation of insulin. *Biochemical and biophysical research communications* **2012,** *423* (2), 373-378.
58. Schulz, G. E.; Schirmer, R. H., Noncovalent Forces Determining Protein Structure. In *Principles of Protein Structure*, Springer: 1979; pp 27-45.
59. Fass, D., Disulfide bonding in protein biophysics. *Annual review of biophysics* **2012,** *41*, 63-79.
60. Wetzel, R., Harnessing disulfide bonds using protein engineering. *Trends in Biochemical Sciences* **1987,** *12*, 478-482.
61. Schmidt, B.; Ho, L.; Hogg, P. J., Allosteric disulfide bonds. *Biochemistry* **2006,** *45* (24), 7429-7433.
62. Wong, J. W.; Hogg, P. J., Allosteric disulfide bonds. In *Folding of Disulfide Proteins*, Springer: 2011; pp 151-182.
63. Hogg, P. J., Targeting allosteric disulphide bonds in cancer. *Nat Rev Cancer* **2013,** *13* (6), 425-431.
64. Craik, D. J.; Daly, N. L.; Bond, T.; Waine, C., Plant cyclotides: A unique family of cyclic and knotted proteins that defines the cyclic cystine knot structural motif. *Journal of Molecular Biology* **1999,** *294* (5), 1327-1336.
65. Clark, R. J.; Akcan, M.; Kaas, Q.; Daly, N. L.; Craik, D. J., Cyclization of conotoxins to improve their biopharmaceutical properties. *Toxicon* **2012,** *59* (4), 446-455.
66. Scott, C. P.; Abel-Santos, E.; Wall, M.; Wahnon, D. C.; Benkovic, S. J., Production of cyclic peptides and proteins in vivo. *Proceedings of the National Academy of Sciences of the United States of America* **1999,** *96* (24), 13638-13643.
67. Besse, D.; Moroder, L., Synthesis of selenocysteine peptides and their oxidation to diselenide-bridged compounds. *Journal of Peptide Science* **1997,** *3* (6), 442-453.
68. Willey, J. M.; van der Donk, W. A., Lantibiotics: peptides of diverse structure and function. *Annual review of microbiology* **2007,** *61*, 477-501.
69. Williams, G. M.; Lee, K.; Li, X.; Cooper, G. J.; Brimble, M. A., Replacement of the CysA7–CysB7 disulfide bond with a 1, 2, 3-triazole linker causes unfolding in insulin glargine. *Organic & biomolecular chemistry* **2015,** *13* (13), 4059-4063.
70. Rijkers, D. T., Synthesis of cyclic peptides and peptidomimetics by metathesis reactions. In *Synthesis of Heterocycles by Metathesis Reactions*, Springer: 2015; pp 191-244.
71. Jošt, K.; Barth, T.; Krejčí, I.; Fruhaufová, L.; Procházka, Ž.; Šorm, F., Amino acids and peptides. CXIII. Carba 1-oxytocin: Synthesis and some of its biological properties. *Collection of Czechoslovak Chemical Communications* **1973,** *38* (4), 1073-1083.
72. Keller, O.; Rudinger, J., Synthesis of [1, 6-α, α′-Diaminosuberic acid] oxytocin ('Dicarba-oxytocin'). *Helvetica chimica acta* **1974,** *57* (5), 1253-1259.
73. Veber, D. F.; Strachan, R. G.; Bergstrand, S. J.; Holly, F. W.; Homnick, C. F.; Hirschmann, R.; Torchiana, M. L.; Saperstein, R., Nonreducible cyclic analogues of somatostatin. *Journal of the American Chemical Society* **1976,** *98* (8), 2367-2369.
74. Cui, H. K.; Guo, Y.; He, Y.; Wang, F. L.; Chang, H. N.; Wang, Y. J.; Wu, F. M.; Tian, C. L.; Liu, L., Diaminodiacid-based solid-phase synthesis of peptide disulfide bond mimics. *Angewandte Chemie* **2013,** *52* (36), 9558-62.

75. Trnka, T. M.; Grubbs, R. H., The development of L2X2Ru CHR olefin metathesis catalysts: an organometallic success story. *Accounts of Chemical Research* **2001,** *34* (1), 18-29.
76. Pérez de Vega, M. J.; García-Aranda, M. I.; González-Muñiz, R., A role for ring-closing metathesis in medicinal chemistry: Mimicking secondary architectures in bioactive peptides. *Medicinal research reviews* **2011,** *31* (5), 677-715.
77. Miller, S. J.; Grubbs, R. H., Synthesis of Conformationally Restricted Amino Acids and Peptides Employing Olefin Metathesis. *Journal of the American Chemical Society* **1995,** *117* (21), 5855-5856.
78. Miller, S. J.; Blackwell, H. E.; Grubbs, R. H., Application of ring-closing metathesis to the synthesis of rigidified amino acids and peptides. *Journal of the American Chemical Society* **1996,** *118* (40), 9606-9614.
79. Blackwell, H. E.; Grubbs, R. H., Highly efficient synthesis of covalently cross-linked peptide helices by ring-closing metathesis. *Angewandte Chemie* **1998,** *37* (23), 3281-3284.
80. Schafmeister, C. E.; Po, J.; Verdine, G. L., An all-hydrocarbon cross-linking system for enhancing the helicity and metabolic stability of peptides. *Journal of the American Chemical Society* **2000,** *122* (24), 5891-5892.
81. Stymiest, J. L.; Mitchell, B. F.; Wong, S.; Vederas, J. C., Synthesis of biologically active dicarba analogues of the peptide hormone oxytocin using ring-closing metathesis. *Organic letters* **2003,** *5* (1), 47-49.
82. Whelan, A. N.; Elaridi, J.; Harte, M.; Smith, S. V.; Jackson, W. R.; Robinson, A. J., A tandem metathesis–hydrogenation route to dicarba analogues of cystine-containing cyclic peptides. *Tetrahedron Letters* **2004,** *45* (52), 9545-9547.
83. Robinson, A. J.; Elaridi, J.; Van Lierop, B. J.; Mujcinovic, S.; Jackson, W. R., Microwave-assisted RCM for the synthesis of carbocyclic peptides. *Journal of peptide science : an official publication of the European Peptide Society* **2007,** *13* (4), 280-5.
84. Illesinghe, J.; Guo, C. X.; Garland, R.; Ahmed, A.; van Lierop, B.; Elaridi, J.; Jackson, W. R.; Robinson, A. J., Metathesis assisted synthesis of cyclic peptides. *Chemical communications* **2009,** (3), 295-7.
85. Robinson, A. J.; van Lierop, B. J.; Garland, R. D.; Teoh, E.; Elaridi, J.; Illesinghe, J. P.; Jackson, W. R., Regioselective formation of interlocked dicarba bridges in naturally occurring cyclic peptide toxins using olefin metathesis. *Chemical communications* **2009,** (28), 4293-5.
86. Hossain, M. A.; Rosengren, K. J.; Zhang, S.; Bathgate, R. A. D.; Tregear, G. W.; van Lierop, B. J.; Robinson, A. J.; Wade, J. D., Solid phase synthesis and structural analysis of novel A-chain dicarba analogs of human relaxin-3 (INSL7) that exhibit full biological activity. *Organic & Biomolecular Chemistry* **2009,** *7* (8), 1547-1553.
87. MacRaild, C. A.; Illesinghe, J.; Lierop, B. J. v.; Townsend, A. L.; Chebib, M.; Livett, B. G.; Robinson, A. J.; Norton, R. S., Structure and Activity of (2, 8)-Dicarba-(3, 12)-cystino α-ImI, an α-Conotoxin Containing a Nonreducible Cystine Analogue†. *Journal of medicinal chemistry* **2009,** *52* (3), 755-762.
88. van Lierop, B. J.; Whelan, A. N.; Andrikopoulos, S.; Mulder, R. J.; Jackson, W. R.; Robinson, A. J., Methods for Enhancing Ring Closing Metathesis Yield in Peptides: Synthesis of a Dicarba Human Growth Hormone Fragment. *International Journal of Peptide Research and Therapeutics* **2010,** *16* (3), 133-144.
89. Robinson, A.; Gooding, S., Methods for the synthesis of alkyne-containing dicarba bridges in peptides. WO2011146974A1, Google Patents: 2011.
90. van Lierop, B. J.; Bornschein, C.; Jackson, W. R.; Robinson, A. J., Ring-closing Metathesis in Peptides–the Sting is in the Tail! *Australian Journal of Chemistry* **2011,** *64* (6), 806-811.
91. Robinson, A.; Van Lierop, B., Insulin analogues. Google Patents: 2012.

92. van Lierop, B. J.; Robinson, S. D.; Kompella, S. N.; Belgi, A.; McArthur, J. R.; Hung, A.; MacRaild, C. A.; Adams, D. J.; Norton, R. S.; Robinson, A. J., Dicarba alpha-conotoxin Vc1.1 analogues with differential selectivity for nicotinic acetylcholine and GABAB receptors. *ACS chemical biology* **2013,** *8* (8), 1815-21.
93. McArthur, C. M. A Selective and Succesive Metathesis Approach to Multi-Dicarba Peptides. Monash University, 2015.
94. Gleeson, E. C.; Wang, Z. J.; Robinson, S. D.; Chhabra, S.; MacRaild, C. A.; Jackson, W. R.; Norton, R. S.; Robinson, A. J., Stereoselective synthesis and structural elucidation of dicarba peptides. *Chemical communications* **2016**.
95. van Lierop, B.; Ong, S. C.; Belgi, A.; Delaine, C.; Andrikopoulos, S.; Haworth, N. L.; Menting, J. G.; Lawrence, M. C.; Robinson, A. J.; Forbes, B. E., Insulin in motion: The A6-A11 disulfide bond allosterically modulates structural transitions required for insulin activity. *Scientific reports* **2017,** *7* (1), 17239.
96. Belgi, A. B., James V.; Gooding, Simon G.; MacRaild, Chris A.; Chhabra, Sandeep; Robinson, Samuel D.; Tae, Han-Shen; Bartels, Peter; Zhao, Fei-Yue; Wei, Haifeng; Spanswick, David; Adams, David J.; Norton, Raymond S.; Robinson, Andrea J., Synthesis and structural and biological evaluation of novel dicarba analogues of a–conotoxin Vc1.1: [2-8]-alkyne Vc1.1 and [2-8]-alkane Vc1.1. *Unpublished Manuscript* **2019**.
97. Ong, S. C.; Belgi, A.; van Lierop, B.; Delaine, C.; Andrikopoulos, S.; MacRaild, C. A.; Norton, R. S.; Haworth, N. L.; Robinson, A. J.; Forbes, B. E., Probing the correlation between insulin activity and structural stability through introduction of the rigid A6–A11 bond. *Journal of Biological Chemistry* **2018**, jbc. RA118. 002486.
98. Hua, Q.-X.; Hu, S.-Q.; Frank, B. H.; Jia, W.; Chu, Y.-C.; Wang, S.-H.; Burke, G. T.; Katsoyannis, P. G.; Weiss, M. A., Mapping the functional surface of insulin by design: structure and function of a novel A-chain analogue. *Journal of molecular biology* **1996,** *264* (2), 390-403.
99. Xu, B.; Hua, Q.-x.; Nakagawa, S. H.; Jia, W.; Chu, Y.-C.; Katsoyannis, P. G.; Weiss, M. A., Chiral mutagenesis of insulin's hidden receptor-binding surface: structure of an Allo-isoleucineA2 analogue1. *Journal of molecular biology* **2002,** *316* (3), 435-441.
100. Katsoyannis, P. G.; Zalut, C., Synthesis of deamino-A1 sheep insulin. *Biochemistry* **1972,** *11* (7), 1128-1132.
101. Geiger, R.; Geisen, K.; Regitz, G.; Summ, H.-D., [A1-β-Alanin] Insulin. *Hoppe-Seyler´ s Zeitschrift für physiologische Chemie* **1976,** *357* (2), 1267-1270.
102. Cosmatos, A.; Cheng, K.; Okada, Y.; Katsoyannis, P., The chemical synthesis and biological evaluation of [1-L-alanine-A]-and [1-D-alanine-A] insulins. *J. Biol. Chem* **1978,** *253*, 6586-6590.
103. Geiger, R.; Geisen, K.; Regitz, G.; Summ, H.; Langner, D., Insulin analogues with substitution of A1-glycine by D-amino acids and omega-amino acids (author's transl). *Hoppe-Seyler's Zeitschrift fur physiologische Chemie* **1980,** *361* (4), 563-570.
104. Nakagawa, S. H.; Tager, H. S., Importance of aliphatic side-chain structure at positions 2 and 3 of the insulin A chain in insulin-receptor interactions. *Biochemistry* **1992,** *31* (12), 3204-3214.
105. Nanjo, K.; Sanke, T.; Miyano, M.; Okai, K.; Sowa, R.; Kondo, M.; Nishimura, S.; Iwo, K.; Miyamura, K.; Given, B., Diabetes due to secretion of a structurally abnormal insulin (insulin Wakayama). Clinical and functional characteristics of [LeuA3] insulin. *Journal of Clinical Investigation* **1986,** *77* (2), 514.
106. Sieber, P.; Eisler, K.; Kamber, B.; Riniker, B.; Rittel, W.; Märki, F.; De Gasparo, M., Synthesis and biological activity of two disulphide bond isomers of human insulin:[A7-A11, A6-B7-cystine]-and [A6-A7, A11-B7-cystine] insulin (human). *Biological Chemistry* **1978,** *359* (1), 113-124.

107. Eisler, K.; Kamber, B.; Riniker, B.; Rittel, W.; Sieber, P.; De Gasparo, M.; Märki, F., Synthesis and biological activity of five D-Cys analogs of human insulin. *Bioorganic Chemistry* **1979,** *8* (4), 443-450.
108. Scholl, M.; Ding, S.; Lee, C. W.; Grubbs, R. H. J. O. L., Synthesis and activity of a new generation of ruthenium-based olefin metathesis catalysts coordinated with 1, 3-dimesityl-4, 5-dihydroimidazol-2-ylidene ligands. **1999,** *1* (6), 953-956.
109. Whelan, A. N.; Elaridi, J.; Mulder, R. J.; Robinson, A. J.; Jackson, W. R. J. C. j. o. c., Metal-catalysed tandem metathesis-hydrogenation reactions for the synthesis of carba analogues of cyclic peptides. **2005,** *83* (6-7), 875-881.
110. Büllesbach, E.; Schwabe, C., Synthesis and conformational analysis of the insulin-like 4 gene product. *The Journal of Peptide Research* **2001,** *57* (1), 77-83.
111. Lin, F.; Otvos, L.; Kumagai, J.; Tregear, G. W.; Bathgate, R. A.; Wade, J. D., Synthetic human insulin 4 does not activate the G-protein-coupled receptors LGR7 or LGR8. *Journal of Peptide Science* **2004,** *10* (5), 257-264.
112. Chenault, H. K.; Dahmer, J.; Whitesides, G. M., Kinetic resolution of unnatural and rarely occurring amino acids: enantioselective hydrolysis of N-acyl amino acids catalyzed by acylase I. *Journal of the American Chemical Society* **1989,** *111* (16), 6354-6364.
113. Rensing, D. T.; Uppal, S.; Blumer, K. J.; Moeller, K. D., Toward the selective inhibition of G proteins: total synthesis of a simplified YM-254890 analog. *Organic Letters* **2015,** *17* (9), 2270-2273.
114. Gu, X.; Ying, J.; Agnes, R. S.; Navratilova, E.; Davis, P.; Stahl, G.; Porreca, F.; Yamamura, H. I.; Hruby, V. J., Novel design of bicyclic β-turn dipeptides on solid-phase supports and synthesis of [3.3. 0]-bicyclo [2, 3]-Leu-enkephalin analogues. *Organic letters* **2004,** *6* (19), 3285-3288.
115. Denley, A.; Bonython, E. R.; Booker, G. W.; Cosgrove, L. J.; Forbes, B. E.; Ward, C. W.; Wallace, J. C., Structural determinants for high-affinity binding of insulin-like growth factor II to insulin receptor (IR)-A, the exon 11 minus isoform of the IR. *Molecular Endocrinology* **2004,** *18* (10), 2502-2512.
116. Frasca, F.; Pandini, G.; Scalia, P.; Sciacca, L.; Mineo, R.; Costantino, A.; Goldfine, I.; Belfiore, A.; Vigneri, R., Insulin receptor isoform A, a newly recognized, high-affinity insulin-like growth factor II receptor in fetal and cancer cells. *Molecular and cellular biology* **1999,** *19* (5), 3278-3288.
117. Soos, M.; Siddle, K., Immunological relationships between receptors for insulin and insulin-like growth factor I. Evidence for structural heterogeneity of insulin-like growth factor I receptors involving hybrids with insulin receptors. *Biochemical Journal* **1989,** *263* (2), 553-563.
118. Burnley, J.; Jackson, W. R.; Robinson, A. J., One-Pot Selective Homodimerization/Hydrogenation Strategy for Sequential Dicarba Bridge Formation. *The Journal of organic chemistry* **2015,** *80* (18), 9057-9063.
119. Wengrovius, J. H.; Sancho, J.; Schrock, R. R., Metathesis of acetylenes by tungsten (VI)-alkylidyne complexes. *Journal of the American Chemical Society* **1981,** *103* (13), 3932-3934.
120. Bindl, M.; Stade, R.; Heilmann, E. K.; Picot, A.; Goddard, R.; Fürstner, A., Molybdenum Nitride Complexes with Ph3SiO Ligands Are Exceedingly Practical and Tolerant Precatalysts for Alkyne Metathesis and Efficient Nitrogen Transfer Agents. *Journal of the American Chemical Society* **2009,** *131* (27), 9468-9470.
121. Heppekausen, J.; Stade, R.; Kondoh, A.; Seidel, G.; Goddard, R.; Fürstner, A., Optimized Synthesis, Structural Investigations, Ligand Tuning and Synthetic Evaluation of Silyloxy-Based Alkyne Metathesis Catalysts. *Chemistry – A European Journal* **2012,** *18* (33), 10281-10299.

122. Ghalit, N.; Poot, A. J.; Furstner, A.; Rijkers, D. T.; Liskamp, R. M., Ring-closing alkyne metathesis approach toward the synthesis of alkyne mimics of thioether A-, B-, C-, and DE-ring systems of the lantibiotic nisin Z. *Org Lett* **2005,** *7* (14), 2961-4.
123. Ghalit, N.; Rijkers, D. T.; Liskamp, R. M., Alkene-and alkyne-bridged mimics of nisin as potential peptide-based antibiotics. *Journal of Molecular Catalysis A: Chemical* **2006,** *254* (1), 68-77.
124. Cromm, P. M.; Schaubach, S.; Spiegel, J.; Fürstner, A.; Grossmann, T. N.; Waldmann, H., Orthogonal ring-closing alkyne and olefin metathesis for the synthesis of small GTPase-targeting bicyclic peptides. *Nature Communications* **2016,** *7*.
125. Cromm, P. M.; Wallraven, K.; Glas, A.; Bier, D.; Fürstner, A.; Ottmann, C.; Grossmann, T. N., Constraining an Irregular Peptide Secondary Structure through Ring-Closing Alkyne Metathesis. *ChemBioChem* **2016**.
126. Ghalit, N.; Rijkers, D. T.; Kemmink, J.; Versluis, C.; Liskamp, R. M., Pre-organization induced synthesis of a crossed alkene-bridged nisin Z DE-ring mimic by ring-closing metathesis. *Chemical communications* **2005,** (2), 192-4.
127. Ijsselstijn, M.; Aguilera, B.; van der Marel, G. A.; van Boom, J. H.; van Delft, F. L.; Schoemaker, H. E.; Overkleeft, H. S.; Rutjes, F. P. J. T.; Overhand, M., Ring-closing alkyne metathesis mediated synthesis of cyclic β-turn mimetics. *Tetrahedron Letters* **2004,** *45* (22), 4379-4382.
128. Heppekausen, J.; Stade, R.; Goddard, R.; Fürstner, A., Practical new Silyloxy-based alkyne metathesis catalysts with optimized activity and selectivity profiles. *Journal of the American Chemical Society* **2010,** *132* (32), 11045-11057.
129. Fairlie, D. P.; Abbenante, G.; March, D. R., Macrocyclic peptidomimetics-forcing peptides into bioactive conformations. *Current medicinal chemistry* **1995,** *2* (2), 654-686.
130. Chalker, J. M., Allyl Sulfides: Reactive Substrates for Olefin Metathesis. *Australian Journal of Chemistry* **2015,** *68* (12), 1801-1809.
131. Schmiedeberg, N.; Kessler, H., Reversible backbone protection enables combinatorial solid-phase ring-closing metathesis reaction (RCM) in peptides. *Organic letters* **2002,** *4* (1), 59-62.
132. Chalker, J. M.; Lin, Y. A.; Boutureira, O.; Davis, B. G., Enabling olefin metathesis on proteins: chemical methods for installation of S-allyl cysteine. *Chemical communications* **2009,** (25), 3714-3716.
133. Carpino, L. A.; Sadat-Aalaee, D.; Chao, H. G.; DeSelms, R. H., [(9-Fluorenylmethyl) oxy] carbonyl (FMOC) amino acid fluorides. Convienient new peptide coupling reagents applicable to the FMOC/tert-butyl strategy for solution and solid-phase syntheses. *Journal of the American Chemical Society* **1990,** *112* (26), 9651-9652.
134. Wöhr, T.; Wahl, F.; Nefzi, A.; Rohwedder, B.; Sato, T.; Sun, X.; Mutter, M., Pseudo-prolines as a solubilizing, structure-disrupting protection technique in peptide synthesis. *Journal of the American Chemical Society* **1996,** *118* (39), 9218-9227.
135. Chatterjee, A. K.; Choi, T.-L.; Sanders, D. P.; Grubbs, R. H., A general model for selectivity in olefin cross metathesis. *Journal of the American Chemical Society* **2003,** *125* (37), 11360-11370.
136. van Lierop, B. Dicarba Mimetics of Cysteine-Containing Peptides. Monash University, 2010.
137. Sohma, Y.; Hua, Q. X.; Whittaker, J.; Weiss, M. A.; Kent, S. B., Design and folding of [GluA4 (OβThrB30)] insulin ("ester insulin"): a minimal proinsulin surrogate that can be chemically converted into human insulin. *Angewandte Chemie* **2010,** *122* (32), 5621-5625.
138. Sohma, Y.; Kent, S. B., Biomimetic synthesis of lispro insulin via a chemically synthesized "mini-proinsulin" prepared by oxime-forming ligation. *Journal of the American Chemical Society* **2009,** *131* (44), 16313-16318.

139. Tofteng, A. P.; Jensen, K. J.; Schäffer, L.; Hoeg-Jensen, T., Total Synthesis of desB30 Insulin Analogues by Biomimetic Folding of Single-Chain Precursors. *ChemBioChem* **2008,** *9* (18), 2989-2996.
140. Kemmler, W.; Peterson, J. D.; Steiner, D. F., Studies on the conversion of proinsulin to insulin I. Conversion in vitro with trypsin and carboxypeptidase B. *Journal of Biological Chemistry* **1971,** *246* (22), 6786-6791.
141. Frank, B.; Chance, R., Two routes for producing human insulin utilizing recombinant DNA technology. *MMW, Munchener medizinische Wochenschrift* **1983**, S14-20.
142. Frank, B. H.; Prouty, W. E.; Heiney, R. E.; Walden, M. R., Treating with trypsin and carboxypeptidase b in aqueous medium containing nickel ions in specified concentrations and weight ratios. Google Patents: 1995.
143. Chang, S.; Kim, D.; Choi, K.; Shin, J.; Shin, H., Human insulin production from a novel mini-proinsulin which has high receptor-binding activity. *Biochem. J* **1998,** *329*, 631-635.
144. Ashcroft, F. M.; Ashcroft, S. J., *Insulin: molecular biology to pathology*. Oxford University Press: 1992.
145. Thim, L.; Hansen, M. T.; Norris, K.; Hoegh, I.; Boel, E.; Forstrom, J.; Ammerer, G.; Fiil, N. P., Secretion and processing of insulin precursors in yeast. *Proceedings of the National Academy of Sciences* **1986,** *83* (18), 6766-6770.
146. Dawson, P. E.; Muir, T. W.; Clark-Lewis, I.; Kent, S., Synthesis of proteins by native chemical ligation. *Science* **1994,** *266* (5186), 776-779.
147. Malins, L. R.; Mitchell, N. J.; McGowan, S.; Payne, R. J., Oxidative Deselenization of Selenocysteine: Applications for Programmed Ligation at Serine. *Angewandte Chemie* **2015,** *127* (43), 12907-12912.
148. Raj, M.; Wu, H.; Blosser, S. L.; Vittoria, M. A.; Arora, P. S., Aldehyde Capture Ligation for Synthesis of Native Peptide Bonds. *Journal of the American Chemical Society* **2015**.
149. Pusterla, I.; Bode, J. W., An oxazetidine amino acid for chemical protein synthesis by rapid, serine-forming ligations. *Nature Chemistry* **2015**.
150. Chan, W. C.; White, P. D., *Fmoc solid phase peptide synthesis*. Oxford University Press: 2000.
151. Isidro-Llobet, A.; Alvarez, M.; Albericio, F., Amino acid-protecting groups. *Chemical reviews* **2009,** *109* (6), 2455-2504.
152. Given, B.; Cohen, R.; Shoelson, S.; Frank, B.; Rubenstein, A.; Tager, H., Biochemical and clinical implications of proinsulin conversion intermediates. *Journal of Clinical Investigation* **1985,** *76* (4), 1398.
153. Siodłak, D.; Macedowska-Capiga, A.; Broda, M. A.; Kozioł, A. E.; Lis, T., The cis-trans isomerization of N-methyl-α, β-dehydroamino acids. *Peptide Science* **2012,** *98* (5), 466-478.
154. Burk, M. J.; Gross, M. F.; Martinez, J. P., Asymmetric catalytic synthesis of .beta.-branched amino acids via highly enantioselective hydrogenation of .alpha.-enamides. *Journal of the American Chemical Society* **1995,** *117* (36), 9375-9376.
155. Doi, T.; Fujimoto, N.; Watanabe, J.; Takahashi, T., Palladium (0)-catalyzed Mizoroki–Heck reaction and Rh (I)-catalyzed asymmetric hydrogenation of polymer-supported dehydroalanine system. *Tetrahedron letters* **2003,** *44* (10), 2161-2165.
156. Jiang, J.; Ma, Z.; Castle, S. L., Bulky α, β-dehydroamino acids: their occurrence in nature, synthesis, and applications. *Tetrahedron* **2015,** *71* (34), 5431-5451.
157. Siodłak, D., α,β-Dehydroamino acids in naturally occurring peptides. *Amino Acids* **2015,** *47* (1), 1-17.
158. Bonauer, C.; Walenzyk, T.; König, B., α,β-Dehydroamino Acids. *Synthesis* **2006,** *2006* (01), 1-20.

159. Schmidt, U.; Lieberknecht, A.; Wild, J., Didehydroamino Acids (DDAA) and Didehydropeptides (DDP). *Synthesis* **1988,** *1988* (03), 159-172.
160. Gupta, A.; Chauhan, V. S., Synthetic and conformational studies on dehydroalanine-containing model peptides. *Biopolymers* **1990,** *30* (3-4), 395-403.
161. Skropeta, D.; Jolliffe, K. A.; Turner, P., Pseudoprolines as Removable Turn Inducers: Tools for the Cyclization of Small Peptides. *The Journal of Organic Chemistry* **2004,** *69* (25), 8804-8809.
162. Le, D. N.; Riedel, J.; Kozlyuk, N.; Martin, R. W.; Dong, V. M., Cyclizing Pentapeptides: Mechanism and Application of Dehydrophenylalanine as a Traceless Turn-Inducer. *Organic letters* **2016,** *19* (1), 114-117.
163. Liu, D.; Zhang, X., Practical P-chiral phosphane ligand for Rh-catalyzed asymmetric hydrogenation. *European journal of organic chemistry* **2005,** *2005* (4), 646-649.
164. Lu, S.-P.; Lewin, A. H., Enamine/imine tautomerism in α, β-unsaturated-α-amino acids. *Tetrahedron* **1998,** *54* (50), 15097-15104.
165. Makowski, M.; Rzeszotarska, B.; Kubica, Z.; Pietrzyński, G., Synthesis of Peptides with α,β-Dehydroamino Acids, II. Synthesis of tert-Butyloxycarbonyldipeptides of Dehydroalanine and Dehydrophenylalanine. *Liebigs Annalen der Chemie* **1985,** *1985* (5), 893-900.
166. Makowski, M.; Rzeszotarska, B.; Kubica, Z.; Wieczorek, P., Synthesis of Peptides with α,β-Dehydroamino Acids, I. Synthesis of N-Benzyloxycarbonyl and N-Trifluoroacetyl Dipeptides of Dehydroalanine and Dehydrophenylalanine. *Liebigs Annalen der Chemie* **1984,** *1984* (5), 920-928.
167. Pozdnev, V. F., Activation of carboxylic acids by pyrocarbonates. Application of di-tert-butyl pyrocarbonate as condensing reagent in the synthesis of amides of protected amino acids and peptides. *Tetrahedron letters* **1995,** *36* (39), 7115-7118.
168. Jiang, J.; Luo, S.; Castle, S. L., Solid-phase synthesis of peptides containing bulky dehydroamino acids. *Tetrahedron Letters* **2015,** *56* (23), 3311-3313.
169. Wilson, K. R.; Sedberry, S.; Pescatore, R.; Vinton, D.; Love, B.; Ballard, S.; Wham, B. C.; Hutchison, S. K.; Williamson, E. J., Microwave-assisted cleavage of Alloc and Allyl Ester protecting groups in solid phase peptide synthesis. *Journal of Peptide Science* **2016,** *22* (10), 622-627.
170. Kazmaier, U.; Hebach, C.; Watzke, A.; Maier, S.; Mues, H.; Huch, V., A straightforward approach towards cyclic peptides via ring-closing metathesis—scope and limitations. *Organic & biomolecular chemistry* **2005,** *3* (1), 136-145.
171. Gille, F.; Kirschning, A., Studies on the synthesis of peptides containing dehydrovaline and dehydroisoleucine based on copper-mediated enamide formation. *Beilstein Journal of Organic Chemistry* **2016,** *12* (1), 564-570.
172. Djuric, S.; Venit, J.; Magnus, P., Silicon in synthesis: stabase adducts-a new primary amine protecting group: alkylation of ethyl glycinate. *Tetrahedron Letters* **1981,** *22* (19), 1787-1790.
173. Ciampini M.D., Prosser A. R., Robinson A.J., An amine transprotection reaction: A one-step stabase to carbamate protection. *Unpublished* **1998**.
174. Prosser, A. R. A Catalytic Asymmetric Approach to Sulfur-Containing β-Lactam Molecules. Monash University, 1998.
175. Lalonde, M.; Chan, T., Use of organosilicon reagents as protective groups in organic synthesis. *Synthesis* **1985,** *1985* (09), 817-845.
176. Leßmann, T.; Waldmann, H., Enantioselective synthesis on the solid phase. *Chemical communications* **2006,** (32), 3380-3389.
177. Najera, C.; Sansano, J. M., Catalytic asymmetric synthesis of α-amino acids. *Chemical reviews* **2007,** *107* (11), 4584-4671.

178. Ojima, I.; Tsai, C.-Y.; Zhang, Z., Catalytic asymmetric synthesis of peptides on polymer support. *Tetrahedron letters* **1994,** *35* (32), 5785-5788.
179. Wilson, K. R.; Sedberry, S.; Pescatore, R.; Vinton, D.; Love, B.; Ballard, S.; Wham, B. C.; Hutchison, S. K.; Williamson, E. J., Microwave-assisted cleavage of Alloc and Allyl Ester protecting groups in solid phase peptide synthesis. *Journal of Peptide Science* **2016**.
180. Jad, Y. E.; Acosta, G. A.; Naicker, T.; Ramtahal, M.; El-Faham, A.; Govender, T.; Kruger, H. G.; Torre, B. G. d. l.; Albericio, F., Synthesis and biological evaluation of a teixobactin analogue. *Organic letters* **2015,** *17* (24), 6182-6185.
181. Debaene, F.; Mejias, L.; Harris, J. L.; Winssinger, N., Synthesis of a PNA-encoded cysteine protease inhibitor library. *Tetrahedron* **2004,** *60* (39), 8677-8690.